

AD_____

AWARD NUMBER: W81XWH-07-1-0286

TITLE: Development of Complement Inhibitors to Limit Tissue as Adjuvants to Resuscitation

PRINCIPAL INVESTIGATOR: Yuang-Taung JUANG, Ph.D.

CONTRACTING ORGANIZATION: Beth Israel Deaconess Medical Center
Boston, MA 02215

REPORT DATE: March 2010

TYPE OF REPORT: Annual Summary

PREPARED FOR: U.S. Army Medical Research and Materiel Command
Fort Detrick, Maryland 21702-5012

DISTRIBUTION STATEMENT: Approved for Public Release;
Distribution Unlimited

The views, opinions and/or findings contained in this report are those of the author(s) and should not be construed as an official Department of the Army position, policy or decision unless so designated by other documentation.

REPORT DOCUMENTATION PAGE			<i>Form Approved</i> <i>OMB No. 0704-0188</i>		
Public reporting burden for this collection of information is estimated to average 1 hour per response, including the time for reviewing instructions, searching existing data sources, gathering and maintaining the data needed, and completing and reviewing this collection of information. Send comments regarding this burden estimate or any other aspect of this collection of information, including suggestions for reducing this burden to Department of Defense, Washington Headquarters Services, Directorate for Information Operations and Reports (0704-0188), 1215 Jefferson Davis Highway, Suite 1204, Arlington, VA 22202-4302. Respondents should be aware that notwithstanding any other provision of law, no person shall be subject to any penalty for failing to comply with a collection of information if it does not display a currently valid OMB control number. PLEASE DO NOT RETURN YOUR FORM TO THE ABOVE ADDRESS.					
1. REPORT DATE 1 March 2010		2. REPORT TYPE Annual Summary		3. DATES COVERED 23 Mar 2007 – 22 Feb 2010	
4. TITLE AND SUBTITLE Development of Complement Inhibitors to Limit Tissue as Adjuvants to Resuscitation			5a. CONTRACT NUMBER		
			5b. GRANT NUMBER W81XWH-07-1-0286		
			5c. PROGRAM ELEMENT NUMBER		
6. AUTHOR(S) Yuang-Taung JUANG, Ph.D. E-Mail: yjuang@bidmc.harvard.edu			5d. PROJECT NUMBER		
			5e. TASK NUMBER		
			5f. WORK UNIT NUMBER		
7. PERFORMING ORGANIZATION NAME(S) AND ADDRESS(ES) Beth Israel Deaconess Medical Center Boston, MA 02215			8. PERFORMING ORGANIZATION REPORT NUMBER		
9. SPONSORING / MONITORING AGENCY NAME(S) AND ADDRESS(ES) U.S. Army Medical Research and Materiel Command Fort Detrick, Maryland 21702-5012			10. SPONSOR/MONITOR'S ACRONYM(S)		
			11. SPONSOR/MONITOR'S REPORT NUMBER(S)		
12. DISTRIBUTION / AVAILABILITY STATEMENT Approved for Public Release; Distribution Unlimited					
13. SUPPLEMENTARY NOTES					
14. ABSTRACT We have produced evidence to urge the development of six new drugs/biologics to use in battlefield injury. We have established that DAF limits tissue injury and moved it to large animals of polytrauma injury. We have defined the importance of C5a in tissue injury and we have recommended that C5a inhibitors may be of value in limiting tissue injury. Finally we have introduce a novel inhibitor, CRlg, in the field of tissue injury. We have established that T cells and B cells are important in the execution of injury. We have demonstrated the importance of Annexin IV in instigating tissue injury. A discovery approach has revealed yet novel targets that may limit tissue injury. Our first finding was that actin polymerization is important for the expression of tissue injury. While ourselves are moving some of them to the next phase, we believe that the information that we have published will be of value to the industry and government agencies in carrying on large animal and clinical studies.					
15. SUBJECT TERMS None provided.					
16. SECURITY CLASSIFICATION OF:			17. LIMITATION OF ABSTRACT	18. NUMBER OF PAGES	19a. NAME OF RESPONSIBLE PERSON
a. REPORT	b. ABSTRACT	c. THIS PAGE			19b. TELEPHONE NUMBER (include area code)
U	U	U	UU	102	

Table of Contents

	<u>Page</u>
Introduction.....	2
Body.....	8
Key Research Accomplishments.....	13
Reportable Outcomes.....	14
Conclusion.....	15
References.....	16
Appendices.....	19

Introduction

Hemorrhage is seen as a challenge in multiple clinical conditions and is the primary cause of casualties on the battlefield and in civilian trauma. Data suggest that half of wartime casualties die due to hemorrhagic shock. Many casualties are resuscitated with fluids that enhance the tissue damage due to hemorrhage. [1, 2]. A prime example of this was the use of crystalloid resuscitation fluids during the Vietnam conflict that resulted in Da Nang lung and has been renamed to acute respiratory distress syndrome (ARDS).

Hemorrhage results in decreased blood flow throughout the body, blood is directed away from non-critical organs, such as the intestines, to vital organs such as the brain. Hemorrhagic shock is associated with intestinal ischemia [3]. These conditions lead to a reduction of blood volume that is believed to result in splanchnic vasoconstriction and functional if not true ischemia of the gut [4-8]. The splanchnic circulation is a large vascular bed that receives as much as 25-30% of the total blood flow bringing oxygen and nutrients to the intestine. As blood flow to the intestine decreases, the flow to the various circuits is not decreased equally with more flow shunted to the mucosa than to other networks. The rapid turnover of the mucosa makes it extremely sensitive to low oxygenation. Therefore, severe decreased blood flow to the intestine for a limited amount of time, as little as 20 min, results in damage to the mucosal surfaces with villi disruption. However, during resuscitation and the increased blood volume, the intestine is reperfused, resulting in pathological changes to the tissue. These alterations of hemorrhagic shock cause additional local inflammation characterized by complement activation and deposition, neutrophil infiltration and eicosanoid generation that coincide with mucosal injury and increased vascular permeability [7, 9, 10]. The role of complement in mediating this injury and the possibilities to inhibit complement activation is the focus of the current proposal.

Currently, there are pig and rat models that have been used to investigate the correlation between hemorrhage, ischemia/reperfusion, and tissue injury. We developed a mouse model so that we can take advantage of inbred genetically modified animals. Using the mice, we have developed a time course of intestinal damage when removing 30% of the blood. Our preliminary data indicate that hemorrhage induces complement activation and deposition, inflammation and tissue damage similar to that seen in other animal models.

Complement activation

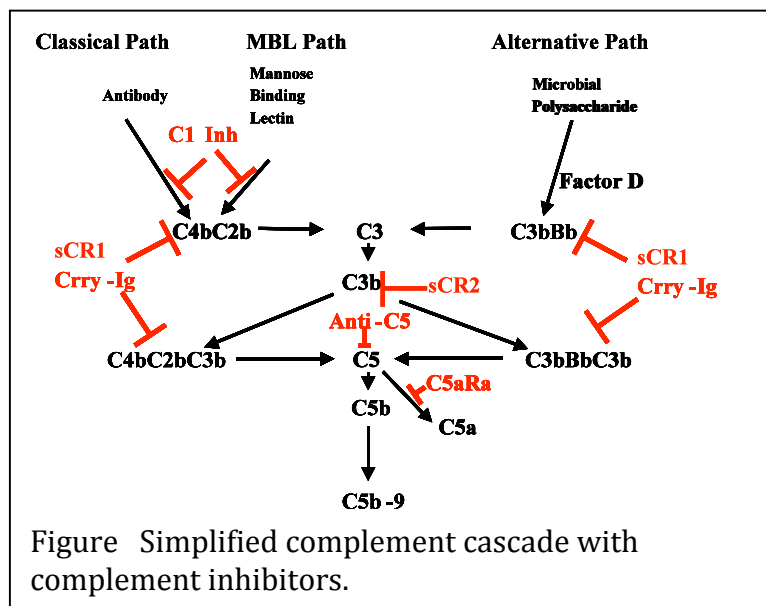
The complement system is composed of more than 30 proteins that interact in a proteolytic cascade. The cascade uses three different initiation pathways that unite into a common terminal pathway. Complement-mediated injury is responsible for a number of clinical scenarios associated with tissue damage. These clinical settings include hemorrhagic shock, thermal injury (burns), myocardial infarction, ARDS, and compartment syndrome following extremity

ischemia and mesenteric ischemia. Our preliminary data indicate a role for complement induced damage in hemorrhage and resuscitation.

When activated complement provides a critical link between the innate and adaptive immune responses. The cascade has 3 initiating arms, the classical, lectin and alternative pathways each activated in a distinct mechanism: antibody initiates the classical pathway, mannose binding lectin and bacterial polysaccharides initiate the lectin and alternative pathways, respectively. Each initiating arm produces enzymatic complexes, C3 and C5 convertases. The cleavage of C3 and C5 continues the cascade with all 3 pathways culminating in a common terminal pathway. The terminating complex, the membrane attack complex (MAC) is a lytic complex that inserts into the membrane forming a pore in the cell. In addition to cell lysis, the cascade also increases phagocytosis, recruits inflammatory molecules, and instructs the adaptive response to produce an appropriate humoral response.

During activation, all three initiating pathways of the complement system result in the formation and release of the anaphylatoxins, C3a and C5a. These small molecules, 9 and 11.2 kDa respectively, are potent chemotactic proteins that not only recruit granulocytes but also induce degranulation of phagocytes and basophils and mast cells, release of hydrolytic enzymes from neutrophils, smooth muscle contraction, and increased vascular permeability [11]. This proinflammatory response can prevent pathogen invasion but can also induce host tissue injury when inappropriately produced. Therefore, although beneficial, in excess C3a and C5a maybe potent mediators of remote organ injury during trauma.

Capable of extreme damage, complement regulatory molecules are essential and occur naturally at multiple points within the cascade. However, in many clinical conditions, unregulated complement activation induces additional tissue injury. Inappropriate



complement activation and subsequent tissue damage occurs during tissue inflammation, myocardial or intestinal ischemia, blunt trauma, hemorrhagic shock, and after exposure to bacterial toxins.

Complement activation contributes to cell injury in a number of ways. The central events in complement activation involve the activation of plasma proteins, C3 and C5. All initiating pathways result in the generation of C3b and C5b and the formation of C5b-9 the MAC. As the result of the common terminal pathway, MAC inserts itself as a pore into cell membranes causing cell death.

Complement inhibitors

Complement is controlled by 10 or more inhibitory proteins found either in the serum or on cell membranes [12]. A deficiency in some of these inhibitory molecules causes increased susceptibility to immune complexes that are found frequently in patients with rheumatic diseases. Without complement inhibitors to prevent continued growth, the lattice of antibody/antigen complexes becomes extremely large and precipitate in organs. In addition, complement coating of the complexes aids phagocytosis of the complexes by binding to surface erythrocyte complement receptors and trafficking to the liver and spleen. Because of the similarities of the 3 pathways, many of the regulatory molecules can inhibit multiple pathways. In addition, the convergence of all pathways at the formation of the MAC, allows inhibitors downstream of C5 to regulate all forms of complement activation. The primary function of these natural regulatory proteins is to control the C3 and C5 convertases by degrading the components.

With the advent of molecular biology, a number of recombinant engineered inhibitors have been designed. Although there are some high molecular weight bivalent molecules that exist, the more recent inhibitors are small peptides. The use of peptides in complement inhibition has a number of distinct advantages: they are very specific, small, defined by complement components and therefore an antibody response is not expected, and maybe delivered orally.

Recently, Compstatin, a synthetic peptide, has been described that binds to C3 and inhibits both C3a release and MAC formation [13, 14]. In vitro and ex vivo animal models have shown that Compstatin is a useful complement inhibitor for transplantation and cardiopulmonary bypass-related pathology [14, 15]. As an inhibitor that is useful in primates, it is also likely, that Compstatin blockade of C3 will prevent excessive complement activation during trauma.

C5a Receptor antagonist (C5aRa) is recent synthetic small peptide inhibitor that is currently being used in a number of animal models of tissue injury [16, 17]. The anaphylatoxin C5a mediates its effects by binding the G-protein coupled cell surface receptor, CD88. C5aRa has been shown to inhibit C5a induced neutrophil chemotaxis in response to sepsis and recently to attenuate both cardiac and mesenteric ischemia and reperfusion local damage in rodents [16, 18]. In addition, it prevents neutrophil mediated systemic damage in a similar animal model [18]

Research efforts at limiting complement-mediated tissue injury have focused on inhibitors of complement. The complement cascade also involves soluble and membrane bound inhibitor proteins that act at various different points in the cascade. Manipulation of these natural inhibitors inhibits complement mediated tissue damage during mesenteric ischemia and reperfusion and may be useful in a hemorrhagic shock model. Studies are currently underway to examine the ability of C1-Inh or sCR1 to inhibit complement activation in hemorrhage. In addition, the ability to create soluble forms of naturally membrane bound inhibitors may provide targeted inhibitors. Two such membrane bound molecules in the mouse are complement receptor 1-related gene/protein y (Crry) and complement receptor 2 (Cr2).

In mice, Crry is a membrane regulatory protein altering the activity of both the classical and alternative complement pathways. Using a recombinant soluble form of Crry fused to the hinge, CH2, and CH3 domains of mouse IgG1 (Crry-Ig), mice were pretreated either 5 min prior to, or 30 min after, the initiation of the reperfusion phase of mesenteric IR [7]. IR-induced injury was reduced after Crry-Ig was administered. Pre-treatment with Crry-Ig reduced the local intestinal mucosal injury and decreased generation of LTB₄ [7]. When given 30 min after the beginning of the reperfusion phase, Crry-Ig resulted in a decrease in IR-induced intestinal mucosal injury comparable to when it was given 5 min prior to initiation of the reperfusion phase. Despite the presence of substantial number of neutrophils, Crry-Ig administered 30 min after the initiation of the reperfusion prevented the IR-induced tissue injury damage [7]. This indicates that although neutrophils may have a role in the damage, complement inhibition is beneficial.

Complement receptor type 2 (Cr2/CD21) is an important membrane receptor that binds complement iC3b/C3d-bound antigens and greatly enhances B cell receptor mediated activation by engaging the Cr2/CD19/CD81 signaling complex [19-22]. This recognition mechanism lowers the threshold for activation of B cells [19, 20, 23]. In mice, Cr2 is encoded along with the larger complement receptor type 1 (CR1) by the *Cr2* gene, which produces both proteins through alternative splicing of a common mRNA [24, 25]. As a soluble molecule, it is likely that Cr2 will bind excess C3b products preventing excessive complement activation and antibody production.

Complement activation in hemorrhage and resuscitation

Patients who have experienced a severe loss of blood or blood volume activate complement. C1 activation and the classical complement pathway are activated by the coagulation pathway and factor XII [26, 27]. In addition, there are indications that the alternative pathway is also activated however the triggering factors are not well defined [26]. Recent studies have focused on determining if complement activation induces damage or if complement activation is merely a side effect of the tissue damage. Younger et al used a rat model of hemorrhagic shock (HS) to show that induction of complement activation by treatment with cobra venom factor increased mortality while complement depletion prior to HS attenuated injury [28]. In addition, they showed that C5a mediated the lethal effects of HS as indicated by experiments that showed that blocking C5a clearance was lethal in at least 80% of the animals -- suggesting that C5a is at least one of the critical players in the pathology of HS [28].

During HS the sympathetic nerve response decreases splanchnic circulation causing intestinal ischemia. As discussed above, at least two mechanisms, complement and polymorphonuclear cells (PMN) infiltration mediate damage to the intestine. In a rat model of HS, inhibition of complement by administering sCR1 prior to resuscitation maintained the splanchnic circulation thus preventing HS induced intestinal ischemia [29]. Two complement inhibitors, C1 inh and soluble CR1 have recently been shown to prevent PMN infiltration [27]. To recruit PMN into the intestine requires a chemotactic signal followed by increase adhesion molecule expression on the vascular endothelium. This is followed by leukocyte rolling and adhering to the vasculature. C1 Inh attenuates adhesion and rolling of leukocytes within the mesenteric vascular endothelium [27, 30]. The PMN chemotactic signal may be either C5a [28] or PLA2 derived eicosanoids [31]. Finally, there is evidence that hemorrhage may alter the intestinal barrier such that macrophages in the lamina propria are exposed to bacterial products. The presence of these products may also activate the complement cascade.

Military Significance

The principal cause of death among soldiers who die within the first hour of wounding is hemorrhage. The frequency and associated morbidity of peripheral vascular injury sustained during wartime has been well documented. In DeBakey's review of 2471 acute battle injuries resulting in vascular trauma from World War II, the limb amputation rate in extremity vascular injury was 40% [32]. Hughes reviewed the treatment of vascular injuries from the Korean conflict during which time the principle of vascular repair to restore arterial continuity was practiced rather than vessel ligation [2]. While this preserved limb viability in a greater number of cases, ischemia/reperfusion (IR) in the revascularized injured limb presented additional problems. Rich's review of vascular injuries sustained during the Vietnam conflict, again illustrates the high numbers of vascular injuries, the repair of which risk IR, that continue to be observed in modern armed combat [2]. Despite advances in the early resuscitative management and definitive repair of such injuries, limb loss has remained a concern as evidenced

by the amputation rates reported from these conflicts. In a review of 1,000 cases of acute major arterial injury reported from Vietnam between 1965 and 1968, the amputation rate was significantly less than prior conflicts, but was still 13.5% [2]. Given the frequency of major arterial injury and hemorrhagic shock due to combat injuries, and that many of the adverse sequelae of these injuries are at least in part mediated by complement activation, an effective inhibitor of complement activation would have tremendous therapeutic potential in the setting of combat casualty care. The extension of the window of opportunity in which a limb can be saved would be of great value especially in a limited environment such as peacekeeping missions. The overall goal of this proposal is to identify complement activation inhibitors that can be used effectively and safely in injured soldiers or other appropriate clinical settings. We anticipate that some of these biologics will be part of the initial-first aid- kit that will prevent or limit the magnitude of the injury. More specifically, an appropriate inhibitor can be part of a patch or initial intravenous fluids that are given by the field medic to limit the effects of complement mediated tissue damage. We know that complement activation in damaging tissues and therefore limiting its injurious effects should be desirable. We aim at reducing the resuscitation fluid volume required for resuscitation to the minimum possible. We aim reducing mortality by 70%. We aim at limiting morbidity by 70%.

Public Purpose:

Hemorrhage is a frequent consequence of automobile, farm and occupational accidents. Therefore, any inhibitors which are useful on the battlefield will also be useful in the paramedic's bag in the ambulance or for the physician in the emergency room.

BODY

A. Decay-accelerating factor attenuates remote ischemia-reperfusion-initiated organ damage.

A.1. As discussed in the introduction, complement activation contributes to the expression of local and remote organ injury in animal models of ischemia-reperfusion (IR). We demonstrated here that a soluble form of decay-accelerating factor (DAF) protects normal C57Bl/6 and autoimmunity-prone B6.MRL/lpr mice subjected to hindlimb IR from remote intestinal and lung injury without affecting the degree of local skeletal muscle injury. In addition, DAF treatment attenuated remote organ injury in mice subjected to mesenteric IR. Soluble DAF allowed the deposition of complement 3 in local and remote injury sites while it limited the presence of terminal membrane attack complex and did not increase animal susceptibility to sepsis. These data provide evidence that soluble DAF might offer clinical benefit to patients suffering remote intestinal or lung damage in response to muscle or other organ injury (*see attached Publication for detailed report of the data. APPENDIX 1*).

A.2. Because tissue injury occurs invariably in the setting of inflammation, we wished to explore whether tissue injury occurring in the setting of systemic inflammation. A marker and causative agent of tissue inflammation is C-reactive protein (CRP). CRP is an acute pro-inflammatory mediator that has been demonstrated to enhance ischemia/reperfusion (IR) injury by virtue of activating the complement system. CRP is able to interact with complement proteins such as C1q, complement factor H, and C4b-binding protein. Since complement activation is central in the expression of tissue injury following IR, we have investigated the effects of human decay-accelerating factor (DAF), a complement inhibitor, on CRP-potentiated complement activation and tissue injury in mice subjected to mesenteric IR.

Male C57B1/6 mice were allocated into eight groups: (1) Sham-operated group without IR injury; (2) CRP+Sham group; (3) IR group; (4) CRP+IR group; (5) DAF group; (6) CRP+DAF group; (7) IR+DAF group, and (8) CRP+IR+DAF group. Intestinal and lung injury, neutrophil infiltration, myeloperoxidase (MPO) expression, complement component deposition, and interleukin-6 (IL-6) production were assessed for each treatment group of mice.

We found that administration of DAF significantly attenuates the CRP-enhanced intestinal injury as well as remote lung damages following acute mesenteric IR in mice, while DAF inhibits complement activation, suppresses neutrophil infiltration, and reduces IL-6 production.

We concluded that that inhibition complement activation with DAF may prove useful

for the treatment of post-ischemic inflammatory injuries associated with an increased production of CRP. *Details on the experimental data can be found in the attached PDF of the published paper APPENDIX 2.*

The data from this series of studies have been used to move on to determine whether DAF can prevent tissue injury in a swine polytrauma model. If this is successful, we will propose a phase I/II clinical trial.

B. A Novel Inhibitor of the Alternative Pathway of Complement (CR1g) Attenuates Intestinal Ischemia/Reperfusion-Induced Injury.

Complement activation has been demonstrated to contribute significantly to the expression of IR-induced tissue damage. Each of the three complement pathways, classic, alternative, and lectin, has been implicated in the instigation of tissue pathology. We used a selective inhibitor of the alternative pathway, that is, a soluble form of complement receptor of the immunoglobulin superfamily (CR1g-Fc) to determine whether it can prevent IR tissue injury. We demonstrated that treatment of C57Bl/6 mice prior to mesenteric IR prevents local (intestinal) and remote (lung) injury by limiting deposition of complement and entry of polymorphonuclear cells to the sites of injury. Our results show that CR1g-Fc represents a candidate to limit IR injury as it occurs in various clinical conditions. *Details on the experimental data can be found in the attached PDF of the published paper APPENDIX 3.*

The data from this series of studies provide the required rationale to move on to determine whether DAF can prevent tissue injury in a swine polytrauma model. If this is successful, we will propose a phase I/II clinical trial.

C. Complement component C5a mediates hemorrhage-induced intestinal damage.

Complement has been implicated in the pathogenesis of intestinal damage and inflammation in multiple animal models. Although the exact mechanism is unknown, inhibition of complement prevents hemodynamic alterations in hemorrhage.

C57Bl/6, complement 5 deficient (C5^{-/-}) and sufficient (C5^{+/+}) mice were subjected to 25% blood loss. In some cases, C57Bl/6 mice were treated with C5a receptor antagonist (C5aRa) post-hemorrhage. Intestinal injury, leukotriene B₄, and myeloperoxidase production were assessed for each treatment group of mice.

Mice subjected to significant blood loss without major trauma develop intestinal inflammation and tissue damage within 2 hours. We report here that complement

5 (C5) deficient mice are protected from intestinal tissue damage when subjected to hemorrhage (injury score = 0.36 compared with wildtype hemorrhaged animal injury score = 2.89; $P < 0.05$). We present evidence that C5a represents the effector molecule because C57Bl/6 mice treated with a C5a receptor antagonist displayed limited intestinal injury (injury score = 0.88), leukotriene B4 (13.16 pg/mg tissue), and myeloperoxidase (115.6 pg/mg tissue) production compared with hemorrhaged C57Bl/6 mice ($P < 0.05$). Complement activation is important in the development of hemorrhage-induced tissue injury and C5a generation is critical for tissue inflammation and damage. *Details on the experimental data can be found in the attached PDF of the published paper APPENDIX 4.*

We believe that therapeutics targeting C5a may be useful therapeutics for hemorrhage-associated injury.

D. Annexin IV represents an antigen expressed by injured cells which binds natural antibodies, activated complement and instigates damage.

Previously we had shown that intestinal ischemia-reperfusion injury is initiated when natural IgM Abs recognize neo-epitopes that are revealed on ischemic cells. The target molecules and mechanisms whereby these neo-epitopes become accessible to recognition are not well understood. Proposing that isolated intestinal epithelial cells (IEC) may carry IR-related neo-epitopes, we used in vitro IEC binding assays to screen hybridomas created from B cells of unmanipulated wild-type C57BL/6 mice. We identified a novel IgM mAb (mAb B4) that reacted with the surface of IEC by flow cytometric analysis and was alone capable of causing complement activation, neutrophil recruitment and intestinal injury in otherwise IR-resistant Rag1(-/-) mice. mAb B4 was found to specifically recognize mouse annexin IV. Preinjection of recombinant annexin IV blocked IR injury in wild-type C57BL/6 mice, demonstrating the requirement for recognition of this protein to develop IR injury in the context of a complex natural Ab repertoire. Humans were also found to exhibit IgM natural Abs that recognize annexin IV. These data in toto identify annexin IV as a key ischemia-related target Ag that is recognized by natural Abs in a pathologic process required in vivo to develop intestinal IR injury. *Details on the experimental data can be found in the attached PDF of the published paper APPENDIX 5.*

The data from this series of studies provide the required rationale to use Annexin IV to prevent tissue injury. A patent has been submitted which includes WRAIR (RADII) and the University of Colorado and BIDMC.

E. Actin polymerization accounts for the binding of natural antibodies to ischemic tissues.

Ischemia-reperfusion (IR) injury represents a major clinical challenge, which contributes to morbidity and mortality during surgery. The critical role of natural immunoglobulin M (IgM) and complement in tissue injury has been

demonstrated. However, cellular mechanisms that result in the deposition of natural IgM and the activation of complement are still unclear. In this report, using a murine intestinal IR injury model, we demonstrated that the beta-actin protein in the small intestine was cleaved and actin filaments in the columnar epithelial cells were aggregated after a transient disruption during 30 min of ischemia. Ischemia also led to deposition of natural IgM and complement 3 (C3). A low dose of cytochalasin D, a depolymerization reagent of the actin cytoskeleton, attenuated this deposition and also attenuated intestinal tissue injury in a dose-dependent manner. In contrast, high doses of cytochalasin D failed to worsen the injury. These data indicate that ischemia-mediated aggregation of the actin cytoskeleton, rather than its disruption, results directly in the deposition of natural IgM and C3.

We concluded that ischemia-mediated aggregation of the actin cytoskeleton leads to the deposition of natural IgM and the activation of complement, as well as tissue injury. *Details on the experimental data can be found in the attached PDF of the published paper APPENDIX 6.*

F. B cells contribute to ischemia/reperfusion-mediated tissue injury.

Multiple elements are known to participate in ischemia/reperfusion (I/R)-mediated tissue injury. Amongst them, B cells have been shown to contribute by the production of antibodies that bind to ischemic cells and fix complement. It is currently unknown whether B cells participate through antibody-independent mechanisms in the pathogenesis of I/R. In a mesenteric I/R model we found that B cells infiltrate the injured intestine of normal and autoimmune mice 2h after reperfusion is established. B cell depletion protected mice from the development of I/R-mediated intestinal damage. The protection conferred by B cell depletion was significantly greater in MRL/lpr mice. Finally, we show that ischemic tissue expressed the B cell-attractant CXCL13 and infiltrating B cells expressed the corresponding receptor CXCR5. Our data grant B cells an antibody-independent role in the pathogenesis of intestinal I/R and suggest that B cells accumulate in the injured tissue in response to the chemokine CXCL13. *Details on the experimental data can be found in the attached PDF of the published paper APPENDIX 7.*

These data suggest that B cell depletion using available and approved by the FDA to control tissue injury due to ischemia.

G. IL-17 producing CD4+ T cells mediate accelerated ischemia/reperfusion-induced injury in autoimmunity-prone mice.

Elements of the innate and adaptive immune response have been implicated in the development of tissue damage after ischemic reperfusion (I/R). We demonstrated that T cells infiltrate the intestine of C57BL/6 mice subjected to intestinal I/R during the first hour of reperfusion. The intensity of the T cell

infiltration was higher in B6.MRL/lpr mice subjected to intestinal I/R and reflected more severe tissue damage than that observed in control mice. Depletion of T cells limited I/R damage in B6.MRL/lpr mice, whereas repletion of B6.MRL/lpr lymph node-derived T cells into the I/R-resistant Rag-1(-/-) mouse reconstituted tissue injury. The tissue-infiltrating T cells were found to produce IL-17. Finally, IL-23 deficient mice, which are known not to produce IL-17, displayed significantly less intestinal damage when subjected to I/R. *Details on the experimental data can be found in the attached PDF of the published paper APPENDIX 8.*

Our data assign T cells a major role in intestinal I/R damage by virtue of producing the pro-inflammatory cytokine IL-17. Anti-IL-17 biologics that are being now developed for a number of medical conditions may serve also trauma patients in the civilian and battlefield arena.

Key accomplishments:

1. Demonstrated the importance of DAF in limiting tissue injury and especially after inflammatory conditions.
2. Demonstrated that complement component C5a mediates hemorrhage-induced intestinal damage.
3. A novel inhibitor of the alternative pathway of complement attenuates intestinal ischemia-reperfusion-induced injury.
4. Demonstrated that Ischemia-mediated aggregation of the actin cytoskeleton is one of the major initial events resulting in ischemia-reperfusion injury
5. Proved that IL-17 producing CD4+ T cells mediate accelerated ischemia/reperfusion-induced injury in mice.
6. Showed first evidence that B cells contribute to ischemia/reperfusion-mediated tissue injury.

Reportable outcomes

Publications

1. Weeks, C. M. Moratz, C., Zacharia, A., Stracener, C., Peckham, R., Moore, Jr., F. D., Tsokos, G. C. (2007). Decay-accelerating factor attenuates remote ischemia/reperfusion-initiated organ damage. *Clin. Immunol.* 124: 311-327.
2. Lu, X., Li, Y., Simovic, M., Peckham, R. M., Fallabella, M., Wang, Y., Tsokos, G. C. and Dalle Lucca, J. J. Decay accelerating factor mitigates C-reactive protein –augmented tissue in mice with mesenteric ischemia reperfusion. *J. Surg. Res.* In press.
3. Chen, J., Crispin, J. C., van Lookeren Champagne, M., Dalle Lucca J. J., and Tsokos, G. C. A novel inhibitor of the alternative pathway of complement attenuates intestinal ischemia/reperfusion-induced injury. *J. Surg. Res.* In press.
4. Fleming, S. D., Phillips, L., Lambris, J.D. and Tsokos, G. C. (2008). Complement component C5a mediates hemorrhage-induced intestinal damage. Submitted. *J. Surg. Res.* 150:196-203.
5. Shi, T., Moulton, V. R., Lapchak, P. H., Deng, G. M., Dalle Lucca, J. J. and Tsokos, G. C., Ischemia-mediated aggregation of the actin cytoskeleton is one of the major initial events resulting in ischemia/reperfusion injury . *Amer. J. Physiol. (Gastroenterology and Liver Physiology)* 296:G339-47.
6. Kulik, L., Fleming, S. D., Moratz, C., Reuter, J. W., Novikov, A., Chen, K., Andrews, K. T., Markayan, A., Quigg, R. J., Silverman, G. J., Tsokos, G. C. and Holers, V. M. (2009). Pathogenic natural antibodies recognizing Annexin IV are required in to develop intestinal ischemia-reperfusion injury. *J. Immunol.* 182: 5363–5373.
7. Chen, J., Crispin, J. C., Tedder, T., Dalle Lucca, J. J. and Tsokos, G. C. (2009). B cells participate in the ischemia/reperfusion-initiated tissue injury in an antibody-independent manner. *J. Autoimmun.* 32: 195-200
8. Edgerton, C., Crispin, J. C. Moratz, C. M., Simovic, M., Zacharia, A., Egan, R., Chen, J., DalleLucca, J. J., Juang, Y. T. and Tsokos, G. C. (2009). IL-17 producing CD4⁺ T cells mediate accelerated ischemia/reperfusion-induced injury in autoimmunity-prone mice. *Clin. Immunol.* 130: 313-321.

Patents

1. Prevention and Treatment of Ischemia-Reperfusion Injury and Related Conditions.” U.S. Provisional Patent 60/685,289, international PCT/US2007/065125
2. WRAIR 09-45 - "Use of Complement Inhibitors to Decrease Mortality and Morbidity due to Hemorrhage"

Conclusions

We have established that DAF limits tissue injury and moved it to large animals of polytrauma injury. We have defined the importance of C5a in tissue injury and we have recommended that C5a inhibitors may be of value in limiting tissue injury. Finally we have introduced a novel inhibitor, CRIg, in the field of tissue injury. We have established that T cells and B cells are important in the execution of injury. We have demonstrated the importance of Annexin IV in instigating tissue injury. A discovery approach has revealed yet novel targets that may limit tissue injury. Our first finding was that actin polymerization is important for the expression of tissue injury.

In sum, SIX new approaches to the treatment of tissue injury have been introduced. While ourselves are moving some of them to the next phase, we believe that the information that we have published will be of value to the industry and government agencies in carrying on large animal and clinical studies.

REFERENCES

1. Burns BJ, Brandt LJ. Intestinal ischemia. *Gastroenterol Clin North Am* 2003;32(4):1127-43.
2. Rich NM, Baugh JH, Hughes CW. Acute arterial injuries in Vietnam: 1,000 cases. *J Trauma* 1970;10:359-69.
3. Trunage RH, Guice KS, Oldham KT. Endotoxemia and remote organ injury following intestinal reperfusion. *J Surg Res* 1994; 56:571-.
4. Austen WG, Zhang m, chan R, Friend D, hechtman HB, Carroll mC, Moore FD. Murine hindlimb reperfusion injury can be initiated by a self-reactive monoclonal IgM. *Surgery* 2004;136(2):401-6.
5. Dong J, Pratt JR, Smith RAG, Dodd I, Sacks SH. Strategies for targeting complement inhibitors in ischaemia/reperfusion injury. *Mol Immunol* 1999;36:957-63.
6. Kilgore KS, Todd RF, Lucchesi BR. Reperfusion injury. In: Gallin JI, Snyderman R, eds. *Inflammation:basic principles and clinical correlates*. Philadelphia:Lippincott Williams and Wilkins, 1999:1047-60.
7. Rehrig S, Fleming SD, Anderson J, *et al*. Complement inhibitor, complement receptor 1-related gene/protein γ -Ig attenuates intestinal damage after the onset of mesenteric ischemia/reperfusion injury in mice. *J Immunol* 2001;167(10):5921-7.
8. Williams TJ, Jose PJ, Wedmore CV, Peck MJ, Forrest MJ. Mechanisms underlying inflammatory edema: the importance of synergism between prostaglandins, leukotrienes, and complement-derived peptides. In: Samuelsson B, Paoletti R, Ramwell P, eds. *Advances in prostaglandin, thromboxane and leukotriene research, Vol. 11*. New York:Raven Press, 1983:33-7.
9. Conner WC, Gallagher CM, Miner TJ, Tavaf-Motamen H, Wolcott KM, Shea-Donohue T. Neutrophil priming state predicts capillary leak after gut ischemia in rats. *J Surg Res* 1999;84:24-30.
10. Eror AT, Stojadinovic A, Starnes BW, Makrides SC, Tsokos GC, Shea-Donohue T. Anti-inflammatory effects of soluble complement receptor type 1 promote rapid recovery of ischemia/reperfusion injury in rat small intestine. *Clin Immunol* 1999;90:266-75.
11. Sahu A, Morikis D, Lambris JD. Complement inhibitors targeting C3, C4, and C5. In: Lambris JD, Holers VM, eds. *Therapeutic interventions in the complement system*. Totowa, NJ:Humana Press, 2000:75-112.
12. Morgan BP. Clinical complementology: recent progress and future trends. *Eur J Clin Invest* 1994;24:219-28.
13. Morikis D, Assa-Munt N, Sahu A, Lambris JD. Solution structure of Compstatin, a potent complement inhibitor. *Protein Sci* 1998;7:619-27.
14. Nilsson B, Larsson R, Hong J, Elgue G, Ekdahl KN, Sahu A, Lambris JD. Compstatin inhibits complement and cellular activation in whole blood in two models of extracorporeal circulation. *Blood* 1998;92:1661-7.

15. Fiame AE, Mollens TE, Videm V, *et al.* Compstatin, a peptide inhibitor of C3, prolongs survival of ex vivo perfused pig xenografts. *Xenotransplantation* 1999;6:52-65.
16. Arumugam TV, Shiels IA, Woodruff TM, Reid RC, Fairlie DP, Taylor SM. Protective effect of a new C5a receptor antagonist against ischemia-reperfusion injury in the rat small intestine. *J Surg Res* 2002;103:260-7.
17. Haynes DR, Harkin DG, Bignold LP, Hutchens MJ, Taylor SM, Fairlie DP. Inhibition of C5a-induced neutrophil chemotaxis and macrophage cytokine production in vitro by a new C5a receptor antagonist. *Biochem Pharmacol* 2000;60:729-33.
18. Fleming SD, Mastellos D, Karpel-Massler G, Shea-Donohue T, Lambris JD, Tsokos GC. C5a causes limited, polymorphonuclear cell-independent, mesenteric ischemia/reperfusion-induced injury. *Clin Immunol* 2003;108:263-73.
19. Carter RH, Fearon DT. CD19: lowering the threshold for antigen receptor stimulation of B lymphocytes. *Science* 1992;256:105.
20. Carter RH, Spycher MO, Ng YC, Hoffman R, Fearon DT. Synergistic interaction between complement receptor type 2 and membrane IgM on B lymphocytes. *J Immunol* 1998;141:457.
21. Fearon DT, Carter RH. The CD19/CR2/TAPA-1 complex of B lymphocytes: linking natural to acquired immunity. *Annual Reviews of Immunology* 1995;13:127.
22. Tsokos GC, Lambris JD, Finkelman FD, Anastassiou ED, June CH. Monovalent ligands of complement receptor 2 inhibit whereas polyvalent ligands enhance anti-Ig-induced human B cell intracytoplasmic free calcium concentration. *J Immunol* 1990;144:1640-5.
23. Carroll MC. Role of complement receptors CD21/CD35 in B lymphocyte activation and survival. *Curr Top Microbiol Immunol* 1999;246:63-7.
24. Kurtz CB, O'Toole E, Christensen SM, Weis JH. The murine complement receptor gene family. IV. Alternative splicing of Cr2 gene transcripts predicts two distinct gene products that share homologous domains with both human CR2 and CR1. *J Immunol* 1990;144:3581-91.
25. Molina H, T. Kinoshita, K. Inoue, J.-C. Carel, and V. M. Holers. A molecular and immunochemical characterization of mouse CR2: Evidence for a single gene model of mouse Complement Receptors 1 and 2. *J Immunol* 1990;145:2974-83.
26. Kaplan AP, Ghebrehiwet B, Silverberg M, Sealey JE. The intrinsic coagulation-kinin pathway, complement cascades, plasma renin-angiotensin system and their interrelationships. *CRC Crit Rev Immunol* 1981:75-93.
27. Spain DA, Fruchterman TM, Matheson PJ, Wilson MA, Martin AW, Garrison RN. Complement activation mediates intestinal injury after resuscitation from hemorrhagic shock. *J Trauma* 1999;46:224-33.
28. Younger JG, Sasaki N, Waite MD, *et al.* Detrimental effects of complement activation in hemorrhagic shock. *J Appl Physiol* 2001;90:441-6.

29. Fruchterman TM, Spain DA, Wilson MA, Harris PD, Garrison RN. Complement inhibition prevents gut ischemia and endothelial cell dysfunction after hemorrhage/resuscitation. *Surgery* 1998;124:782-92.
30. Horstick G, Kempf T, Lauterbach M, *et al.* C1-esterase-inhibitor treatment at early reperfusion of hemorrhagic shock reduces mesentery leukocyte adhesion and rolling. *Microcirculation* 2001;8:427-33.
31. Gelfand JA, Donelan M, Burke JF. Preferential activation and depletion of the alternative complement pathway by burn injury. *Ann Surg* 1983;198:58-62.
32. DeBakey ME, Simeone FA. Battle injuries of the arteries in World War II: an analysis of 2,471 cases. *Ann Surg* 1946;123:534-79.
33. Fleming SD, Shea-Donohue T, Guthridge JM, Kulik L, Waldschmidt TJ, Gipson MG, Tsokos GC, Holers VM. Mice deficient in complement receptors 1 and 2 lack a tissue injury-inducing subset of the natural antibody repertoire. *J Immunol* 2002;169:2126-33.



available at www.sciencedirect.com



www.elsevier.com/locate/yclim



Decay-accelerating factor attenuates remote ischemia–reperfusion-initiated organ damage[☆]

Christine Weeks^{a,b}, Chantal Moratz^c, Athina Zacharia^c, Catherine Stracener^b, Ryan Egan^c, Russell Peckham^b, Francis D. Moore Jr.^a, George C. Tsokos^{b,c,d,*}

^a Department of Surgery, Brigham and Women's Hospital, Boston, MA 02115, USA

^b Department of Cellular Injury, Walter Reed Army Institute of Research, Silver Spring, MD 20910-7500, USA

^c Department of Medicine, Uniformed Services University of the Health Sciences, Bethesda, MD 20910-7500, USA

^d Division of Rheumatology, Beth Israel Deaconess Medical Center, Harvard Medical School, Boston MA 02115, USA

Received 5 January 2007; accepted with revision 8 May 2007

Available online 12 July 2007

KEYWORDS

Complement;
Inflammation;
Lung;
Cell surface molecules;
Ischemia–reperfusion

Abstract Complement activation contributes to the expression of local and remote organ injury in animal models of ischemia–reperfusion (IR). We demonstrate here that a soluble form of decay-accelerating factor (DAF) protects normal C57Bl/6 and autoimmunity-prone B6.MRL/lpr mice subjected to hindlimb IR from remote intestinal and lung injury without affecting the degree of local skeletal muscle injury. In addition, DAF treatment attenuates remote organ injury in mice subjected to mesenteric IR. Soluble DAF allowed the deposition of complement 3 in local and remote injury sites while it limited the presence of terminal membrane attack complex and did not increase animal susceptibility to sepsis. These data provide evidence that soluble DAF might offer clinical benefit to patients suffering remote intestinal or lung damage in response to muscle or other organ injury.

© 2007 Elsevier Inc. All rights reserved.

Introduction

Ischemia–reperfusion (IR) is a common clinical entity encountered in diverse fields such as vascular surgery, trauma, cardiac surgery, transplant, and cardiovascular medicine. The acute inflammatory response following an ischemic insult instigates pathology in local and remote organs leading to significant

morbidity and mortality. The critical role of complement activation in tissue injury has been amply demonstrated, resulting in various attempts at therapeutic intervention.

Observations of decreased myocardial inflammation with transient depletion of complement (C) 3 [1] and of the beneficial effect of soluble complement receptor 1 (sCR1) on IR pathology [2–7] implicated a role for complement in IR tissue damage. Studies in C3- and C4-deficient mice provided the first convincing evidence that IR-initiated tissue injury is complement-dependent [8,9].

The fact that *Rag-2*^{-/-} mice lacking serum Ig are protected from IR damage and that this protection is abrogated with infusion of wild-type Ig indicated that natural antibodies play a critical role in augmented IR injury [8,9]. Further, evidence that *Cr 2*^{-/-} mice displaying altered Ig responses were also

[☆] Supported by The Complement Program of the Medical Research and Materiel Command. C.M.W. is a National Research Council Associate.

* Corresponding author. Division of Rheumatology, Beth Israel Deaconess Medical Center, 4 Blackfan Circle, HIM-244, Boston MA 02115, USA. Fax: +1 617 975 5299.

E-mail address: gtsokos@bidmc.harvard.edu (G.C. Tsokos).

resistant to IR injury despite normal circulating levels of IgG and IgM, and that injury was restored with Ig from wild-type mice, suggested the presence of a distinct subset of Abs responsible for the initiation of IR injury [10,11].

Recent work has further narrowed the pathogenic natural Ig repertoire and revealed likely initial target antigens. An antibody directed against non-muscle myosin heavy chain type II (NMHC-II) was found to reconstitute damage in IR-resistant mice [12–14] as were anti-DNA, anti-histone [15], and anti-phospholipid antibodies [16]. It appears that multiple specificities are involved in Ag-Ab reactions leading to IR damage, and with the number of downstream events in the cascade, various targets for intervention exist.

Therapeutic inhibition of the complement system has been tried successfully in multiple animal models of IR injury [2–6,17–20]. However, indiscriminate suppression of complement may increase susceptibility to infection, especially in already immunocompromised individuals. Concern over infectious risks of systemic complement inhibition led to design of complement inhibitors directed to sites of complement activation. A fusion protein consisting of complement receptor 2 and a complement inhibitor protein (Crry) effectively limited organ injury without altering the susceptibility of mice to sepsis [21].

Decay-accelerating factor (DAF) is a glycosylphosphatidylinositol (GPI)-anchored membrane protein which contains four short consensus repeat (SCR) modules and a C-terminal O-glycosylated extension [22]. DAF binds CD97 through its first SCR [23]. Through its 2nd and 3rd SCR, DAF binds to and dissociates C3 and C5 convertases assembling on host cells [22–42], thereby protecting cells from complement activation on their surfaces and preventing C5b-9 formation [25,26,43–51]. Because DAF accelerates convertase decay and interrupts the complement amplification loop, we reasoned that both local and, more prominently, remote injury should be attenuated by DAF treatment.

Our results demonstrate that administration of soluble human DAF reduces remote intestinal and lung damage in a hindlimb IR model as well as remote injury in a mesenteric IR model in normal and autoimmunity prone mice while conserving resistance to polymicrobial sepsis.

Materials and methods

Animals

C57Bl/6 mice ages 8 to 12 weeks were used in the hindlimb model of skeletal muscle IR. B6.MRL/*lpr* autoimmune mice were used in the IR model at age 5 to 6 months (after their autoimmune phenotype had sufficient time to express). Animals in this study were maintained in accordance with the guidelines of the Laboratory Animal Medicine Department/IACUC of USUHS and the Committee on the Care and Use of Laboratory Animals of the Institute of Laboratory Animal Resources, National Research Council.

Hindlimb model of IR

C57Bl/6 mice ages 8–12 weeks or B6.MRL/*lpr* mice ages 5–6 months were exposed to 2 h of hindlimb ischemia and 3 h of reperfusion as previously described [8,13]. Anesthesia was

administered with injection of a mixture of ketamine and xylazine. Two rubber bands (Latex-O-Rings; Miltex, Inc.) were applied above the greater trochanter of one hindlimb following 2 min of hindlimb elevation to decrease venous congestion using a McGivney Hemorrhoid Ligator (Miltex, Inc., York, PA). Sham mice did not undergo banding. Mice were kept anesthetized for the duration of the experiment. Five minutes prior to reperfusion, mice were injected with the indicated dose per animal DAF (rhCD55/DAF, R&D Systems, Minneapolis, MN) or 0.2 ml sterile 1× PBS intravenously by tail vein injection. At the 2-h time point, rubber bands were cut, and limb reperfusion was confirmed by return of pink color to formerly dusky ischemic limbs. Animals were allowed to reperfuse for 3 h under anesthesia prior to sacrifice. Harvested tissues (lung, intestine, liver, kidney, spleen, muscle) were fixed overnight in 10% formalin (for paraffin blocks) or 4% paraformaldehyde (for frozen sections). Frozen section tissues stored in 4% paraformaldehyde were washed in PBS and sucrose and made into blocks for future sectioning.

Determination of DAF deposition

To determine time in circulation of rhCD55/DAF, C57Bl/6 mice were subjected to hindlimb IR as described above. After 2 h of hindlimb ischemia, mice were injected with either PBS vehicle control or 2 μg DAF by tail vein injection 5 min prior to reperfusion. Tissues were harvested 5 min post-reperfusion (10 min after DAF or PBS injection) and 55 min post-reperfusion (1 h after DAF or PBS injection). Muscle, intestine, and lung were harvested and placed in 4% paraformaldehyde overnight for fixation. Organs were placed into blocks to obtain frozen sections. Sections were cut and stained with anti-DAF or anti-C3-FITC.

Mesenteric model of IR

Five-month-old B6.MRL/*lpr* and C57Bl/6 mice were exposed to laparotomy and clamping of the superior mesenteric artery (SMA) following 30 min of equilibration after opening the abdomen as previously described [15]. Clamp was released after 30 min and animals were allowed to reperfuse for 2 h prior to sacrifice by anesthetic overdose. Five minutes prior to reperfusion, mice were injected with 2 μg per animal DAF (rhCD55/DAF, R&D Systems, Minneapolis, MN) or 0.2 ml sterile 1× PBS intravenously by tail vein injection. Mice were kept anesthetized for the duration of the experiment. Harvested tissues (lung, intestine, liver, kidney, spleen, muscle) were fixed overnight in 10% formalin (for paraffin blocks) or 4% paraformaldehyde (for frozen sections). Frozen section tissues stored in 4% paraformaldehyde were washed in PBS and sucrose and made into blocks for future sectioning.

Cecal ligation and puncture (CLP) model of polymicrobial sepsis

C57Bl/6 mice ages 3–8 weeks were allowed to acclimate to the USUHS animal facility for 1–2 weeks prior to use in experiments. Mice were anesthetized with 4% isoflurane in a sealed canister using VetEquip inhalant anesthesia equipment (VetEquip, Incorporated, Pleasanton, CA). Following induction of anesthesia, mice were moved to nose cones with

flow rates of 0.5 l/min isoflurane for the duration of the procedure. The abdomen was shaved with an electric razor and then prepped with betadine prior to draping. Midline incision was made using a 10 blade and the peritoneal cavity opened with iris scissors. The cecum was retrieved and ligated with 4–0 silk (Ethicon) 15 mm from the cecal pole, taking care to ensure intestinal continuity so as not to cause bowel obstruction. An 18-gauge needle was then employed to punch a full thickness hole in the cecum. The cecum was squeezed to allow a drop of stool to exude before replacing it in the abdominal cavity. Peritoneal cavity and skin/fur were closed in one layer with 3–0 vicryl (Ethicon). Following abdominal closure, mice were injected i.v. (by tail vein injection) with 2 µg/animal (0.2 ml) DAF (rhCD55/DAF, R&D Systems, Minneapolis, MN) or 0.2 ml sterile 1× PBS. They also received a subcutaneous injection of 1 cm³ warm normal saline prior to placement in their cages postoperative. Mice were maintained on a heating pad throughout the experiment and for 4 h postoperative. Mice were observed every 4 h for the first 48 h postoperative then every 8 h up to a time point of 240 h (10 days). They were allowed access to food and water *ad libitum* and were provided with gel in the floor of their cages and non-irritant bedding postoperative. No antibiotics or anti-inflammatories were administered. The endpoint was hours survived postoperatively.

Cobra venom factor (CVF)-treated animals were used as positive controls in this experiment. C57Bl/6 mice were injected I.P. with two separate injections of 3 µg per animal CVF (Cobra Venom Factor, *Naja naja kaouthia*, Calbiochem, La Jolla, CA) on the 2 days prior to the planned CLP procedure. Therefore, each mouse received a total of 6 µg/animal CVF (roughly equal to one unit functional activity). Procedure was carried out as above except that CVF-treated mice received no postoperative intravenous injection.

Scoring

Formalin-fixed tissues were made into paraffin blocks and slides were created from these blocks. Intestines harvested were opened and pinned flat prior to fixation. Intestine and muscle were cut two sections per slide, while lung was cut three sections per slide in serial sections 5 mm apart to obtain a representative group for scoring. Slides were stained with hematoxylin and eosin (H&E) prior to scoring for injury.

Intestine

Intestine was scored for injury as previously described [15,16]. Points were given for edema (0 to 1), hemorrhage (0 to 1), and an average score of villi destruction ranging from 0 to 6 (normal intact villi to denuded villi with hemorrhage and exuding lamina propria). Scoring was performed in a blind manner (animals coded by color). An average of 72 villi were scored for injury per animal in nearly all cases unless this number of villi were not present due to poor sectioning.

Lung

Lung sections were cut three sections per animal 5 mm apart and placed on slides. They were scored in a method

described by Cooke et al. [52]. First, lung was scored on a scale of 0 to 3 for pneumonitis (parenchymal consolidation) at low power. The extent of involvement by pneumonitis in each lung section was scored and the three values averaged for a total extent involvement score for the animal. The pneumonitis score and extent involvement by pneumonitis were multiplied together to obtain a “pneumonitis index.” Next, perivascular infiltrate was assessed on a scale of 0 to 3 for multiple vessels in each lung section and averaged to obtain a final average score for the animal. On average, twenty to forty vessels were scored per animal for perivascular infiltrate. Again at low power, extent of involvement by perivascular infiltrate in each lung was estimated for each section and averaged to determine perivascular infiltrate extent of involvement for the animal. The perivascular infiltrate value was multiplied by extent of involvement to give each animal’s “perivascular infiltrate index.” The total injury index for each animal was then the pneumonitis index added to the perivascular infiltrate index.

Muscle

Local injury to the hindlimb muscle was scored according to the method published in previous studies [8,53,53]. As it is difficult to identify individual muscle fiber borders when injury is present, percentage of the specimen where damage exists was assessed and given a numerical score. Additional points were given for notable edema (0 to 1) and hemorrhage (0 to 1) in specimens. Maximum total injury score was 6.

Lung density determination

Lung slides stained with H&E were used for lung density quantification. Pictures were taken on the Olympus Leica microscope at 200× magnification along the perimeter of each lung section. Using the Image J program (NIH, Bethesda, MD), image was changed to black and white pixels with black representing lung parenchyma and white open space. Approximately 20 to 26 pictures were taken per animal and Image J values averaged to determine total percentage of open space for oxygen exchange present in each animal. These scores are shown on scatter plots to reveal the variation between animals within each group. Pictures were also taken on the Leica microscope of vessels to assess perivascular infiltrate. These pictures were analyzed using Image J (NIH, Bethesda, MD) in the same manner and an average calculated for perivascular infiltrate density. 15 to 25 vessels were assessed for density of perivascular infiltrate per animal. Scatter plot was made separately of perivascular infiltrate density.

Immunohistochemistry: C3 and MAC (C5b-9) staining

Formalin-fixed paraffin sections of muscle, intestine, and lung were subjected to rehydration and antigen retrieval in a standard protocol. Staining was done for C3 (ABCAM Rabbit polyclonal to C3c) as well as for MAC/C5b-9 (Anti-complement C5b-9 rabbit polyclonal Ab, Calbiochem, La Jolla, CA). Control used was 1:10 rabbit IgG. Secondary antibody

employed was a Biotin JP conjugated Affinipure F(ab')₂ fragment donkey anti-rabbit IgG (H&L) (Jackson, Bar Harbor, ME). A Vector Nova Red kit (Vector NovaRED substrate kit (for peroxidase) SK-4800, Vector, Burlingame, CA) was used to develop the slides.

Immunofluorescence: C3 and GR-1 staining

Frozen section blocks were made of muscle, intestine, lung, liver, kidney, and spleen for each animal. Six-micrometer sections were cut using a cryostat. These sections were stained for C3 using directly conjugated FITC-C3 (ICN/Cappel fluorescein-conjugated goat F(ab')₂ fragment to mouse complement C3, Aurora, OH) with control antibody FITC-conjugated goat anti-human IgM (Cappel fluorescein-conjugated goat affinity purified F(ab')₂ fragment to human IgM (5FC μ), West Chester, PA). Slides were also stained with FITC-GR1 (FITC anti-mouse Ly-6G(GR1) and Ly-6C(RB6-8C5), Pharmingen) in a standard immunofluorescence protocol. Control used for GR-1 staining was FITC-conjugated IgG2α (FITC rat IgG2α, κ isotype control, Pharmingen).

Immunofluorescence: DAF staining

Frozen section blocks were made of muscle, intestine, lung, liver, kidney, and spleen tissues for each animal. Six-micrometer sections were cut using a cryostat. The sections were stained with biotinylated anti-human CD55/DAF antibody (R&D Systems, Minneapolis, MN) as a primary and streptavidin-PE as a fluorescence-conjugated secondary antibody. The mounting medium contained DAPI.

Quantification of immunofluorescence (C3, DAF deposits)

Multiple pictures were taken on the Olympus Leica microscope at 200× magnification of the fluorescent stained side and control side of each slide stained with anti-C3-FITC or anti-DAF antibody (and respective control antibodies). Four to six images were taken per animal. Images were then opened using the Adobe Photoshop program and adjusted until only fluorescent deposits and no background tissue was visible. Using the Image J program (NIH, Bethesda, MD), image was changed to black and white pixels with black representing deposits of C3 or DAF, and white representing nonstained areas of the image. Image was then changed to red and white, with fluorescent deposits in red, using the Image Adjust Threshold command. Finally, image was analyzed to give the total area in red (=fluorescent deposit area) in pixels squared. This number was entered into a Microsoft Excel spreadsheet for each animal and treatment group. Individual pictures for each animal slide of the control and fluorescent stained sections were analyzed and total area of fluorescent deposit (in pixels squared) for fluorescent side and control side was averaged to obtain an average value for each animal. Next, total area values for all animals in the DAF- and PBS-treated groups were averaged to give average area of fluorescent deposit for stained and control sides of each treatment group. These average values were graphed for comparison on the Graphpad Prism program.

Results

Effect of DAF on local hindlimb IR injury

Local skeletal muscle damage from 2-h occlusion of the femoral artery and vein followed by 3 h of reperfusion was assessed by grading histological skeletal muscle injury with a standard scoring system assigning an injury score of 0 to 4 for histological damage as previously published [8,9,53], which we modified to add one additional point for both edema and hemorrhage, for a maximum injury score of 6 per muscle sample. Local skeletal muscle injury from hindlimb ischemia appeared comparable following treatment of C57Bl/6 mice with DAF (2 μg per animal) 5 min prior to reperfusion (muscle injury score 2.75±1.71 versus 3.83±1.17 in C57Bl/6 mice, $p=0.286$, Mann–Whitney test, Fig. 1A). Scoring was repeated in transverse sections of muscle to confirm results with the same conclusion of comparable local muscle injury in PBS- and DAF-treated mice. Although the overall local injury of DAF- and PBS-treated animals was not appreciably different by grading, the quality of the injury was altered following treatment with DAF. It was noted that a larger percentage of muscle samples from DAF-treated mice showed significant edema on histology, rather than frank necrosis and muscle fiber destruction, which occur later in ischemic injury and were more prevalent in PBS-treated mice (Fig. 1B).

Immunohistochemistry as well as immunofluorescence confirmed C3 deposition in the skeletal muscle of all animals subjected to IR (Fig. 1C). Upon quantification, C3 deposits in local muscle, though less, were not significantly ($p>0.05$) different in DAF-treated animals when compared to PBS-treated vehicle controls (Fig. 2A). However, in DAF-treated animals no MAC deposition was seen on immunohistochemistry (Fig. 1C).

Treatment with DAF attenuates remote intestinal injury in the hindlimb model of skeletal muscle IR

With the finding that local injury was not significantly attenuated with DAF treatment, we assessed remote damage from hindlimb IR. C57Bl/6 mice treated with 2 μg/animal DAF 5 min prior to reperfusion exhibited reduced remote intestinal damage as assessed using a pathology score (Fig. 3A). DAF-treated mice had a mean pathology score of 1.19±0.22 compared to 2.39±0.73 for PBS-treated mice undergoing IR (Fig. 3A, $p=0.01$, Mann–Whitney test). Animals not exposed to skeletal muscle ischemia (sham) had a mean intestine pathology score of 0.396±0.15 (Fig. 3A). Intestinal injury in all animals was scattered, with areas of preserved, normal villi alternating with heavily damaged stretches of broken, denuded villi. Remote intestinal injury was subtle on H&E staining, but DAF-treated animals demonstrated fewer areas of extensive villus injury and disruption with more areas of mild villus injury compared to PBS-treated animals subjected to IR. C3 deposition was readily detectable by immunohistochemistry and immunofluorescence in all animals undergoing IR while no MAC deposition was noted in DAF-treated animals (Fig. 3B). Fluorescence quantification revealed less C3 deposition in intestines of DAF-treated animals than in the PBS-treated

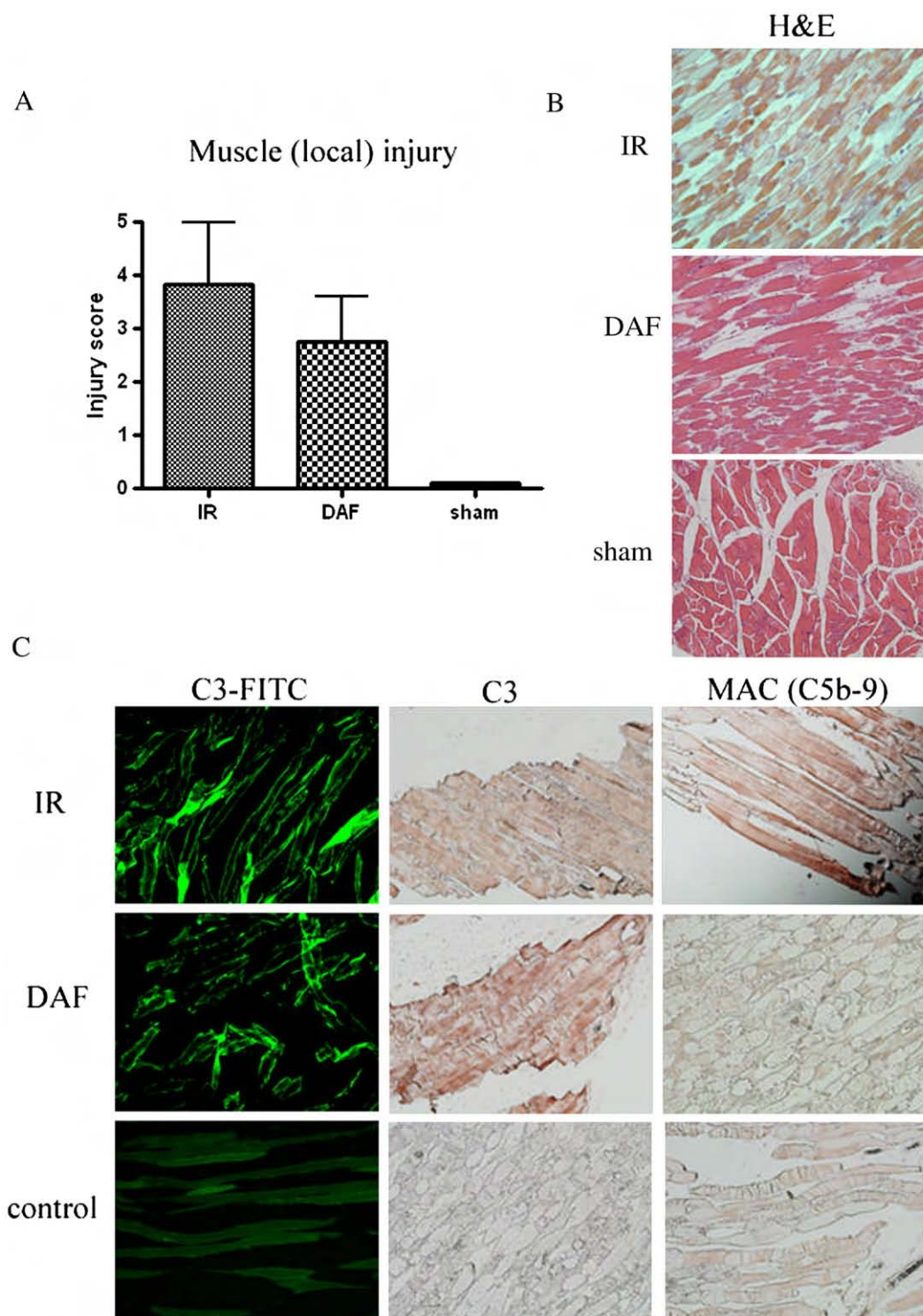


Figure 1 DAF treatment does not reduce significantly local skeletal muscle injury. (A) Cumulative local damage scores of mice subjected to hindlimb IR and treated with 2 μ g/animal DAF or 0.2 ml PBS 5 min prior to reperfusion ($n=12$, 4 separate experiments). Error bars represent standard deviations. (B) Representative H&E sections from DAF-treated, PBS-treated, and sham animals (C) Immunohistochemical and immunofluorescent detection of C3 and C5b-9 deposition in DAF- and PBS-treated mice.

control group, although the values did not reach statistical significance (Fig. 2B). C3 and DAF deposits colocalized on fluorescent stained sections of DAF-treated animals, while only C3 was deposited in intestines of PBS-treated animals exposed to IR.

Treatment with DAF attenuates remote lung injury in the hindlimb model of skeletal muscle IR

Remote lung injury is a hallmark of the systemic inflammatory response to reperfusion following an ischemic insult

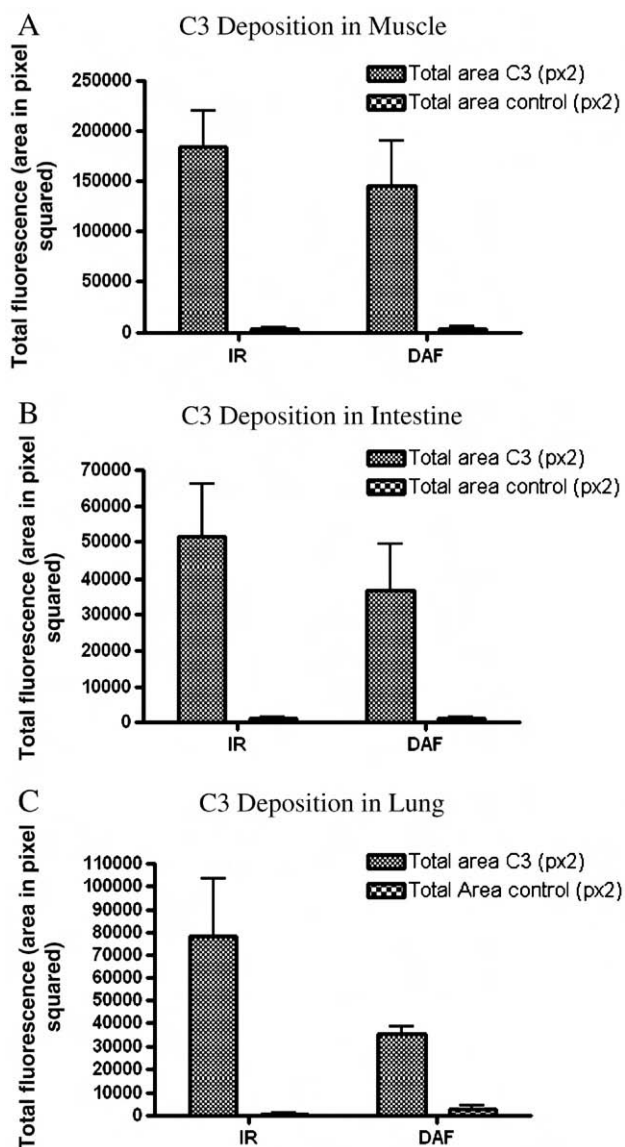


Figure 2 C3 deposition by fluorescence quantification in DAF- and PBS-treated animals following hindlimb IR. (A) C3 deposition in local muscle of DAF- and PBS-treated animals. Error bars represent standard deviations. (B) C3 deposition in remote intestine of DAF- and PBS-treated animals. Error bars represent standard deviations. (C) C3 deposition in remote lung of DAF- and PBS-treated animals. Error bars represent standard deviations.

[54–56]. Animals were subjected to hindlimb IR and administered DAF (2 $\mu\text{g}/\text{animal}$) or PBS (0.2 ml) 5 min prior to reperfusion. Lung damage was scored by assessing pneumonitis and perivascular infiltrates in H&E stained slides using a previously described grading system [52]. Total lung injury index in DAF-treated animals was 1.64 ± 2.00 versus 7.51 ± 2.14 for PBS-treated mice (Fig. 4A, $p=0.01$, Mann–Whitney test). H&E stained slides showed a clear decrease in consolidation and inflammatory damage in DAF-treated animals (Fig. 4B). As evidenced by the large standard deviation in both experimental groups, lung injury (like intestinal damage) was discontinuous, with an irregular distribution of spared and significantly damaged lung tissue

in the specimens scored. Comparison of pneumonitis scores with perivascular infiltrate scores in animals subjected to IR revealed marked reduction in both pneumonitis and perivascular infiltrate indices in DAF-treated mice compared to PBS-treated controls (1.50 ± 1.73 and 0.143 ± 0.29 versus 5.84 ± 1.93 and 1.66 ± 1.24 , respectively). Both pneumonitis and perivascular infiltrate scores were significantly reduced in DAF-treated animals ($p=0.02$ for pneumonitis, $p=0.02$ for perivascular infiltrate, Mann–Whitney test). Sham animals lacked any evidence of lung injury.

H&E slides from lungs of PBS-treated controls exposed to hindlimb IR showed visibly more parenchymal consolidation and less open alveolar space for oxygen exchange than lungs of both DAF-treated animals and sham animals (Fig. 4B). To quantify the difference apparent in histological sections, lung density calculations were carried out to provide another measure of remote damage from IR (Figs. 4C and D). Amount of open space was compared to space occupied by parenchymal lung tissue in H&E stained lung sections using the Image J program (see Materials and methods). Lung density in DAF-treated animals was less than that in both sham animals and PBS-treated vehicle controls exposed to IR, though there was wide variation between animals in all three groups (Figs. 4C and D).

While C3 deposition in the lungs of all animals exposed to IR was confirmed by immunohistochemistry and immunofluorescence, MAC was present only in animals treated with PBS and not in animals treated with DAF (Fig. 4E). C3 deposition in the lung was localized primarily to the endothelium of the lung vasculature (Fig. 4F). C3 deposits in the lung, when quantified, were less in the DAF group than in the PBS-treated group of animals, though the difference did not reach significance (Fig. 2C). Fluorescent staining revealed deposited DAF colocalized with C3 in lung endothelium of DAF-treated animals exposed to hindlimb IR, while animals administered PBS exhibited lung C3 deposits only (Fig. 6E).

DAF inhibits remote organ injury in the hindlimb model in a dose-dependent manner

In order to determine the *in vivo* effective dose at which inhibition of remote IR injury is achieved with DAF, C57Bl/6 mice were subjected to 2 h of hindlimb ischemia and administered PBS vehicle (0 μg DAF), 0.2 μg DAF, 2.0 μg DAF, or 20 μg DAF 5 min prior to reperfusion. As the titration curves for intestinal (Fig. 5A) and lung (Fig. 5B) IR injury demonstrate, the minimal effective dose at which significant attenuation of remote damage is seen appears to be 2 μg . There is little additional benefit in terms of reduction of injury scores seen after treatment with a dose 10 times larger (in the 20 μg DAF group).

Human DAF is deposited in murine tissues 10 min after i.v. injection

DAF staining of mouse tissues with biotinylated anti-human DAF antibody conjugated to fluorescence (see Materials and methods) was quantified using the Image J Program. As shown in Fig. 6, fluorescence quantification revealed DAF deposition in DAF-treated animals at both 10 min and 1 h after DAF injection (Fig. 6). We did not notice any DAF deposition in the

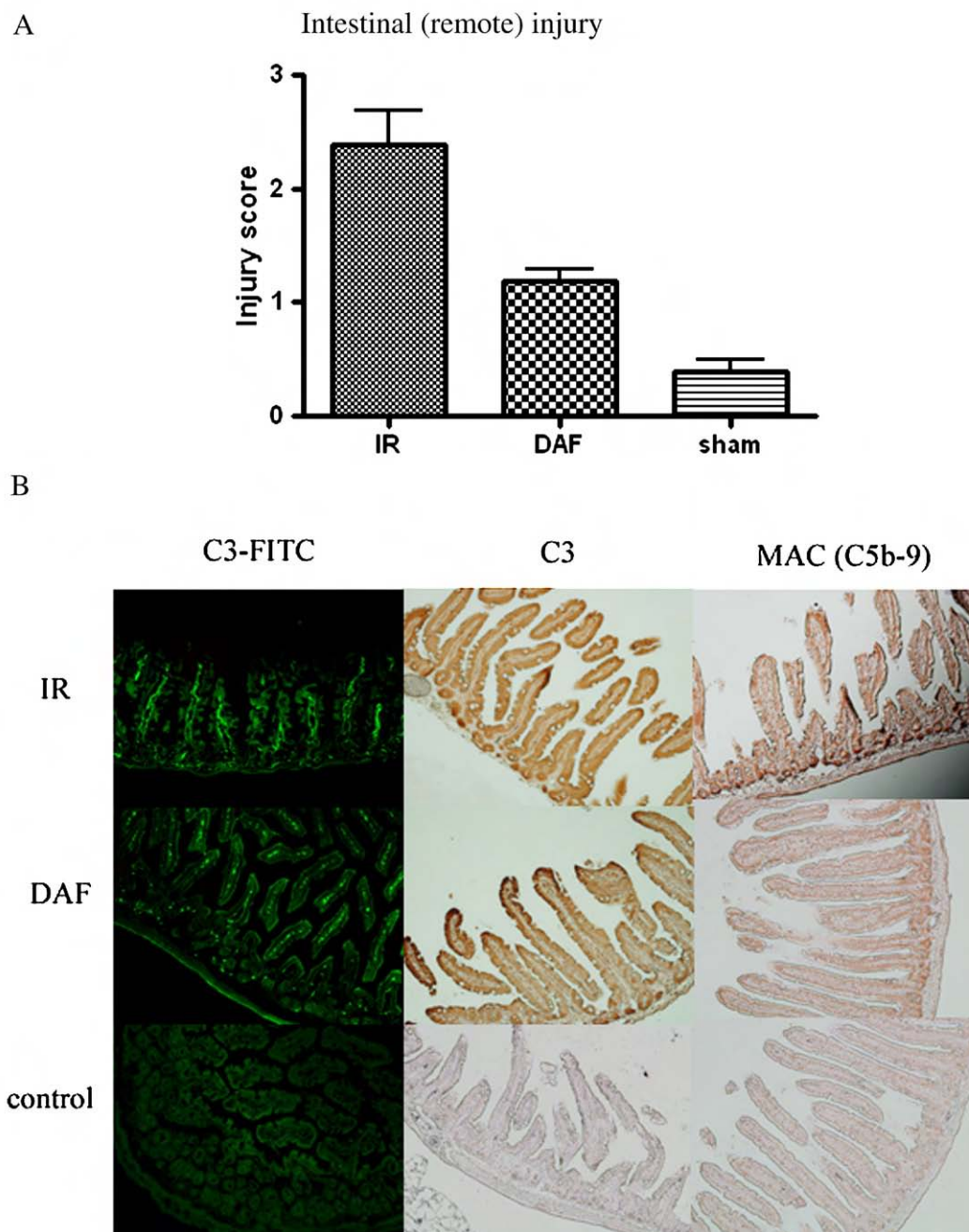


Figure 3 DAF treatment attenuates remote intestinal damage following hindlimb IR. (A) Composite intestinal injury score in PBS-treated, DAF-treated, and sham animals. Error bars represent standard deviations. (B) Immunohistochemical and immunofluorescent staining for C3 deposition and MAC (C5b-9) formation in PBS- and DAF-treated animals.

PBS-treated animals. DAF in sham animals was deposited in both lung and intestine at 10 min post-injection and was still visible at 1 h post-injection. In the lung, more DAF deposition was noted at 10 min post-injection than at 1 h, while DAF deposits in the intestine were greater at the 1-h time point than at 10 min (Fig. 6). Using ELISA we did not detect any circulating DAF at 10 min and 1 h post-injection (2 μ g dose, data not shown), suggesting that the majority of DAF injected is deposited in the tissues within 10 min.

Since DAF is likely upregulated in endogenous tissues with IR, use of a biotinylated anti-human DAF antibody in the

mouse was used to distinguish exogenously administered human DAF from murine DAF deposited in the membranes of tissues.

DAF treatment attenuates remote intestinal and lung IR damage without affecting local hindlimb skeletal muscle injury in B6.MRL/lpr mice

B6.MRL/lpr mice have been shown previously to exhibit increased mesenteric IR injury attributed to the presence of high titers of anti-DNA and anti-histone antibodies [15]. B6.

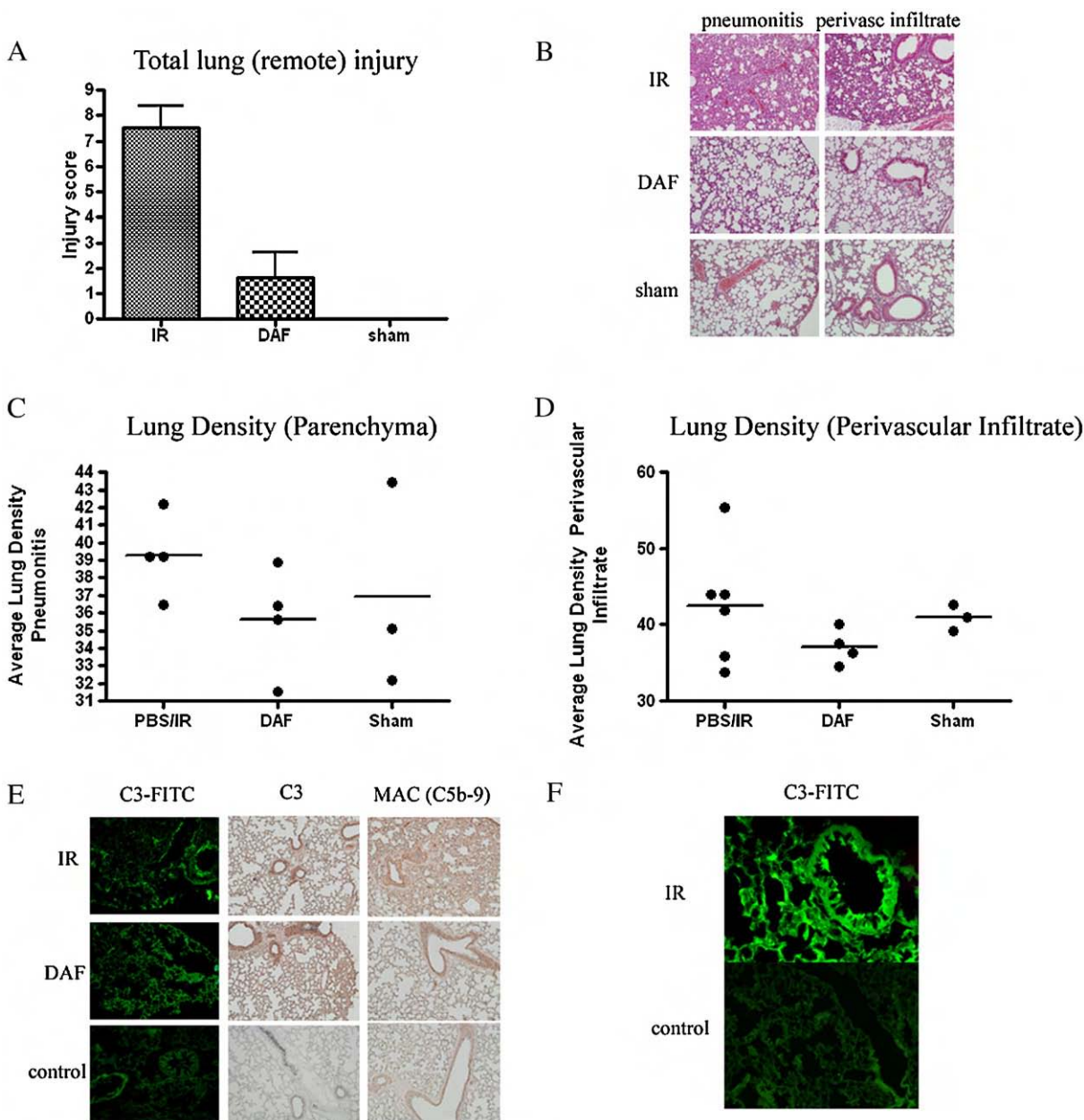


Figure 4 DAF treatment reduces remote lung injury. (A) Total average lung histological injury scores in PBS-treated, DAF-treated, and sham mice. Error bars represent standard deviations. (B) Representative H&E stained lung sections from treated, vehicle control, and sham animals. (C and D) Lung density measurements of pneumonitis and perivascular infiltrate in PBS-treated, DAF-treated, and sham mice. (E) C3 and MAC (C5b-9) deposition by immunohistochemistry and immunofluorescent staining. (F) C3 deposition on endothelium of lung vasculature by immunofluorescence (400 \times magnification).

MRL/*lpr* mice displayed comparable local skeletal muscle injury in response to hindlimb IR. Similar to C57Bl/6 mice, muscle damage scores in B6.MRL/*lpr* mice were comparable in DAF- and PBS-treated animals (muscle injury score 4.00 ± 0.0 versus 3.67 ± 0.52 respectively, Fig. 7A, $p=0.317$, Mann-Whitney test). This scoring was confirmed in transverse muscle sections of B6.MRL/*lpr* mice with similar local muscle injury seen in both PBS and DAF treatment groups. C3 deposits were confirmed by staining in all muscle samples from animals undergoing IR (Fig. 7B). MAC (C5b-9) staining was negative in animals treated with DAF but was positive in all other animals undergoing IR (Fig. 7B).

Intestinal pathology score in 5-month-old B6.MRL/*lpr* mice treated with DAF was 1.36 ± 0.56 compared to 3.04 ± 1.22 in PBS vehicle-treated animals, showing significant reduction in remote villus injury with DAF treatment (Fig. 8A, $p=0.01$, Mann-Whitney test). H&E sections from intestines of DAF-treated and PBS control mice demonstrated markedly reduced villus injury in DAF-treated animals (Fig. 8B). Intestines of DAF-treated animals on H&E stained slides were much closer in appearance to sham animal intestines than to their PBS control IR counterparts (Fig. 8B).

Total lung injury index was 6.63 ± 3.34 in DAF-treated animals compared to 9.69 ± 4.71 in PBS-treated mice,

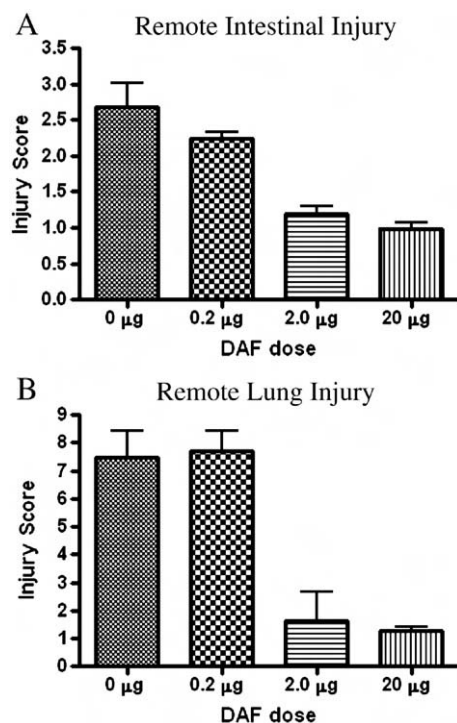


Figure 5 DAF attenuates remote IR injury in a dose-dependent manner. (A) Dose titration curve: intestinal IR injury scores of animals subjected to hindlimb IR and administered PBS vehicle, 0.2 µg DAF, 2.0 µg DAF, or 20 µg DAF 5 min prior to reperfusion. Error bars represent standard deviations. (B) Dose titration curve: lung IR injury scores of animals subjected to hindlimb IR and administered PBS vehicle, 0.2 µg DAF, 2.0 µg DAF, and 20 µg DAF 5 min prior to reperfusion. Error bars represent standard deviations.

indicating a trend towards attenuated injury that did not reach significance due to large differences between lung injury scores in each treatment group in the autoimmune animals (Fig. 9A, $p=0.28$, Mann–Whitney test). H&E stained sections showed slightly less consolidation and perivascular infiltrate in the DAF-treated animals, but again the injury scores do not reach significance since scores between animals range widely within each treatment group ($p=0.13$ for pneumonitis, $p=0.617$ for perivascular infiltrate, Mann–Whitney test). Similarly, lung density calculations were widely variable in the B.6MRL/*lpr* mice and did not exhibit statistically significant difference between treatment groups.

As demonstrated previously, C3 deposition was seen by immunohistochemical and immunofluorescent staining in all animals undergoing IR, while MAC (C5b-9) staining was only positive in animals not undergoing DAF treatment and exposed to IR (Figs. 8C and 9C).

Effect of DAF treatment on mesenteric IR local and remote injury

Next, we used mesenteric IR to determine whether the beneficial effect of soluble DAF extended to an additional model of IR injury. The superior mesenteric artery (SMA) was clamped for 30 min followed by 2 h of reperfusion; 2 µg/

animal DAF or 0.2 ml PBS was administered 5 min prior to reperfusion. Average intestine injury score was 2.18 ± 0.56 in DAF-treated mice compared to 2.94 ± 0.14 in PBS-treated animals (Fig. 10A, $n=14$, $p=0.05$, Mann–Whitney test). As in the hindlimb experiments, local injury was not drastically affected by DAF treatment. In contrast, we noted marked reduction in remote lung injury (total lung injury index of 14.5 ± 0.89 in PBS-treated mice compared to 3.43 ± 2.48 in DAF-treated animals, Fig. 10B, $p=0.01$, Mann–Whitney test). Pneumonitis and perivascular infiltrate scores were also much reduced in animals treated with DAF (2.24 ± 1.59 versus 8 ± 1.73 for pneumonitis, 1.18 ± 0.92 versus 6.52 ± 1.68 for perivascular infiltrate, $p=0.01$ for both pneumonitis and perivascular infiltrate, Mann–Whitney test). Finally, lung density calculations demonstrating decreased pneumonitis and perivascular infiltrate in DAF-treated mice provided further support for attenuated overall remote lung damage (Figs. 10C and D).

DAF treatment does not increase susceptibility to infection

Because we saw evidence that DAF treatment limits C5b-9 formation but permits C3 deposition in both local and remote organs after IR, we asked whether DAF treatment compromises resistance to infection. This question was addressed using the CLP model of polymicrobial sepsis in a survival study [21]. The CLP model has long been used to study sepsis as a result of controlled peritoneal contamination and hematogenous dissemination of a significant bacterial load [57,58].

Mice subjected to CLP and treated with DAF showed no significant difference in survival when compared to their PBS-treated counterparts (Fig. 11A, $p=0.48$, log rank test, $n=89$). Most animals succumbed to sepsis and death within 48 h, while a few mice in each group survived beyond this critical initial period. One mouse in the DAF group and one in the PBS group even survived to the chosen endpoint of 10 days (240 h). Mice treated with cobra venom factor (CVF), which depletes animals of C3, did not survive past 48 h, with most dying in the initial 24 h postoperative. Because this protocol exposes animals to a significant initial bacterial load, possibly eliminating subtle differences between groups subjected to various modalities of complement inhibition with an overwhelming septic insult, we repeated CLP experiments with the addition of a normal saline abdominal rinse prior to abdominal closure. In this experiment ($n=21$), survival curves separated in the initial 48 h postoperative (Fig. 11B). No CVF animals in this experiment survived more than 32 h. Again, no significant difference was seen between survival curves of PBS and DAF animals in this smaller group of animals (Fig. 11B, $p=0.29$, log test, $n=18$).

Discussion

We present evidence that treatment of C57Bl/6 mice exposed to hindlimb skeletal muscle or mesenteric IR with soluble human DAF results in significantly reduced remote organ injury with mild effect on local skeletal muscle or local intestinal damage. Similarly, treatment of B.6MRL/*lpr* mice subjected to hindlimb IR with soluble human DAF resulted in significant attenuation of remote organ injury.

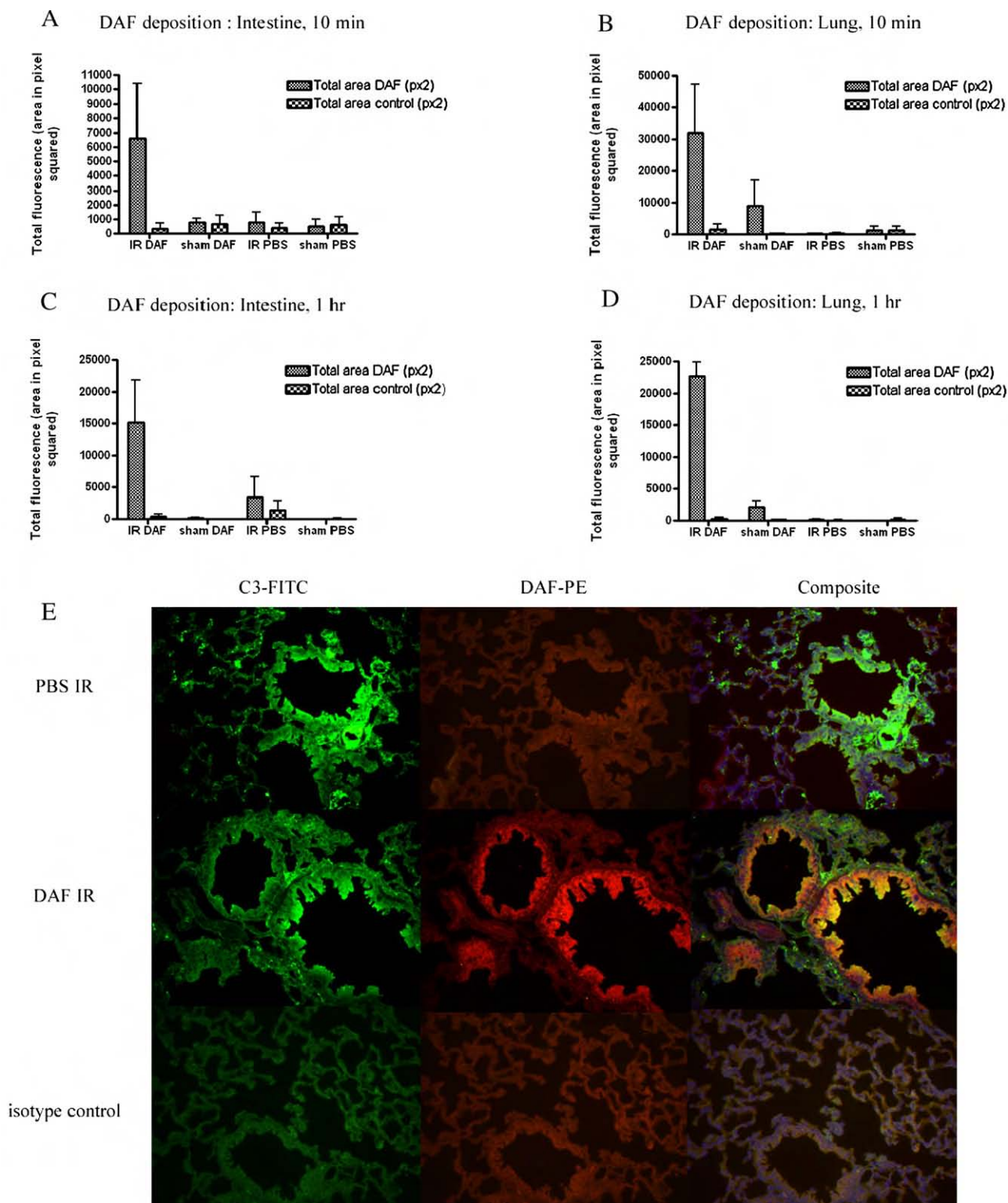


Figure 6 DAF is deposited in remote intestine and lung of DAF-treated animals following hindlimb IR. DAF deposits are visible at both 10 min and 1 h post-injection. All error bars represent standard deviations. (A) Fluorescence quantification: area of DAF deposition in intestines of animals following hindlimb IR, 10 min after injection. (B) Fluorescence quantification: area of DAF deposition in lungs of animals following hindlimb IR, 10 min after injection. (C) Fluorescence quantification: area of DAF deposition in intestines of animals following hindlimb IR, 1 h after injection. (D) Fluorescence quantification: area of DAF deposition in lungs of animals following hindlimb IR, 1 h after injection. (E) C3-FITC, DAF-PE, and composite stained (C3-FITC, DAF-PE, and DAPI) representative lung sections from PBS- and DAF-treated animals compared to isotype controls. C3 staining (green) is present in both PBS and DAF animals with DAF staining (red) only in the DAF-treated group. Simultaneous DAF and C3 deposits (yellow) are present on the endothelium of vessels in the lungs of DAF-treated animals.

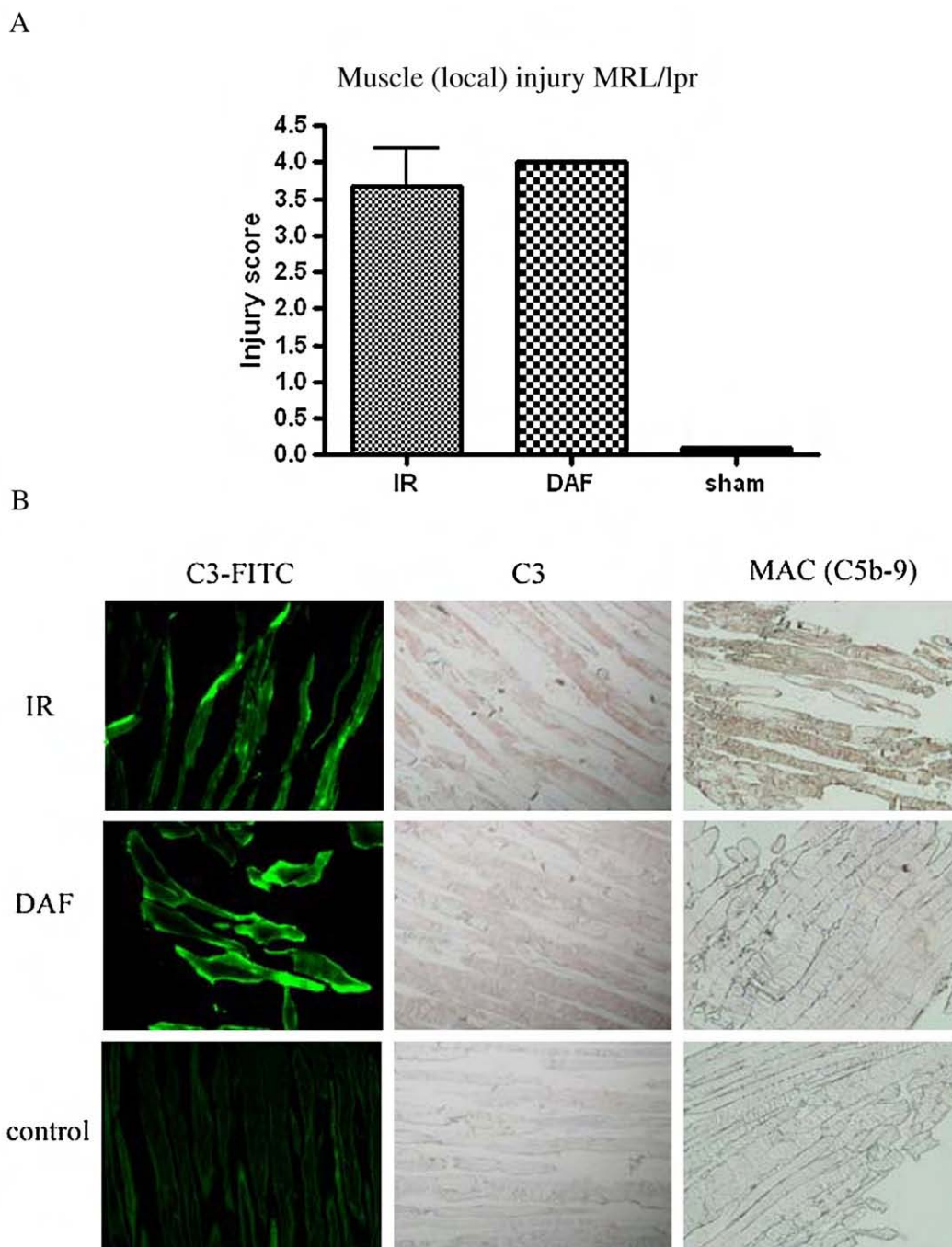


Figure 7 DAF treatment does not affect local muscle injury in autoimmune phenotype B6.MRL/*lpr* mice. (A) Local composite muscle injury scores in PBS treated, DAF-treated, and sham mice ($n=5$ separate experiments). Error bars represent standard deviations. (B) C3 and MAC (C5b-9) staining by immunohistochemistry and immunofluorescence in MRL mice treated with PBS or DAF.

Both intestinal and hindlimb models of ischemia–reperfusion have been demonstrated to involve the binding of natural antibodies with diverse specificities [12–14,16] to ischemia-conditioned tissues followed by activation of complement, resulting in further tissue damage. Complement activation leads to generation of anaphylatoxins C3a and C5a, which are thought to contribute to the development of remote organ injury. Accordingly, multiple complement activation inhibitors have been used to limit both local and remote organ damage. C1 inhibitor, functioning at the

earliest steps of the classical and mannose binding lectin (MBL) pathways while at the same time inhibiting coagulation factors XIa and XIIa, kallikrein, and plasma and tissue-type plasminogen activators [59], has been shown to attenuate complement-induced IR injury in multiple animal models. These models include skeletal muscle IR [60,61] and mesenteric IR [17] in mice, liver IR in rats, and myocardial IR in rabbits [62], cats [63], and pigs [64]. In addition, soluble CR1 [2–6], Crry-Ig [21], anti-C5 antibodies [17,18], and C5a receptor antagonists [19,20,65] have all displayed

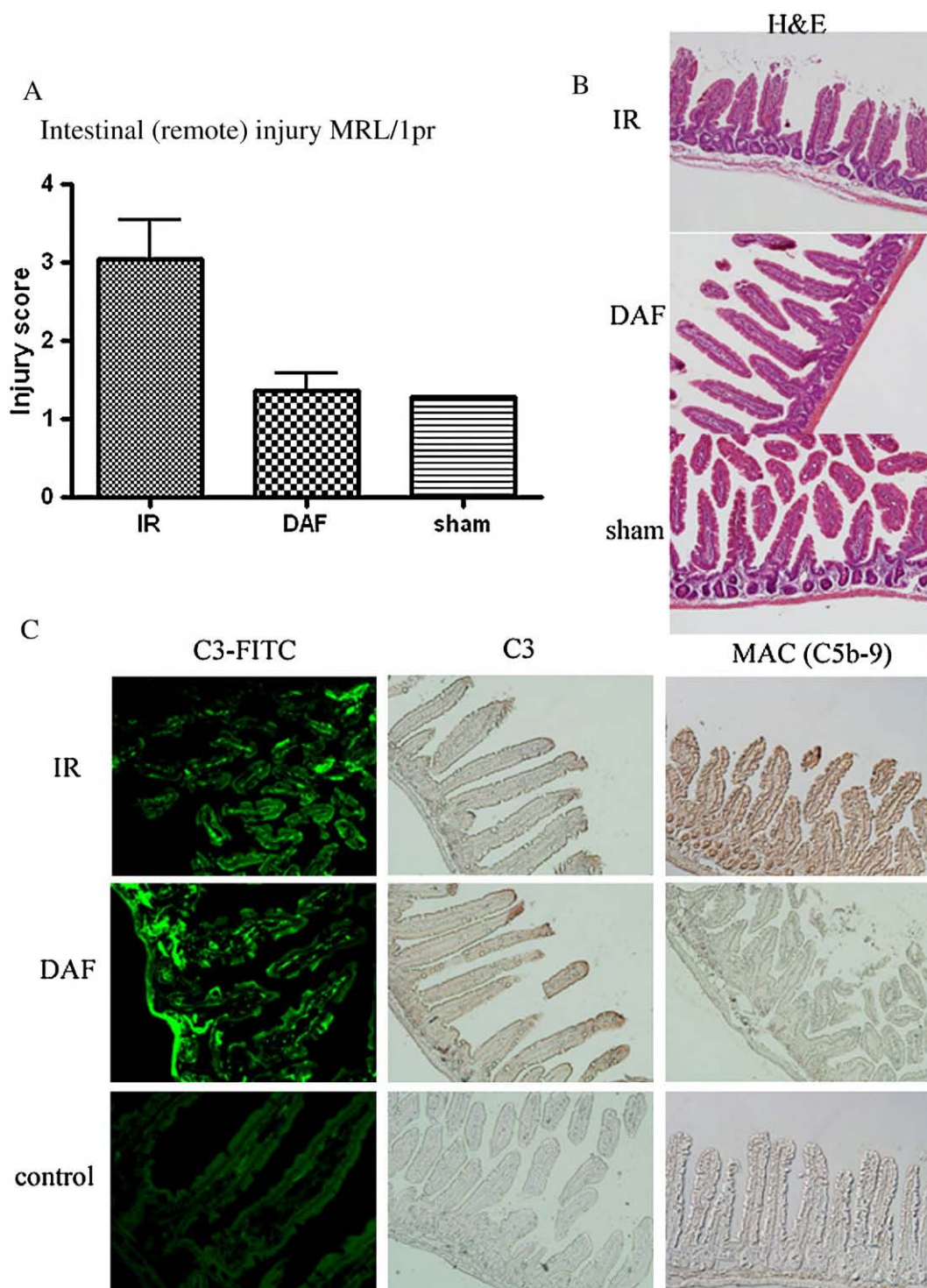


Figure 8 DAF treatment reduces significantly remote intestinal injury in B6.MRL/lpr mice. (A) Average intestinal injury scores in B6.MRL/lpr mice. Error bars represent standard deviations. (B) H&E stained representative sections of intestine from MRL/lpr mice administered 2 μ g/animal DAF or 0.2 ml PBS 5 min prior to reperfusion compared to sham animals. (C) C3 and MAC deposition by immunohistochemical and immunofluorescent staining in the intestines of DAF-treated and PBS vehicle-treated mice.

therapeutic effect on IR injury. Inflammatory inhibitors such as carboxypeptidase R have proven beneficial as well in limiting severity of anaphylatoxin-mediated damage [66]. However, all of these agents demonstrate potential to impair innate resistance to infection by systemically

inhibiting complement and weakening host defense. Those agents targeting early events in complement activation, including C1 inhibitor and sCR1, threaten to increase susceptibility to infection by the same means successfully employed to attenuate IR injury—a potent anti-inflammatory

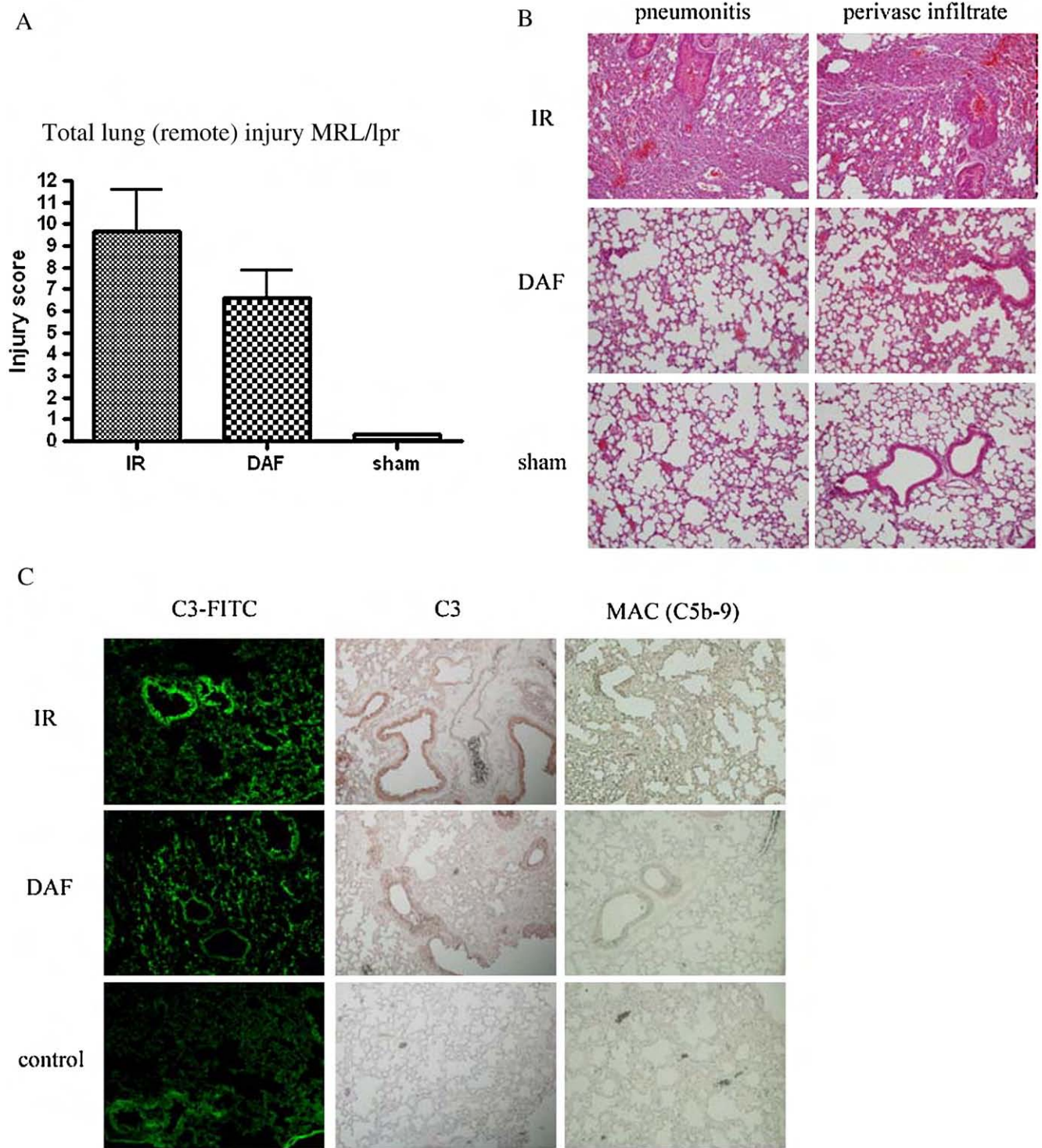


Figure 9 Effect of DAF treatment on remote lung injury in B6.MRL/*lpr* mice. (A) Average total lung histological injury scores for each treatment group of MRL mice. Error bars represent standard deviations. (B) Representative H&E lung sections from DAF-treated, PBS-treated, and sham animals. (C) Immunohistochemical and immunofluorescent detection of C3 and MAC (C5b-9) deposition in lungs of DAF- and PBS-treated mice.

effect. The ability to mount an immune response should be preserved by targeting the complement amplification loop rather than initial activation of all complement.

DAF is a GPI-anchored complement regulatory protein inhibiting formation of C3 and C5 convertases on host cell

membranes and rapidly dissociating any assembled C3/C5 convertase on cell surfaces, thereby limiting progression of the C3b/C5b-initiated terminal complement cascade [22,28,67]. Clinical use of DAF to limit complement activation-mediated tissue damage was first attempted in

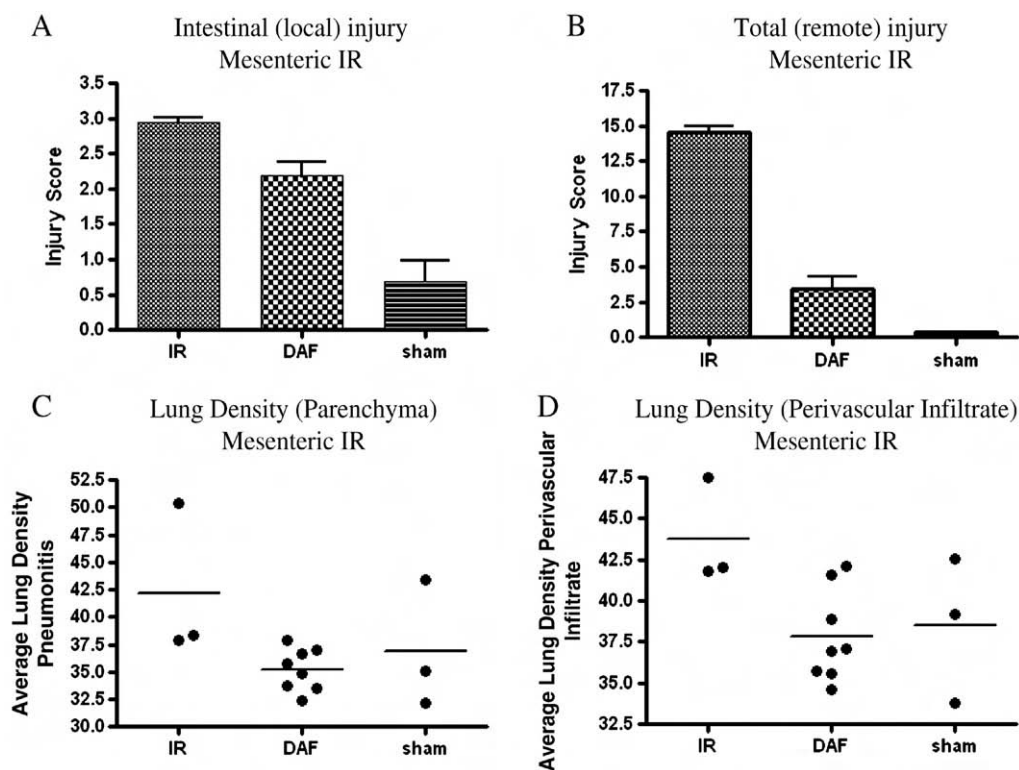


Figure 10 DAF attenuates both local intestinal damage and remote lung injury in the mesenteric IR model. (A) Composite local intestinal injury scores of PBS-treated, DAF-treated, and sham animals subjected to 30 min of intestinal ischemia and 2 h of reperfusion ($n=14$, 3 separate experiments). Error bars represent standard deviations. (B) Average total lung injury index of PBS-treated, DAF-treated, and sham animals. Error bars represent standard deviations. (C and D) Lung density measurements of pneumonitis and perivascular infiltrate in PBS-treated, DAF-treated, and sham mice undergoing mesenteric IR.

xenotransplantation to prevent hyperacute rejection of organs due to preformed host natural antibodies [38–42]. Human DAF has been studied clinically mainly in the context of paroxysmal nocturnal hemoglobinuria (PNH), a disease in which its absence along with the absence of CD59, another GPI-anchored complement regulatory protein, leads to increased susceptibility of human erythrocytes to complement-mediated destruction [67–72].

DAF expression on the surface membrane limits complement activation; processes that engage complement, as predicted, appear to be exacerbated when the *DAF* gene is eliminated. Specifically, *DAF*^{-/-} mice suffer more severe renal IR [42] and nephrotoxic serum-induced nephritis [35]. Absence of the *DAF* gene increases severity of both organ-specific autoimmune disease, such as experimental autoimmune encephalomyelitis [36], and systemic autoimmune disease, such as the skin disease that develops in the MRL/*lpr* mouse [73]. A recent report that T cells lacking DAF display enhanced T cell responses [37] may explain why the above autoimmune processes, both known to be T-cell-dependent, manifest exacerbated damage in the absence of DAF.

The C3 and C5 convertases on which DAF exercises its regulatory influence have been termed the “amplifying enzymes” of the complement cascade [33]. By targeting the amplification loop of the systemic inflammatory response, DAF significantly reduces remote organ damage from IR. Previous published work has shown that once incorporated into the membrane, DAF functions mainly to prevent

convertase assembly rather than to dissociate already assembled convertases, and that it can function only intrinsically [33]. Our results reveal that DAF is significantly deposited in remote organs (lung, intestine) by 10 min post-injection, and that DAF continues to be present in the tissues for at least 1 h post-injection. In this way, DAF incorporated into the cell membrane of remote tissues precludes assembly of C3 and C5 convertases, limiting the amount of anaphylatoxins C3a and C5a produced following enzymatic cleavage. C3 deposition occurs in both DAF- and PBS-treated animals, with subsequent complement activation and damage at the local injury site that is not notably affected by DAF treatment. Action of DAF at the amplification loop of the cascade inhibits remote damage preferentially over local injury. This may occur by multiple mechanisms—membrane incorporation of DAF and limitation of convertase formation, reduced anaphylatoxin release, suppression of T cell effector response, and decreased neutrophil migration and cytokine release downstream. The failure of DAF to attenuate local injury significantly in our results stands in contrast to those agents acting early in the complement cascade, such as C1 inhibitor and sCR1, which protect against local IR injury as well as remote damage, at the likely expense of preservation of immune resistance.

The dose of 2 μg DAF used in these experiments was confirmed to be the minimum effective dose using dose titration experiments in the hindlimb model. Though significantly less than the 75 μg dose necessary to inhibit the

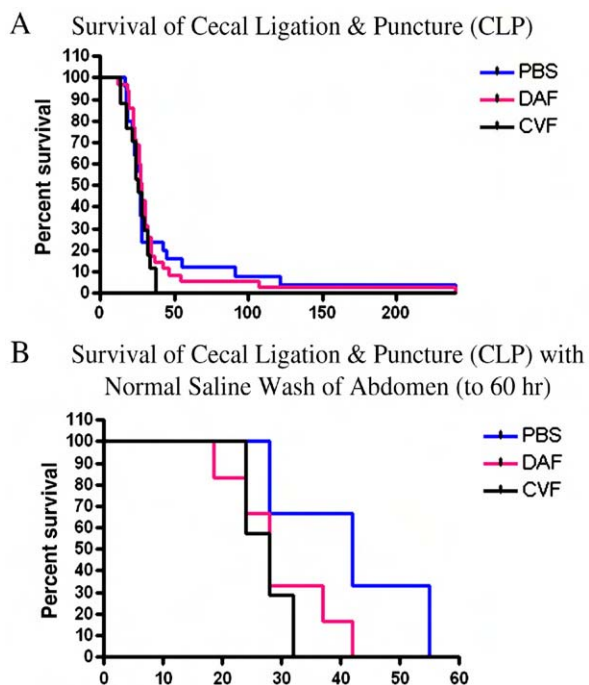


Figure 11 DAF-treated animals demonstrate comparable susceptibility to infection compared to PBS controls. (A) Kaplan–Meier survival curves in mice subjected to cecal ligation and puncture in the CLP model of polymicrobial sepsis ($n=89$ animals, 6 separate experiments). (B) Kaplan–Meier survival curves in the first 60 h postoperative when the abdomen is rinsed with normal saline after cecal ligation and puncture and prior to abdominal closure ($n=21$ animals, 1 experiment).

reverse passive Arthus reaction (RPAR) in rats, this difference in the effective dose can be attributed to already recognized variation in dose ranges among species [74], and to the fact that the RPAR can be compared to local damage rather than remote injury from systemic inflammation (and local injury was not significantly reduced with DAF). In other published work, doses of rsCD46 greater than or equal to 2.2 μg per site were shown to inhibit the RPAR in rats, and rsCD35 showed effect in the RPAR at only 0.3 μg per site [74]. From our DAF ELISA and DAF deposition data, it seems that although DAF has a very short half life in circulation, with quantities too low for detection by ELISA 10 min after injection, DAF is still deposited in remote organs at 10 min post-injection and remains incorporated into the membranes of remote organs and exerting its inhibitory effect at 1 h post-injection. Published work has shown that only a small number of incorporated DAF molecules (<100) have a marked effect on hemolytic activity in vitro [33]. Though human DAF appears to be less effective on mouse complement than it is on complement of humans and rats [75], its effect on C3 and C5 convertases is potent enough to strikingly reduce remote IR damage while preserving immune resistance.

Since deposited DAF acts intrinsically [33] to prevent convertase assembly and to dissociate already formed complexes on the membrane in which it is incorporated [76], it is not surprising that DAF exerts minimal systemic effect on hemolysis in the CH50 assay 10 min after injection (data not shown). Our staining reveals deposited DAF

colocalized with C3 in remote organ membranes at 10 min and 2 h after injection in DAF-treated animals exposed to hindlimb IR (Fig. 6). Local DAF inhibitory activity on remote organ membranes is critical despite DAF's short serum half life, and the lack of sustained systemic complement inhibition at the 2 μg dose of DAF preserves immune resistance to infection as shown in the CLP sepsis model (Fig. 11). By exerting its intrinsic inhibitory effect, deposited DAF preferentially binds catalytically active convertases [77] in addition to limiting local convertase assembly [33]. DAF is more stable and active on membrane-associated complement complexes [76,77]; once incorporated, it appears to function to prevent that amplification of the complement cascade which results in systemic IR damage.

The data presented herein establish the clinical value of soluble DAF in preventing remote organ injury from IR. Soluble DAF limited remote organ injury in two distinct models of IR, hindlimb skeletal muscle and mesenteric IR, in two mouse species, normal C57Bl/6 mice and autoimmune B6.MRL/lpr mice. This preclinical information suggests strongly that human soluble DAF can be used in surgical and medical conditions known to be associated with complement-mediated remote lung and intestinal injury following ischemia, hemorrhage, resuscitation and organ transplantation.

Acknowledgments

We would like to thank Dr. Michael Zidanic for his assistance with microscopy and Dr. Bob Burge for his help with statistical analysis.

References

- [1] J.H. Hill, P.A. Ward, The phlogistic role of C3 leukotactic fragments in myocardial infarcts of rats, *J. Exp. Med.* 133 (1971) 885–900.
- [2] H.F. Weisman, T. Bartow, M.K. Leppo, H.C. Marsh Jr., G.R. Carson, M.F. Concino, M.P. Boyle, K.H. Roux, M.L. Weisfeldt, D.T. Fearon, Soluble human complement receptor type 1: in vivo inhibitor of complement suppressing post-ischemic myocardial inflammation and necrosis, *Science* 249 (1990) 146–151.
- [3] A.T. Eror, A. Stojadinovic, B.W. Starnes, S.C. Makrides, G.C. Tsokos, T. Shea-Donohue, Antiinflammatory effects of soluble complement receptor type 1 promote rapid recovery of ischemia/reperfusion injury in rat small intestine, *Clin. Immunol.* 90 (1999) 266–275.
- [4] J. Huang, L.J. Kim, R. Mealey, H.C. Marsh Jr., Y. Zhang, A.J. Tenner, E.S. Connolly Jr., D.J. Pinsky, Neuronal protection in stroke by an sLex-glycosylated complement inhibitory protein, *Science* 285 (1999) 595–599.
- [5] P.J. Chai, R. Nassar, A.E. Oakeley, D.M. Craig, G. Quick Jr., J. Jagers, S.P. Sanders, R.M. Ungerleider, P.A. Anderson, Soluble complement receptor-1 protects heart, lung, and cardiac myofilament function from cardiopulmonary bypass damage, *Circulation* 101 (2000) 541–546.
- [6] J. Hill, T.F. Lindsay, F. Ortiz, C.G. Yeh, H.B. Hechtman, F.D. Moore Jr., Soluble complement receptor type 1 ameliorates the local and remote organ injury after intestinal ischemia–reperfusion in the rat, *J. Immunol.* 149 (1992) 1723–1728.
- [7] H. Zhao, M.C. Montalto, K.J. Pfeiffer, L. Hao, G.L. Stahl, Murine model of gastrointestinal ischemia associated with complement-dependent injury, *J. Appl. Physiol.* 93 (2002) 338–345.
- [8] M.R. Weiser, J.P. Williams, F.D. Moore Jr., L. Kobzik, M. Ma, H.B. Hechtman, M.C. Carroll, Reperfusion injury of ischemic

- skeletal muscle is mediated by natural antibody and complement, *J. Exp. Med.* 183 (1996) 2343–2348.
- [9] J.P. Williams, T.T. Pechet, M.R. Weiser, R. Reid, L. Kobzik, F.D. Moore Jr., M.C. Carroll, H.B. Hechtman, Intestinal reperfusion injury is mediated by IgM and complement, *J. Appl. Physiol.* 86 (1999) 938–942.
- [10] S.D. Fleming, T. Shea-Donohue, J.M. Guthridge, L. Kulik, T.J. Waldschmidt, M.G. Gipson, G.C. Tsokos, V.M. Holers, Mice deficient in complement receptors 1 and 2 lack a tissue injury-inducing subset of the natural antibody repertoire, *J. Immunol.* 169 (2002) 2126–2133.
- [11] R.R. Reid, S. Woodcock, A. Shimabukuro-Vornhagen, W.G. Austen Jr., L. Kobzik, M. Zhang, H.B. Hechtman, F.D. Moore Jr., M.C. Carroll, Functional activity of natural antibody is altered in Cr2-deficient mice, *J. Immunol.* 169 (2002) 5433–5440.
- [12] M. Zhang, W.G. Austen Jr., I. Chiu, E.M. Alicot, R. Hung, M. Ma, N. Verna, M. Xu, H.B. Hechtman, F.D. Moore Jr., M.C. Carroll, Identification of a specific self-reactive IgM antibody that initiates intestinal ischemia/reperfusion injury, *Proc. Natl. Acad. Sci. U. S. A.* 101 (2004) 3886–3891.
- [13] W.G. Austen Jr., M. Zhang, R. Chan, D. Friend, H.B. Hechtman, M.C. Carroll, F.D. Moore Jr., Murine hindlimb reperfusion injury can be initiated by a self-reactive monoclonal IgM, *Surgery* 136 (2004) 401–406.
- [14] M. Zhang, E.M. Alicot, I. Chiu, J. Li, N. Verna, T. Vorup-Jensen, B. Kessler, M. Shimaoka, R. Chan, D. Friend, U. Mahmood, R. Weissleder, F.D. Moore, M.C. Carroll, Identification of the target self-antigens in reperfusion injury, *J. Exp. Med.* 203 (2006) 141–152.
- [15] S.D. Fleming, M. Monestier, G.C. Tsokos, Accelerated ischemia/reperfusion-induced injury in autoimmunity-prone mice, *J. Immunol.* 173 (2004) 4230–4235.
- [16] S.D. Fleming, R.P. Egan, C. Chai, G. Girardi, V.M. Holers, J. Salmon, M. Monestier, G.C. Tsokos, Anti-phospholipid antibodies restore mesenteric ischemia/reperfusion-induced injury in complement receptor 2/complement receptor 1-deficient mice, *J. Immunol.* 173 (2004) 7055–7061.
- [17] G. Karpel-Massler, S.D. Fleming, M. Kirschfink, G.C. Tsokos, Human C1 esterase inhibitor attenuates murine mesenteric ischemia/reperfusion induced local organ injury, *J. Surg. Res.* 115 (2003) 247–256.
- [18] K. Wada, M.C. Montalto, G.L. Stahl, Inhibition of complement C5 reduces local and remote organ injury after intestinal ischemia/reperfusion in the rat, *Gastroenterology* 120 (2001) 126–133.
- [19] T.V. Arumugam, I.A. Shiels, A.J. Strachan, G. Abbenante, D.P. Fairlie, S.M. Taylor, A small molecule C5a receptor antagonist protects kidneys from ischemia/reperfusion injury in rats, *Kidney Int.* 63 (2003) 134–142.
- [20] B. de Vries, J. Kohl, W.K. Leclercq, T.G. Wolfs, A.A. van Bijnen, P. Heeringa, W.A. Buurman, Complement factor C5a mediates renal ischemia–reperfusion injury independent from neutrophils, *J. Immunol.* 170 (2003) 3883–3889.
- [21] C. Atkinson, H. Song, B. Lu, F. Qiao, T.A. Burns, V.M. Holers, G. C. Tsokos, S. Tomlinson, Targeted complement inhibition by C3d recognition ameliorates tissue injury without apparent increase in susceptibility to infection, *J. Clin. Invest.* 115 (2005) 2444–2453.
- [22] P. Lukacik, P. Roversi, J. White, D. Esser, G.P. Smith, J. Billington, P.A. Williams, P.M. Rudd, M.R. Wormald, D.J. Harvey, M.D. Crispin, C.M. Radcliffe, R.A. Dwek, D.J. Evans, B.P. Morgan, R.A. Smith, S.M. Lea, Complement regulation at the molecular level: the structure of decay-accelerating factor, *Proc. Natl. Acad. Sci. U.S.A.* 101 (2004) 1279–1284.
- [23] S. Lea, Interactions of CD55 with non-complement ligands, *Biochem. Soc. Trans.* 30 (2002) 1014–1019.
- [24] M.E. Medof, D.M. Lublin, V.M. Holers, D.J. Ayers, R.R. Getty, J.F. Leykam, J.P. Atkinson, M.L. Tykocinski, Cloning and characterization of cDNAs encoding the complete sequence of decay-accelerating factor of human complement, *Proc. Natl. Acad. Sci. U. S. A.* 84 (1987) 2007–2011.
- [25] A. Herbert, J. O’leary, M. Krych-Goldberg, J.P. Atkinson, P.N. Barlow, Three-dimensional structure and flexibility of proteins of the RCA family – a progress report, *Biochem. Soc. Trans.* 30 (2002) 990–996.
- [26] T. Miwa, W.C. Song, Membrane complement regulatory proteins: insight from animal studies and relevance to human diseases, *Int. Immunopharmacol.* 1 (2001) 445–459.
- [27] P. Williams, Y. Chaudhry, I.G. Goodfellow, J. Billington, R. Powell, O.B. Spiller, D.J. Evans, S. Lea, Mapping CD55 function. The structure of two pathogen-binding domains at 1.7 Å, *J. Biol. Chem.* 278 (2003) 10691–10696.
- [28] D.D. Kim, W.C. Song, Membrane complement regulatory proteins, *Clin. Immunol.* 118 (2006) 127–136.
- [29] W.C. Song, Membrane complement regulatory proteins in autoimmune and inflammatory tissue injury, *Curr. Dir. Autoimmun.* 7 (2004) 181–199.
- [30] W.C. Song, M.R. Sarrias, J.D. Lambris, Complement and innate immunity, *Immunopharmacology* 49 (2000) 187–198.
- [31] W.G. Brodbeck, C. Mold, J.P. Atkinson, M.E. Medof, Cooperation between decay-accelerating factor and membrane cofactor protein in protecting cells from autologous complement attack, *J. Immunol.* 165 (2000) 3999–4006.
- [32] T.J. Kroshus, C.T. Salerno, C.G. Yeh, P.J. Higgins, R.M. Bolman III, A.P. Dalmaso, A recombinant soluble chimeric complement inhibitor composed of human CD46 and CD55 reduces acute cardiac tissue injury in models of pig-to-human heart transplantation, *Transplantation* 69 (2000) 2282–2289.
- [33] M.E. Medof, T. Kinoshita, V. Nussenzweig, Inhibition of complement activation on the surface of cells after incorporation of decay-accelerating factor (DAF) into their membranes, *J. Exp. Med.* 160 (1984) 1558–1578.
- [34] V.M. Holers, T. Kinoshita, H. Molina, The evolution of mouse and human complement C3-binding proteins: divergence of form but conservation of function, *Immunol. Today* 13 (1992) 231–236.
- [35] H. Sogabe, M. Nangaku, Y. Ishibashi, T. Wada, T. Fujita, X. Sun, T. Miwa, M.P. Madaio, W.C. Song, Increased susceptibility of decay-accelerating factor deficient mice to anti-glomerular basement membrane glomerulonephritis, *J. Immunol.* 167 (2001) 2791–2797.
- [36] J. Liu, T. Miwa, B. Hilliard, Y. Chen, J.D. Lambris, A.D. Wells, W.C. Song, The complement inhibitory protein DAF (CD55) suppresses T cell immunity in vivo, *J. Exp. Med.* 201 (2005) 567–577.
- [37] P.S. Heeger, P.N. Lalli, F. Lin, A. Valujskikh, J. Liu, N. Muqim, Y. Xu, M.E. Medof, Decay-accelerating factor modulates induction of T cell immunity, *J. Exp. Med.* 201 (2005) 1523–1530.
- [38] I. Shimizu, N.R. Smith, G. Zhao, E. Medof, M. Sykes, Decay-accelerating factor prevents acute humoral rejection induced by low levels of anti- α Gal natural antibodies, *Transplantation* 81 (2006) 95–100.
- [39] Y.T. Ghebremariam, S.A. Smith, J.B. Anderson, D. Kahn, G.J. Kotwal, Intervention strategies and agents mediating the prevention of xenorejection, *Ann. N. Y. Acad. Sci.* 1056 (2005) 123–143.
- [40] D.M. Lublin, Review: Cromer and DAF: role in health and disease, *Immunohematology* 21 (2005) 39–47.
- [41] C.A. Verbakel, S. van Duikeren, R.W. de Bruin, R.L. Marquet, J.N. IJzermans, Human decay-accelerating factor expressed on rat hearts inhibits leukocyte adhesion, *Transpl. Int.* 16 (2003) 168–172.
- [42] K. Yamada, T. Miwa, J. Liu, M. Nangaku, W.C. Song, Critical protection from renal ischemia reperfusion injury by CD55 and CD59, *J. Immunol.* 172 (2004) 3869–3875.
- [43] H. Schafer, D. Mathey, F. Hugo, S. Bhakdi, Deposition of the terminal C5b-9 complement complex in infarcted areas of human myocardium, *J. Immunol.* 137 (1986) 1945–1949.
- [44] S.R. Robert-Offerman, M.P. Leers, R.J. van Suylen, M. Nap, M.J.

- Daemen, P.H. Theunissen, Evaluation of the membrane attack complex of complement for the detection of a recent myocardial infarction in man, *J. Pathol.* 191 (2000) 48–53.
- [45] J.W. Homeister, P. Satoh, B.R. Lucchesi, Effects of complement activation in the isolated heart. Role of the terminal complement components, *Circ. Res.* 71 (1992) 303–319.
- [46] W.G. Austen Jr., C. Kyriakides, J. Favuzza, Y. Wang, L. Kobzik, F.D. Moore Jr., H.B. Hechtman, Intestinal ischemia–reperfusion injury is mediated by the membrane attack complex, *Surgery* 126 (1999) 343–348.
- [47] S.D. Fleming, D. Mastellos, G. Karpel-Massler, T. Shea-Donohue, J.D. Lambris, G.C. Tsokos, C5a causes limited, polymorphonuclear cell-independent, mesenteric ischemia/reperfusion-induced injury, *Clin. Immunol.* 108 (2003) 263–273.
- [48] K.S. Kilgore, J.L. Park, E.J. Tanhehco, E.A. Booth, R.M. Marks, B.R. Lucchesi, Attenuation of interleukin-8 expression in C6-deficient rabbits after myocardial ischemia/reperfusion, *J. Mol. Cell. Cardiol.* 30 (1998) 75–85.
- [49] W. Ito, H.J. Schafer, S. Bhakdi, R. Klask, S. Hansen, S. Schaarschmidt, J. Schofer, F. Hugo, T. Hamdoch, D. Mathey, Influence of the terminal complement-complex on reperfusion injury, no-reflow and arrhythmias: a comparison between C6-competent and C6-deficient rabbits, *Cardiovasc. Res.* 32 (1996) 294–305.
- [50] W. Zhou, C.A. Farrar, K. Abe, J.R. Pratt, J.E. Marsh, Y. Wang, G.L. Stahl, S.H. Sacks, Predominant role for C5b-9 in renal ischemia/reperfusion injury, *J. Clin. Invest.* 105 (2000) 1363–1371.
- [51] E. Lupia, L. Del Sorbo, S. Bergerone, G. Emanuelli, G. Camussi, G. Montrucchio, The membrane attack complex of complement contributes to plasmin-induced synthesis of platelet-activating factor by endothelial cells and neutrophils, *Immunology* 109 (2003) 557–563.
- [52] K.R. Cooke, L. Kobzik, T.R. Martin, J. Brewer, J. Delmonte Jr., J.M. Crawford, J.L. Ferrara, An experimental model of idiopathic pneumonia syndrome after bone marrow transplantation: I. The roles of minor H antigens and endotoxin, *Blood* 88 (1996) 3230–3239.
- [53] R.K. Chan, G. Ding, N. Verna, S. Ibrahim, S. Oakes, W.G. Austen Jr., H.B. Hechtman, F.D. Moore Jr., IgM binding to injured tissue precedes complement activation during skeletal muscle ischemia–reperfusion, *J. Surg. Res.* 122 (2004) 29–35.
- [54] M.M. Yassin, D.W. Harkin, A.A. Barros D’Sa, M.I. Halliday, B.J. Rowlands, Lower limb ischemia–reperfusion injury triggers a systemic inflammatory response and multiple organ dysfunction, *World J. Surg.* 26 (2002) 115–121.
- [55] C. Mukundan, M.F. Gurish, K.F. Austen, H.B. Hechtman, D.S. Friend, Mast cell mediation of muscle and pulmonary injury following hindlimb ischemia–reperfusion, *J. Histochem. Cytochem.* 49 (2001) 1055–1056.
- [56] C. Kyriakides, J. Favuzza, Y. Wang, W.G. Austen Jr., F.D. Moore Jr., H.B. Hechtman, Recombinant soluble P-selectin glycoprotein ligand 1 moderates local and remote injuries following experimental lower-torso ischaemia, *Br. J. Surg.* 88 (2001) 825–830.
- [57] S. Maier, T. Traeger, M. Entleutner, A. Westerholt, B. Kleist, N. Huser, B. Holzmann, A. Stier, K. Pfeffer, C.D. Heidecke, Cecal ligation and puncture versus colon ascendens stent peritonitis: two distinct animal models for polymicrobial sepsis, *Shock* 21 (2004) 505–511.
- [58] W. Tao, D.J. Deyo, D.L. Traber, W.E. Johnston, E.R. Sherwood, Hemodynamic and cardiac contractile function during sepsis caused by cecal ligation and puncture in mice, *Shock* 21 (2004) 31–37.
- [59] M. Kirschfink, Targeting complement in therapy, *Immunol. Rev.* 180 (2001) 177–189.
- [60] E.W. Nielsen, T.E. Mollnes, J.M. Harlan, R.K. Winn, C1-inhibitor reduces the ischaemia–reperfusion injury of skeletal muscles in mice after aortic cross-clamping, *Scand. J. Immunol.* 56 (2002) 588–592.
- [61] D. Inderbitzin, G. Beldi, I. Avital, G. Vinci, D. Candinas, Local and remote ischemia–reperfusion injury is mitigated in mice overexpressing human C1 inhibitor, *Eur. Surg. Res.* 36 (2004) 142–147.
- [62] M. Buerke, H. Schwertz, W. Seitz, J. Meyer, H. Darius, Novel small molecule inhibitor of C1s exerts cardioprotective effects in ischemia–reperfusion injury in rabbits, *J. Immunol.* 167 (2001) 5375–5380.
- [63] M. Buerke, T. Murohara, A.M. Lefer, Cardioprotective effects of a C1 esterase inhibitor in myocardial ischemia and reperfusion, *Circulation* 91 (1995) 393–402.
- [64] G. Horstick, A. Heimann, O. Gotze, G. Hafner, O. Berg, P. Boehmer, P. Becker, H. Darius, H.J. Rupperecht, M. Loos, S. Bhakdi, J. Meyer, O. Kempfski, Intracoronary application of C1 esterase inhibitor improves cardiac function and reduces myocardial necrosis in an experimental model of ischemia and reperfusion, *Circulation* 95 (1997) 701–708.
- [65] T.V. Arumugam, T.M. Woodruff, S.Z. Stocks, L.M. Proctor, S. Pollitt, I.A. Shiels, R.C. Reid, D.P. Fairlie, S.M. Taylor, Protective effect of a human C5a receptor antagonist against hepatic ischaemia–reperfusion injury in rats, *J. Hepatol.* 40 (2004) 934–941.
- [66] William Campbell, Noriko Okada, Hidechika Okada, Carboxypeptidase R is an inactivator of complement-derived inflammatory peptides and an inhibitor of fibrinolysis, *Immunol. Rev.* 180 (2001) 162–167 (Ref Type: Generic).
- [67] D.M. Lublin, J.P. Atkinson, Decay-accelerating factor: biochemistry, molecular biology, and function, *Annu. Rev. Immunol.* 7 (1989) 35–58.
- [68] A. Nicholson-Weller, J.P. March, S.I. Rosenfeld, K.F. Austen, Affected erythrocytes of patients with paroxysmal nocturnal hemoglobinuria are deficient in the complement regulatory protein, decay accelerating factor, *Proc. Natl. Acad. Sci. U. S. A.* 80 (1983) 5066–5070.
- [69] M.K. Pangburn, R.D. Schreiber, H.J. Muller-Eberhard, Deficiency of an erythrocyte membrane protein with complement regulatory activity in paroxysmal nocturnal hemoglobinuria, *Proc. Natl. Acad. Sci. U. S. A.* 80 (1983) 5430–5434.
- [70] W.F. Rosse, C.J. Parker, Paroxysmal nocturnal haemoglobinuria, *Clin. Haematol.* 14 (1985) 105–125.
- [71] A. Nicholson-Weller, J. Burge, D.T. Fearon, P.F. Weller, K.F. Austen, Isolation of a human erythrocyte membrane glycoprotein with decay-accelerating activity for C3 convertases of the complement system, *J. Immunol.* 129 (1982) 184–189.
- [72] C.J. Parker, Historical aspects of paroxysmal haemoglobinuria: ‘defining the disease’, *Br. J. Haematol.* 117 (2002) 3–22.
- [73] T. Miwa, M.A. Maldonado, L. Zhou, X. Sun, H.Y. Luo, D. Cai, V.P. Werth, M.P. Madaio, R.A. Eisenberg, W.C. Song, Deletion of decay-accelerating factor (CD55) exacerbates autoimmune disease development in MRL/lpr mice, *Am. J. Pathol.* 161 (2002) 1077–1086.
- [74] Dale Christiansen, Julie Milland, Bruce R. Thorley, Ian F.C. McKenzie, Bruce E. Loveland, A functional analysis of recombinant soluble CD46 in vivo and a comparison with recombinant soluble forms of CD55 and CD35 in vitro, *Eur. J. Immunol.* 26 (1996) 578–585.
- [75] C.L. Harris, O.B. Spiller, B.P. Morgan, Human and rodent decay-accelerating factors (CD55) are not species restricted in their complement inhibiting activities, *Immunology* 100 (2000) 462–470.
- [76] M.K. Pangburn, Differences between the binding sites of the complement regulatory proteins DAF, CR1, and factor H on C3 convertases, *J. Immunol.* 136 (1986) 2216–2221.
- [77] C.L. Harris, R.J. Abbott, R.A. Smith, B.P. Morgan, S.M. Lea, Molecular dissection of interactions between components of the alternative pathway of complement and decay accelerating factor (CD55), *J. Biol. Chem.* 280 (2005) 2569–2578.

Decay-Accelerating Factor Attenuates C-Reactive Protein-Potentiated Tissue Injury After Mesenteric Ischemia/Reperfusion

Xinyue Lu, M.D., Ph.D.,* Yansong Li, M.D.,* Milomir O. Simovic, M.D.,* Russell Peckham, M.D.,* Ying Wang, M.D.,* George C. Tsokos, M.D.,† and Jurandir J. Dalle Lucca, M.D., Ph.D.*¹

*Division of Military Casualty Research, Walter Reed Army Institute of Research, Silver Spring, Maryland; and †Department of Medicine, Beth Israel Deaconess Medical Center, Harvard Medical School, Boston, Massachusetts

Submitted for publication June 24, 2009

Background. C-reactive protein (CRP) is an acute pro-inflammatory mediator that has been demonstrated to enhance ischemia/reperfusion (IR) injury by virtue of activating the complement system. CRP is able to interact with complement proteins such as C1q, complement factor H, and C4b-binding protein. Since complement activation is central in the expression of tissue injury following IR, we have investigated the effects of human decay-accelerating factor (DAF), a complement inhibitor, on CRP-potentiated complement activation and tissue injury in mice subjected to mesenteric IR.

Materials and Methods. Male C57B1/6 mice were allocated into eight groups: (1) Sham-operated group without IR injury; (2) CRP+Sham group; (3) IR group; (4) CRP+IR group; (5) DAF group; (6) CRP+DAF group; (7) IR+DAF group, and (8) CRP+IR+DAF group. Intestinal and lung injury, neutrophil infiltration, myeloperoxidase (MPO) expression, complement component deposition, and interleukin-6 (IL-6) production were assessed for each treatment group of mice.

Results. We report that administration of DAF significantly attenuates the CRP-enhanced intestinal injury as well as remote lung damages following acute mesenteric IR in mice, while DAF inhibits complement activation, suppresses neutrophil infiltration, and reduces IL-6 production.

Conclusions. Our study suggests that inhibition complement activation with DAF may prove useful for the treatment of post-ischemic inflammatory in-

juries associated with an increased production of CRP. Published by Elsevier Inc.

Key Words: complement; C-reactive protein; inflammation; rodent; mesenteric ischemia.

INTRODUCTION

Ischemia/reperfusion (IR) represents a model of tissue injury in which circulation is reinstalled in an organ transiently deprived of blood flow. The ischemic insult alters the affected tissue making it susceptible to inflammatory damage during reperfusion. Furthermore, mediators produced in the ischemic areas diffuse when circulation is restored causing inflammation in remote organs not exposed to ischemia [1]. Several molecular and cellular mechanisms have been implicated in IR. These include mainly elements of the innate immune response, such as reactive oxygen species, cytokines, and chemokines, complement, natural antibodies, and neutrophils [1]. More recently, elements of the adaptive immune response have been shown to play significant roles. Specifically, T [2] and B cells [3] have been shown to be directly involved in the expression of tissue injury and depletion of either T or B cells prior to mesenteric IR limit both local and remote tissue injury. Complement (C) activation and neutrophil stimulation represent two major pathogenetic processes of IR-induced organ dysfunction, and local and remote tissue injury [4, 5]. Suppression of the C activities either by C inhibitors or in C-deficient animals has been demonstrated to attenuate tissue injury in various IR animal models. Studies which have demonstrated that C inhibition reduces IR tissue injury in various organs, including myocardium [6], lung [7], liver [8], intestine [9], kidney [10], and skeletal muscle

¹ To whom correspondence and reprint requests should be addressed at Division of Military Casualty Research, Walter Reed Army Institute of Research, 503 Robert Grant Ave. Room 1A32, Silver Spring, MD 20910 E-mail: jurandir.dallelucca@us.army.mil.



[9], clearly identify the C system as a promising therapeutic target.

C-reactive protein (CRP), an acute phase reactant, which can increase in the blood plasma up to 1000-fold following inflammation, infection, or tissue injury in patients and animals, is part of the innate system as well as the C [11]. Unlike humans, CRP is not an acute-phase protein in mice [12, 13]. Accordingly, administration of human CRP to mice is a good model to study its functions. Mesenteric IR in rats induced endogenous CRP expression, and its deposition correlated with the deposition of C3, suggesting a role for CRP in the C activation [14]. We have reported that exogenous human CRP augments intestinal injury in a C-dependent manner in murine model of mesenteric IR [15]. These results suggest that CRP augmented IR-induced gut injury is strongly associated with C activation, and therefore implicate that C regulatory proteins or inhibitors would reduce tissue injury enhanced by CRP.

Decay-accelerating factor (DAF), a ubiquitously expressed intrinsic C-regulatory protein, is a glycosylphosphatidylinositol (GPI)-anchored membrane associated C regulatory protein, and is known to protect host tissue from autologous C activation. DAF contains four short consensus repeats (SCR) for binding CD97 and C3, C5 convertases and a heavily O-glycosylated region rich in serine and threonine. DAF inhibits C activation at the C3 and C5 convertase levels after binding to the convertases through its SCR2, SCR3, and SCR4 in both of classic and alternative C pathways, thereby limiting local C3a/C5a and subsequent blocking C5b-9 (MAC) production [16, 17].

We have shown that soluble human DAF attenuates local intestinal and remote lung injury in mice subjected to mesenteric IR [18]. Since human and rodent DAFs are not species restricted in their complement-inhibiting activity [19], we hypothesized that IR animals treated with human DAF would down-regulate human CRP-amplified C activity and effectively ameliorate tissue injury induced by mesenteric IR. We report in this study that CRP potentiates IR-triggered intestinal injury as well as remote lung damage, whereas the treatment with human DAF remarkably attenuates the CRP-induced injury *via* inhibition of complement activation and cytokine release. Our work supports the concept of utilizing C inhibitor as a therapeutic approach for IR related injury.

MATERIALS AND METHODS

Mouse Mesenteric IR Model

Research was conducted in compliance with the Animal Welfare Act and other Federal statutes and regulations relating to animals and experiments involving animals, and adhered to principles stated in the Guide for the Care and Use Laboratory Animals. All procedures were reviewed and approved by the Institute's Animal Care and

Use Committee, and performed in a facility accredited by the Association for Assessment and Accreditation of Laboratory Animal Care, International. Male C57Bl/6 mice, aged 8 to 12 wk (Jackson Laboratory, Bar Harbor, ME) underwent at least 7-d acclimatization prior to experimentation.

Purified, sodium azide-free human CRP was obtained from US Biological (Swampscott, MA) and diluted to working concentrations in Tris-buffered saline (TBS, 10 mM Tris, 15 mM NaCl, 2 mM CaCl₂). To confirm purity, 1 and 5 μ g of CRP were loaded on SDS-PAGE gel followed by using Silver and Coomassie Blue staining, which revealed a single 24 kD band. Endotoxin was not detectable (<0.03 EU/mL) in aliquots of CRP solution (1 mg/mL) as measured with Limulus Amebocyte Lysate Test Kit (Cambrex, East Rutherford, NJ).

Mice were assigned to the following experimental groups: (1) Sham (control, TBS injection, without mesenteric IR); (2) CRP+Sham; (3) IR; (4) CRP+IR; (5) DAF; (6) CRP+DAF; (7) IR+DAF, and (8) CRP+IR+DAF ($n = 5-8$ mice/group). Briefly, a midline laparotomy was performed followed by a 30-min equilibration period. The superior mesenteric artery was isolated and a small nontraumatic vascular clamp (Roboz Surgical Instruments, Gaithersburg, MD) was applied for 30 min. After this ischemic phase the clamp was removed, the laparotomy incisions were sutured and the intestine was reperused for 2 h. Two hours prior to surgery, animals were injected i.p. with 0.25 mg/animal of purified human CRP or an equivalent volume of sterile TBS. Mice were anesthetized with ketamine (16 mg/kg) and xylazine (8 mg/kg) injected by i.p. All procedures were performed with the animal breathing spontaneously and maintained on 37 °C water-circulating heating pad. Animals were subjected to mesenteric I/R as previously described [20]. For DAF treatment, 5 min prior to reperfusion, mice were injected with either 2 μ g per animal DAF (rhCD55/DAF; R and D Systems, Minneapolis, MN) or 0.2 mL sterile saline *via* tail vein injection. Mice were under anesthesia during the experiment and before euthanasia.

Serum and Tissue Collection and Preparation

Blood samples were collected by cardiac puncture at the time of euthanasia. Serum was separated immediately and stored at -80 °C for later analysis. After euthanasia the small intestine and lung specimens were removed, and each organ collected was immediately divided into three fractions, one was stored at -80 °C, the others were separately fixed in 10% buffered formalin phosphate and 4% paraformaldehyde.

The 4% paraformaldehyde-fixed tissues were washed twice (5 min each) in cold PBS, then sunk into 20% sucrose in PBS on a rocker in 4 °C-cold room for 2 h. The tissues were embedded in Tissue Tek Cryomold Standard Vinyl Specimen Disposable mold with Tissue Tek O.C.T compound (Sakura Finetek USA, Inc., Torrance, CA), and frozen on dry-ice. The frozen blocks were stored at -80 °C until section cut. Frozen blocks were cut at 5- μ m sections using a cryostat and mounted on poly-L-lysine-coated slides.

Histopathology and Immunohistochemistry

The 10% formalin-fixed tissues were embedded in paraffin, sectioned at 5 μ m transversely, and stained with hematoxylin and eosin (H & E). For each intestinal section, at least 50 villi were graded on a six-tiered scale for mucosal damage score and the mean score was recorded as described previously [21]. A score of 0 was assigned to a normal villus; villi with tip distortion were scored as 1; villi lacking goblet cells and containing Gugenheim's spaces were scored as 2; villi with patchy disruption of the epithelial cells were scored as 3; villi with exposed but intact lamina propria and epithelial cell sloughing were assigned a score of 4; villi in which the lamina propria was exuding were scored as 5; and villi displaying hemorrhage or denuded villi were scored as 6. All histologic analysis was performed in a blinded manner.

Severity of lung injury was scored in a method described by Nishina *et al.* [22]. Briefly, lung was scored by using a 5-point scale according to combined assessments of alveolar congestion, hemorrhage,

infiltration or aggregation of neutrophils in airspace or vessel wall, and thickness of alveolar wall/hyaline membrane formation: 0 = normal, 1 = minimum damage, 2 = mild damage, 3 = moderate damage, 4 = severe damage, and 5 = maximum damage. Pictures were taken on the Olympus Leica microscope at 400× magnification along the perimeter of each lung section.

Frozen slides were dried at room temperature, then fixed in cold acetone for 5–10 min. After another air-dry for 30 min, slides were washed with PBS and blocked for 30 min with 2.5% bovine serum albumin solution in PBS. Slides were then incubated with various primary antibodies (goat anti-mouse C3 IgG; MP Biomedical LLC, Solon, OH; rat anti-mouse C5a; BD Biosciences, San Jose, CA; rabbit anti-complement C5b-9 polyclonal Ab; Calbiochem, La Jolla, CA; goat anti-human DAF/CD55, R and D Systems, Minneapolis, MN; rat anti-mouse IL-6, Beckman Coulter, Fullerton, CA; rat anti-mouse neutrophils; AbD Serotec, Raleigh NC; rabbit anti-CD32; Santa Cruz Biotechnology, Santa Cruz, CA) at 1:100–1:1000 dilution for 60 min. Slides were incubated with appropriate secondary antibodies for 1 h (donkey anti-goat IgG-Alexa 488, Donkey anti-rabbit IgG-Alexa 594, goat anti-rat IgG-Alexa 594 secondary antibodies, Invitrogen, Carlsbad, CA). Finally, slides were mounted with ProLong Gold antifade, counterstained with DAPI (4',6'-diamidino-2-phenylindole; Invitrogen, Carlsbad, CA), and observed under a confocal laser scanning microscope (Radiance 2100; Bio-Rad, Hercules, CA). Recorded digital images were processed using Image J software (NIH Bethesda, MD).

Western Blotting

Extracted proteins (20 ~ 50 µg) from frozen intestinal and lung tissue were separated in SDS-PAGE and transferred onto a polyvinylidene difluoride membrane (Pierce, Rockford IL). The membranes were blocked with 5% nonfat dry milk in TBST buffer for 1 h, and then incubated with primary antibodies (chicken anti-mouse C3/C3a; AbD Serotec, Raleigh NC; goat anti-mouse C5/C5a; Quidel, San Diego; CA; rabbit anti-rat C9; gift from Dr. B. Paul Morgan; goat anti-mouse MPO; R and D Systems, Minneapolis, MN) at 1:1000–1:2000 dilution for 1 h, followed by incubation with appropriate HRP-conjugated secondary Abs (goat anti-chicken IgY-HRP; AbD Serotec, Raleigh NC; donkey anti-goat IgG-HRP, goat anti-rabbit IgG-HRP; Santa Cruz Biotechnology, Santa Cruz, CA;) at 1:000–1:3000 dilution for 1 h. Specific bands were visualized by an ECL method (Amersham Biosciences, Piscataway, NJ) and captured with Fujifilm LAS-3000 System Configured for Chemiluminescence (Fujifilm Life Science, Edison, NJ). The density of each band was measured using QuantityOne Software (Bio-Rad).

ELISA

The serum concentrations of exogenous human CRP and endogenous mouse interleukin-6 (IL-6) were determined by an ultra-sensitive human-CRP specific enzyme-linked immunosorbent assay (ELISA) (Diagnostic Systems Laboratories, Webster TX) and a mouse IL-6 ELISA kit (eBioscience, San Diego, CA), respectively, according to the manufacturer's protocols.

Statistical Analysis

Data were expressed as mean ± SD unless otherwise stated. The two-tailed *t*-test or one-way ANOVA with Tukey's *post-hoc* test were performed using GraphPad Prism ver. 4 (GraphPad Software, San Diego, CA). *P* value < 0.05 was considered as significant.

RESULTS

DAF Prevents Enhanced Local Intestinal IR Injury Due to CRP

Our recent study showed that CRP administration (250–1000 µg/mouse) amplified the mesenteric

IR-induced intestinal damage [15]. In this study, we pretreated mice with human CRP (250 µg/mouse, i.p.) at 2.5 h prior to ischemia. The concentrations of human CRP in murine sera were monitored at 30 min after of the occlusion of mesenteric artery, and 2 h after reperfusion using human CRP-specific ELISA kit. No significant differences were found in serum CRP levels in the CRP-sham (33.55 ± 5.24 µg/mL, *n* = 7) and CRP-IR (37.79 ± 8.13 µg/mL, *n* = 8) groups. Human CRP was not detected in animals without treatment of CRP.

Human DAF deposition in the intestinal and lung tissue was determined by specific immunostaining in DAF-treated mice due to its characteristic binding to membrane. We noticed a marked deposition of DAF in the gut and lung tissue in DAF-treated animals 2 h after injection, whereas DAF was not detected in the tissues of mice which did not receive DAF (unpublished results).

The mucosal damage induced by IR in various *t* groups was assessed histologically by H and E staining and microscopic observation using an established scale. As demonstrated in Fig. 1A and B, IR-induced intestinal injury was enhanced in animals that received human CRP. The injury score was 2.61 ± 0.42 in the CRP+IR group compared with 1.88 ± 0.08 in the IR group (*P* < 0.001). Treatment with DAF (2 µg/mouse, i.v., 5 min prior to reperfusion) not only reduced the damage induced by IR (the DAF+IR: 1.43 ± 0.13 versus the IR, *P* < 0.05), but also significantly attenuated the CRP-mediated enhancement of the IR-induced injury (the CRP+DAF+IR: 1.50 ± 0.09 versus the CRP+IR, *P* < 0.001). DAF did not completely prevent local injury in mice subjected to IR as gut damage scores in DAF-treated and DAF+CRP-treated IR mice were still markedly higher than those in relevant Sham groups (DAF + IR versus Sham: 1.43 ± 0.13 versus 0.40 ± 0.08 , *P* < 0.001; DAF+CRP+IR versus CRP: 1.50 ± 0.09 versus 0.51 ± 0.10 , *P* < 0.001).

DAF Ameliorates Lung Tissue Injury Following CRP-Augmented Intestinal IR

The mesenteric IR model was used for determining whether the protective effect of DAF treatment can be extended to remote or systemic injury after local IR. The lung is particularly susceptible to damage in the setting of intestinal ischemia [23]. Following intestinal IR, lung sections were analyzed to assess the severity of histological injury (Fig. 2A and B). In animals exposed to mesenteric IR, H and E staining revealed a great number of alveolar septal and interstitial capillaries that were congested with erythrocytes, and alveolar walls were thickened with neutrophil infiltration and edema compared with the Sham group. The average damage score in the animals subjected to IR was increased by 6.7-fold of

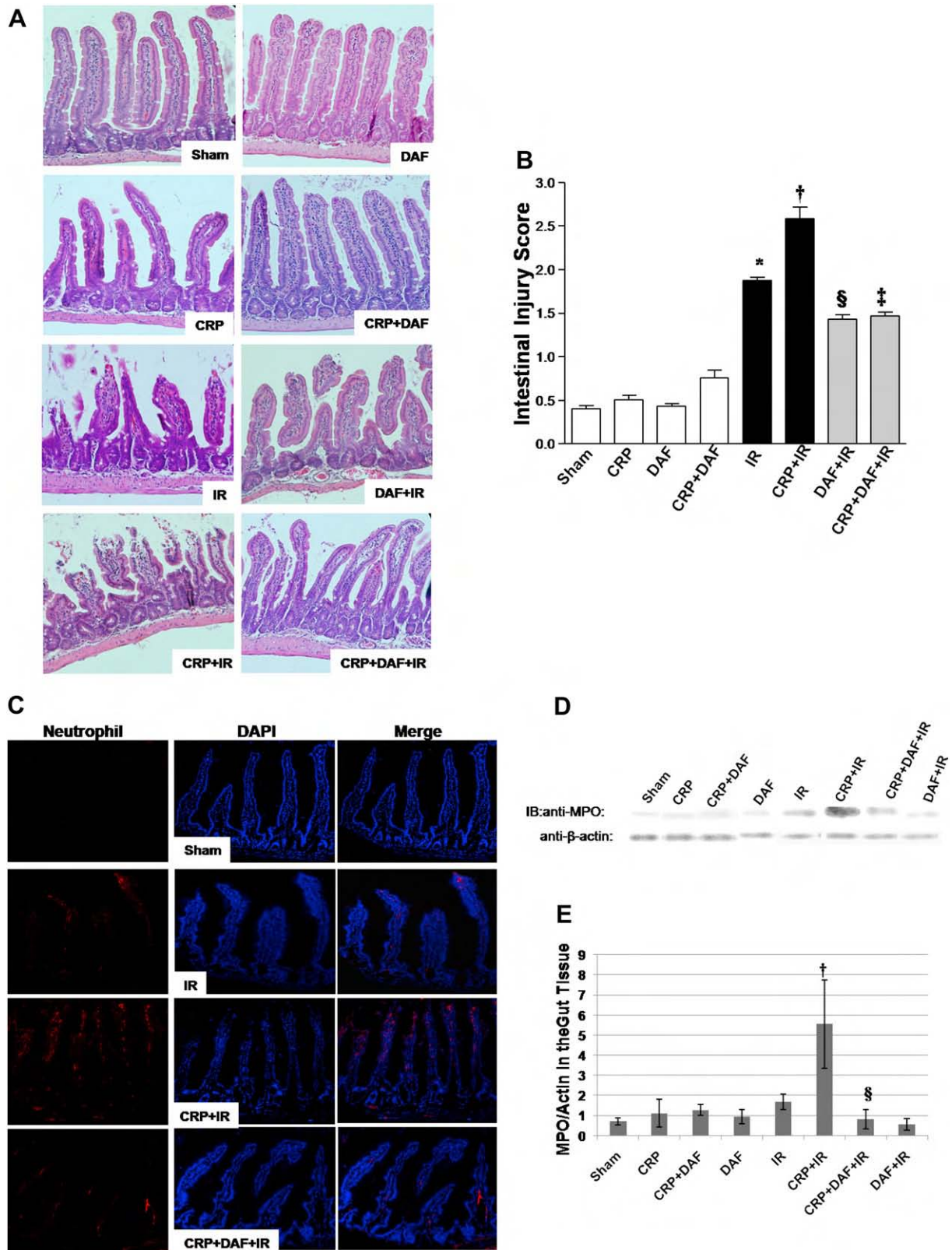


FIG. 1. DAF treatment mitigates CRP-amplified local intestinal IR injury. (A) Representative H and E stained slides from the small intestine of mice ($n = 5-8$) subjected to IR or Sham procedure and pretreated with TBS, CRP ($500 \mu\text{g}/\text{mouse}$), DAF ($2 \mu\text{g}/\text{mouse}$) were visualized and pictures were captured under a light microscope. Original magnification: $\times 200$. (B) H and E-stained intestinal sections from various treatment groups were scored for intestinal mucosal damage as described in the **Materials and Methods** section. Group data were compared using one-way ANOVA followed by the Tukey's multiple comparison test with P values of $P < 0.05$ considered as significant. ANOVA: $P < 0.0001$; Tukey:

that in the Sham group (IR *versus* Sham: 2.49 ± 0.73 *versus* 0.37 ± 0.10 , $P < 0.001$). CRP-pretreated animals subjected to mesenteric IR displayed more serious pulmonary injury with alveolar fibrin deposition, hemorrhage, and widespread edema, neutrophil infiltration, atelectasis, disruption of alveoli than in animals only subjected to mesenteric IR. The injury score was significantly elevated in the CRP+IR group compared with the IR group (4.17 ± 0.55 and 2.49 ± 0.73 , $P < 0.001$). The lung tissue in DAF-treated animals had a reduction in these morphologic changes compared with the mesenteric IR and the CRP+IR groups. The damage scores were significantly reduced in the DAF+IR and CRP+DAF+IR groups compared with the IR and CRP+IR groups ($P < 0.001$ and $P < 0.001$, respectively). DAF not only had protective effects on local intestinal injury, but also played an effective role in protecting against CRP-enhanced acute pulmonary injury associated with mesenteric ischemia-reperfusion.

DAF Decreases PMN Infiltration in Injured Local and Remote Tissues

It has been suggested that neutrophil infiltration mediates local tissue damage in response to mesenteric IR. We reported that human CRP induced marked myeloperoxidase (MPO) activity in local damaged intestinal tissue in mice subjected to mesenteric IR [15]. To determine whether the protective effect of DAF on CRP-augmented IR injury was associated with decreased neutrophil infiltration, the neutrophils in injured areas were assessed using an anti-neutrophil antibody. Infiltrated neutrophils in frozen intestinal sections were not detected in the Sham group but were detected in mice subjected to mesenteric IR and clearly increased in the CRP+IR group. DAF injection prior to reperfusion, dramatically down-regulated the infiltration of neutrophils in the CRP+DAF+IR group compared with those in the CRP+IR group (Figs. 1C and 2C). This finding demonstrates that human DAF has a role in attenuating leukocyte recruitment in local and remote organs during acute inflammation following mesenteric IR, and that DAF reduces tissue damage associated with down-regulation of neutrophil activation.

DAF Reduces MPO Release in Damaged Tissues After Mesenteric IR

Acute tissue inflammation in this model was also evident from the MPO evaluation with western blotting. Consistent with increased neutrophil infiltration in dam-

aged tissues, increased tissue MPO release was detected 2 h after reperfusion in the IR animals compared with the Sham group (Figs. 1D, E and 2D, E). Animals subjected to IR and pretreated with CRP (given at 180 min prior to reperfusion) exhibited significant increases in MPO deposition in the intestine and lungs. Administration of DAF 5 min prior to reperfusion significantly decreased MPO expression in the CRP+DAF+IR group compared with mice in the CRP+IR group. However, CRP, DAF alone, or CRP+DAF did not show obvious effect on MPO release in intestinal tissues compared with the Sham group.

DAF Reduced Deposition of C3 in Injured Tissues from Mice in the IR and IR+CRP Groups

Mesenteric IR results in C3 deposition on the villi [24]. To investigate whether DAF reduces complement deposition in CRP-enhanced intestinal injury, we performed immunohistochemical staining for C3. Our findings revealed significant accumulation of C3 in mice from the IR and CRP+IR groups while Sham animals did not show detectable levels of C3 in tissues. C3 accumulation in intestinal sections from the CRP+IR group was significantly greater in comparison to animals subjected to IR alone. C3 deposition in the villi was markedly reduced in DAF-treated mice subjected to mesenteric IR and pretreated with CRP (Fig. 3A). Thus, the treatment with human DAF inhibited complement activation and prevented C3 deposition in CRP-amplified mesenteric IR injury in mice.

Deposition of C3 in the lungs of mice subjected to mesenteric IR and CRP+IR was also observed. The specific C3 fluorescent signal was not as strong as that in local intestinal injury. Treatment with DAF significantly reduced CRP-enhanced intensity of C3 signal in the lung tissue following intestinal IR (Fig. 4A).

DAF Inhibits Production of Activated C5a in CRP-Accelerated Tissue Injury

C5a is an anaphylatoxin that has been identified as a major complement factor responsible for induction of the reperfusion-associated inflammatory response. In the present study, C5a accumulation was detected in local and remote injured tissues from the IR groups. In addition, a significant increase in C5a levels was detected in the CRP+IR treated animals compared with the IR and Sham controls (Fig. 3B, C and Fig. 4B, C). Administration of DAF resulted in a significant reduction of C5a deposition in the intestine and lung tissues in CRP + IR treated animals. These results indicate that a low dose

* $P < 0.001$ *versus* Sham; † $P < 0.001$ *versus* Sham, CRP and IR; ‡ $P < 0.05$ *versus* IR; § $P < 0.001$ *versus* CRP+IR. (C) Neutrophil infiltration was evaluated by probing with anti-neutrophil antibody in frozen intestinal sections (original magnification: $\times 200$). (D) MPO was detected by Western blot in gut tissues. (E) The bands of MPO were quantitated densitometrically and normalized to β -actin. † $P < 0.001$ *versus* Sham, ‡ $P < 0.05$ *versus* IR; § $P < 0.01$ *versus* CRP+IR (one-way ANOVA; Tukey post test; $n = 3 \sim 5$).

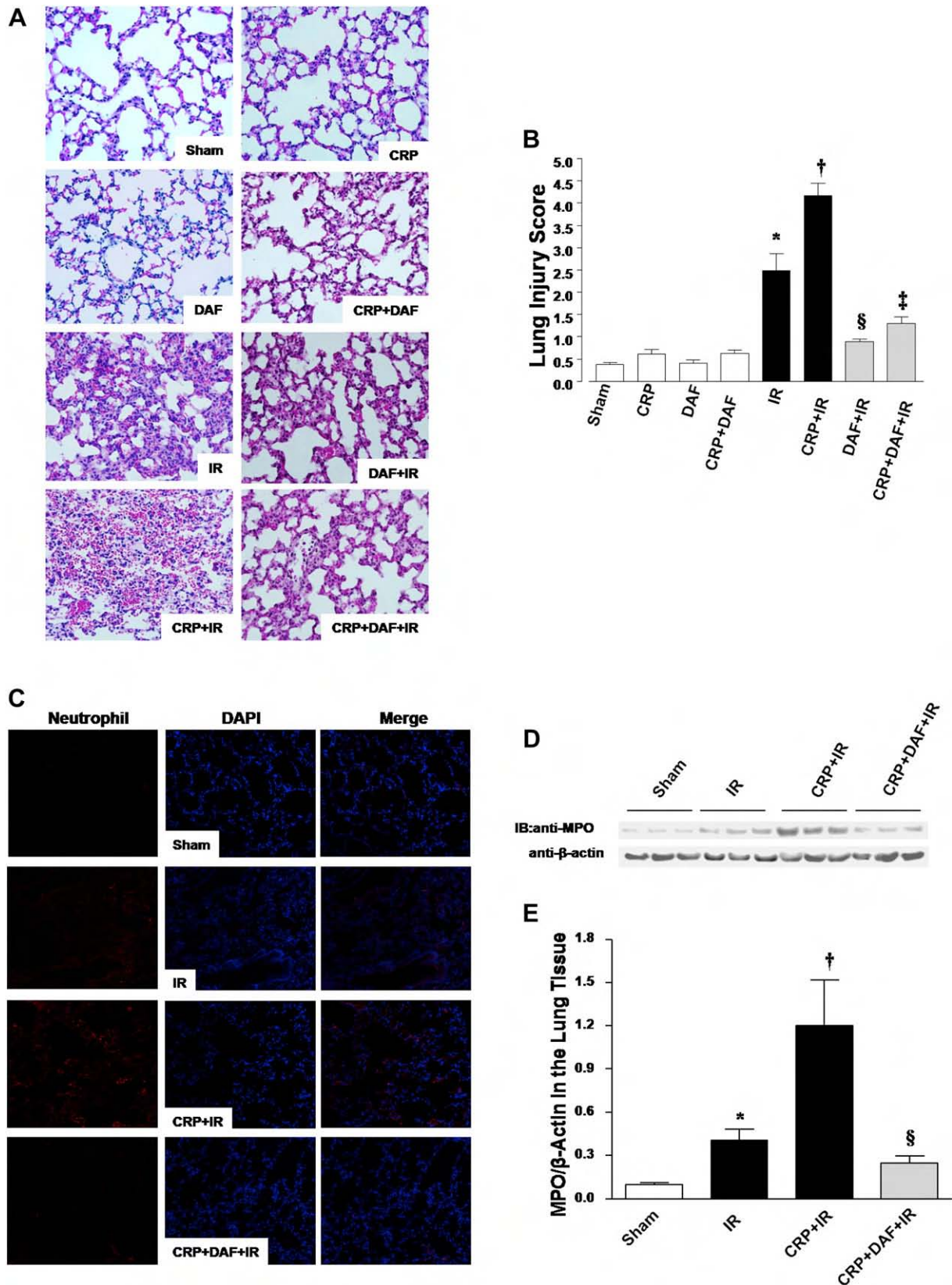


FIG. 2. DAF ameliorates detrimental effects of CRP in the lung tissue following mesenteric IR. (A) Representative H and E stained paraffin sections of the lung tissue were subjected to the same treatments as shown in Figure 1A (magnification: $\times 400$). (B) Lung injury scores from each group were determined based on a criterion as shown in the Materials and Methods section. Group data were compared using one-way ANOVA followed by the Tukey's multiple comparison test, with $P < 0.05$ considered as significant. ANOVA: $P < 0.0001$; Tukey: * $P < 0.001$ versus Sham; † $P < 0.001$ versus IR; ‡ $P < 0.001$ versus CRP+IR; § $P < 0.001$ versus IR+DAF.

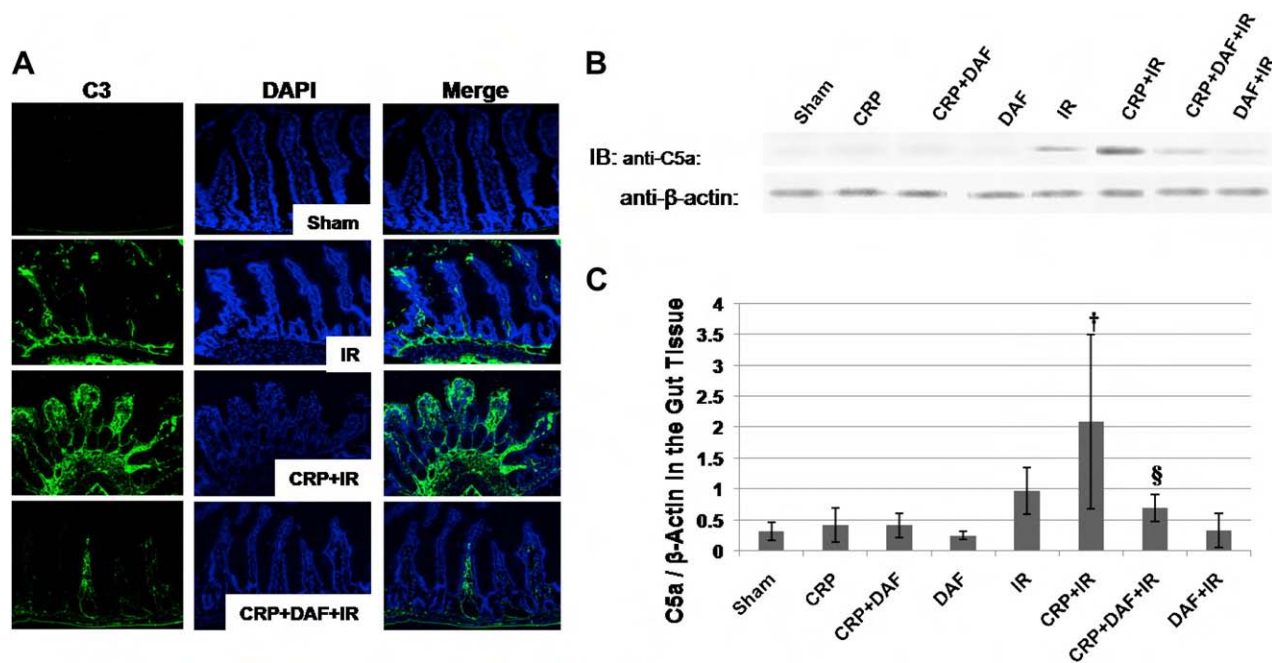


FIG. 3. DAF attenuates CRP-augmented C3 and C5a deposition in the IR-injured gut tissue. (A) Frozen sections of the small intestinal tissue were stained with anti-C3 antibody. The stained slides were observed and images were recorded under a confocal microscope equipped with a digital camera. Representative data from 5 to 8 mice were shown. Original magnification: $\times 200$. (B) C5a of intestinal tissues was detected the western blot using anti-mouse C5a antibody. (C) The bands of C5a were quantified densitometrically and normalized to β -actin. [†] $P < 0.01$ versus Sham, $P < 0.05$ versus IR; [§] $P < 0.01$ versus CRP+IR (one-way ANOVA; Tukey post test; $n = 3 \sim 8$).

of DAF ($2 \mu\text{g}/\text{mouse}$) administration effectively attenuated the generation of C5a in damaged tissues, whereas injury was enhanced by human CRP. There was no clear difference in the C5a deposition in the gut among Sham, CRP, DAF, and CRP+DAF groups.

DAF Prevents the Formation of C5b-9 in Mesenteric IR Injury

Intestinal ischemia-reperfusion injury is mediated by and dependent on the membrane attack complex (MAC, C5b-9) [25]. In our study, DAF treatment led to decreased formation of the terminal complement component, a membrane attack complex, in CRP-augmented both local and remote injury as was demonstrated by immuno-fluorescence staining (Fig. 4D and Fig. 5A). MAC was not detected in the Sham group or CRP-treated group (data not shown). The MAC signal was stronger in the CRP+IR than IR group. CRP and MAC were co-localized in luminal membrane and surface of damaged villi of intestine or on alveolar surface and vascular endothelium in damaged lung tissue. The co-localization of CRP and MAC implicate the association and/or interaction of human CRP and murine MAC in local mesenteric IR and remote lung injury.

[†] $P < 0.001$ versus Sham, CRP and IR; [§] $P < 0.001$ versus IR; [‡] $P < 0.001$ versus CRP+IR ($n = 4-6$). (C) Neutrophil infiltration in the lung tissue was determined using an anti-neutrophil antibody conjugated to fluorescence (original magnification: $\times 200$). (D) MPO expression in lung tissue was detected by the western blot. (E) The bands of MPO were quantitated densitometrically and normalized to β -actin. $*P < 0.05$ versus Sham; [†] $P < 0.05$ versus IR; [§] $P < 0.05$ versus CRP+IR (two-tailed t -test; $n = 3$).

Western blot data revealed that C9, a component of MAC and usually considered as a representative of MAC, was significantly decreased in local gut and remote lung tissues of animals undergoing mesenteric IR and pretreated with both CRP and DAF than in the CRP +IR group (Fig. 4E and F and Fig. 5B and C). This observation further confirms that DAF reduces the MAC formation in CRP-enhanced mesenteric IR injury. No difference in C5b-9 expression in the gut was observed in Sham, CRP, DAF, or CRP+DAF animals.

DAF Suppresses Production of IL-6 in Injured Tissues Following Intestinal IR

A report indicated that intestinal IR stimulates mRNA expression of pro-inflammatory cytokines in local and remote organs in dogs [26]. Previously, we found that CRP increases gene expression of a number of pro-inflammatory cytokines, such as $\text{TNF-}\alpha$, $\text{IL-1}\beta$, and IL-6 in the intestinal tissue after mesenteric IR (30–120 min) [15]. We asked whether the treatment with CRP enhances expression and deposition of pro-inflammatory cytokines in injured tissue or results in the systemic response in mice undergoing intestinal IR. We

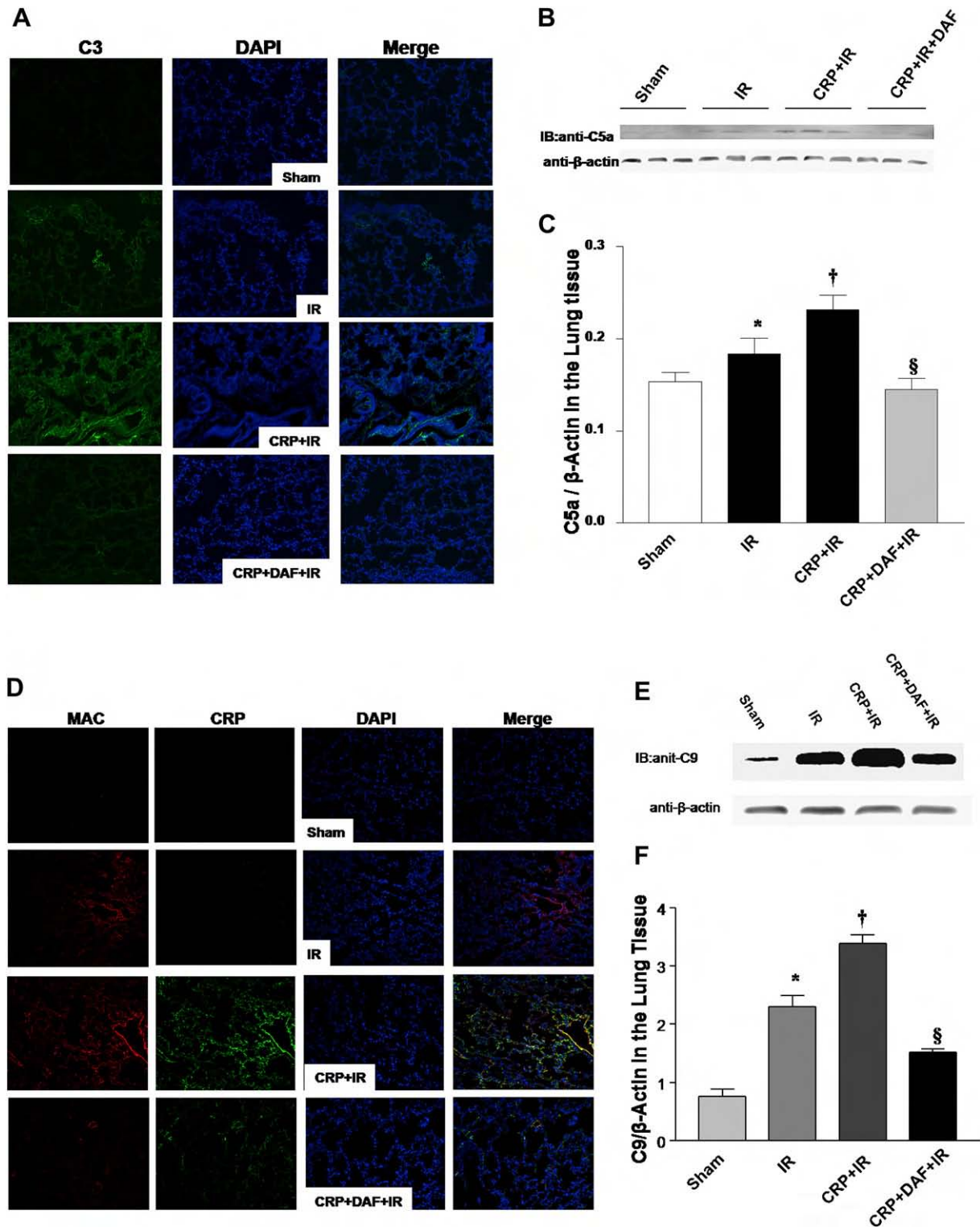


FIG. 4. DAF reduces CRP-exacerbated C3, C5a, and MAC deposition in the lung tissue following mesenteric IR. (A) C3 deposition in the lung tissue was assessed by immunofluorescent staining and confocal microscopy. Each image is representative of three experiments. Original magnification: $\times 200$. (B) Deposition of C5a was analyzed by immunoblotting the lysates from lung tissue. (C) The bands were scanned and the density related to β -actin was calculated. * $P < 0.05$ versus Sham; † $P < 0.05$ versus Sham; § $P = 0.01$ versus CRP+IR (two-tailed t -test; $n = 3$). (D) MAC deposition was detected by immunolabeling frozen section of lung tissues with anti-MAC and anti-CRP antibodies, and representative micro-photographs from three mice were shown at $\times 200$ magnification. (E) C9 was analyzed in the lung tissue by the Western blot and each band was representative of three experiments. (F) The C9 bands were quantitated densitometrically and the ratio was calculated to β -actin. * $P < 0.001$ versus Sham; † $P < 0.001$ versus Sham, < 0.01 versus IR; § $P < 0.05$ versus IR, < 0.001 versus CRP+IR (one-way ANOVA; Tukey post test, $n = 3$).

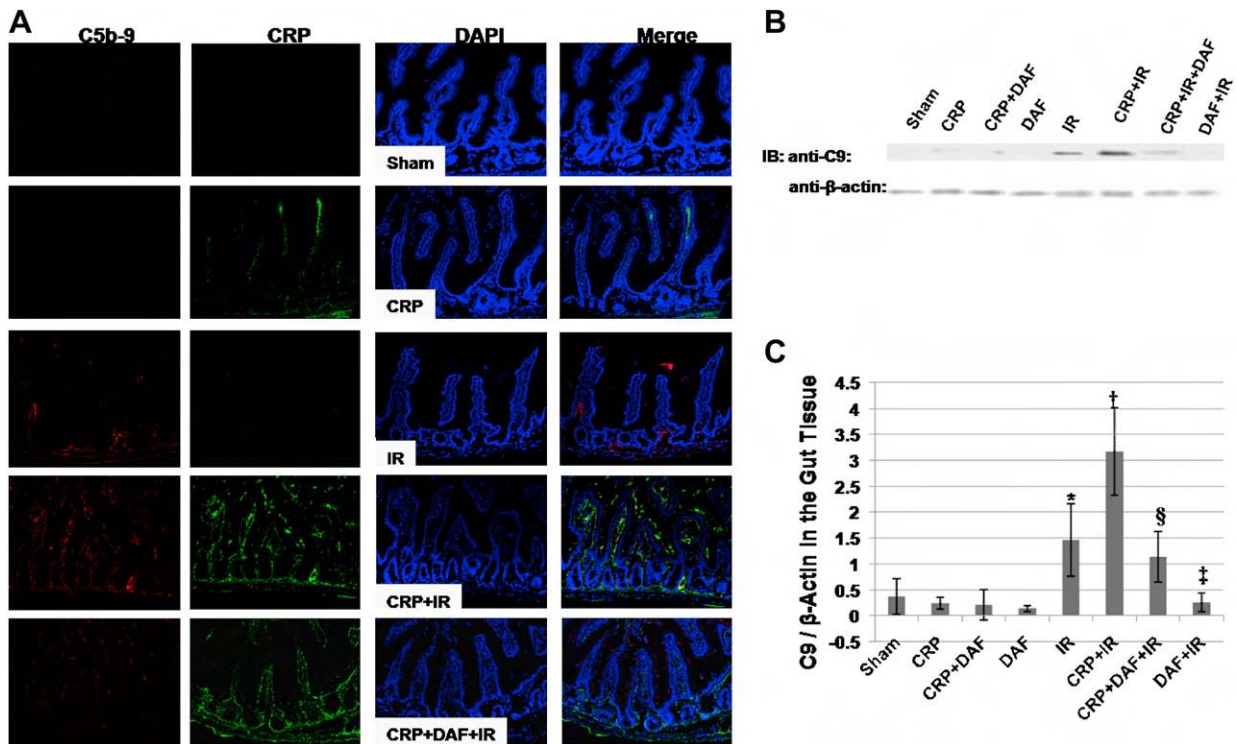


FIG. 5. DAF weakens CRP-strengthened deposition of C9 in the IR-damaged intestinal tissue. (A) Frozen sections from the gut tissues were stained with anti-MAC and anti-CRP antibodies, then stained slides were visualized by confocal microscopy. Image is representative of three sections from at least three different mice. Original magnification: $\times 200$. (B) Gut tissue was lysed and immunoblotted with anti-C9 and anti- β -actin antibodies to detected C9 deposition. (C), C9 was quantified by densitometry and the ratio to β -actin was calculated for each sample. Cumulated data from three independent experiments are shown. * $P < 0.01$ versus Sham; † $P < 0.001$ versus Sham and IR; ‡ $P < 0.001$ versus CRP+IR; § $P < 0.05$ versus IR (one-way ANOVA; Tukey post test, $n = 3 \sim 8$).

also asked whether DAF, as a G-coupled protein, can reduce inflammatory cytokines during mesenteric IR in mice. We used ELISA to determine IL-6 levels in murine sera. The serum concentration of IL-6 was significantly increased in the IR group (125.65 ± 31.45 pg/mL versus Sham 31.53 ± 21.83 pg/mL, $P = 0.0034$) and the CRP+IR group (148.98 ± 41.43 pg/mL versus CRP+Sham 71.95 ± 19.78 pg/mL, $P = 0.0017$). This indicates that IR injury triggers IL-6 expression and release, leading to its elevated blood concentration. There was no significant difference between the CRP and IR group, the CRP and Sham group, the CRP+DAF and Sham group in the serum IL-6 level. Administration of DAF ($2 \mu\text{g}/\text{mouse}$) markedly down-regulated serum IL-6 levels in the DAF+IR group (DAF+IR 75.97 ± 29.09 versus IR 125.65 ± 31.45 , $P < 0.05$), but DAF did not significantly decrease serum IL-6 in the CRP+DAF+IR group (Fig. 6A).

Deposition of IL-6 in damaged tissue following mesenteric IR has not been reported before. We found that IL-6 was expressed and deposited 2 h after reperfusion, not only locally in the intestinal tissue, but also in remote lung tissue. IL-6 was not detected in these tissues of the Sham group. As shown in Fig. 6B and C, human CRP enhanced IL-6 deposition and co-localized with

murine IL-6 in the intestinal and lung tissues in the CRP+IR group. The treatment with DAF remarkably reduced deposition of IL-6 in the intestinal and lung tissues in the CRP+DAF+IR group. Therefore, these data indicate that IL-6 is induced in the early phase of mesenteric IR and might have participated in the IR-initiated acute inflammatory reaction. DAF, a complement inhibitor, plays a protective role against CRP-augmented mesenteric IR injury, at least partially, by the inhibition of local and systemic IL-6 activity.

DISCUSSION

In this study, we have demonstrated that DAF clearly reduces CRP-enhanced intestinal and lung injury following acute mesenteric IR in mice. In particular, a direct or an indirect effect of DAF on inhibition of the complement activation, suppression of the neutrophil infiltration, and reduction of the IL-6 production plays a key role in its protective actions on CRP-enhanced murine tissue injury of mesenteric IR. This is the first report of beneficial effects of DAF on CRP-potentiated local and systemic injury.

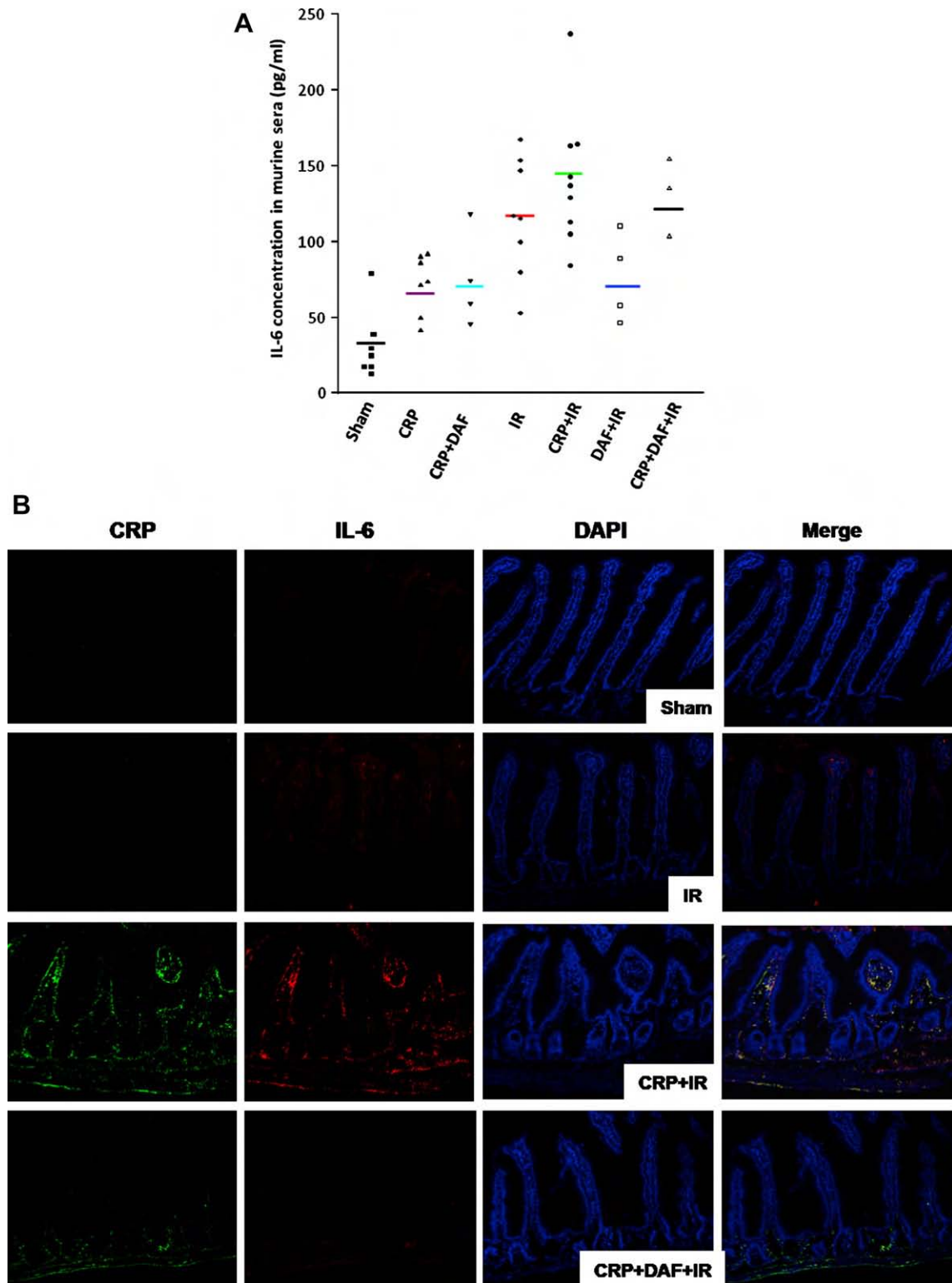


FIG. 6. DAF decreases production of IL-6 locally and systemically after mesenteric IR. (A) Serum IL-6 concentration was determined by ELISA. Red bar indicates a significant difference *versus* Sham, $P < 0.05$; green bar displays significant difference *versus* Sham, $P < 0.001$, *versus* CRP, $P < 0.01$, *versus* CRP+DAF, $P < 0.05$; blue bar indicates significant difference *versus* IR, CRP+IR, $P < 0.05$ (one-way ANOVA; Tukey post test). (B) Expression of IL-6 in the intestinal tissue was measured by immunostaining with anti-IL-6 antibody. Presented data is from a representative experiment of three separate studies. Original magnification: $\times 200$. (C) Production of IL-6 in lung tissue after intestinal IR was determined by immunofluorescent labeling using anti-IL-6 antibody. Each image is representative of three separate experiments. Original magnification: $\times 600$.

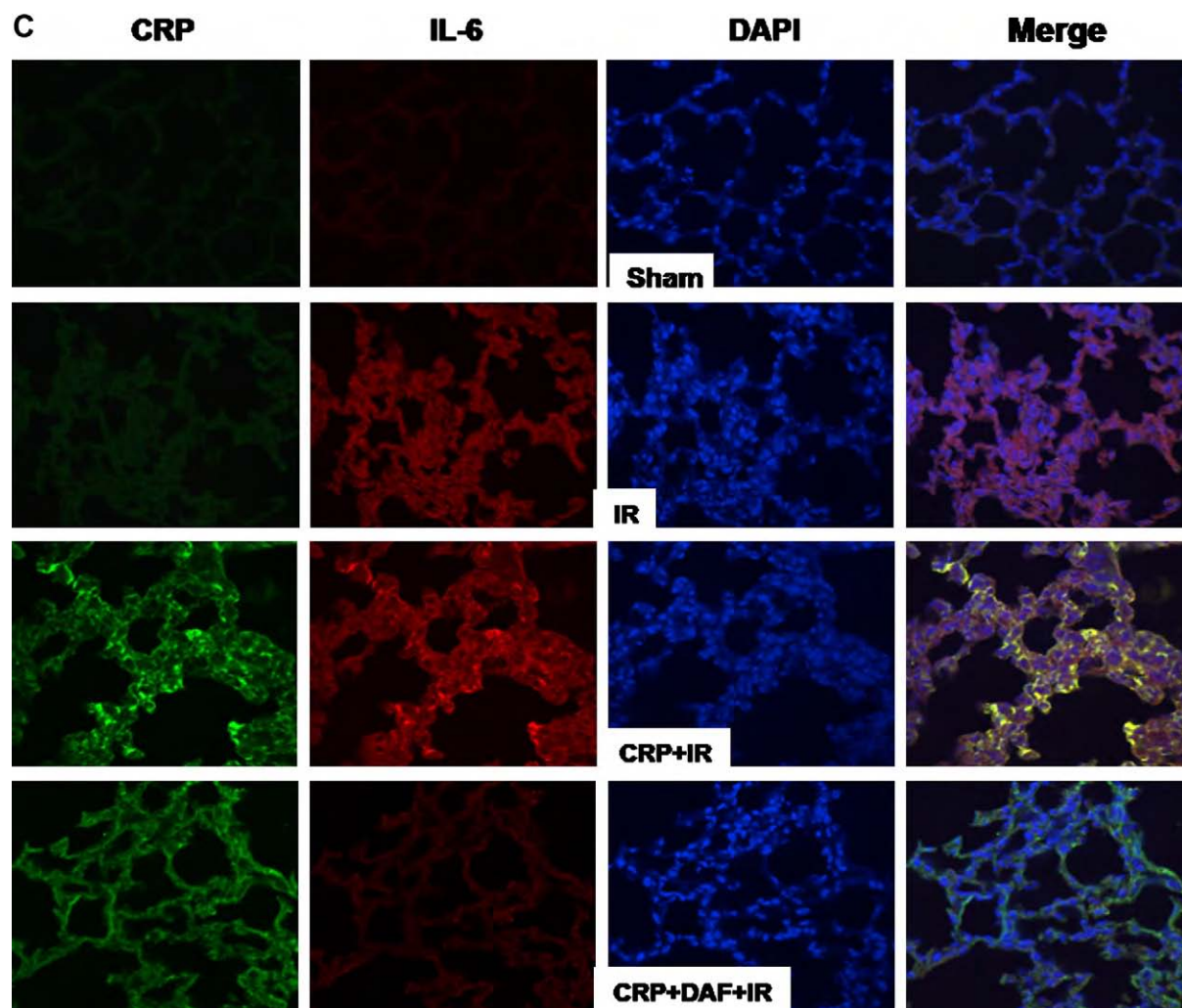


FIG. 6. (continued).

CRP is known to initiate the complement classic pathway [27] and it is the key molecule that boosts the immune response [28]. Complement activation has a critical role in the pathologic alterations following mesenteric IR in animals [4]. Further, the endogenous and exogenous CRP takes part in the pathogenesis and potentiates intestinal IR injury [14, 15]. We have shown that CRP enhanced mesenteric IR in a complement-dependent manner. This synergistic effect of CRP on tissue damage can be prevented by the complement depletion with cobra venom factor [15]. Studies reported that the inhibition of complement activation using membrane complement regulatory proteins, including endogenous [17] and exogenous DAF [18], provided us with an important insight into protection against the potentiating effect of CRP on IR injury.

We selected the therapeutic dose of DAF as 2 μg per mouse in this study as per our previous report [18]. In

this study, human DAF concentration in murine serum was not monitored since it has been reported that human DAF has a very short half-life in the circulation, and that the majority of DAF rapidly binds to and deposits on the cell membranes in local and remote tissues 10 min after administration [18]. Immunofluorescent staining showed that DAF deposition still remained bound to the epithelial and endothelial surface in the intestinal and to the endothelial surface in the lung tissue 2 h after injection in all treated mice (unpublished results). DAF is more stable and active on membrane-associated complement complexes [29, 30]. Once bound and incorporated, it seems to inhibit activation and amplification of complement cascade, which leads to local and systemic damage. The Western blot indicated that administration with as low as 2 μg of DAF effectively reduced C5a formation in local intestinal and remote lung tissue following mesenteric IR in mice pretreated with CRP. DAF significantly attenuated

CRP-augmented morphologic injury and neutrophil infiltration in both intestinal and lung tissues. This was consistent with an observed decrease of C5a and C5b-9 deposition in the tissues.

Mesenteric IR causes local and systemic inflammatory derangements, including release of pro-inflammatory cytokines, and is associated with complement activation. Reports indicate the intestine is a source of cytokine production following intestinal IR injury [31, 32]. In the present study, IL-6 release was found not only in local intestinal tissue, but also in remote lung tissue. The secretion of IL-6 from damaged intestinal and lung tissue may contribute to the increase of the systemic level of IL-6 in mice subjected to mesenteric IR. We did not evaluate the IL-6 production in other tissues and, therefore, we do not know the possible contribution of IL-6 release from these tissues.

The exact mechanism involved in CRP-induced IL-6 secretion remains unclear. Generation of IL-6 appeared to require the involvement of Fc γ receptors, such as CD16 and CD32, on inflammatory cells [33]. CRP has been shown to bind to Fc γ receptors and subsequently lead to activation of PI3 K/Akt, ERK, and NF- κ B pathways [33]. Activation of these signal pathways have been known to up-regulate cytokine production [33]. In this study, the pretreatment of animals with human CRP prior to ischemia obviously enhances the IL-6 release in both intestinal and lung tissues. This effect of CRP on IL-6 release could be explained by CRP binding to its ligands on the surface of activated macrophages and neutrophils in injured tissues. Indeed, human CRP co-localization with murine CD32 rather than CD16 was observed on the surface of inflammatory cells in IR-damaged tissues (unpublished results). It implies that human CRP may interact with murine CRP ligand undergoing IR *in vivo*, which initiates or enhances activation of PI3 K/Akt, ERK, and NF- κ B pathways, thereby potentiating IL-6 production in mesenteric IR injury.

The fact that DAF can effectively reduce the CRP-enhanced IL-6 release from injured tissues is the most important finding in this study. DAF inhibits C3 and C5 convertases in both the classic and the alternative complement pathways and, thus, suppresses the generation of C3a and C5a. These anaphylatoxins, especially C5a, can induce synthesis and release of pro-inflammatory cytokines by leukocytes [34]. DAF-deficient mice are more susceptible to complement-mediated inflammatory injury [17, 35], and produce extraordinary serum levels of IL-6 upon stimulation with lipopolysaccharide compared with wild-type animals [35]. Our data showed that C5a was significantly decreased in damaged gut and lung tissues in mice pretreated with CRP and then treated with DAF prior to intestinal reperfusion than in control, which are mice with mesen-

teric IR only pretreated with CRP. Thus, the attenuation of IL-6 expression by DAF in damaged tissues could be, at least partly, attributed to the inhibition of an anaphylatoxin, C5a.

One of the serious consequences of mesenteric IR is multiple organ failure, which is also referred to as secondary organ injury [36]. Complement activation leads to the generation of anaphylatoxin C3a and C5a, which contribute to the development of remote organ injury [18, 37]. Other studies reported that intestinal IR-induced pro-inflammatory cytokines and chemokines exert their effects *via* a direct toxic action on target cells in distant organs [38, 39]. Complement activation results in the release of chemoattractants C3a and C5a, which can be released directly or indirectly through the activation of endothelial cells expressing other various chemokines and adhesion molecules and subsequently activate neutrophils [35, 40].

A previous study suggested that the membrane attack complex (C5b-9) also solely mediated neutrophil infiltration following mesenteric IR injury in mice [18]. The influx of neutrophils into IR tissue can cause degranulation and superoxide production, which damages tissue and subsequently amplifies the neutrophil response. The accurate mechanisms regulating remote lung injury are not fully explained but probably involve complement activation, cytokine/chemokine generation, leukocyte infiltration, and release of reactive oxygen species (ROS) and proteases into remote tissue. In this study, DAF inhibited C5a formation, IL-6 expression, accumulation of neutrophils, and release of MPO in both intestinal and lung tissue in mice with CRP-enhanced mesenteric IR injury. By inhibition of C5a production and MAC formation, DAF blocks the downstream signaling of C5a/C5a receptor (C5aR) and MAC. This infers that complement-mediated inflammation can be modulated at C5a/C5aR level, resulting in prevention of local and remote organ injury. Our study suggests that DAF may be useful for the treatment of acute intestinal injury associated with bowel obstruction, necrotic enterocolitis, repair of abdominal aortic aneurysms, and acute mesenteric ischemia.

ACKNOWLEDGMENTS

The authors acknowledge support for this work by the Department of Defense Combat Casualty Care Research Program.

The opinions and assertions contained herein are the private views of the authors and are not to be construed as official or reflecting the views of the United States Department of the Army, or the United States Department of Defense.

The authors thank Michael Falabella for his technical expertise.

REFERENCES

1. Fleming SD, Tsokos GC. Complement, natural antibodies, auto-antibodies and tissue injury. *Autoimmun Rev* 2006;5:89.

2. Edgerton C, Crispin JC, Moratz CM, et al. IL-17 producing CD4 + T cells mediate accelerated ischemia/reperfusion-induced injury in autoimmunity-prone mice. *Clin Immunol* 2009;130:313.
3. Chen J, Crispin JC, Tedder TF, et al. B cells contribute to ischemia/reperfusion-mediated tissue injury. *J Autoimmune* 2009;32:195.
4. Arumugam TV, Shiels IA, Woodruff TM, et al. The role of the complement system in ischemia-reperfusion injury. *Shock* 2004;21:401.
5. Riedmann NC, Ward PA. Complement in ischemia reperfusion injury. *Am J Pathol* 2003;162:363.
6. Mollnes TE, Song WC, Lambris JD. Complement in inflammatory tissue damage and disease. *Trends Immunol* 2002;23:41.
7. Asghar SS, Pasch MC. Therapeutic inhibition of the complement system. Y2 K update. *Front Biosci* 2000;5:E63.
8. Montalvo-Jave EE, Escalante-Tattersfield T, Ortega-Salgado JA, et al. Factors in the pathophysiology of the liver ischemia-reperfusion injury. *J Surg Res* 2008;147:153.
9. Diepenhorst GM, van Gulik TM, Hack CE. Complement-mediated ischemia-reperfusion injury: Lessons learned from animal and clinical studies. *Ann Surg* 2009;249:889.
10. Jang HR, Rabb H. The innate immune response in ischemic acute kidney injury. *Clin Immunol* 2009;130:41.
11. Krijnen PA, Meischl C, Nijmeijer R, et al. Inhibition of sPLA2-IIA, C-reactive protein or complement: New therapy for patients with acute myocardial infarction? *Cardiovasc Hematol Disord Drug Targets* 2006;6:113.
12. Suresh MV, Singh SK, Ferguson DA, Jr., et al. Role of the property of C-reactive protein to activate the classical pathway of complement in protecting mice from pneumococcal infection. *J Immunol* 2006;176:4369.
13. Whitehead AS, Zahedi K, Rits M, et al. Mouse C-reactive protein: Generation of cDNA clones structure analysis and induction of mRNA during inflammation. *Biochem J* 1990;266:283.
14. Padilla ND, van Vliet AK, Schoots IG, et al. C-reactive protein and natural IgM antibodies are activators of complement in a rat model of intestinal ischemia and reperfusion. *Surgery* 2007;142:722.
15. Lu X, Peckham R, Falabella M, et al. Human C-reactive protein augments the gut ischemia/reperfusion injury in mice. *Clin Immunol* 2006;123(Suppl):S185.
16. Kim DD, Song WC. Membrane complement regulatory proteins. *Clin Immunol* 2006;118:127.
17. Yamada K, Miwa T, Liu J, et al. Critical protection from renal ischemia reperfusion injury by CD55 and CD59. *J Immunol* 2004;172:3869.
18. Weeks C, Moratz C, Zacharia A, et al. Decay-accelerating factor attenuates remote ischemia-reperfusion-initiated organ damage. *Clin Immunol* 2007;124:311.
19. Harris CL, Spiller OB, Morgan BP. Human and rodent decay-accelerating factor (CD55) are not species restricted in their complement-inhibiting activities. *Immunology* 2000;100:462.
20. Rehrig S, Fleming SD, Anderson J, et al. Complement inhibitor, complement receptor 1-related gene/protein γ -Ig attenuates intestinal damage after the onset of mesenteric ischemia/reperfusion injury in mice. *J Immunol* 2001;167:5921.
21. Fleming SD, Monestier M, Tsokos GC. Accelerated ischemia/reperfusion-induced injury in autoimmunity-prone mice. *J Immunol* 2004;173:4230.
22. Nishina K, Mikawa K, Yakao Y, et al. ONO-5046, an elastase inhibitor, attenuates endotoxin-induced acute lung injury in rabbits. *Anesth Analg* 1997;84:1097.
23. Atkinson C, Song H, Lu B, et al. Targeted complement inhibition by C3d recognition ameliorates tissue injury without apparent increase in susceptibility to infection. *J Clin Invest* 2005;115:2444.
24. Karpel-Massler G, Fleming SD, Kirschfink M, et al. Human C1 esterase inhibitor attenuates murine mesenteric ischemia/reperfusion induce local organ injury. *J Surg Res* 2003;115:247.
25. Austern WG, Jr., Kyriakides C, Favuzza J, et al. Intestinal ischemia-reperfusion injury is mediated by the membrane attack complex. *Surgery* 1999;126:343.
26. Nezu Y, Nezu Y, Shigihara K, et al. Effects of small intestinal ischemia and reperfusion on expression of tumor necrosis factor- α and interleukin-6 messenger RNAs in the jejunum, liver and lungs of dog. *Am J Vet Res* 2008;69:512.
27. Marnell L, Mold C, Du Clos TW. C-reactive protein: Ligands, receptors and role in inflammation. *Clin Immunol* 2005;117:104.
28. Ng PM, Le Saux A, Lee CM, et al. C-reactive protein collaborates with plasma lectins to boost immune response against bacteria. *Embo J* 2007;26:3431.
29. Pangburn MK. Differences between the binding sites of the complement regulation proteins DAF, CR1, and factor H on C3 convertases. *J Immunol* 1986;136:2216.
30. Harris CL, Abbott RJ, Smith RA, et al. Molecular dissection of interactions between components of the alternative pathway of complement and decay accelerating factor (CD55). *J Biol Chem* 2005;280:2569.
31. Grotz MR, Deitch EA, Ding J, et al. Intestinal cytokine response after gut ischemia: Role of gut barrier failure. *Ann Surg* 1999;229:478.
32. Roccourt DV, Mehta VB, Besner GE. Heparin-binding EGF-like growth factor (HB-EGF) decreases inflammatory cytokine expression after intestinal ischemia/reperfusion injury. *J Surg Res* 2007;139:269.
33. Yang J, Wezeman M, Zhang X, et al. Human C-reactive protein binds activating Fc γ receptor and protects myeloma tumor cells from apoptosis. *Cancer Cell* 2007;12:252.
34. Haas PJ, van Strijp J. Anaphylatoxins: Their role in bacterial infection and inflammation. *Immunol Res* 2007;37:161.
35. Zhang X, Kimura Y, Fang C, et al. Regulation of Toll-like receptor-mediated inflammatory response by complement *in vivo*. *Blood* 2007;110:228.
36. Harward TR, Brooks DL, Flynn TC, et al. Multiple organ dysfunction after mesenteric artery revascularization. *J Vasc Surg* 1993;18:459.
37. Fleming SD, Mastellos D, Karpel-Massler G, et al. C5a causes limited, polymorphonuclear cell-independent, mesenteric ischemia/reperfusion-induced injury. *Clin Immunol* 2003;108:263.
38. Ward PA. Recruitment of inflammatory cells into lung: Roles of cytokines, adhesion molecules, and complement. *J Lab Clin Med* 1997;129:400.
39. Frangogiannis NG. Chemokines in ischemia and reperfusion. *Thromb Haemost* 2007;97:738.
40. Proctor LM, Arumugam TV, Shiels I, et al. Comparative anti-inflammatory activities of antagonists to C3a and C5a receptors in a rat model of intestinal ischemia/reperfusion injury. *Br J Pharmacol* 2004;142:756.

A Novel Inhibitor of the Alternative Pathway of Complement Attenuates Intestinal Ischemia/Reperfusion-Induced Injury

Jie Chen, Ph.D.,* José C. Crispín, M.D.,* Jurandir Dalle Lucca, M.D., Ph.D.,† and George C. Tsokos, M.D.*¹

*Division of Rheumatology, Beth Israel Deaconess Medical Center, Harvard Medical School, Boston, Massachusetts; and †Department of Cellular Injury, Walter Reed Army Institute of Research, Silver Spring, Maryland

Submitted for publication April 16, 2009

Complement activation has been demonstrated to contribute significantly to the expression of IR-induced tissue damage. Each of the three complement pathways, classic, alternative, and lectin, has been implicated in the instigation of tissue pathology. In this study, we used a selective inhibitor of the alternative pathway, that is, a soluble form of complement receptor of the immunoglobulin superfamily (CRIg-Fc) to determine whether it can prevent IR tissue injury. We demonstrate that treatment of C57B1/6 mice prior to mesenteric IR prevents local (intestinal) and remote (lung) injury by limiting deposition of complement and entry of polymorphonuclear cells to the sites of injury. Our results show that CRIg-Fc represents a candidate to limit IR injury as it occurs in various clinical conditions. © 2009 Elsevier Inc. All rights reserved.

Key Words: ischemia/reperfusion injury; CRIg-Fc; complement; alternative pathway.

INTRODUCTION

Transient loss of blood flow followed by reperfusion, known as ischemia/reperfusion (IR) causes an intense local and systemic inflammatory response. IR injury is frequently encountered in a number of common clinical settings, including surgery, transplantation, and shock [1]. The ischemic insult induces local cellular changes that cause the tissue to become susceptible to immune-mediated damage. When blood flow is restored, molecules expressed by the hypoxic tissue activate elements

of the innate and adaptive immune response instigating inflammation. Complement activation is an essential step in the initiation and amplification of the inflammatory response induced by IR. Accordingly, deficiency or depletion of complement factors protects animals from developing IR injury [2–4]. Moreover, inhibition of complement activity through a variety of approaches has been shown to diminish the intensity of IR-mediated organ damage (reviewed in reference [5]).

The mechanisms by which complement is activated by ischemic tissue are probably numerous, and involve the classic, the alternative, and the mannose-binding lectin (MBL) pathways [6–8]. Activation of the classic and MBL pathways probably occurs early, and depends on the recognition of tissue antigens exposed in response to the ischemic insult by antibodies and lectins, respectively [7, 9]. On the other hand, the alternative pathway incorporates a powerful amplification mechanism that has been shown to be essential in other complement-mediated processes, such as antiphospholipid antibody-induced fetal resorption [10].

CRIg is a recently identified complement receptor of the immunoglobulin superfamily expressed by macrophages [11]. CRIg participates in pathogen clearance and has also been shown to possess the capacity to inhibit complement activation. It does so by binding to C3b and inhibiting the C3 and C5 convertases of the alternative pathway [12]. Inhibition of the complement alternative pathway with a soluble form of CRIg (CRIg-Fc, a chimeric molecule comprised of the extracellular portion of murine CRIg and the Fc portion of murine IgG1) has shown to be useful in a number of settings, highlighting the role of the alternative pathway as an amplifier of the inflammatory response [13]. We decided to use CRIg-Fc in a model of murine IR-induced tissue

¹ To whom correspondence and reprint requests should be addressed at Beth Israel Deaconess Medical Center, Harvard Medical School, 330 Brookline Avenue, CLS-937. Boston, MA 02115. E-mail: gtsokos@bidmc.harvard.edu.



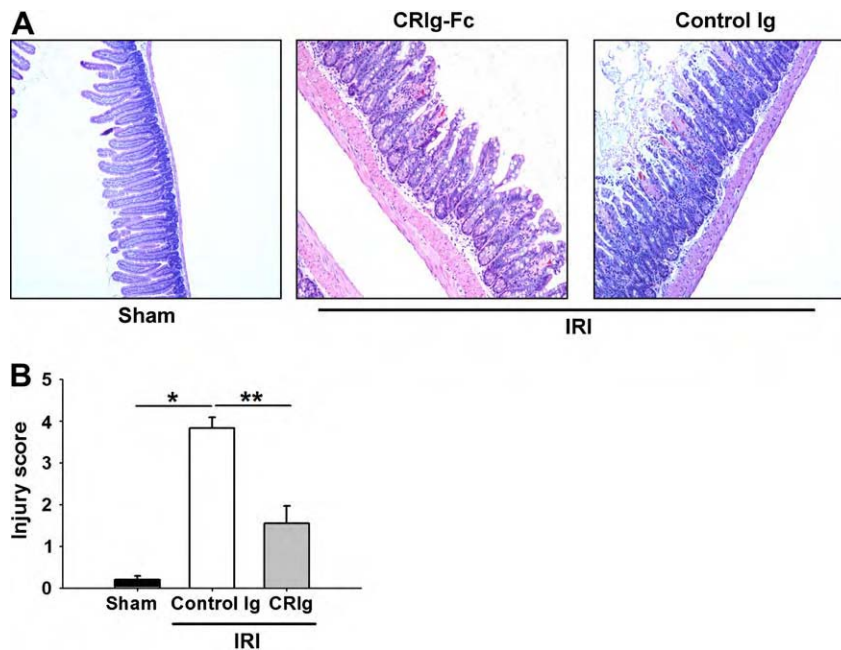


FIG. 1. CRlg-Fc significantly decreases ischemia/reperfusion-induced intestinal injury. (A) Representative photographs of a B6 mouse subjected to sham (left panel) or I/R procedure (middle and right panels). Administration of CRlg-Fc before the induction of IRI significantly decreases intestinal injury. (B) Cumulative data of one experiment ($n = 3$ mice per group). * $P < 0.001$; ** $P = 0.001$.

injury to investigate the local and systemic repercussions of blocking the alternative pathway in a setting where complement activation plays a central role.

MATERIALS AND METHODS

Mice

Eight-week old C57Bl/6 mice were used for mesenteric IR. Animals in this study were maintained in accordance with the guidelines of the Laboratory Animal Medicine Department and the Committee on the Care and Use of Laboratory Animals of the Institute of Laboratory Animals.

Reagents

FITC-labeled anti-mouse C3 (MP Biomedical, LLS, Solon, OH) and FITC-labeled anti-mouse Gr-1 (BD Pharmingen, San Jose, CA) were used for immunofluorescence studies and confocal microscope imaging. Rat anti-mouse B220 (BD Pharmingen) and rat anti-mouse CD3 (BD Pharmingen) were used in immunohistochemistry studies. Murine CRlg-Fc was a kind gift from Dr. Menno van Lookeren Campagne [11]. A monoclonal anti-gp-120 IgG1 antibody was used as an isotype control.

Intestinal Model of Ischemia/Reperfusion

Eight-week-old C57Bl/6 male mice were weighed and anesthetized with a mixture of ketamine (100 mg/kg), xylazine (20 mg/kg), and acepromazine (3 mg/kg). Anesthesia was maintained during the entire experiment. Body temperature was kept at 37 °C using warm-mate. I/R group: mice underwent intestinal ischemia for 30 min through occlusion of the mesenteric artery with a vascular clamp, followed by 3 h reperfusion. Sham mice underwent the same operative intervention except for clamping of the superior mesenteric artery. Mice were sacrificed by anesthetic overdose. Harvested intestine were fixed overnight in 10% formalin (for paraffin blocks) or directly stored in embedding media (for frozen sections). In some mice, Peyer's patches were harvested, and single cell sus-

pensions were prepared for flow cytometry analyses. Mice received either CRlg-Fc (12 mg/K) or isotype control in a single subcutaneous injection before IR surgery.

Histology and Tissue Injury Scoring

To prepare specimens for histological analysis, 2 cm segments of small intestine specimens were fixed in 10% buffered Formalin phosphate immediately after euthanasia. Next, tissues were embedded in paraffin, sectioned transversely in 5- to 7 μ m sections, and stained with H and E. For some experiments, CD3 and B220⁺ cells were detected by immunohistochemistry. In each section, 100 villi were graded on a six-tiered scale, as previously described [14]. Briefly, a score of 0 was assigned to a normal villus; villi with tip distortion were scored as 1; villi lacking goblet cells and containing Guggenheims' spaces were scored as 2; villi with patchy disruption of the epithelial cells were scored as 3; villi with exposed but intact lamina propria and epithelial cell sloughing were assigned a score of 4; villi in which the lamina propria was exuding were scored as 5; and finally, villi displaying hemorrhage or denudation were scored as 6. All histologic analysis was performed in a blinded manner.

Three parameters were scored in lung sections to determine distal injury: (A) periluminal infiltrates (airways/vessels): 0, when no infiltrates were observed; 1, when infiltrates were formed by 1 to 3 cell layers; 2, when infiltrates were 4 to 10 cell layers thick; 3, when they were >10 cell layers thick. (B) Pneumonitis (alveolar/interstitial): 0, when no infiltrates were observed; 1, when infiltrating cells were evident only at high magnification ($\times 400$); 2, when cell infiltrates were easily observed; 3, when lung consolidation by inflammatory cells was evident. (C) Percentage of affected lung tissue: 0, 0%; 1, 5% to 25%; 2, 26% to 50%; 3, >50%.

Immunofluorescence

For immunofluorescence, small intestine or lung fragments were snap-frozen to -70 °C, and sections were cut with a cryostat and fixed in acetone. Samples were blocked in PBS + 10% FCS. Sections were

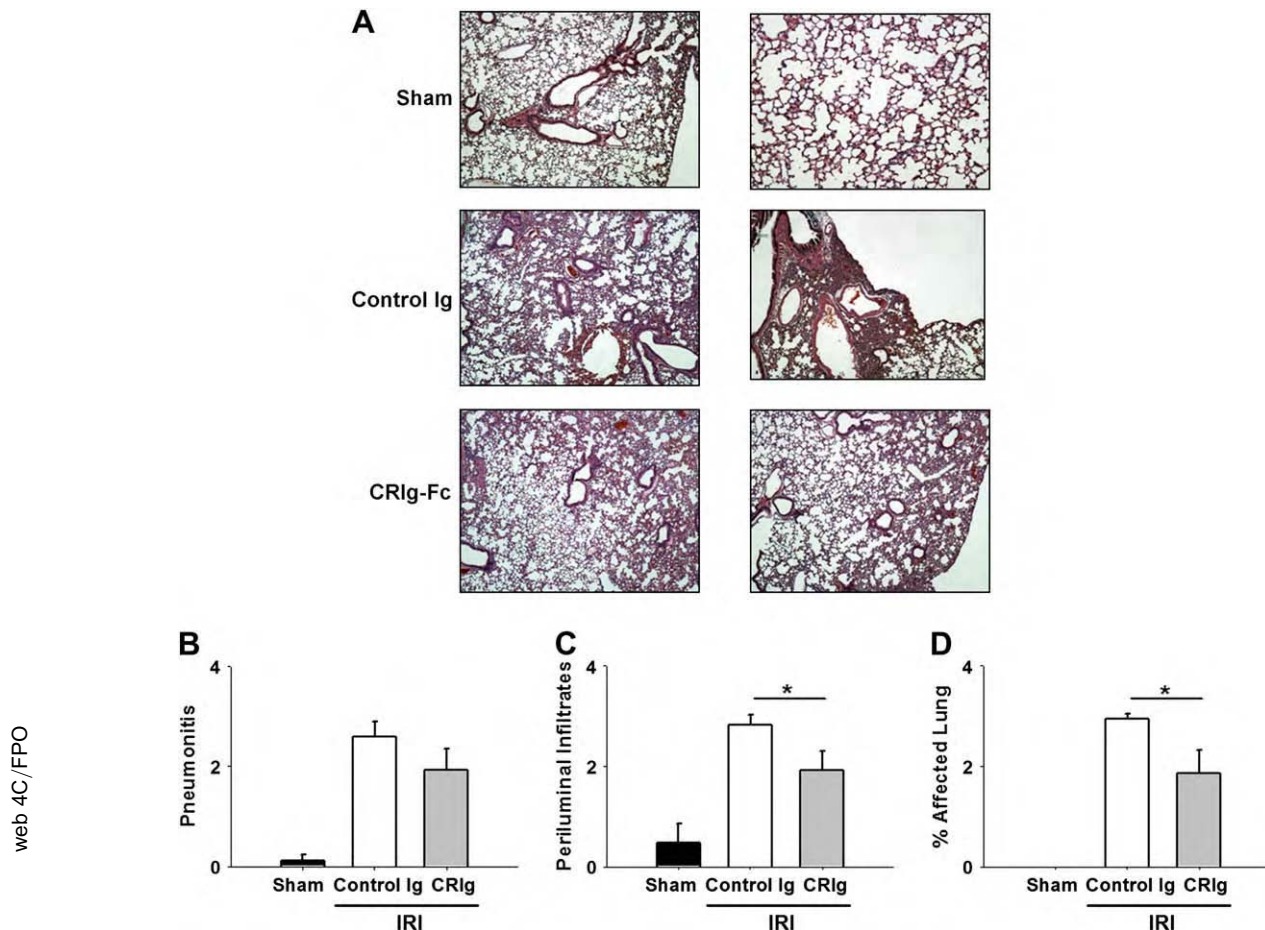


FIG. 2. CRIG-Fc treatment reduces remote organ damage induced by ischemia/reperfusion. (A) Representative photographs of lung sections from mice subjected to 30 min mesenteric ischemia followed by 3 h reperfusion. Upper panels show normal lung parenchyma; middle panels show dense infiltrates in a mouse that received control Ig; lower panels show milder inflammation in a mouse treated with CRIG-Fc. Lung inflammation was evaluated considering three parameters: pneumonitis (B), periluminal infiltrates (C), and percentage of affected lung parenchyma (D). Treatment with CRIG significantly decreased the magnitude of the observed periluminal infiltrates, as well as the percentage of affected lung parenchyma (* $P < 0.02$). Although CRIG showed a tendency to diminish pneumonitis, the difference did not reach statistical significance.

incubated overnight with primary antibodies (1:100). After thorough washing, secondary antibodies were incubated for 1 h. Sections were mounted using anti-fade solution (Slowfade Gold; Invitrogen, Carlsbad, CA). Finally, slides were scanned in a Nikon Eclipse Ti confocal microscope (Melville, NY). Images were analyzed with EZ-C1 ver. 3.6 software (Nikon). To quantify cellular infiltrates, digital photomicrographs of stained sections were processed with the Nikon NIS-Elements software. Five random fields (at a power of $\times 200$) were examined per tissue per animal in a blinded fashion.

Statistical Analyses

Student's *t*-test was used to compare data among groups. Data are expressed as mean \pm SD. A $P < 0.05$ was considered significant.

RESULTS

Inhibition of the Alternative Pathway Decreases Ischemia/Reperfusion-Induced Intestinal and Lung Injury

To determine whether inhibition of the alternative pathway of the complement was able to reduce tissue

damage induced by IR, we injected CRIG-Fc or an appropriate isotype control to B6 mice before subjecting them to 30 min mesenteric ischemia. As shown in Fig. 1, mice that received the control antibody developed intense intestinal injury after reperfusion (5.1 ± 0.04). In contrast, intestinal damage was significantly limited (3.9 ± 0.11 , $P = 0.001$) in mice that received CRIG-Fc.

The inflammation elicited in the ischemic tissue is distributed systemically when blood flow is restored, causing injury in distant organs such as the kidney and lungs. As shown in Fig. 2, treatment with CRIG-Fc also reduced significantly lung organ damage (Fig. 2). Pneumonitis diminished, albeit not significantly, in mice treated with CRIG-Fc (2.6 ± 0.3 versus 1.9 ± 0.4 ; $P = 0.09$). The magnitude of the periluminal infiltrates decreased significantly, from 2.8 ± 0.2 to 1.9 ± 0.4 in CRIG-Fc-treated animals ($P = 0.02$). Likewise, treated mice had a lower percentage of affected

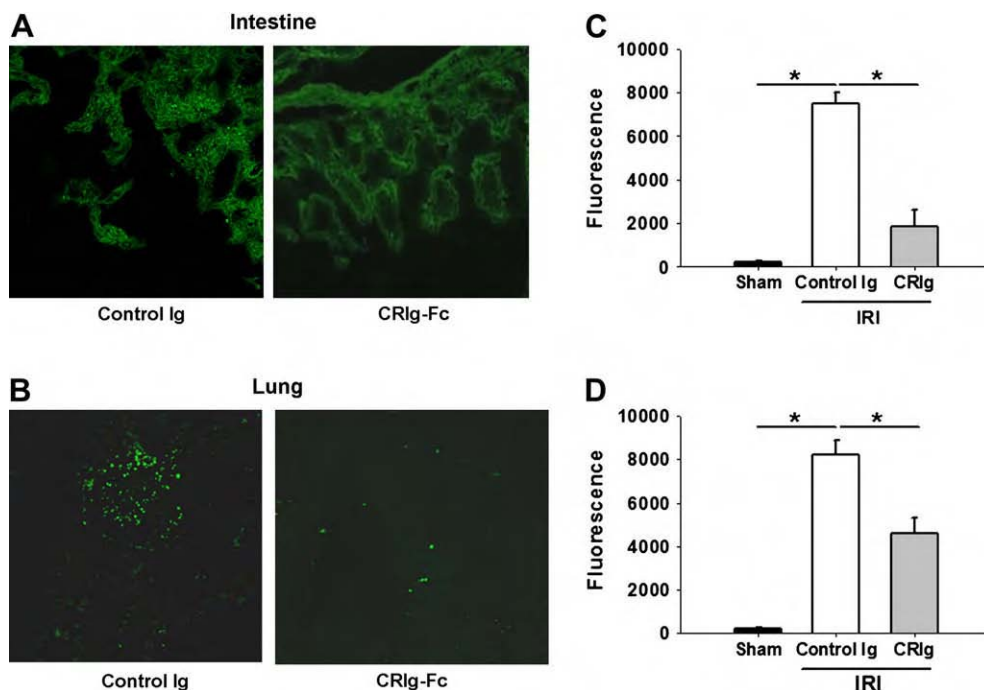


FIG. 3. CRlg-Fc reduces complement deposition in intestine and lung. Frozen sections from intestine (A) and lung (B) of mice treated with control Ig or CRlg-Fc prior to induction of ischemia/reperfusion were stained with anti-C3-FITC and scanned in a confocal microscope. Treatment with CRlg-Fc conspicuously decreased complement deposition in both organs. (C) Cumulative data ($n = 7$ mice per group) as quantified by an image-analyzing software (Nikon NIS-Elements). $*P < 0.001$

lung parenchyma than mice in which isotype control was administered (2.9 ± 0.1 versus 1.8 ± 0.5 ; $P = 0.02$). These results are summarized in Fig. 2.

Administration of CRlg-Fc Effectively Blocks Complement Deposition

IR-induced tissue injury leads to complement activation by the classic and MBL pathways [1]. In order to

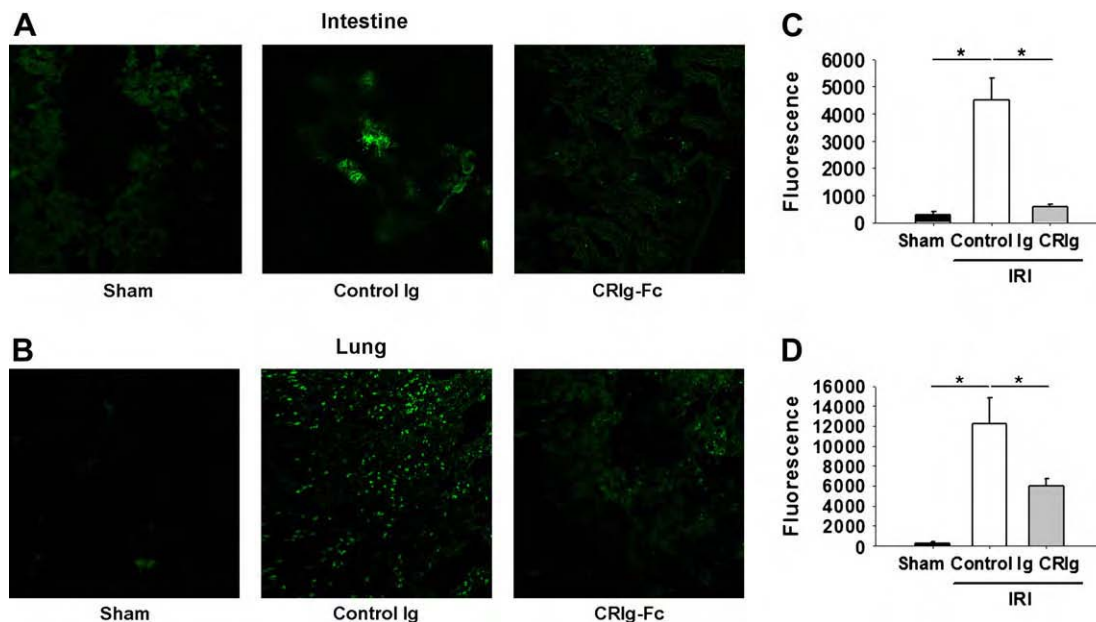


FIG. 4. CRlg-Fc reduces neutrophil infiltration in intestine and lung. Frozen sections from intestine (A) and lungs (B) of mice treated with control Ig or CRlg-Fc prior to induction of ischemia/reperfusion were stained with anti-Gr1-FITC and scanned in a confocal microscope. Treatment with CRlg-Fc decreased the number of neutrophils and inflammatory monocytes in both tissues. Cumulative data ($n = 7$ mice per group) of Gr-1⁺ cells in the intestine (C) and lung (D) as quantified by an image-analyzing software (Nikon NIS-Elements). $*P < 0.001$

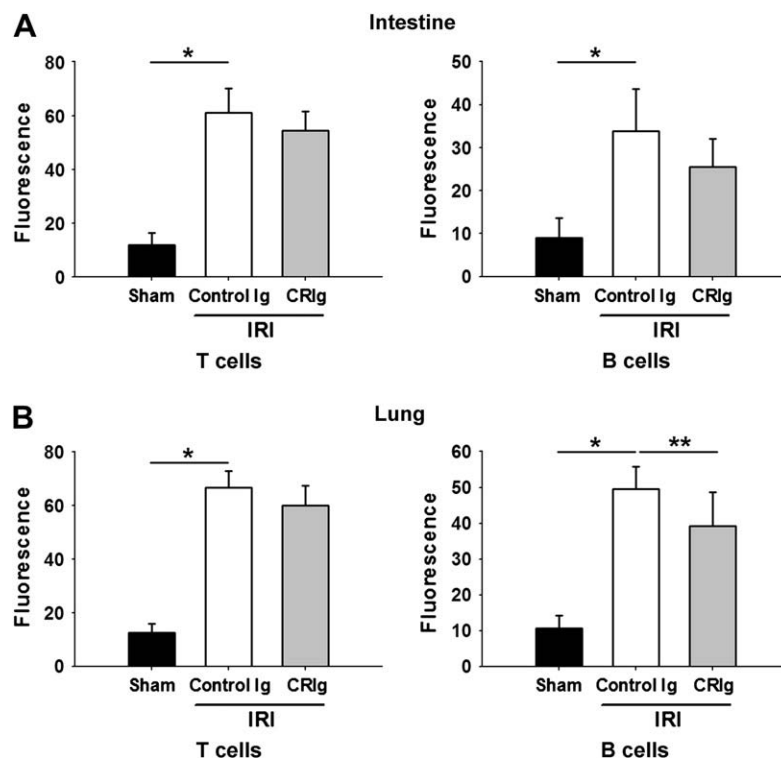


FIG. 5. CRIg-Fc has no significant effect on T and B cell infiltration. Sections from intestine (A) and lungs (B) of mice treated with control Ig or CRIg-Fc prior to induction of ischemia/reperfusion were stained by immunohistochemistry with rat anti-CD3 or rat anti-B220. Cells were quantified by counting positive cells in five high-power fields. Treatment with CRIg-Fc did not modify the numbers of intestine- and lung-infiltrating T cells; it did decrease the magnitude of B cell infiltration in the lung in a significant manner (* $P = 0.03$).

determine to what extent CRIg-Fc could block complement activation and deposition, we stained frozen sections from intestinal and lung tissues of mice subjected to IR. As shown in Fig. 3, treatment with CRIg-Fc effectively blocked C3 deposition in both organs.

CRIg-Fc Prevents Neutrophil Infiltration

Neutrophils are key mediators of IR-mediated tissue injury [15]. They enter the ischemic tissue early during reperfusion attracted by chemotactic factors, including C5a. Since CRIg-Fc blocked the activation and deposition of complement, we hypothesized that its protective effect could be mediated by the prevention of neutrophil infiltration. As shown in Fig. 4, CRIg-Fc decreased significantly the quantity of neutrophils in the intestine and lung 3 h after reperfusion ($P < 0.001$).

CRIg-Fc Does Not Affect Significantly the Magnitude of T and B Cell Infiltration

We have previously shown that T and B cells are important players in IR-mediated tissue injury [16, 17]. They enter the tissue during the first hours of reperfusion, guided by locally released chemokines [17]. We stained intestine and lung sections with anti-CD3 and anti-B220, and quantified the number of infiltrating T

and B cells. As shown in Fig. 5, IR led to a significant increase in the number of T and B cells in both intestine and lung parenchyma ($P < 0.01$). Treatment with CRIg-Fc did not modify the magnitude of T lymphocyte infiltration. It decreased B cell entry into lung parenchyma in a moderate, albeit statistically significant, fashion (Fig. 5).

DISCUSSION

In this article, we demonstrate that the complement alternative pathway inhibitor, CRIg-Fc, prevents local and remote tissue injury induced by IR. Such effect is accompanied by a significant reduction in C3 deposition in both intestine and lung, and is associated with an obvious reduction in tissue infiltration by Gr-1⁺ polymorphonuclear cells. We also show that protection is largely independent of T and B cell infiltration.

Complement activation is known to play a central role in the instigation and amplification of IR-mediated tissue injury [18]. Absence of complement factors, as well as inhibition of complement activation, have been shown to protect tissues from IR-initiated damage [2–4]. Complement activation in the setting of IR has been shown to involve mainly the classic and MBL pathways [7]. Natural autoantibodies present in normal serum bind to negatively charged phospholipids

exposed on ischemic cells and initiate the complement cascade [1, 19]. This phenomenon is exacerbated in autoimmune-prone mice by the presence of antiphospholipid and anti-DNA antibodies [9, 14]. The importance of the alternative pathway as an amplification mechanism has been observed in a variety of settings, including IR-mediated injury [6, 20] and murine models of antiphospholipid syndrome [21].

Inhibition of the alternative pathway has been shown to be protective against tissue injury in the model of intestinal IR [3, 22]. In this paper, we confirm these findings, and demonstrate that an infusible biologic CRIg-Fc can be used effectively in clinical settings that involve IR injury. We show that although C3 deposition and neutrophil infiltration are dramatically reduced in local and remote organs, T and B lymphocyte infiltration is not affected. Our findings suggest that IR-induced tissue infiltration by lymphocytes and neutrophils is guided by different signals. The absence of complement activation dampens injury produced by polymorphonuclear cells, but not by lymphocytes [16, 17].

The demonstration of CRIg-Fc as an effective inhibitor of IR-induced tissue injury adds a potential therapeutic option that may prove useful in the clinical setting. The effect of CRIg-Fc is limited to the inhibition of the alternative pathway convertases [12]. Because it does not block the activation of complement through the classic and MBL pathways, it does not block the initial steps of complement activation and, in this respect, it may limit the immunosuppression that results from indiscriminate suppression of the complement system.

In summary, we show that CRIg-Fc, an inhibitor of the complement alternative pathway, is able to protect from IR-induced local and remote organ damage in a neutrophil-dependent manner. Our results show that CRIg represents a candidate to limit IR injury as it occurs in various clinical conditions.

ACKNOWLEDGMENTS

The authors acknowledge support for this work by the RADII of Medical Research and Materiel Command, USA, Fort Detrick, MD. The authors would like to thank Dr. Menno van Lookeren Campagne for providing the Murine CRIg-Fc and the monoclonal anti-gp-120 IgG1 antibody that were used in this study.

REFERENCES

1. Fleming SD, Tsokos GC. Complement, natural antibodies, autoantibodies and tissue injury. *Autoimmun Rev* 2006;5:89.
2. Fleming SD, Mastellos D, Karpel-Massler G, et al. C5a causes limited, polymorphonuclear cell-independent, mesenteric ischemia/reperfusion-induced injury. *Clin Immunol* 2003;108:263.
3. Atkinson C, Song H, Lu B, et al. Targeted complement inhibition by C3d recognition ameliorates tissue injury without apparent increase in susceptibility to infection. *J Clin Invest* 2005; 115:2444.
4. Fleming SD, Anderson J, Wilson F, et al. C5 is required for CD49d expression on neutrophils and VCAM expression on vascular endothelial cells following mesenteric ischemia/reperfusion. *Clin Immunol* 2003;106:55.
5. Fleming SD. Natural antibodies, autoantibodies and complement activation in tissue injury. *Autoimmunity* 2006;39:379.
6. Stahl GL, Xu Y, Hao L, et al. Role for the alternative complement pathway in ischemia/reperfusion injury. *Am J Pathol* 2003; 162:449.
7. Williams JP, Pechet TT, Weiser MR, et al. Intestinal reperfusion injury is mediated by IgM and complement. *J Appl Physiol* 1999; 86:938.
8. Fleming SD, Shea-Donohue T, Guthridge JM, et al. Mice deficient in complement receptors 1 and 2 lack a tissue injury-inducing subset of the natural antibody repertoire. *J Immunol* 2002; 169:2126.
9. Fleming SD, Egan RP, Chai C, et al. Anti-phospholipid antibodies restore mesenteric ischemia/reperfusion-induced injury in complement receptor 2/complement receptor 1-deficient mice. *J Immunol* 2004;173:7055.
10. Girardi G, Berman J, Redecha P, et al. Complement C5a receptors and neutrophils mediate fetal injury in the antiphospholipid syndrome. *J Clin Invest* 1994;203:112.
11. Helmy KY, Katschke KJ, Jr., Gorgani NN, et al. CRIg: A macrophage complement receptor required for phagocytosis of circulating pathogens. *Cell* 2006;124:915.
12. Wiesmann C, Katschke KJ, Yin J, et al. Structure of C3b in complex with CRIg gives insights into regulation of complement activation. *Nature* 2006;444:217.
13. Katschke KJ, Jr., Helmy KY, Steffek M, et al. A novel inhibitor of the alternative pathway of complement reverses inflammation and bone destruction in experimental arthritis. *J Exp Med* 2007;204:1319.
14. Fleming SD, Monestier M, Tsokos GC. Accelerated ischemia/reperfusion-induced injury in autoimmunity-prone mice. *J Immunol* 2004;173:4230.
15. Simpson R, Alon R, Kobzik L, et al. Neutrophil and nonneutrophil-mediated injury in intestinal ischemia-reperfusion. *Ann Surg* 1993;218:444.
16. Edgerton C, Crispin JC, Moratz CM, et al. IL-17 producing CD4 + T cells mediate accelerated ischemia/reperfusion-induced injury in autoimmunity-prone mice. *Clin Immunol* 2009;130:313.
17. Chen J, Crispin JC, Tedder TF, et al. B cells contribute to ischemia/reperfusion-mediated tissue injury. *J Autoimmun* 2009; 32:195.
18. Tsokos CG, Fleming SD. Autoimmunity, complement activation, tissue injury and back. *Curr Dir Autoimmun* 2004;7:149.
19. Weiser MR, Williams JP, Moore FD, Jr., et al. Reperfusion injury of ischemic skeletal muscle is mediated by natural antibody and complement. *J Exp Med* 1996;183:2343.
20. Thurman JM, Holers VM. The central role of the alternative complement pathway in human disease. *J Immunol* 2006; 176:1305.
21. Girardi G, Redecha P, Salmon JE. Heparin prevents antiphospholipid antibody-induced fetal loss by inhibiting complement activation. *Nat Med* 2004;10:1222.
22. Huang Y, Qiao F, Atkinson C, et al. A novel targeted inhibitor of the alternative pathway of complement and its therapeutic application in ischemia/reperfusion injury. *J Immunol* 2008; 181:8068.

Complement Component C5a Mediates Hemorrhage-Induced Intestinal Damage

Sherry D. Fleming, Ph.D.,^{*1} Lauren M. Phillips, B.S.,^{*} John D. Lambris, Ph.D.,[†] and George C. Tsokos, M.D.[‡]

^{*}Division of Biology, Kansas State University, Manhattan, Kansas; [†]Pathology and Laboratory Medicine, University of Pennsylvania, Philadelphia, Pennsylvania; and [‡]Division of Rheumatology, Beth Israel Deaconess Medical Center, Harvard Medical School, Boston, Massachusetts

Submitted for publication September 1, 2007

Background. Complement has been implicated in the pathogenesis of intestinal damage and inflammation in multiple animal models. Although the exact mechanism is unknown, inhibition of complement prevents hemodynamic alterations in hemorrhage.

Materials and methods. C57Bl/6, complement 5 deficient (C5^{-/-}) and sufficient (C5^{+/+}) mice were subjected to 25% blood loss. In some cases, C57Bl/6 mice were treated with C5a receptor antagonist (C5aRa) post-hemorrhage. Intestinal injury, leukotriene B₄, and myeloperoxidase production were assessed for each treatment group of mice.

Results. Mice subjected to significant blood loss without major trauma develop intestinal inflammation and tissue damage within 2 hours. We report here that complement 5 (C5) deficient mice are protected from intestinal tissue damage when subjected to hemorrhage (injury score = 0.36 compared with wildtype hemorrhaged animal injury score = 2.89; $P < 0.05$). We present evidence that C5a represents the effector molecule because C57Bl/6 mice treated with a C5a receptor antagonist displayed limited intestinal injury (injury score = 0.88), leukotriene B₄ (13.16 pg/mg tissue), and myeloperoxidase (115.6 pg/mg tissue) production compared with hemorrhaged C57Bl/6 mice ($P < 0.05$).

Conclusions. Complement activation is important in the development of hemorrhage-induced tissue injury and C5a generation is critical for tissue inflammation and damage. Thus, therapeutics targeting C5a may be useful therapeutics for hemorrhage-associated injury. © 2008 Elsevier Inc. All rights reserved.

Key Words: complement; mucosa; rodent.

INTRODUCTION

Hemorrhage and the accompanying hemorrhagic shock result in clinical complications and systemic inflammation [1, 2]. During hemorrhage, there is decreased systemic perfusion, leading to decreased blood flow to the intestine, kidney, and skeletal muscle [3, 4]. As the intestine normally receives more blood from the heart than any other organ with the splanchnic circulation consisting of up to 25% to 30% of the total blood volume, hemorrhage-induced decreased intestinal blood flow and associated vasoconstriction may result in a functional intestinal ischemia [5]. In other models of ischemia, this process leads to local and systemic damage and is suggested to be critical in the induction of multiple organ failure [6]. Mechanisms of ischemia and subsequent reperfusion-induced intestinal mucosal injury include oxidative stress and excessive complement activation [7–9].

Excessive complement activation results in tissue damage in many animal models, including septic shock, transplantation, and mesenteric or skeletal muscle ischemia (reviewed in [10]). Previously, we showed that C5a has a significant role in a mouse model of intestinal ischemia/reperfusion-induced damage and eicosanoid production [8]. In addition, others have shown that C5 and specifically, C5a is critical for neutrophil and monocyte chemotaxis in either myocardial or mesenteric ischemic models [11–14]. Finally, in a renal ischemia/reperfusion model, C5a blockade prevents damage that is not dependent on neutrophil infiltration, but by alteration of the chemokine profile [13]. Thus, therapeutics that target complement activation in the intestine prevent damage in other animal models and the same therapeutics may be beneficial in hemorrhage.

¹To whom correspondence and reprint requests should be addressed at Division of Biology, 18 Ackert Hall, Kansas State University, Manhattan, KS 66506. E-mail: sdflemin@ksu.edu.



Complement activation is also critical in rat models of hemorrhagic shock. Depletion of complement prevented clinical signs of hemorrhagic shock [15] and hemodynamic changes were prevented with complement inhibition with soluble complement receptor 1 [3, 16] or C1-inhibitor [17]. Recent studies showed that anti-C5 antibody treatment decreases the resuscitation fluid volume required to improve mean arterial pressure [18]. Total inhibition of complement activation and the membrane attack complex, however, may lead to sepsis and other infectious complications due to the inhibition of all complement cascades. It is critical therefore, to identify the specific molecules involved in the complement mediated damage to achieve targeted complement inhibition. Excess of C5a is lethal in a rat hemorrhage model [15] and a C5a receptor antagonist decreased the inflammatory response within rat intestine and lungs in a model of intestinal ischemia with hemorrhage [19]. However, it is unclear if inhibition of C5a activity is sufficient to prevent or attenuate intestinal damage and its sequelae.

Many animal models of hemorrhage involve rats and include traumatic injury [19–24] and the use of heparin [3, 16], which complicates determination of the complement activation factors. In addition, rat models of hemorrhagic shock preclude the use of genetically modified animals.

Here we show that in the absence of major trauma, loss of one-quarter of the total blood volume in mice results in significant intestinal inflammation and damage. We present evidence that C5 deficient mice do not develop signs of inflammation and tissue damage and more importantly, blockade of the action of C5a with a synthetic C5a receptor antagonist limited tissue damage in wild type mice.

MATERIALS AND METHODS

Mice

C57Bl/6, B10.D2-Hc⁰H2^dH2-T18⁰SnJ and B10.D2-Hc¹H2^dH2-T18ⁿSnJ (C5^{-/-} and C5^{+/+}, respectively) male mice (6 to 8 wk old) were obtained from The Jackson Laboratory (C5^{+/+}, and C5^{-/-}) or bred (C57Bl/6) and maintained in the Division of Biology at Kansas State University. All mice were allowed food and water *ad libitum* and kept in 12-h light-to-dark facilities. Research was conducted in compliance with the Animal Welfare Act and other federal statutes and regulations relating to animals and experiments involving animals, and experiments were performed according to the principles set forth in the Guide for the Care and Use of Laboratory Animals (Institute of Laboratory Animal Resources, National Research Council, 1996 edition).

Hemorrhage Protocol

After a 1-wk acclimatization period, mice were anesthetized using ketamine (16 mg/kg) and xylazine (80 mg/kg). All procedures were performed with the animals breathing spontaneously and body temperature maintained at 37°C using a water-circulating heating pad. Mice undergoing hemorrhage were subjected to retro-orbital removal of 25% of the calculated blood volume (approximately 0.5 mL) over a 90 s period [25, 26]. Volume of blood to be removed was based on weight and ranged from 400 μ L to 600 μ L; (body weight in grams \times

0.02 [27]. The determined blood volume was measured in water and marked on both the collection tubes and the capillary tubing used for retro-orbital punctures. This ensured that the correct amount would be withdrawn. A single retro-orbital puncture was sufficient for blood collection. The 2 h mortality rate was less than 1%. Sham mice were subjected to similar procedures with no blood removal. In some studies, the murine C5aRa (25 μ g/mouse) was injected intravenously 5 to 15 min after either hemorrhage or sham treatment [28]. An additional experimental group consisted of mice subjected to hemorrhage followed 1 h later by administration of 200 μ L normal saline i.v. C5aRa was synthesized and similar dosages administered as described previously [28]. To prevent spontaneous complement activation, all studies were performed in the absence of heparin. At 2 h post-hemorrhage, mice were euthanized and tissues collected for analysis. Intestinal tissues were formalin fixed for analysis of injury and frozen sections were obtained for immunohistochemistry.

Injury Score

Formalin fixed tissue sections were transversely sectioned and H and E stained for analysis of injury. Injury was scored by an observer unaware of the treatment given using a six-tiered scale adapted from Chiu *et al.* that was described previously [7, 8, 29]. The average damage score was assigned to an approximately 2 cm section of mid-jejunum intestine (75 to 150 villi) after grading each villus from 0–6. Normal villi were assigned a score of zero; villi with tip distortion were assigned a score 1; score 2 was assigned when Guggenheims' spaces were present; villi with patchy disruption of the epithelial cells were assigned a score of 3; score 4 was assigned to villi with exposed but intact lamina propria with epithelial sloughing; a score of 5 was assigned when the lamina propria was exuding; and villi that displayed hemorrhage or were denuded were assigned a score of 6.

Villus Height/Crypt Depth

Villus height/crypt depth ratio of at least 15 individual villi per animal was measured using MetaVue computer software (Molecular Devices, Sunnyvale, CA). The average of three to eight animals per treatment group is reported.

Leukotriene B₄, Myeloperoxidase, and Total Peroxidase Production

Ex vivo intestinal supernatants were generated for total peroxidase, leukotriene B₄ (LTB₄), and myeloperoxidase (MPO) analysis as described previously [30, 31]. Briefly, 1 cm mid-jejunum sections were minced, washed, and resuspended in oxygenated Tyrode's buffer (Sigma, St. Louis, MO) for 20 min at 37°C. Following incubation, the supernatants and tissues were collected and stored at –80°C until assayed. Commercially available LTB₄ EIA kit (Cayman Chemicals #520111; Cayman Chemicals, Ann Arbor, MI) and MPO specific enzyme-linked immunosorbent assay kit (Cell Sciences #HK201; Cell Sciences, Canton, MA) were used to determine LTB₄ and MPO concentrations. Total tissue peroxidase was determined by incubating supernatants with 3, 3', 5, 5' tetramethylbenzidine (KPL Chemicals, Rockville, MD) and the reaction stopped with 0.18 M sulfuric acid. The OD450 was determined and compared with a horseradish peroxidase (Sigma) standard. The concentration of each factor was reported as pg/mg intestinal tissue.

Immunohistochemistry

Tissues snap frozen in TBS freezing media (ThermoFisher, Waltham, MA) were sectioned at 6 to 8 μ for immunohistochemistry staining as described previously [7, 8]. Briefly, nonspecific antibody binding sites were blocked by treatment with a solution of 20% rabbit serum (Jackson ImmunoResearch, West Grove, PA) in phosphate-buffered saline (PBS) for 30 min prior to incubation with rabbit anti-mouse C3 antibody (Cell Sciences #HP8012) overnight at 4°C. The

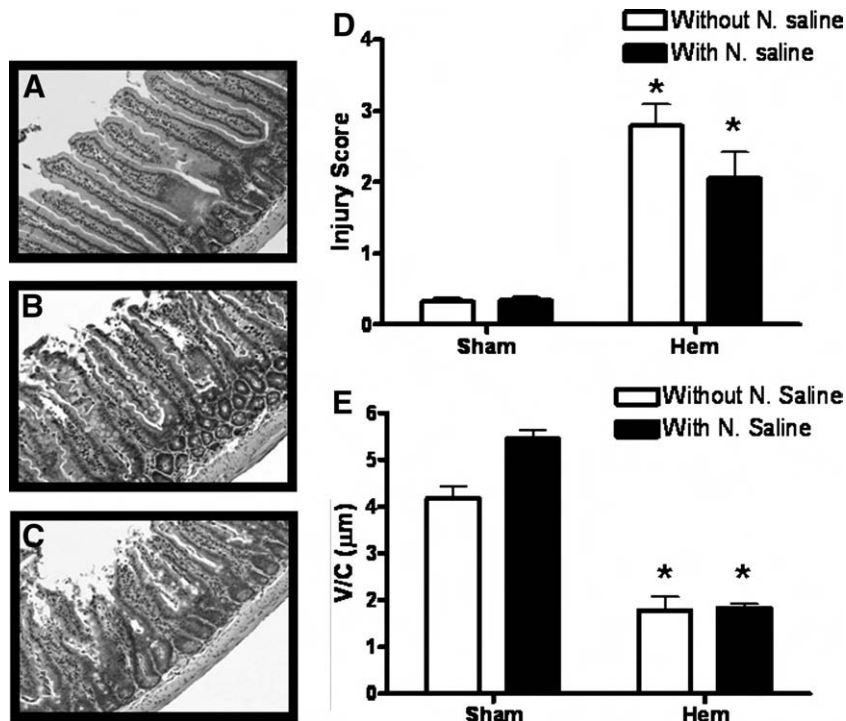


FIG. 1. Hemorrhage induces intestinal injury. Wildtype mice which were subjected to sham treatment (A) or hemorrhage (B) followed by a 2 h recovery period. Intestinal sections were stained with H and E. Additional mice were subjected to hemorrhage followed by an injection of normal saline (C). Formalin fixed intestinal sections from each treatment group were scored for mucosal injury (0–6) as described in the Materials and Methods section (D). Open bars represent no resuscitation fluid, solid bars represent resuscitation fluids were administered. Each bar represents the average \pm SEM with 4 to 10 mice per group. Villus height/crypt depth ratio of individual villi was measured using Metavue computer software (E). All measurements were obtained at a $\times 200$ magnification. Open bars represent no normal saline, solid bars represent normal saline was administered. Each bar is the average \pm SEM with 3 mice per group. Using ANOVA with Newman-Keuls post hoc test, the asterisk indicates significant difference from the respective sham treatment group ($P \leq 0.05$).

tissue was then incubated with donkey anti-rabbit secondary antibody conjugated to Texas Red (Jackson ImmunoResearch). After washing, the slides were mounted with ProLong Gold (Invitrogen, Carlsbad, CA). A blinded observer examined the slides by fluorescent microscopy using a Nikon 80i fluorescent microscope equipped with appropriate filters and CoolSnapCf camera (Photometrics, Tucson, AZ) and analyzed by MetaVue Imaging software (Molecular Devices).

Statistics

The data are presented as mean \pm SEM and compared by one-way analysis of variance (ANOVA) with Neuman-Keuls post hoc analysis (GraphPad, San Diego, CA). Differences were considered significant when $P < 0.05$.

RESULTS

Hemorrhage Induces Intestinal Damage

A recent study showed that during porcine hemorrhage, intestinal blood flow decreased proportionally to total volume, but these studies did not examine the extent of intestinal damage [4]. To confirm that blood loss induced intestinal damage, mice were sham-treated or retro-orbitally bled to remove 25% blood volume based on weight. Previous reports indicated that removal of 25% blood volume induced liver dam-

age and inflammation [27]. In addition, preliminary data indicated the presence of significant intestinal damage. Intestinal tissues were collected 2 h post-bleeding and analyzed for mucosal injury. As shown in Fig. 1A and D, sham treatment did not result in damage of the intestines as indicated by preservation of villi tips (Fig. 1A) and low injury score (Fig. 1D). In contrast, significant mucosal damage occurred at 2 h post-hemorrhage as shown in Fig. 1B and D. Intestinal damage at 2 h post-hemorrhage included disintegration of the epithelial integrity and exuding lamina propria from the villi (Fig. 1B), which resulted in increased injury score (Fig. 1D). Also indicative of damage, hemorrhage resulted in significantly shorter villi without altering the crypt depth as indicated by villus height/crypt depth ratio (Fig. 1E).

Previous studies indicate that administration of even small volumes of normal saline, alters inflammation and organ damage [18, 20]. Because future studies will require treatment with small volumes of complement inhibitor suspended in saline, it was necessary to determine if these quantities of saline altered intestinal damage and inflammation. Therefore, some groups of both sham and hemorrhaged mice were adminis-

C57Bl/6 mice, the complement sufficient mice subjected to hemorrhage developed significant intestinal damage (Fig. 3A and B) manifested by increased injury scores and decreased villus height/crypt depth ratio compared with sham-treated mice. In contrast, hemorrhage-induced intestinal damage was significantly attenuated in C5^{-/-} mice compared with the C5^{+/+} mice with mean injury scores of 0.36 and 2.89, respectively (Fig. 3A, B, and C). Villi remained tall, the villus height/crypt depth ratio did not change, and the epithelial layer remained intact in C5^{-/-} mice after hemorrhage (Fig. 3C). As expected, C3 was deposited in both C5^{+/+} and C5^{-/-} mice despite the lack of damage (data not shown).

Excessive inflammation, characterized by neutrophil infiltration, mediates hemorrhage-induced liver and lung injury [17, 26, 32]. To determine if hemorrhage induces intestinal neutrophil infiltration, the production of chemotactic factor LTB₄ was determined. As shown in Fig. 4A, hemorrhage induced significant LTB₄ production. In addition, intestinal tissues from hemorrhaged, complement sufficient mice contained increased amounts of myeloperoxidase when compared with sham-treated mice (Fig. 4B). In contrast, when C5^{-/-} mice were subjected to hemorrhage, the release of LTB₄ was significantly reduced, suggesting that the recruitment of neutrophils to the intestine is complement dependent (Fig. 4A). In addition, intestinal tissue from C5^{-/-} mice subjected to hemorrhage did not contain any myeloperoxidase (Fig. 4B).

C5a Receptor Antagonist Attenuates Intestinal Damage and Inflammation

We considered it likely that C5a generated following complement activation is responsible for the observed neutrophil infiltration in C5 sufficient mice subjected to hemorrhage and that inhibition of its action would limit the inflammatory response and tissue damage. To test this possibility we treated male C57Bl/6 mice with murine C5a receptor antagonist or an equivalent vol-

ume of PBS 5–10 min after hemorrhage. In contrast to the PBS-treated C57Bl/6 mice (Fig. 5B), mice injected with C5a receptor antagonist displayed attenuated intestinal mucosal damage (Fig. 5C) with pathology similar to that recorded in the sham group of animals (Fig. 5A). Hemorrhage-induced intestinal injury was decreased significantly in C5a receptor antagonist-treated mice compared to the PBS-treated group of hemorrhaged mice and was comparable to tissue injury observed in the sham group of mice (Fig. 5D). C5a production occurs downstream of C3 activation; therefore, C5a receptor antagonist should not alter C3 deposition. C5a receptor antagonist treatment did not limit the amounts of C3 deposited to the intestine of hemorrhaged mice (Figs. 2 and 6) and the observed C3 deposition in these mice was increased compared to the sham group of animals (Fig. 6A and B). As expected, administration of C5a receptor antagonist decreased LTB₄ production in both sham and hemorrhaged mice (Fig. 7A) and eliminated the hemorrhage-induced increase in myeloperoxidase content (Fig. 7B). Together these data indicate that C5a receptor antagonist can attenuate the hemorrhage-induced chemotactic activity and intestinal tissue damage.

DISCUSSION

Hemorrhage induces intestinal mucosal damage and inflammation with complement activation and influx of neutrophils [3, 16]. Complement inhibition prevents intestinal damage and decreases vasoconstriction and the subsequent requirement for fluid to maintain the mean arterial pressure [18, 19, 33]. Our study shows that low blood volume also leads to intestinal damage and inflammation in complement sufficient but not in C5 deficient mice. C5a which is produced during complement activation appears to be the culprit because inhibition of its action by C5a receptor antagonist limits both the inflammatory response and intestinal tissue damage.

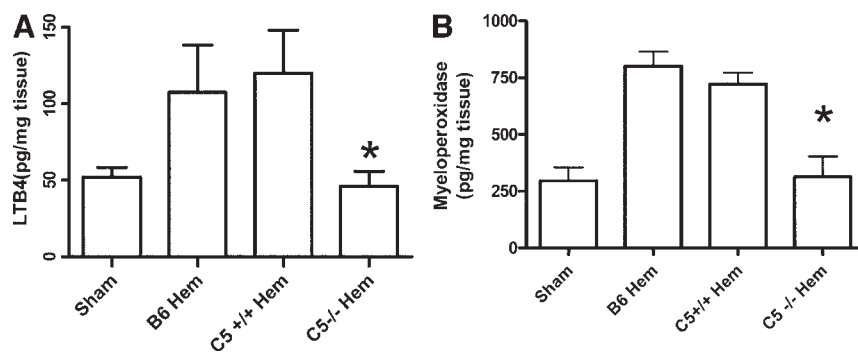


FIG. 4. Hemorrhage induces a complement-dependent inflammatory response. *Ex vivo*, intestinal LTB₄ (A) and myeloperoxidase (B) production from each treatment group was determined by enzyme immunoassays as described in the Materials and Methods section. Each bar represents the average \pm SEM with four to six animals per group. Using ANOVA with Newman-Keuls post hoc test, the asterisk indicates significant difference from the wildtype treatment groups.

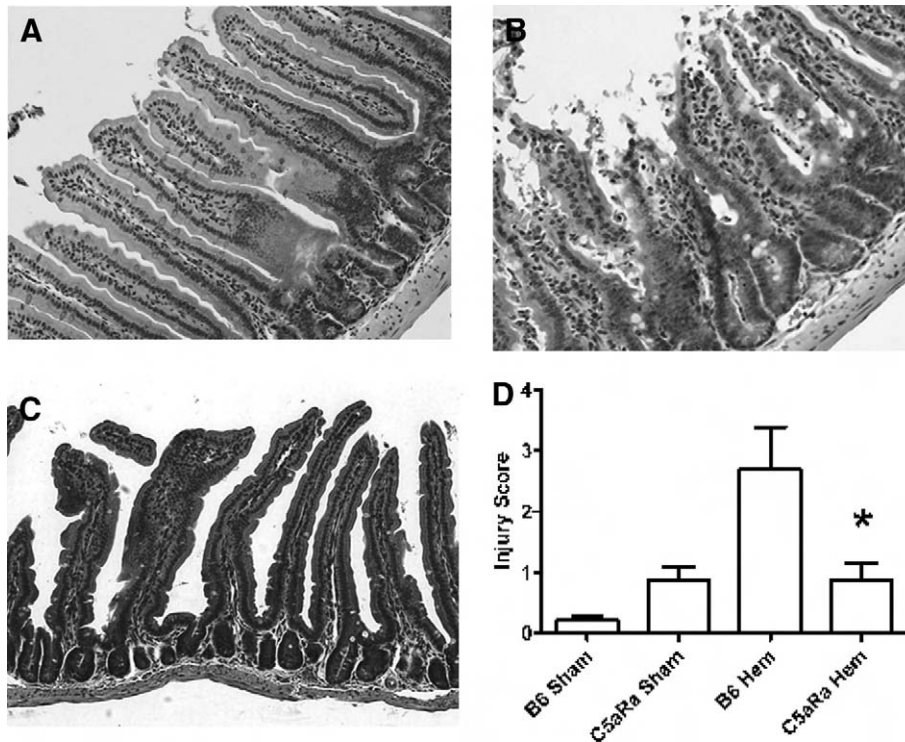


FIG. 5. Administration of C5a receptor antagonist after hemorrhage prevents intestinal damage. H and E intestinal sections of wildtype mice (B6) with (A) and (C) or without (B) C5a receptor antagonist (C5aRa) treatment were subjected to sham treatment (A) or hemorrhage (B) and (C). Mucosal injury (0–6) was determined as described in the Materials and Methods section (D). Using ANOVA with Newman-Keuls post hoc test, the asterisk indicates significant difference from C57Bl/6 hemorrhage group (B6 Hem).

Complement is known to have a role in the intestinal damage, but the specific pathway or molecules involved are unknown. In ischemia and sepsis models of intestinal damage, C5a has been shown to be required for neutrophil infiltration [8, 14, 19, 34, 35]. Inhibition of C3a and C5a in rat models of hemorrhage or hemorrhage with vascular clamping prevented decrease in mean arterial pressure and the appearance of acidosis, intestinal permeability and tissue damage [15, 19]. Our studies extend these observations and suggest the recorded beneficiary effects of complement inhibition on physiological parameters such as mean arterial blood pressure and acid-base balance are probably due

to the preceding inhibition of the tissue inflammatory response and damage. Indeed, the administration of C5a receptor antagonist limited the production of the chemotactic factor, LTB_4 , and the infiltration of the intestinal tissue by neutrophils as manifested by decreased myeloperoxidase content. C5a receptor antagonist has been shown to be effective in other animal models of inflammation [35, 36], including a murine model of mesenteric ischemia/reperfusion [8].

In many animal models, C5a and selective C5a agonists induce hypotension and vascular permeability which are inhibited by blockade of C5a receptor binding [19, 33]. In other animal models, C5a receptor

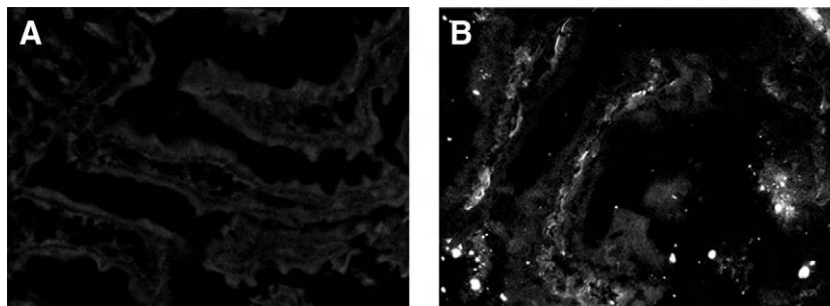


FIG. 6. C5a receptor antagonist does not prevent C3 deposition on intestinal tissue. Wildtype mice were subjected to sham (A) or hemorrhage (B) prior to treatment with C5a receptor antagonist (C5aRa), and frozen intestinal sections were stained for C3 deposition as described in the Materials and Methods section. Original magnification is $\times 200$. Data are representative of three individual experiments.

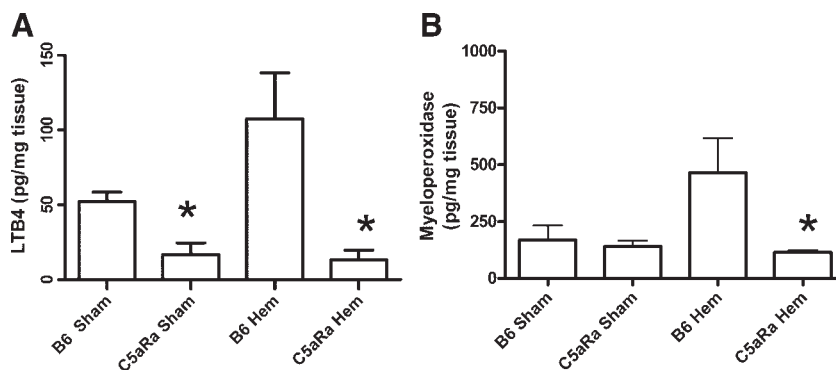


FIG. 7. C5a receptor antagonist attenuates leukotriene B4 and myeloperoxidase production in response to hemorrhage. *Ex vivo*, intestinal LTB₄ (A) and myeloperoxidase (B) production by each treatment group was determined by enzyme immunoassays as described in the Materials and Methods section. Each bar is average \pm SEM with three to eight animals per group. Using ANOVA with Newman-Keuls post hoc test, asterisks indicate significant difference from the respective wildtype treatment groups (B6).

antagonists attenuate the cobra venom factor mediated or xenotransplant-induced blood pressure changes [37, 38]. However, in other hemorrhage studies, complement depletion did not significantly alter mean arterial pressures within the first 2 h after hemorrhage [15]. Thus, it is possible that administration of the C5 receptor antagonist prevents the hemorrhage-induced hypotension. Additional studies will be needed to determine the exact mechanism of protection provided by the C5a receptor antagonist.

It is possible that the administration of C5 receptor antagonist alters the cytokine milieu that leads to intestinal damage. Previous studies have illustrated that monocytes treated with C5a produce IL-6 [39]. Other studies have shown that hemorrhage increases KC, MCP-1, IL-6 and IL-10 serum concentrations in a TLR4-dependent manner [22, 40, 41]. In addition, Meng *et al.* showed that IL-6 is critical for the induction of lung and liver damage in response to hemorrhage [32]. Therefore, IL-6 and possibly other cytokines or chemokines may be involved in hemorrhage-induced intestinal damage and it is possible that C5a receptor antagonist alters the inflammatory cytokine response.

Previous studies have shown that complement inhibition prevents intestinal damage and decreased vasoconstriction in rat models of hemorrhage [3, 16]. In a rat model of hemorrhage and mesenteric ischemia, the combination of heparin and C5a receptor antagonist decreased intestinal permeability and tumor necrosis factor production [19]. The unavoidable use of heparin in practically all hemorrhage models complicates the interpretation of the data because of the extensive interaction of the complement and coagulation activation cascades [42]. Our studies offer a unique model to study the role of complement activation in a murine model of hemorrhage without the interference of confounding factors such as trauma, tubing and the need for anti-coagulation drugs.

In conclusion, we present evidence in a simple model of murine hemorrhage which does not involve the use

of trauma or anti-coagulants that complement activation is responsible for inflammation and tissue damage in the intestine. C5 deficient mice were found to be completely protected from hemorrhage-induced intestinal damage and the administration of a C5a receptor antagonist limits both the inflammatory response and tissue damage in the intestine of mice subjected to hemorrhage. The use of complement inhibitors may therefore be of clinical value in people who hemorrhage and they may limit the need for resuscitation fluids.

ACKNOWLEDGMENTS

This study was supported by the following: a grant from the Department of Defense (to G.C.T. and to S.D.F.), NIH grants GM-62134 (to J.D.L.), and P20-RR017686 and P20-RR016475 from the Institutional Development Award (IDeA) Program of the NCRR, HHMI Undergraduate Science Educational Grant, Terry C. Johnson Center for Cancer Research, and the Division of Biology, Kansas State University, (to S.D.F.).

LMP was supported as an HHMI Undergraduate Scholar.

The authors thank Tiffany Moses and Diana Hylton for their technical expertise.

The opinions or assertions contained herein are the private views of the authors and are not to be construed as official or reflecting the views of the United States Department of the Army, or the United States Department of Defense.

REFERENCES

- DeBakey ME, Simeone FA. Battle injuries of the arteries in World War II: An analysis of 2,471 cases. *Ann Surg* 1946;123:534.
- Bellamy RF. The causes of death in conventional land warfare: Implications for combat casualty care research. *Military Med* 1984;149:55.
- Fruchterman TM, Spain DA, Wilson MA, et al. Complement inhibition prevents gut ischemia and endothelial cell dysfunction after hemorrhage/resuscitation. *Surgery* 1998;124:782.
- Kvarstein G, Mirtheri P, Tonnessen TI. Detection of organ ischemia during hemorrhagic shock. *Acta Anaesthesiol Scand* 2003;675.
- Shea-Donohue T, Anderson J, Swiecki C. Ischemia/reperfusion injury. In: Tsokos GC, Atkins JL, Eds. *Combat Medicine*. Totowa, NJ: Humana Press, 2003:219–248.

6. Tavaf-Motamen H, Miner TJ, Starnes BW, et al. Nitric oxide mediates acute lung injury by modulation of inflammation. *J Surg Res* 1998;78:137.
7. Fleming SD, Anderson J, Wilson F, et al. C5 is required for CD49d expression on neutrophils and VCAM expression on vascular endothelial cells following mesenteric ischemia/reperfusion. *Clin Immunol* 2003;105:55.
8. Fleming SD, Mastellos D, Karpel-Massler G, et al. C5a causes limited, polymorphonuclear cell-independent, mesenteric ischemia/reperfusion-induced injury. *Clin Immunol* 2003;108:263.
9. Rehrig S, Fleming SD, Anderson J, et al. Complement inhibitor, complement receptor 1-related gene/protein γ -Ig attenuates intestinal damage after the onset of mesenteric ischemia/reperfusion injury in mice. *J Immunol* 2001;167:5921.
10. Fleming SD, Tsokos GC. Complement inhibitors in rheumatic diseases. In: Tsokos GC, Ed. *Modern therapeutics in Rheumatic Diseases*. Totowa, NJ: Humana Press, 2000:443–452.
11. Birdsall HH, Green DM, Trial J, et al. Complement C5a, TGF- β 1, and MCP-1, in sequence, induce migration of monocytes into ischemic canine myocardium within the first 1 to 5 hours after reperfusion. *Circulation* 1997;95:684.
12. Ivey CL, Williams FM, Collins PD, et al. Neutrophil chemoattractants generated in two phases during reperfusion of ischemic myocardium in the rabbit: Evidence for a role for C5a and interleukin-8. *J Clin Invest* 1995;95:2720.
13. de Vries B, Kohl J, Leclercq WKG, et al. Complement factor C5a mediates renal ischemia/reperfusion injury independent of neutrophils. *J Immunol* 2003;170:3883.
14. Arumugam TV, Shiels IA, Woodruff TM, et al. Protective effect of a new C5a receptor antagonist against ischemia/reperfusion injury in the rat small intestine. *J Surg Res* 2002;103:260.
15. Younger JG, Sasaki N, Waite MD, et al. Detrimental effects of complement activation in hemorrhagic shock. *J Appl Physiol* 2001;90:441.
16. Spain DA, Fruchterman TM, Matheson PJ, et al. Complement activation mediates intestinal injury after resuscitation from hemorrhagic shock. *J Trauma* 1999;46:224.
17. Horstick G, Kempf T, Lauterbach M, et al. C1-esterase-inhibitor treatment at early reperfusion of hemorrhagic shock reduces mesentery leukocyte adhesion and rolling. *Microcirculation* 2001;8:427.
18. Peckham RM, Handrigan MT, Bentley TB, et al. C5-blocking antibody reduces fluid requirements and improves responsiveness to fluid infusion in hemorrhagic shock managed with hypotensive resuscitation. *J Appl Physiol* 2007;102:673.
19. Harkin DW, Romaschin A, Taylor SM, et al. Complement C5a receptor antagonist attenuates multiple organ injury in a model of ruptured abdominal aortic aneurysm. *J Vasc Surg* 2004;39:196.
20. Homma H, Deitch EA, Feketeova E, et al. Small volume resuscitation with hypertonic saline is more effective in ameliorating trauma-hemorrhagic shock-induced lung injury, neutrophil activation, and red blood cell dysfunction than pancreatic protease inhibition. *J Trauma* 2005;59:266.
21. Kiang JG, Peckham RM, Duke LE, et al. Androstenediol inhibits the trauma-hemorrhage-induced increase in caspase-3 by down-regulating the inducible nitric oxide synthase pathway. *J Appl Physiol* 2007;102:933.
22. Thobe BM, Frink M, Hildebrand F, et al. The role of MAPK in Kupffer cell toll-like receptor (TLR) 2-, TLR4-, and TLR9-mediated signaling following trauma-hemorrhage. *J Cell Physiol* 2007;210:667.
23. Hildebrand F, Thobe BM, Hubbard WJ, et al. Effects of 17 β -estradiol and flutamide on splenic macrophages and splenocytes after trauma-hemorrhage. *Cytokine* 2006;36:107.
24. Hildebrand F, Hubbard WJ, Choudhry MA, et al. Kupffer cells and their mediators: The culprits in producing distant organ damage after trauma-hemorrhage. *Am J Pathol* 2006;169:784.
25. Lomas-Niera JL, Perl M, Chung C-S, et al. Shock and hemorrhage: An overview of animal models. *Shock* 2005;24:33.
26. Arcaroli J, Yang KY, Yum HK, et al. Effects of catecholamines on kinase activation in lung neutrophils after hemorrhage or endotoxemia. *J Leukoc Biol* 2002;72:571.
27. Rajnik M, Salkowski CA, Thomas KE, et al. Induction of early inflammatory gene expression in a murine model of non-resuscitated, fixed-volume hemorrhage. *Shock* 2002;17:322.
28. Mastellos D, Papadimitriou JC, Franchini S, et al. A novel role of complement: Mice deficient in the fifth component of complement (C5) exhibit impaired liver regeneration. *J Immunol* 2001;166:2479.
29. Chiu C-J, McArdle AH, Brown R, et al. Intestinal mucosal lesion in low-flow states. *Arch Surg* 1970;101:478.
30. Fleming SD. Natural antibodies, autoantibodies, and complement activation in tissue injury. *Autoimmunity* 2006;39:379.
31. Fleming SD, Monestier M, Tsokos GC. Accelerated ischemia/reperfusion-induced injury in autoimmunity-prone mice. *J Immunol* 2004;173:4230.
32. Meng ZH, Dyer K, Billiar TR, et al. Essential role for IL-6 in post-resuscitation inflammation in hemorrhagic shock. *Am J Physiol Cell Physiol* 2001;280:C343.
33. Harkin DW, Marron CD, Rother RP, et al. C5 complement inhibition attenuates shock and acute lung injury in an experimental model of ruptured abdominal aortic aneurysm. *Br J Surg* 2005;92:1227.
34. Czermak BJ, Sarma V, Pierson CL, et al. Protective effects of C5a blockade in sepsis. *Nat Med* 1999;5:788.
35. Riedemann NC, Guo RF, Neff TA, et al. Increased C5a receptor expression in sepsis. *J Clin Invest* 2002;110:101.
36. Heller T, Henneke M, Baumann U, et al. Selection of a C5a receptor antagonist from phage libraries attenuating the inflammatory response in immune complex disease and ischemia/reperfusion injury. *J Immunol* 1999;163:985.
37. Gaca JG, Appel JZ III, Lukes JG, et al. Effect of an anti-C5a monoclonal antibody indicates a prominent role for anaphylatoxin in pulmonary xenograft dysfunction. *Transplantation* 2006;81:1686.
38. Proctor LM, Strachan AJ, Woodruff TM, et al. Complement inhibitors selectively attenuate injury following administration of cobra venom factor to rats. *Int Immunopharmacol* 2006;6:1224.
39. Fayyazi A, Scheel O, Werfel T, et al. The C5a receptor is expressed in normal renal proximal tubular but not in normal pulmonary or hepatic epithelial cells. *Immunology* 2000;99:38.
40. Prince JM, Levy RM, Yang R, et al. Toll-like receptor-4 signaling mediates hepatic injury and systemic inflammation in hemorrhagic shock. *J Am Coll Surg* 2006;202:407.
41. Frink M, Lu A, Thobe BM, et al. Monocyte chemoattractant protein-1 influences trauma-hemorrhage-induced distal organ damage via regulation of keratinocyte-derived chemokine production. *Am J Physiol Regul Integr Comp Physiol* 2007;292:R1110.
42. Markiewski MM, Nilsson B, Ekdahl KN, et al. Complement and coagulation: Strangers or partners in crime? *Trends Immunol* 2007;28:184.

Tong Shi, Vaishali R. Moulton, Peter H. Lapchak, Guo-Min Deng, Jurandir J. Dalle Lucca and George C. Tsokos

Am J Physiol Gastrointest Liver Physiol 296:339-347, 2009. First published Dec 18, 2008;
doi:10.1152/ajpgi.90607.2008

You might find this additional information useful...

This article cites 51 articles, 24 of which you can access free at:

<http://ajpgi.physiology.org/cgi/content/full/296/2/G339#BIBL>

Updated information and services including high-resolution figures, can be found at:

<http://ajpgi.physiology.org/cgi/content/full/296/2/G339>

Additional material and information about *AJP - Gastrointestinal and Liver Physiology* can be found at:

<http://www.the-aps.org/publications/ajpgi>

This information is current as of May 5, 2009 .

Ischemia-mediated aggregation of the actin cytoskeleton is one of the major initial events resulting in ischemia-reperfusion injury

Tong Shi,¹ Vaishali R. Moulton,¹ Peter H. Lapchak,¹ Guo-Min Deng,¹ Jurandir J. Dalle Lucca,² and George C. Tsokos¹

¹Division of Rheumatology, Beth Israel Deaconess Medical Center, Harvard Medical School, Boston, Massachusetts; and ²Walter Reed Army Institute of Research, Silver Spring, Maryland

Submitted 22 October 2008; accepted in final form 16 December 2008

Shi T, Moulton VR, Lapchak PH, Deng G, Dalle Lucca JJ, Tsokos GC. Ischemia-mediated aggregation of the actin cytoskeleton is one of the major initial events resulting in ischemia-reperfusion injury. *Am J Physiol Gastrointest Liver Physiol* 296: G339–G347, 2009. First published December 18, 2008; doi:10.1152/ajpgi.90607.2008.—Ischemia-reperfusion (IR) injury represents a major clinical challenge, which contributes to morbidity and mortality during surgery. The critical role of natural immunoglobulin M (IgM) and complement in tissue injury has been demonstrated. However, cellular mechanisms that result in the deposition of natural IgM and the activation of complement are still unclear. In this report, using a murine intestinal IR injury model, we demonstrated that the β -actin protein in the small intestine was cleaved and actin filaments in the columnar epithelial cells were aggregated after a transient disruption during 30 min of ischemia. Ischemia also led to deposition of natural IgM and complement 3 (C3). A low dose of cytochalasin D, a depolymerization reagent of the actin cytoskeleton, attenuated this deposition and also attenuated intestinal tissue injury in a dose-dependent manner. In contrast, high doses of cytochalasin D failed to worsen the injury. These data indicate that ischemia-mediated aggregation of the actin cytoskeleton, rather than its disruption, results directly in the deposition of natural IgM and C3. We conclude that ischemia-mediated aggregation of the actin cytoskeleton leads to the deposition of natural IgM and the activation of complement, as well as tissue injury.

cytochalasin D; complement; deposition

ISCHEMIA-REPERFUSION (IR) injury, resulting in damage to local and remote organs after periods of ischemia, is a major contributor to morbidity and mortality during myocardial infarction, transplantation, stroke, surgery, and trauma (6, 8, 9, 25, 47). However, currently there are no effective therapies because the mechanisms that result in tissue injury are not fully understood.

Although IR injury causes a strong inflammatory response (18, 44, 45, 48), accumulated evidence has shown that complement plays a critical role in IR injury. The finding that chemotactic complement (C)3-cleavage products are found in damaged heart tissue indicates that IR injury is complement dependent (17, 42). Additionally, the myocardium is protected from necrosis by cobra venom factor, which depletes C3 activation via the activation of the alternative pathway (12, 17, 25, 27), and by recombinant soluble human complement receptor (CR)1, which promotes inactivation of C3 by factor I (45). Soluble CR1 also reduces cerebral infarct volume (18) and intestinal injury (13). The observation that C5b-9 deposits

in human myocardial tissue and C5- or C6-deficient mice and rabbits are protected from IR injury strongly suggests that complement is a major mediator of IR injury (15, 36, 51). Studies in C3- and C4-deficient mice and factor B- or factor D-knockout mice suggest that all three complement pathways mediate IR injury (39, 41, 44, 48). Although the significance of complement has been well established, the cellular mechanisms leading to its activation in tissues are not clear.

In addition to the contribution of complement, natural antibodies are also shown to be involved in the pathogenesis of IR injury (20, 44, 48). Recombination activation gene (RAG)1/2-deficient mice lacking natural antibodies and CR1/2-null mice with defects in T-dependent B-2 B cell responses to foreign antigens undergo less IR injury (14). Furthermore, natural immunoglobulin (Ig) M has been identified as one of culprits of IR injury (3, 48, 50). Recently, nonmuscle myosin type II (NM-II) heavy chain A and C have been identified as self-targets of natural IgM and IR injury in both the small intestine and in the skeletal muscle of mice (49). Thus it has been suggested that neoantigens or modified epitopes presented on the cell surface in ischemic tissues may trigger complement activation via natural IgM deposition (49). However, the mechanisms that lead to the exposure of these neoantigens need further investigation.

The actin cytoskeleton is known to play a crucial role in maintaining the functional and structural integrity of cells (21). The three-dimensional network of the actin cytoskeleton interacts with selected plasmalemmal proteins and ATP depletion or ischemia disrupt the actin cytoskeleton in vascular smooth muscle cells, endothelial cells, as well as epithelial cells (21–23, 32, 40). Multiple cleavage of actin protein has been observed in apoptotic cells (19, 28), and one of these cleaved fragments leads to apoptosis-like morphological changes in cultured cells (29).

We hypothesized that alteration of the actin cytoskeleton mediated by ischemia is one of the major initial events that result in the deposition of natural IgM, activation of complement, and further tissue injury. In this paper we establish a definite link between ischemia-mediated alteration of the actin cytoskeleton and the deposition of natural IgM, the activation of complement, and IR injury. We show in a murine intestinal IR injury model that ischemia induces aggregation of the actin cytoskeleton in columnar epithelial cells in small intestinal villi after a period of transient disruption. We also show that ischemia-mediated aggregation of actin filaments and deposition of

Address for reprint requests and other correspondence: T. Shi or G. C. Tsokos, Division of Rheumatology, Beth Israel Deaconess Medical Center, 330 Brookline Ave. CLS 928, Boston, MA 02215 (e-mail: tshi@bidmc.harvard.edu or gtsokos@bidmc.harvard.edu).

The costs of publication of this article were defrayed in part by the payment of page charges. The article must therefore be hereby marked “advertisement” in accordance with 18 U.S.C. Section 1734 solely to indicate this fact.

IgM and C3/C3d fragment are diminished by an optimal dose of cytochalasin D. In addition, low doses of cytochalasin D attenuate IR injury in a dose-dependent manner whereas high doses do not worsen the injury. Taken together, these data reveal that ischemia-mediated aggregation of the actin cytoskeleton plays a crucial role in mediating the deposition of IgM and C3, as well as IR injury.

MATERIALS AND METHODS

Materials. Cytochalasin D was purchased from Sigma-Aldrich (St. Louis, MO). Hoechst 33342, Alexa Fluor 546-labeled phalloidin, and Alexa Fluor 488-labeled DNase I were bought from Invitrogen (Carlsbad, CA). Microvascular clips were obtained from Biomedical Research Instruments (Silver Spring MD). FITC-anti-mouse IgM and C3 antibodies were purchased from Immunology Consultant Laboratory (Newberg, OR). Goat anti-mouse C3d was purchased from R & D Systems (Minneapolis, MN). Mouse anti- β -actin NH₂-terminus antibody was bought from Abcam (Cambridge, MA), and mouse anti- β -actin COOH-terminus antibody was obtained from Santa Cruz Biotechnology (Santa Cruz, CA).

Animal model of murine intestinal IR. All mice used in this study were maintained in specific pathogen-free conditions in the animal research facility at the Beth Israel Deaconess Medical Center (BIDMC). All experiments were performed in accordance with the guidelines and approval of the Institutional Animal Care and Use Committee of the BIDMC. Male C57BL/6 mice aged 8 to 10 wk were purchased from Jackson Laboratory (Bar Harbor, ME) and acclimated for 1 wk. Mice were anesthetized by intraperitoneal injection of a combination of ketamine-xylazine-acepromazine (100:20:3 mg/kg) (1) and subjected to IR as described previously (14) with some modifications that included ischemia for 20 to 30 min and reperfusion for 10 min to 2 h. At various times after ischemia and reperfusion, mice were euthanized and tissues were harvested. Sham mice were subjected to an identical surgical protocol aside from artery clamping. In inhibition experiments, food, but not water, was withdrawn for 24 h before anesthesia. All procedures were performed while maintaining mouse body temperature at 37°C using a controlled heating pad. Mice subjected to inhibition experiments underwent small intestine intraluminal injection 0.5–1.0 ml of cytochalasin D dissolved in dimethyl sulfoxide (DMSO)-PBS immediately after arterial clamping. Vehicle-treated mice were given an equal volume of DMSO.

Histology. About 15 cm of jejunal segment was rinsed and fixed immediately with cold 10% phosphate-buffered formalin. The tissues were then embedded in paraffin, sectioned transversely (5 μ m), and stained with hematoxylin and eosin (H & E). Villus damage was scored according to the severity of injury. The complete destruction of the villus was scored "6" and no injury in the villus was scored "0" (14). The scores of injury were calculated by the following equation: injury score = $\sum(\text{score} \times N_i)/N$. N_i represents the number of villi with the same injury score. N represents the total number of villi counted (250 villi).

Proteomic analysis. Jejunal segments obtained from mice ($n = 3/\text{group}$) subjected to sham, 30-min ischemia, and 30-min ischemia-2 h reperfusion were harvested and sent on dry ice directly for two-dimensional difference gel electrophoresis (2-DIGE) and mass spectrometry analysis provided by Applied Biomics (Hayward, CA).

Western blot assay. Jejunal segments from individual mice subjected to various durations of ischemia and reperfusion were homogenized in buffer (10 mM HEPES, pH 7.9, 1.5 mM MgCl₂, 10 mM KCl, and 1 mM DTT) with complete protease inhibitor cocktail (Roche, Mannheim, Germany). Concentrations of protein extracts were determined using Micro BCA protein assay kit (Pierce, Rockford, IL). Protein extracts were processed under reducing conditions and subjected to standard Western blot analysis. Blots were developed with mouse anti- β -actin antibodies (NH₂ terminus and COOH termi-

nus) and horseradish peroxidase-conjugated secondary antibodies and images were captured using a Fujifilm LAS-40000 luminescent image analyzer (Fujifilm, Valhalla, NY).

Confocal microscopy. Jejunal segments were rinsed with cold PBS and snap frozen in frozen tissue embedding media. The tissues were sectioned transversely (6 μ m), fixed with 10% phosphate-buffered formalin for 10 min, and permeabilized with 0.1% Triton X-100-PBS for another 10 min. Sections were blocked with 1% BSA-PBS at room temperature for 1 h and then incubated with fluorochrome-labeled primary or secondary antibodies at room temperature for 1 h. After being washed and mounted on slides, sections were analyzed by confocal microscopy (Nikon Eclipse Ti, Nikon Instruments, Melville, NY).

To evaluate the ratio of global to filamentous (G/F)-actin using quantitative fluorescence image analysis (35), tissue sections were stained with fluorochrome-labeled DNase I and phalloidin, which bind to global actin and filamentous actin, respectively (24). Fluorescence from the columnar epithelial cells of small intestinal villi was obtained by confocal microscopy under identical conditions. Intensity of fluorescence was analyzed by Nikon EZ-C1 FreeViewer 3_20_615 Gold (Nikon Instruments, Melville, NY). The ratio of G/F-actin was calculated by dividing DNase I fluorescent intensity by phalloidin fluorescent intensity. Increased ratios of G/F-actin reflect disruption of actin filaments, and decreased ratios of G/F-actin indicate aggregation of actin filaments.

Statistical analysis. Data are expressed as means \pm SD. Differences between groups were evaluated by Student's *t*-test. $P \leq 0.05$ was considered statistically significant. A two-tailed distribution and paired *t*-test were used to evaluate the differences in the ratios of G/F-actin. A two-tailed distribution and unpaired *t*-test were employed for the differences in injury scores.

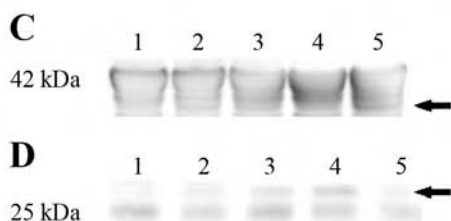
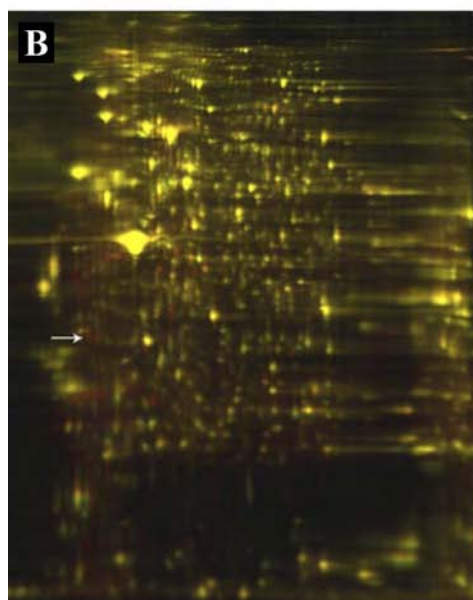
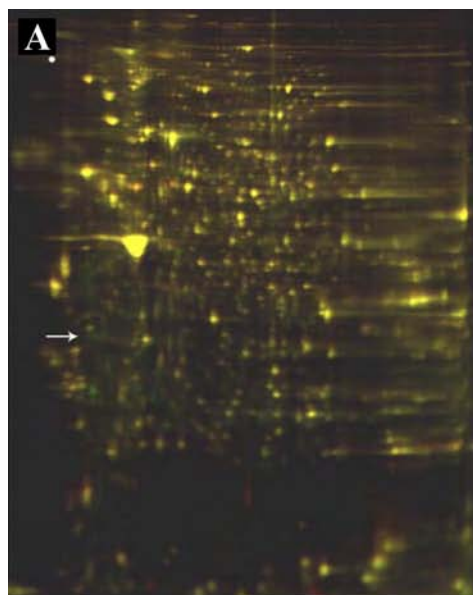
RESULTS

Ischemia induces cleavage of β -actin protein. On the basis of a previous study showing that a 15-kDa fragment of actin leads to morphological changes of cells undergoing apoptosis (29) and our interest to find potentially cleaved proteins in the small intestine, we conducted experiments to compare the differential expression of proteins in sham-, ischemia-, or IR-treated small intestine. The superior mesenteric artery (SMA) was clamped with a microvascular clip to generate ischemia in the jejunum for 30 min followed by reperfusion 2 h. Jejunal segments harvested without clip clamping were designated as sham samples, before clip removal as ischemia samples, and after reperfusion as IR samples. Jejunal segments were processed and subjected to 2-DIGE. One spot with a molecular weight of 30 kDa identified in the ischemia samples (Fig. 1, A and B) was isolated and sequenced. The abundance of this protein was increased 11.43-fold after ischemia and 0.78-fold after IR compared with sham samples. The MAS-COT search engine analysis identified this protein to be β -actin.

Mouse anti- β -actin COOH-terminus antibody identified a band of 40 kDa in the ischemia (Fig. 1C, lanes 2 and 3) and IR samples (Fig. 1C, lanes 4 and 5) but not from sham samples (Fig. 1C, lane 1), indicating that β -actin protein (42 kDa) was cleaved during ischemia and reperfusion. A faint 30-kDa band in 20-min ischemia samples (Fig. 1D, lane 2) and a strong band in 30-min ischemia sample were also visualized in Western blot (Fig. 1D, lane 3). This band was also seen in 10-min reperfusion samples (Fig. 1D, lane 4). However, it disappeared in 2-h reperfusion samples (Fig. 1D, lane 5). These results are consistent with the 2-DIGE results above, indicating that ische-

mia induces cleavage of β -actin and the cleaved fragment is destroyed by reperfusion.

Mouse anti- β -actin NH₂-terminus antibody failed to identify this 30-kDa band (data not shown), indicating that the cleaved fragment represents the COOH terminus of β -actin. In this experiment, 25-kDa bands of the Ig light chain were considered as loading controls since the primary antibody used in the Western blot assay was a mouse immunoglobulin (Fig. 1D).



Ischemia with or without reperfusion results in alteration of the actin cytoskeleton. Disruption of the actin cytoskeleton induced by ATP depletion or ischemia have been reported in various cell types (21–23, 32). However, it has also been demonstrated that the actin cytoskeleton polymerizes at 2 h and then depolymerizes in a camptothecin-induced apoptotic model in HL-60 cells (35). In addition, β -actin is cleaved to yield 40- and 30-kDa bands during ischemia in our intestinal IR model (Fig. 1). Therefore, it is possible that ischemia may alter the actin cytoskeletal network in tissues. We conducted experiments focusing on the alteration of the actin cytoskeleton to address this hypothesis. The SMA was clamped with a microvascular clip to generate jejunal ischemia for 20 or 30 min and reperfused for 10 min or 2 h. Jejunal segments were processed and then stained with fluorochrome-labeled phalloidin and DNase I, Hoechst 33342 or H & E.

H & E staining revealed that 30-min ischemia caused minor injury in small intestinal villi (injury score: 1.54 ± 0.58 , $n = 5$; $P = 0.003$) whereas 2-h reperfusion following 30-min ischemia resulted in severe injury (injury score: 4.18 ± 0.44 , $n = 8$; $P < 0.0001$) compared with sham segments (injury score: 0.18 ± 0.07 , $n = 4$).

Confocal microscopic images showed that phalloidin staining of the actin cytoskeleton in the columnar epithelial cells of the villi is lighter and less dense after 20-min ischemia (Fig. 2B) whereas staining becomes brighter and more dense in 30-min ischemia tissues (Fig. 2C) compared with sham-treated tissues (Fig. 2A). This indicates that ischemia results in an initial disruption of the actin cytoskeleton, followed by aggregation. This was confirmed by a quantitative analysis of G/F-actin; the ratio of G/F-actin was 2.08 ± 1.34 ($n = 6$, Fig. 3) in the columnar epithelial cells from sham mice, which significantly increased to 4.93 ± 3.62 ($n = 6$, $P = 0.038$, Fig. 3) after 20-min ischemia. However, after 30-min ischemia the ratio of G/F-actin was significantly decreased to 2.54 ± 2.52 ($n = 6$, $P = 0.007$, Fig. 3) consistent with the observation above that the actin cytoskeleton aggregates after 30-min ischemia (Fig. 2C). These results indicate that ischemia results in aggregation of actin filaments after an initial transient disruption. However, the actin cytoskeleton was disrupted again when the small intestine was reperfused for 10 min (Fig. 2D) and was destroyed completely after reperfusion for 2 h (Fig. 2E). The disruption induced by reperfusion was also demonstrated by an increase in the ratio of G/F-actin to 4.79 ± 4.58 ($n = 6$) or 4.87 ± 3.69 ($n = 6$) after 10 min or 2 h reperfusion, respectively. These results indicate that the restoration of blood supply damages the actin cytoskeleton.

Fig. 1. Ischemia induces multiple cleavages of β -actin. Jejunal segments were harvested and homogenized in buffer. Proteins, pooled from 3 mice per group, were labeled with various CyDyes and subjected to 2-dimensional difference gel electrophoresis (2-DIGE). **A:** sham-treated sample was labeled in red; 30-min ischemia sample was labeled in green. **B:** 30-min ischemia sample was labeled in red; 2-h reperfusion sample was labeled in green. Arrows indicate the dots that were sequenced. In separate experiments, proteins were subjected to standard Western blot. Blots were developed with mouse anti- β -actin antibodies and horseradish peroxidase-conjugated anti-mouse antibody. *Lane 1*, sham; *lane 2*, 20-min ischemia; *lane 3*, 30-min ischemia; *lane 4*, 30-min ischemia/10-min reperfusion; *lane 5*, 30-min ischemia/2 h reperfusion in **C** and **D**. Arrows indicate 40-kDa protein in **C** and 30-kDa protein in **D**. Western blot images represent 3 independent experiments.

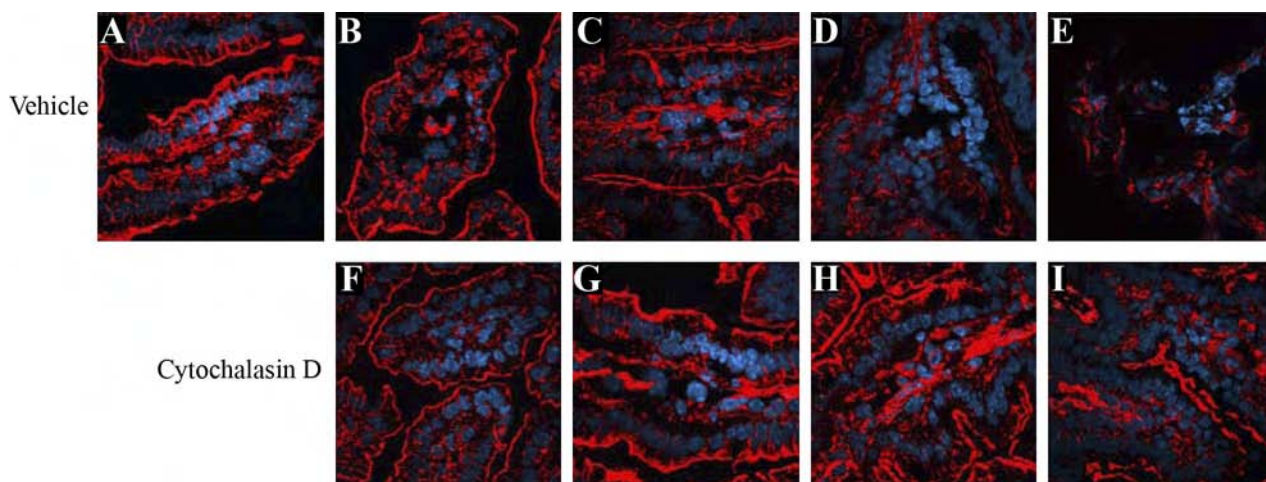


Fig. 2. Ischemia induces disruption and aggregation of the actin cytoskeleton. Jejunal segments were processed and then stained with fluorochrome-labeled phalloidin (red) and Hoechst 33342 (blue). *A*: sham. *B* and *F*: 20-min ischemia. *C* and *G*: 30-min ischemia. *D* and *H*: 30-min ischemia/10-min reperfusion. *E* and *I*: 30-min ischemia/2 h reperfusion. Images represent more than 3 independent experiments.

Ischemia with or without reperfusion induces natural IgM and C3 deposition. To investigate whether ischemia with or without reperfusion results in natural IgM and C3 deposition, we evaluated this deposition in small intestinal villi from mice subjected to various durations of ischemia with or without reperfusion by confocal microscopy. Jejunal segments were processed as described above and stained with FITC-anti-IgM or anti-C3 antibodies, or anti-C3d antibody/FITC-secondary antibody, Alexa Fluor 546-phalloidin, and Hoechst 33342. Confocal microscopy showed IgM deposits on the membranes of villus epithelial cells, which are in close proximity to blood vessels and also on the microvilli of the columnar epithelial cells from mice subjected to 10 min (Fig. 4D) or 2 h reperfusion (Fig. 4E). IgM deposits were clearly visualized (Fig. 4C) in 30-min ischemia samples although minor IgM deposits were observed on cores of the villi in 20-min ischemia samples (Fig. 4B), indicating that ischemia efficiently induces deposition of natural IgM. The IgM deposits on the villi from mice subjected to 30- or 10-min IR confirmed that the deposition of IgM in ischemic tissues is due to specific binding of IgM to the tissues.

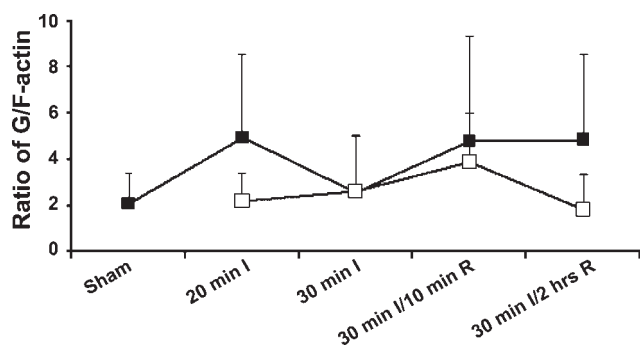


Fig. 3. Kinetic analysis of the ratio of G- to F-actin (G/F-actin) columnar epithelial cells of small intestinal villi during ischemia (I) and reperfusion (R). ■, Vehicle-treated samples; □, cytochalasin D-treated samples. Ischemia results in aggregation of actin filaments after an initial transient disruption. However, the actin cytoskeleton was disrupted again when the small intestine was reperfused for 10 min and was destroyed completely after reperfusion for 2 h.

In contrast, IgM deposits were only detected in blood vessels of sham samples (Fig. 4A).

Both C3 and C3d deposits were observed on the microvilli of the columnar epithelial cells from mice subjected to 30-min or 2-h IR (Fig. 4, *J* and *O*). Both C3 and C3d deposits were also visualized on the villi from mice subjected to 30- or 10-min IR (Fig. 4, *I* and *N*). Deposits of C3 and C3d were clearly detected in tissues from mice subjected to 30-min ischemia (Fig. 4, *H* and *M*) but barely from those subjected to 20-min ischemia (Fig. 4, *G* and *L*). This indicates that ischemia results in deposition of C3 and more specifically C3d. These results reveal that not only reperfusion but also ischemia without reperfusion activates complement in the small intestine.

Ischemia-mediated aggregation of the actin cytoskeleton results in IR-mediated injury. We next hypothesized that ischemia-mediated alteration of the actin cytoskeleton eventually leads to IR tissue injury. Therefore, we used cytochalasin D, a reagent that disrupts and blocks polymerization of actin filaments (37), to alter the actin cytoskeletal network in small intestinal villi to test this hypothesis. Mice were treated as described above. Various doses of cytochalasin D in DMSO-PBS (<0.1% in vol/vol) were injected into the small intestinal lumen immediately after the clip was applied to the SMA. After 30-min or 2-h IR, jejunal segments were processed and stained with H & E. Results of the cytochalasin D dose-response study showed that 1 μ M of cytochalasin D effectively inhibited small intestinal injury (injury score: 1.38 ± 0.55 , $n = 12$, $P < 0.0001$, Fig. 5), compared with the injury score in tissues from vehicle-treated mice (3.83 ± 0.97 , $n = 16$, Fig. 5). This inhibition was dose dependent when doses of cytochalasin D used were less than 1 μ M. This indicates that cytochalasin D dose-dependent alteration of the actin cytoskeleton protects mice from the small intestinal injury. Although cytochalasin D lost its inhibitory effect with gradually increased doses (Fig. 5), higher doses (30 and 100 μ M) of cytochalasin D did not induce additional injury than that from vehicle-treated mice ($P = 0.75$ and $P = 0.86$, respectively). This indicates that cytochalasin D-induced disruption of the actin cytoskeleton does not contribute to the injury. All experimental mice died after 200 μ M

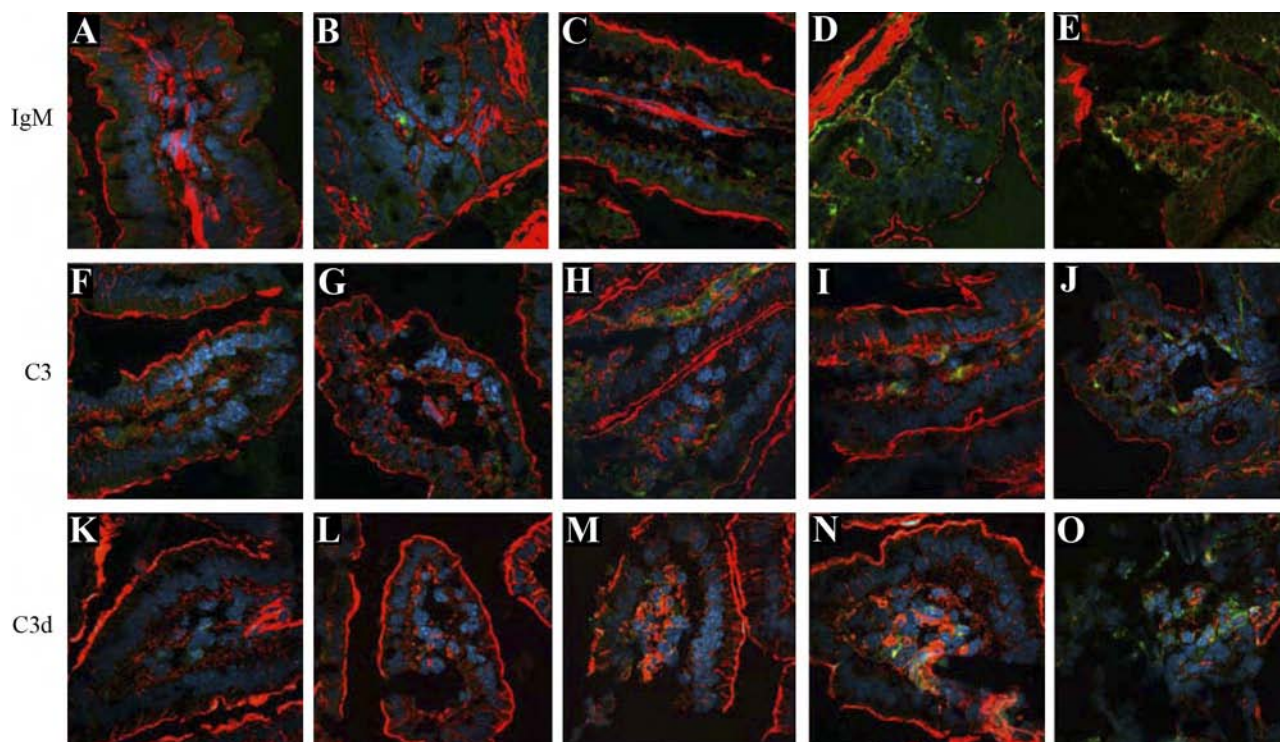


Fig. 4. Ischemia results in deposition of natural IgM and C3/C3d. Jejunal segments were stained with fluorochrome-labeled phalloidin (red), anti-C3 (green), anti-C3d (green), and Hoechst 33342 (blue). A, F, K: sham. B, G, L: 20-min ischemia. C, H, M: 30-min ischemia. D, I, N: 30-min ischemia/10-min reperfusion. E, J, O: 30-min ischemia/2 h reperfusion. Images represent 3 independent experiments.

of cytochalasin D was injected whereas sham-treated mice died within several minutes after 1 μM of cytochalasin D was injected so that we were unable to obtain results from cytochalasin D-treated sham samples. These findings suggest that aggregation of actin filaments ultimately leads to IR tissue injury.

Optimal concentration of cytochalasin D attenuates the alteration of the actin cytoskeleton. To further investigate how cytochalasin D alters the actin cytoskeleton, we observed the

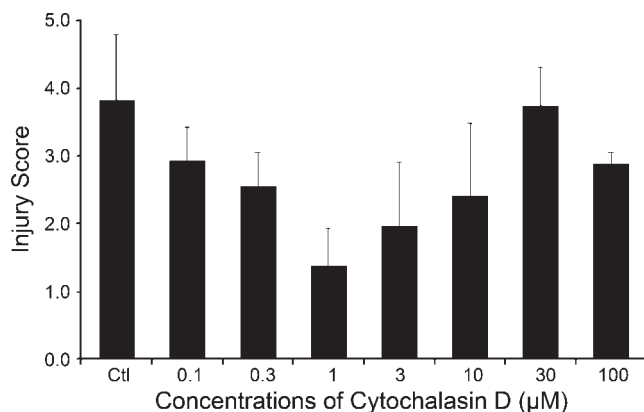


Fig. 5. Cytochalasin D attenuates tissue injury in a dose-dependent manner. Jejunal segments from mice undergo ischemia-reperfusion and injection of various doses of cytochalasin D were processed and stained with hematoxylin and eosin. The inhibition of tissue injury indicates that cytochalasin D dose-dependent alteration of the actin cytoskeleton protects mice from the small intestinal injury. That higher doses of cytochalasin D did not induce additional injury than that from vehicle-treated mice indicates that cytochalasin D-induced disruption of the actin cytoskeleton does not contribute to the injury.

effects of cytochalasin D on IR-induced morphological changes of the actin cytoskeleton. Mice were treated with 1 μM of cytochalasin D or vehicle and subjected to various durations of ischemia and reperfusion. Frozen sections of jejunal segments were stained with fluorochrome-labeled phalloidin and DNase I, as well as Hoechst 33342. Confocal microscopic results showed that the brightness, thickness, and integrity of the actin cytoskeleton in the villus columnar epithelial cells from mice subjected to 20-min ischemia (Fig. 2F) were comparable to those from sham-treated mice without cytochalasin D treatment (Fig. 2A) and were brighter, more dense than those in samples from 20-min ischemia-treated mice treated with vehicle (Fig. 2B). These data indicated that the optimal dose of cytochalasin D blocks the disruption of the actin cytoskeleton. In samples from 30-min ischemia-treated mice treated with cytochalasin D (Fig. 2G) or vehicle (Fig. 2C) the integrity of the actin cytoskeleton was comparable, indicating that the actin cytoskeleton does not undergo aggregation. The actin cytoskeleton network is highly organized in the columnar epithelial cells from mice subjected to 10-min or 2-h reperfusion (Fig. 2, H and I), compared with those from vehicle-treated mice subjected to 10 min or 2 h of reperfusion (Fig. 2D and E). These images demonstrate that cytochalasin D blocks reperfusion-mediated damage of the actin cytoskeleton.

The findings above are supported by changes in the ratio of G/F-actin. The ratio of G/F-actin in the columnar epithelial cells of small intestinal villi from mice subjected to 20-min ischemia (2.19 ± 1.24 , $n = 6$, $P = 0.89$) was comparable to that from sham mice without cytochalasin D treatment (2.08 ± 1.34 , $n = 6$, Fig. 3) and was significantly lower than that from vehicle-treated mice subjected to 20-min ischemia ($4.93 \pm$

3.62, $n = 6$, $P = 0.04$, Fig. 3), consistent with the observation above (Fig. 2F) indicating that 1 μM of cytochalasin D attenuates the disruption of the actin cytoskeleton. The ratio of G/F-actin from mice subjected to 30-min ischemia increased, rather than decreased, slightly to 2.60 ± 2.40 ($n = 6$, $P = 0.54$, Fig. 3), compared with those from mice subjected to 20-min ischemia. This result also agrees with the observation above in which cytochalasin D blocks the aggregation of actin filaments (Fig. 2G). This may also mean that the aggregation of actin filaments may be a result of the initial disruption and actin filaments may be unable to aggregate owing to the blockade of the disruption by cytochalasin D as in tissues from vehicle-treated mice. Thus it can be concluded that the disruption of the actin cytoskeleton initiates the aggregation. The ratios of G/F-actin increased significantly ($n = 6$, $P = 0.02$, Fig. 3) and went down to initial levels ($n = 6$, $P = 0.64$, Fig. 3) after 10 min or 2 h of reperfusion, respectively, compared with that from mice subjected to 20-min ischemia (Fig. 3). The ratios were much lower than those from vehicle-treated mice subjected to 10-min or 2-h reperfusion, respectively (Fig. 3), supporting the conclusion above that cytochalasin D protects the actin cytoskeleton from reperfusion-mediated disruption (Fig. 2, H and I). These data strongly support the hypothesis that cytochalasin D alters ischemia and reperfusion-mediated disruption and aggregation of the actin cytoskeleton.

Ischemia-mediated aggregation of the actin cytoskeleton leads to deposition of IgM and C3. Ischemia-mediated deposition of natural IgM and C3 in small intestinal villi has been shown here and by others (48), and ischemia-mediated aggregation of the actin cytoskeleton is demonstrated above. On this basis, we hypothesized that ischemia-mediated aggregation of the actin cytoskeleton directly results in the deposition of natural IgM and C3. To test this hypothesis, we determined whether cytochalasin D can attenuate ischemia-mediated deposition of IgM and C3/C3d. Mice treated with 1 μM of cytochalasin D or vehicle were subjected to various durations of ischemia and reperfusion. Frozen sections of jejunal segments were stained for IgM and C3/C3d plus phalloidin and Hoechst 33342. Confocal images demonstrate decreased deposition of IgM and C3/C3d on the villi from cytochalasin D-treated mice subjected to various durations of ischemia and reperfusion (Fig. 6) compared with the villi from vehicle-treated mice (Fig. 4). However, cytochalasin D does not interfere with the natural deposition of IgM or C3/C3d in blood vessels (Fig. 6). These results clearly indicate that the optimal concentration of cytochalasin D attenuates the deposition of IgM and C3, and this strongly supports the hypothesis that ischemia-mediated aggregation of the actin cytoskeleton directly leads to the deposition of natural IgM and C3.

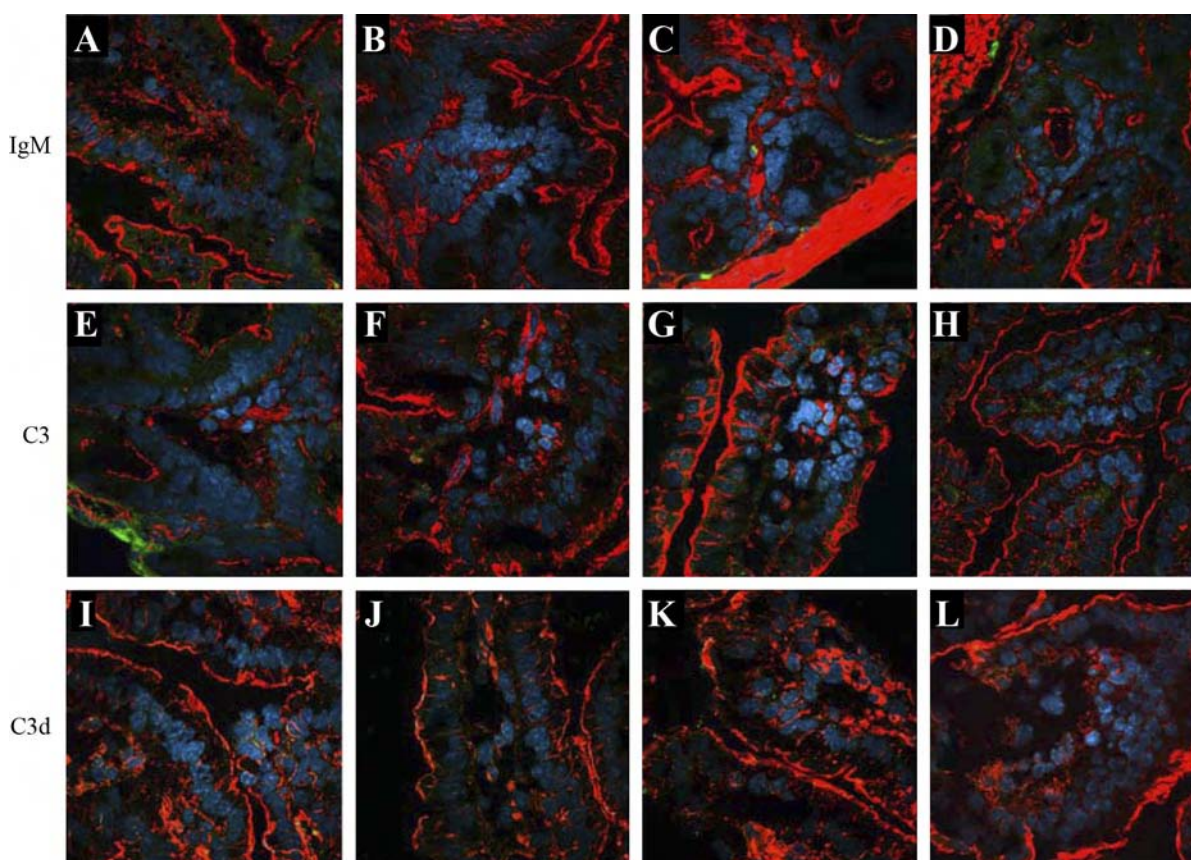


Fig. 6. Cytochalasin D blocks deposition of natural IgM and C3/C3d. Jejunal segments from mice subjected to ischemia-reperfusion and injection of optimal dose of cytochalasin D were stained with fluorochrome labeled-phalloidin (red), anti-C3 (green), anti-C3d (green), and Hoechst 33342 (blue). A, E, I: 20-min ischemia. B, F, J: 30-min ischemia. C, G, K: 30-min ischemia/10-min reperfusion. D, H, L: 30-min ischemia/2 h reperfusion. Images represent 3 independent experiments.

DISCUSSION

In the present study, we investigated the alteration of the actin cytoskeleton during ischemia with or without reperfusion. We demonstrated that ischemia results in multiple cleavages of β -actin (Fig. 1) and aggregation of the actin cytoskeleton after a transient disruption (Figs. 2 and 3). The aggregation of the actin cytoskeleton mediated by ischemia induces deposition of natural IgM and C3 (Fig. 4). Furthermore, cytochalasin D attenuates the aggregation of the actin cytoskeleton (Fig. 2), the subsequent deposition of natural IgM and C3 (Fig. 6), as well as IR injury (Fig. 5).

It has been reported that the actin protein is cleaved by interleukin-1 β converting enzyme (ICE) family proteases, which are active players of programmed cell death (apoptosis) (30), to produce three major peptides (40–41, 30–31, and 14–15 kDa) *in vitro* and in cultured apoptotic cells (19, 28). We demonstrated, *in vivo*, employing 2-DIGE and Western blot analysis in this report, that ischemia-mediated cleavage of β -actin in mouse small intestine yields bands with molecular weights of \sim 30 and 40 kDa (Fig. 1). Our results reveal that ischemia-mediated cleavage of β -actin occurs, *in vivo*, in tissues.

Ischemia-mediated disruption of vascular smooth muscle cells and epithelial cells in the kidney has been reported (21, 23). However, ATP depletion induced by antimycin A in the proximal tubule-derived LLC-PK1 cell line results in disruption of the cortical cytoskeleton, and at same time actin monomers significantly convert into filamentous actin to form large cytoplasmic aggregates (32). Furthermore, energy depletion leads to disintegration of filamentous actin and formation of numerous small clumps of filamentous actin in the cytoplasm of cultured aortic endothelial cells (22). Using an intestinal IR injury model in which small intestinal villi are vulnerable to IR insult, we demonstrated *in vivo* by phalloidin staining that the actin cytoskeleton in the columnar epithelial cells of the small intestinal villi is disrupted initially and then aggregates during a short term of ischemia (Fig. 2). We also demonstrated this result quantitatively by calculating ratios of G/F-actin (Fig. 3). We were unable to measure concentrations of global actin and filamentous actin using the assay of DNase I inhibition described previously (5) because of very high endogenous DNase I activity in intestinal samples, which may come from the pancreas. Our finding of the initial disruption of the actin cytoskeleton is supported by observations that high cytosolic Ca^{2+} concentrations, which increase rapidly after 2-min exposure to a metabolic inhibitor, result in depolymerization of the actin cytoskeleton (22). Thus it is possible that during early ischemia in our study a rapid increase in free cytosolic Ca^{2+} results in the disruption of filamentous actin. Free Ca^{2+} also helps villin, one of the major actin-associated proteins (11), to break or sever filamentous actin (16). The cleavage of actin fragments by ICE family proteases demonstrate impaired capability to block DNase I activity and to polymerize normally (19). Ectopic expression of a 15-kDa fragment of actin, which is cleaved from actin filaments by ICE family proteases during apoptosis, induces morphological changes, very similar to those of apoptotic cells (29). Although we were unable to visualize the 15-kDa fragment of actin by Western blot analysis, the accumulation of these fragments may contribute to the later aggregation of actin filaments.

These data support our observation of actin cytoskeletal aggregation in the small intestine. Ischemia-induced consumption of ATP in the epithelial cells may lead to the aggregation too (22, 32, 35).

Several studies have shown that IR results in the deposition of natural IgM and IgG, the activation of complement (3, 9, 12, 17, 18, 27, 36, 44, 45, 48, 51), and the subsequent formation of the membrane attack complex that results in tissue necrosis (2, 36, 51). It was suggested that natural IgM against NM-II directly causes tissue injury after IR and a peptide mimicking an epitope on NM-II blocks complement activation and prevents tissue injury (49, 50). These studies clearly indicate that the deposition of natural IgM and the activation of complement during IR is due to a turnover of antigens on cell membranes, which are not exposed to the innate immune system under physiological conditions (49). Our observations in this report support these findings. We also observed that actin filaments aggregate after a transient disruption. So we hypothesized that the alteration of the actin cytoskeleton results in the deposition of natural IgM and complement. We used cytochalasin D, a fungal metabolite that binds to the barbed end of actin filaments (37), to test this hypothesis. The fact that cytochalasin D does not inhibit glucose transport (34) makes it acceptable for our ischemia-mediated actin cytoskeletal alteration study. It has been reported that cytochalasin D inhibits the rapid polymerization of actin (10, 46). We developed a novel model that makes it possible to study the effects of cytochalasin D on cell function *in vivo*. In this model, various doses of cytochalasin D were injected immediately into the small intestinal lumen after the SMA was clamped. We believe that SMA clamping blocks the absorption of cytochalasin D into the blood circulation since all animals died several minutes after its injection without SMA clamping. A 1- μM dose of cytochalasin D is optimal to block both disruption and aggregation of actin filaments (Figs. 2 and 3). This finding is consistent with the observation that cytochalasin D treatment of cells induces actin aggregation while simultaneously depolymerizing preexisting actin cytoskeletal components (33). However, higher doses of cytochalasin D, resulting in disruption of actin filaments (43) and detachment of the epithelial cells from the intestinal villi (data not shown), failed to worsen tissue injury (Fig. 5). This indicates that the disruption does not contribute to IgM- or complement-mediated tissue injury (Fig. 4). We conclude that ischemia-mediated aggregation after an initial disruption induces deposition of natural IgM and C3 (Figs. 5 and 6). It is also possible that the subsequent aggregation results from the initial disruption. Under physiological conditions, polymerization and depolymerization may be well balanced whereas this balance is biased to either disruption or aggregation during ischemia.

It has been suggested that NM-II heavy chains, which were identified as targets of natural IgM, may be exposed to the innate immunity during ischemia (49). NM-II binds to actin filaments, playing a critical role in regulating cell motility and polarity (7). It has also been reported that the injection of anti- β_2 -glycoprotein I (β_2 -GPI) antibodies and anti-phospholipid antibodies into Rag1- and CR2-deficient mice restore intestinal injury (14). β_2 -GPI, a plasma protein, was reported to bind to phosphatidylserine (PS) on the outside of the membrane of apoptotic cells (4, 26). These observations indicate that anti- β_2 -GPI and anti-PS antibodies mediate tissue injury

due to the formation of complexes of PS/ β_2 -GPI/antibodies or PS/antibodies on the cell membrane, which lead to the activation of complement. It is possible that ischemia-mediated aggregation of actin filaments results in the turnover or exposure of NM-II, PS, and/or other antigens to the outer surface of cell membrane so that they can be recognized by natural IgM and IgG. Although it is challenging technically for us to test the turnover hypothesis directly using anti-NM-II or anti- β_2 -GPI antibodies, the blockade of ischemia-mediated deposition of natural IgM and C3 by cytochalasin D clearly supports this notion that needs further investigations. Future studies should focus on how ischemia-mediated aggregation leads to the turnover of antigens in the members.

In conclusion, we revealed that the deposition of IgM and complement during IR is a direct result of ischemia-mediated aggregation of the actin cytoskeleton.

ACKNOWLEDGMENTS

The authors thank Dr. K. Frank Austen for critical reading of the manuscript.

GRANTS

The work was supported by Grant no. W81XWH-07-1-0286 from Medical Research and Materiel Command.

REFERENCES

1. Arras M, Autenried P, Rettich A, Spaeni D, Rulicke T. Optimization of intraperitoneal injection anesthesia in mice: drugs, dosages, adverse effects, and anesthesia depth. *Comp Med* 51: 443–456, 2001.
2. Austen WG Jr, Kyriakides C, Favuzza J, Wang Y, Kobzik L, Moore FD Jr, Hechtman HB. Intestinal ischemia-reperfusion injury is mediated by the membrane attack complex. *Surgery* 126: 343–348, 1999.
3. Austen WG Jr, Zhang M, Chan R, Friend D, Hechtman HB, Carroll MC, Moore FD Jr. Murine hindlimb reperfusion injury can be initiated by a self-reactive monoclonal IgM. *Surgery* 136: 401–406, 2004.
4. Balasubramanian K, Schroit AJ. Characterization of phosphatidylserine-dependent beta2-glycoprotein I macrophage interactions. Implications for apoptotic cell clearance by phagocytes. *J Biol Chem* 273: 29272–29277, 1998.
5. Blikstad I, Markey F, Carlsson L, Persson T, Lindberg U. Selective assay of monomeric and filamentous actin in cell extracts, using inhibition of deoxyribonuclease I. *Cell* 15: 935–943, 1978.
6. Bramlett HM, Dietrich WD. Pathophysiology of cerebral ischemia and brain trauma: similarities and differences. *J Cereb Blood Flow Metab* 24: 133–150, 2004.
7. Bresnick AR. Molecular mechanisms of nonmuscle myosin-II regulation. *Curr Opin Cell Biol* 11: 26–33, 1999.
8. Brewster DC, Franklin DP, Cambria RP, Darling RC, Moncure AC, Lamuraglia GM, Stone WM, Abbott WM. Intestinal ischemia complicating abdominal aortic surgery. *Surgery* 109: 447–454, 1991.
9. Busch GJ, Martins AC, Hollenberg NK, Wilson RE, Colman RW. A primate model of hyperacute renal allograft rejection. *Am J Pathol* 79: 31–56, 1975.
10. Casella JF, Flanagan MD, Lin S. Cytochalasin D inhibits actin polymerization and induces depolymerization of actin filaments formed during platelet shape change. *Nature* 293: 302–305, 1981.
11. Craig SW, Powell LD. Regulation of actin polymerization by villin, a 95,000 dalton cytoskeletal component of intestinal brush borders. *Cell* 22: 739–746, 1980.
12. Crawford MH, Grover FL, Kolb WP, McMahan CA, O'Rourke RA, McManus LM, Pinckard RN. Complement and neutrophil activation in the pathogenesis of ischemic myocardial injury. *Circulation* 78: 1449–1458, 1988.
13. Eror AT, Stojadinovic A, Starnes BW, Makrides SC, Tsokos GC, Shea-Donohue T. Antiinflammatory effects of soluble complement receptor type 1 promote rapid recovery of ischemia/reperfusion injury in rat small intestine. *Clin Immunol* 90: 266–275, 1999.
14. Fleming SD, Egan RP, Chai C, Girardi G, Holers VM, Salmon J, Monestier M, Tsokos GC. Anti-phospholipid antibodies restore mesenteric ischemia/reperfusion-induced injury in complement receptor 2/complement receptor 1-deficient mice. *J Immunol* 173: 7055–7061, 2004.
15. Fleming SD, Mastellos D, Karpel-Massler G, Shea-Donohue T, Lambiris JD, Tsokos GC. C5a causes limited, polymorphonuclear cell-independent, mesenteric ischemia/reperfusion-induced injury. *Clin Immunol* 108: 263–273, 2003.
16. Glenney JR Jr, Kaulfus P, Weber K. F actin assembly modulated by villin: Ca⁺⁺-dependent nucleation and capping of the barbed end. *Cell* 24: 471–480, 1981.
17. Hill JH, Ward PA. The phlogistic role of C3 leukotactic fragments in myocardial infarcts of rats. *J Exp Med* 133: 885–900, 1971.
18. Huang J, Kim LJ, Mealey R, Marsh HC Jr, Zhang Y, Tenner AJ, Connolly ES Jr, Pinsky DJ. Neuronal protection in stroke by an sLex-glycosylated complement inhibitory protein. *Science* 285: 595–599, 1999.
19. Kayalar C, Ord T, Testa MP, Zhong LT, Bredesen DE. Cleavage of actin by interleukin 1 beta-converting enzyme to reverse DNase I inhibition. *Proc Natl Acad Sci USA* 93: 2234–2238, 1996.
20. Keith MP, Moratz C, Egan R, Zacharia A, Greidinger EL, Hoffman RW, Tsokos GC. Anti-ribonucleoprotein antibodies mediate enhanced lung injury following mesenteric ischemia/reperfusion in Rag-1(-/-) mice. *Autoimmunity* 40: 208–216, 2007.
21. Kellerman PS, Clark RA, Hoilien CA, Linas SL, Molitoris BA. Role of microfilaments in maintenance of proximal tubule structural and functional integrity. *Am J Physiol Renal Physiol* 259: F279–F285, 1990.
22. Kuhne W, Besselmann M, Noll T, Muhs A, Watanabe H, Piper HM. Disintegration of cytoskeletal structure of actin filaments in energy-depleted endothelial cells. *Am J Physiol Heart Circ Physiol* 264: H1599–H1608, 1993.
23. Kwon O, Phillips CL, Molitoris BA. Ischemia induces alterations in actin filaments in renal vascular smooth muscle cells. *Am J Physiol Renal Physiol* 282: F1012–F1019, 2002.
24. Lindberg U. Purification from calf spleen of two inhibitors of deoxyribonuclease. I. Physical and chemical characterization of the inhibitor II. *Biochemistry* 6: 323–335, 1967.
25. Maclean D, Fishbein MC, Braunwald E, Maroko PR. Long-term preservation of ischemic myocardium after experimental coronary artery occlusion. *J Clin Invest* 61: 541–551, 1978.
26. Manfredi AA, Rovere P, Heltai S, Galati G, Nebbia G, Tincani A, Balestrieri G, Sabbadini MG. Apoptotic cell clearance in systemic lupus erythematosus. II. Role of beta2-glycoprotein I. *Arthritis Rheum* 41: 215–223, 1998.
27. Maroko PR, Carpenter CB, Chiariello M, Fishbein MC, Radvany P, Knostman JD, Hale SL. Reduction by cobra venom factor of myocardial necrosis after coronary artery occlusion. *J Clin Invest* 61: 661–670, 1978.
28. Mashima T, Naito M, Noguchi K, Miller DK, Nicholson DW, Tsuruo T. Actin cleavage by CPP-32/apoptain during the development of apoptosis. *Oncogene* 14: 1007–1012, 1997.
29. Mashima T, Naito M, Tsuruo T. Caspase-mediated cleavage of cytoskeletal actin plays a positive role in the process of morphological apoptosis. *Oncogene* 18: 2423–2430, 1999.
30. Miura M, Zhu H, Rotello R, Hartweg EA, Yuan J. Induction of apoptosis in fibroblasts by IL-1 beta-converting enzyme, a mammalian homolog of the C. elegans cell death gene ced-3. *Cell* 75: 653–660, 1993.
31. Molitoris BA, Dahl R, Geerdes A. Role of the actin cytoskeleton in ischemic injury. *Chest* 101: 52S–53S, 1992.
32. Molitoris BA, Geerdes A, McIntosh JR. Dissociation and redistribution of Na⁺.K⁺-ATPase from its surface membrane actin cytoskeletal complex during cellular ATP depletion. *J Clin Invest* 88: 462–469, 1991.
33. Mortensen K, Larsson LI. Effects of cytochalasin D on the actin cytoskeleton: association of neoformed actin aggregates with proteins involved in signaling and endocytosis. *Cell Mol Life Sci* 60: 1007–1012, 2003.
34. Rampal AL, Pinkofsky HB, Jung CY. Structure of cytochalasins and cytochalasin B binding sites in human erythrocyte membranes. *Biochemistry* 19: 679–683, 1980.
35. Rao JY, Jin YS, Zheng Q, Cheng J, Tai J, Hemstreet GP, 3rd. Alterations of the actin polymerization status as an apoptotic morphological effector in HL-60 cells. *J Cell Biochem* 75: 686–697, 1999.
36. Schafer H, Mathey D, Hugo F, Bhakdi S. Deposition of the terminal C5b-9 complement complex in infarcted areas of human myocardium. *J Immunol* 137: 1945–1949, 1986.
37. Schliwa M. Action of cytochalasin D on cytoskeletal networks. *J Cell Biol* 92: 79–91, 1982.

38. **Schwartz N, Hosford M, Sandoval RM, Wagner MC, Atkinson SJ, Bamburg J, Molitoris BA.** Ischemia activates actin depolymerizing factor: role in proximal tubule microvillar actin alterations. *Am J Physiol Renal Physiol* 276: F544–F551, 1999.
39. **Stahl GL, Xu Y, Hao L, Miller M, Buras JA, Fung M, Zhao H.** Role for the alternative complement pathway in ischemia/reperfusion injury. *Am J Pathol* 162: 449–455, 2003.
40. **Stossel TP.** On the crawling of animal cells. *Science* 260: 1086–1094, 1993.
41. **Thurman JM, Ljubanovic D, Edelstein CL, Gilkeson GS, Holers VM.** Lack of a functional alternative complement pathway ameliorates ischemic acute renal failure in mice. *J Immunol* 170: 1517–1523, 2003.
42. **Tsokos GC, Fleming SD.** Autoimmunity, complement activation, tissue injury and reciprocal effects. *Curr Dir Autoimmun* 7: 149–164, 2004.
43. **Wakatsuki T, Schwab B, Thompson NC, Elson EL.** Effects of cytochalasin D and latrunculin B on mechanical properties of cells. *J Cell Sci* 114: 1025–1036, 2001.
44. **Weiser MR, Williams JP, Moore FD Jr, Kobzik L, Ma M, Hechtman HB, Carroll MC.** Reperfusion injury of ischemic skeletal muscle is mediated by natural antibody and complement. *J Exp Med* 183: 2343–2348, 1996.
45. **Weisman HF, Bartow T, Leppo MK, Marsh HC Jr, Carson GR, Concino MF, Boyle MP, Roux KH, Weisfeldt ML, Fearon DT.** Soluble human complement receptor type 1: in vivo inhibitor of complement suppressing post-ischemic myocardial inflammation and necrosis. *Science* 249: 146–151, 1990.
46. **Wessells NK, Spooner BS, Ash JF, Bradley MO, Luduena MA, Taylor EL, Wrenn JT, Yamaa K.** Microfilaments in cellular and developmental processes. *Science* 171: 135–143, 1971.
47. **Whisnant JP.** Epidemiology of stroke: emphasis on transient cerebral ischemia attacks and hypertension. *Stroke* 5: 68–70, 1974.
48. **Williams JP, Pechet TT, Weiser MR, Reid R, Kobzik L, Moore FD Jr, Carroll MC, Hechtman HB.** Intestinal reperfusion injury is mediated by IgM and complement. *J Appl Physiol* 86: 938–942, 1999.
49. **Zhang M, Alicot EM, Chiu I, Li J, Verna N, Vorup-Jensen T, Kessler B, Shimaoka M, Chan R, Friend D, Mahmood U, Weissleder R, Moore FD, Carroll MC.** Identification of the target self-antigens in reperfusion injury. *J Exp Med* 203: 141–152, 2006.
50. **Zhang M, Austen WG Jr, Chiu I, Alicot EM, Hung R, Ma M, Verna N, Xu M, Hechtman HB, Moore FD Jr, Carroll MC.** Identification of a specific self-reactive IgM antibody that initiates intestinal ischemia/reperfusion injury. *Proc Natl Acad Sci USA* 101: 3886–3891, 2004.
51. **Zhou W, Farrar CA, Abe K, Pratt JR, Marsh JE, Wang Y, Stahl GL, Sacks SH.** Predominant role for C5b-9 in renal ischemia/reperfusion injury. *J Clin Invest* 105: 1363–1371, 2000.



Pathogenic Natural Antibodies Recognizing Annexin IV Are Required to Develop Intestinal Ischemia-Reperfusion Injury¹

Liudmila Kulik,* Sherry D. Fleming,[†] Chantal Moratz,^{‡§} Jason W. Reuter,* Aleksey Novikov,* Kuan Chen,* Kathy A. Andrews,[¶] Adam Markaryan,[#] Richard J. Quigg,[#] Gregg J. Silverman,[¶] George C. Tsokos,^{‡**} and V. Michael Holers^{2*}

Intestinal ischemia-reperfusion (IR) injury is initiated when natural IgM Abs recognize neo-epitopes that are revealed on ischemic cells. The target molecules and mechanisms whereby these neo-epitopes become accessible to recognition are not well understood. Proposing that isolated intestinal epithelial cells (IEC) may carry IR-related neo-epitopes, we used in vitro IEC binding assays to screen hybridomas created from B cells of unmanipulated wild-type C57BL/6 mice. We identified a novel IgM mAb (mAb B4) that reacted with the surface of IEC by flow cytometric analysis and was alone capable of causing complement activation, neutrophil recruitment and intestinal injury in otherwise IR-resistant *Rag1*^{-/-} mice. mAb B4 was found to specifically recognize mouse annexin IV. Preinjection of recombinant annexin IV blocked IR injury in wild-type C57BL/6 mice, demonstrating the requirement for recognition of this protein to develop IR injury in the context of a complex natural Ab repertoire. Humans were also found to exhibit IgM natural Abs that recognize annexin IV. These data in toto identify annexin IV as a key ischemia-related target Ag that is recognized by natural Abs in a pathologic process required in vivo to develop intestinal IR injury. *The Journal of Immunology*, 2009, 182: 5363–5373.

Ischemia-reperfusion (IR)-induced³ injury is a pathologic process that occurs when the normal blood flow to an organ or tissue is interrupted for a period of time that is sufficiently long to result in marked hypoxia and ischemia, following which the recirculation of blood is restored. A central concept in this process is that the introduction of oxygenated blood during the reperfusion phase results in the development of more severe target organ injury than that caused by the ischemia per se (1, 2). The precise mechanism of injury during the reperfusion phase is a subject of intense investigation, because no specific therapy exists at the present time for the treatment of this pathologic process that underlies common clinical events such as myocardial infarction and stroke (3–6). IR-induced injury is especially prominent in the

intestine and is frequently followed by multiple organ dysfunction and infection as secondary complications (7–10).

With regard to the pathogenesis of this condition, complement activation and neutrophil infiltration are two key events that are required for experimental intestinal IR injury induced by ligation and subsequent release of the mesenteric artery, as both neutrophil depletion (11–13) and complement blockade (14–16) protect mice from the development of local tissue damage. Initiation of complement activation by the classical and lectin pathways has been demonstrated after IR of the heart, intestine, and skeletal muscle (15, 17–19), although tissue injury also apparently requires the engagement of the alternative pathway amplification loop (20). Initial evidence that natural Abs are centrally involved in IR-induced injury came from seminal findings that *Rag1*^{-/-} mice are resistant to the induction of IR injury to the intestine as well as other vascularized organs (19, 21, 22). The same mice, when reconstituted with IgM purified from natural Ab in pooled sera from wild-type (wt) mice, become fully susceptible to IR-induced injury (19, 23, 24). As a related finding, *Cr2*^{-/-} mice that lack expression of the B lymphocyte complement receptor (CR)1 and CR2 are also resistant to IR-induced injury, despite exhibiting normal quantitative levels of polyclonal IgM. Infusion of natural IgM and IgG Abs from *Cr2*^{+/+} but not *Cr2*^{-/-} mice, or transfer of peritoneal B cells from *Cr2*^{+/+} to *Cr2*^{-/-} mice, restores intestinal IR injury (23, 25). These data have suggested that there are specific IR-related neo-epitopes against which *Cr2*^{-/-} mice do not develop normal quantitative or qualitative levels of natural Abs.

Natural Abs are Igs that are produced in the absence of deliberate immunization, and they are a major component of the repertoire of B1 cells, which produce IgM and in some cases IgG Abs (26, 27). B1 cells in the adult mouse are found primarily in the peritoneum and pleura (28). Natural Abs are frequently found to be polyreactive at low affinity with multiple self Ags (29, 30), and they are considered as an important part of the innate immune system defense against infection. For example, natural Abs have been found to be protective against challenge with bacterial as well

*Departments of Medicine and Immunology, University of Colorado Denver School of Medicine, Denver, CO 80045; [†]Division of Biology, Kansas State University, Manhattan, KS 66506; [‡]Department of Cellular Injury, Walter Reed Army Institute of Research, Silver Spring, MD 20910; [§]Uniform Services University of the Health Sciences, Bethesda, MD 20814; [¶]Rheumatic Diseases Core Center, University of California, San Diego, La Jolla, CA 92093; [#]Section of Nephrology, Department of Medicine, University of Chicago, Chicago, IL 60637; and ^{**}Rheumatology Division, Beth Israel Deaconess Medical Center, Harvard Medical School, Boston, MA 02115
Received for publication November 26, 2008. Accepted for publication January 17, 2009.

The costs of publication of this article were defrayed in part by the payment of page charges. This article must therefore be hereby marked *advertisement* in accordance with 18 U.S.C. Section 1734 solely to indicate this fact.

¹ This work was funded by U.S. Army Medical Research and Materiel Command (MRMC) Award W81XWH-06-1-0520 and MRCM Award W81XWH-07-1-0286; the Alliance for Lupus Research; and National Institutes of Health Grants R01 AI31105, A161691, AI46637, DK41873, and DK55357.

² Address correspondence and reprint requests to Dr. V. Michael Holers, Departments of Medicine and Immunology, University of Colorado Denver School of Medicine, Mail Stop B115, P.O. Box 6511, Aurora, CO 80045. E-mail address: michael.holers@ucdenver.edu

³ Abbreviations used in this paper: IR, ischemia-reperfusion; CR, complement receptor; DAPI, 4',6-diamidino-2-phenylindole; IEC, intestinal epithelial cell; IEF, isoelectric focusing; LIC, ligation-independent cloning; LTB₄, leukotriene B₄; MPO, myeloperoxidase; MS, mass spectrometry; SA, streptavidin; wt, wild type.

as viral pathogens, and to play an important role in the clearance of endotoxin (31–33). In addition, natural Abs play important roles in the recognition of apoptotic cells, oxidized low-density lipoprotein, and nuclear and cytoplasmic components released from damaged cells (34–36).

The possibility that Abs recognizing specific Ags, or subsets of Ags, could be identified to play essential roles in IR-induced injury was suggested by Fleming et al. (21) in experiments where IgG mAbs against negatively charged phospholipids and β -2-glycoprotein 1, as well as polyclonal antisera with high titers against the same Ags, were able to reconstitute mesenteric IR-induced intestinal and lung injury in $Cr2^{-/-}$ mice. Unlike $Cr2^{-/-}$ mice, though, reconstitution of IR tissue damage in injury-resistant $Rag1^{-/-}$ mice required the infusion of both anti- β -2-glycoprotein 1 and anti-phospholipid IgG mAbs, or polyclonal serum-derived Abs. Another Ab system important in IR injury has been shown to involve natural Abs recognizing an epitope on non-muscle myosin and glycogen phosphorylase (37, 38). In contrast to studies by Fleming et al., an IgM mAb (designated CM22) recognizing these two Ags was found to be capable alone of inducing mesenteric and skeletal muscle IR injury in $Rag1^{-/-}$ mice, and a peptide mimic of the Ag also blocked *in vivo* the IR injury of intestine and skeletal muscle in wt mice (22, 37, 38).

Annexin IV belongs to a family of proteins that are Ca^{2+} - and phospholipid-binding proteins (39, 40). The structure of annexins consists of a conserved Ca^{2+} and membrane binding core of four annexin repeats (eight for annexin VI) and variable N-terminal regions (41). Annexins are soluble cytosolic proteins, but despite the lack of obvious signal sequences and the apparent inability to enter the classical secretory pathway, annexins have been identified in extracellular fluids or associated with the external cell surface through poorly understood binding sites (40, 42–44). Annexin IV is predominantly produced by epithelial cells and is also found at high levels in lung, intestine, pancreas, liver, and kidney. Depending on the cell type, annexin IV has been found either along the basolateral, basal, or apical domains of the plasma membrane, and in some cell types, it has been found to be present throughout the cytoplasm (45–47). With regard to its function, annexin IV has been shown to inhibit the epithelial calcium-activated chloride ion conductance (48), to play a role in the formation of pronephric tubules (49), and to regulate the passive membrane permeability to water and protons (50). Up-regulation of annexin IV has been found in renal cell carcinoma (51, 52). Finally, surface membrane expression of annexin IV has also been recognized as an early marker for apoptotic cell death (53, 54).

Herein we report the identification of a novel pathogenic IgM mAb that is capable of inducing intestinal IR injury in $Rag1^{-/-}$ mice. The mAb was found to specifically recognize mouse annexin IV. Importantly, we also found that normal mouse sera contain natural Abs to annexin IV epitopes and that treatment of wt C57BL/6 mice with recombinant annexin IV before the reperfusion phase prevents IR-induced intestinal injury. We propose that binding sites on annexin IV are essential neo-epitopes that are expressed on ischemic tissues and are targets for natural Ab binding during the reperfusion phase, with subsequent complement activation, neutrophil recruitment, and tissue injury.

Materials and Methods

Mice

Adult male $Rag1^{-/-}$ mice were obtained from The Jackson Laboratory and maintained following shipment for at least a 7-day acclimation period in the Uniformed Services University of Colorado Denver animal facility. Adult male and female $Cr2^{+/+}$ and $Cr2^{-/-}$ mice were maintained and bred as two sublines at University of Colorado Denver as described previously

(23). Animal studies at sites were approved by the local institutional review board. Human studies were approved by the Colorado MultiInstitutional Review Board.

Abs and reagents used for analysis

Biotinylated and FITC-conjugated goat anti-mouse IgG (Fc γ specific) or anti-mouse IgM (μ -chain specific) streptavidin (SA)-FITC and SA-PE were obtained from Jackson ImmunoResearch Laboratories. Alkaline phosphatase-conjugated goat anti-mouse Ig Ab was obtained from Caltag Laboratories. Polyclonal rabbit anti-annexin IV Ab was obtained from ProteinTech Group, and anti-6 \times His mAb was obtained from Novagen. Synthetic peptides were obtained from Synthetic Biomolecules.

Development and purification of IgM mAbs

mAbs B4 and D5 were developed by the fusion of peritoneal, lymph node, and spleen cells from unmanipulated wt C57BL/6 mice with the Sp2/0-Ag14 myeloma cell line by the standard protocol to establish hybridomas. Successful fusions were screened by Western blot analysis using IEC lysates and by flow cytometric analysis of isolated IEC. To purify mAbs, Ab from the exhausted supernatants of cultured B4 and D5 hybridomas was affinity purified on a column of agarose beads with goat anti-human IgM (Sigma-Aldrich). Bound Ab was eluted with a buffer containing 0.1 M glycine (pH 2.3) and collected into a buffer containing 1.5 M Tris (pH 8.8). Eluted mAb was dialyzed against PBS (pH 7.4) for 48 h and concentrated using centrifugal filtration on Centricon Plus-20 (Millipore). Ab concentration was determined by measuring the $A_{280\text{ nm}}$ of the sample, and purity was confirmed by analysis on a 10% SDS-PAGE gel.

IEC isolation and flow cytometric analysis

Isolation of IEC was performed using previously described methods (55, 56). Briefly, after dissection of the mouse intestine into small pieces, the latter were incubated twice in HBSS with 1 mM DTT and 1 mM EDTA for 30 min at 37°C with shaking to detach IEC. By this method of isolation, the cell mixture consists of 93–95% IEC, with <2% intraepithelial lymphocyte contamination (55). Intraepithelial lymphocyte can be readily gated out in time of flow cytometric analysis by size characteristics. Detached free cells and intact crypts were centrifuged and resuspended in HBSS containing Ca^{2+} and Mg^{2+} , or in 5% FBS DMEM culture media. Isolated IEC were washed in the staining buffer (2% FCS/0.01% NaN_3 /PBS), resuspended in the staining buffer containing hybridoma supernatant or pure mAb, and incubated for 30 min at room temperature. After incubation, cells were washed in the staining buffer three times and then incubated with the secondary goat anti-mouse IgM (μ -chain specific) Abs (Jackson ImmunoResearch Laboratories) for 30 min at room temperature. Following incubation, cells were washed as above described and then resuspended in the staining buffer. Flow cytometry was performed using a BD Biosciences FACSCalibur.

Western blot analysis

IEC were lysed on ice for 20 min in a buffer containing 0.5% Triton X-100, 0.5% Chaps, 20 mM Tris-HCl (pH 7.5), 1 mM EDTA, 10 μ g/ml leupeptin, and protease inhibitor mixture (Roche Molecular Biochemicals). Lysates were cleared by centrifugation at 8000 \times g for 5 min. After separation by 8% Tris-glycine SDS-PAGE, the proteins were transferred to a polyvinylidene difluoride membrane. The membrane was blocked overnight with 5% nonfat milk dissolved in PBS. The membrane was washed in PBS and then probed with a primary Ab for 1–2 h in 2% milk/PBS, washed, and then incubated with HRP-conjugated secondary Abs. A positive signal was visualized using the ECL system (PerkinElmer).

Intestinal IR injury

The intestinal IR injury model was performed as previously described (23) by the surgical procedure of opening the abdominal cavity of an anesthetized mouse and occluding the superior mesenteric artery for 30 min, followed by removal of the clamp and 2-h reperfusion of the tissue. Ketamine/xylazine was used for anesthesia.

Histology and immunohistochemistry

Immediately after euthanasia, segments of small intestine specimens were fixed in 10% buffered formalin, embedded in paraffin, cut transversely in 5- μ m sections, and stained with Giemsa. Mucosal injury was graded on a six-tiered scale in a blinded manner, as described previously (23). Briefly, the average of villus damage in an \sim 2-cm intestinal section (50–100 villi) is determined after grading each villus in the section on a 0–6 scale. A score of 0 is assigned to a normal villus; a score of 1 to villi with tip

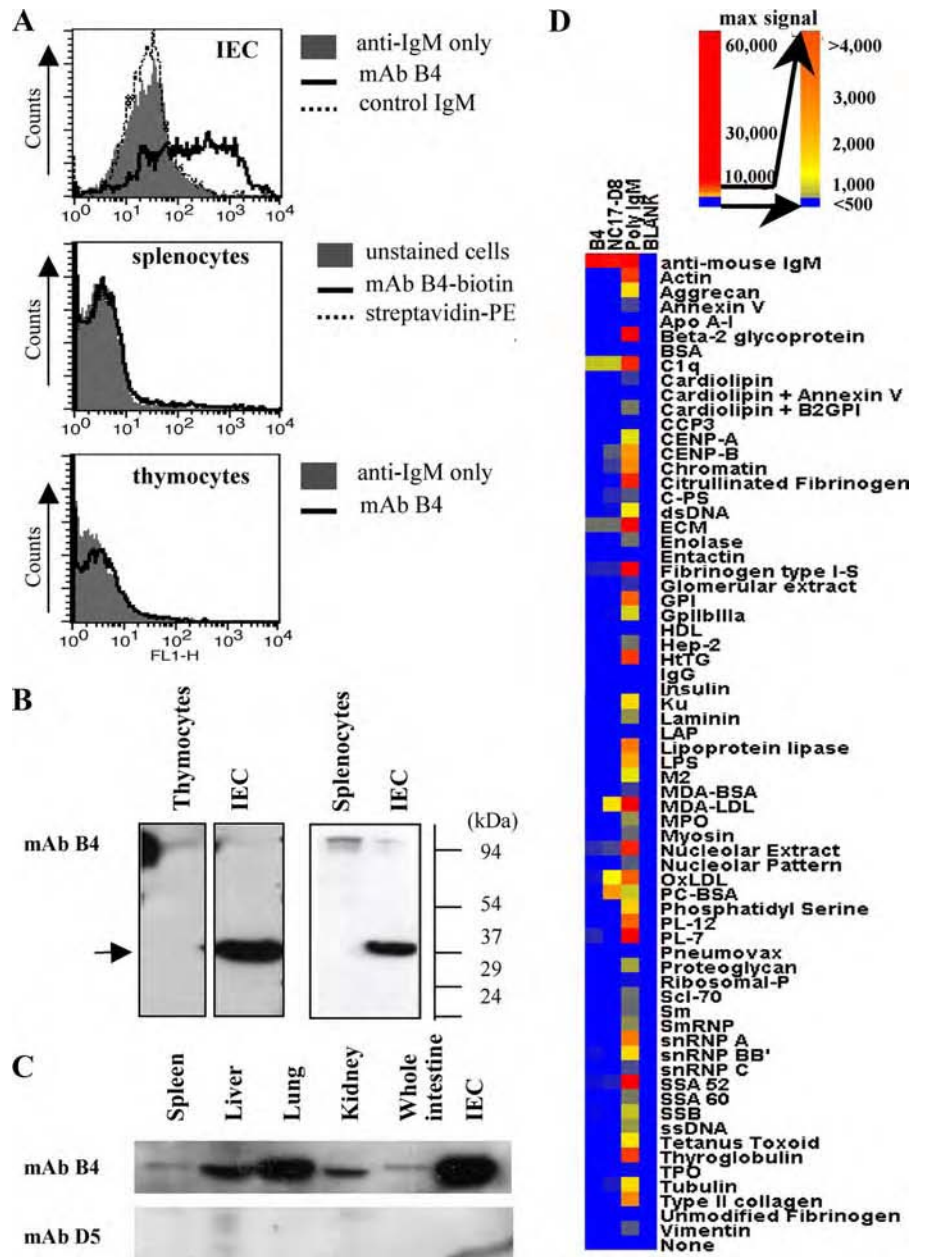


FIGURE 1. Characterization of mAb B4 epitope expression. *A*, Representative flow cytometric histograms show binding of mAb B4 to a single-cell suspension of IEC (*top panel*), splenocytes (*middle panel*), and thymocytes (*bottom panel*). Cells were incubated with mAb B4, and bound Ab was detected by using anti-mouse IgM (μ -chain specific) for IEC and thymocytes. In the case of splenocytes, mAb B4 labeled with biotin was used. *B* and *C*, mAb B4 epitope expression was determined by Western blot analysis of isolated thymus, spleen, or intestine cell in *B*, or lysates were prepared from whole organs in *C*. Data are representative of two independent experiments. *D*, Binding of mAb B4 to proteins typically found as targets of polyreactive natural Abs was studied by microarray analysis. The positive control for mAb B4 binding is C1q and anti-mouse IgM Ab, positive controls for the microarray are mAb NC-17D8 and polyclonal IgM, and the negative control is designated blank.

distortion; a score of 2 is assigned when in addition goblet cells and Gugenheims' spaces are missing; a score of 3 is assigned to villi with patchy disruption of the epithelial cells; a score of 4 is assigned to villi with exposed but intact lamina propria with epithelial cell sloughing; when the lamina propria is exuding a score of 5 is assigned; and lastly, a score of 6 is assigned to villi that display hemorrhage or to villi that are denuded. Additional tissue sections were fixed for 2 h in cold 4% paraformaldehyde in PBS before transfer to PBS for paraffin embedding and preparation of transverse sections. Following removal of paraffin from sections, nonspecific Ab binding sites were blocked by treatment with a blocking solution (DakoCytomation) for 30 min. After washing in PBS, the tissues were incubated with goat anti-mouse C3 (Cappel) or appropriate control IgG (Jackson ImmunoResearch Laboratories) Ab overnight at 4°C. The primary Ab was detected with a biotinylated donkey anti-goat Ig (Jackson ImmunoResearch Laboratories), then SA-HRP (Vector Laboratories), and developed with Vector Nova Red Substrate (Vector Laboratories). For immunohistochemistry, tissues were fixed at 4°C for 2 h in 4% paraformaldehyde in PBS. Nonspecific Ab binding sites were blocked by the incubation with a blocking solution PBS for 30 min. After washing in PBS, the tissues were incubated with isotype control Ab or FITC-conjugated anti-mouse C3, tetramethylrhodamine isothiocyanate-conjugated anti-mouse Ig, and 4',6-diamidino-2-phenylindole (DAPI) to visualize the nucleus. After

washing, the slides were mounted using ProLong Gold antifade reagent with DAPI and analyzed on an Olympus AX80 microscope.

Eicosanoid determination

The ex vivo generation of eicosanoids in small intestine tissue was determined using a previously described method (16, 23). Briefly, sections of minced fresh mid-jejunum were washed and resuspended in 37°C oxygenated Tyrode's buffer (Sigma-Aldrich). After tissues were incubated for 20 min at 37°C, supernatants and tissue were collected and stored at -80°C until assayed. The concentrations of leukotriene B₄ (LTB₄), and PGE₂ were determined using an enzyme immunoassay (Cayman Chemical). The tissue protein content was determined using the bicinchonic acid assay (Pierce) adapted for use with microtiter plates. LTB₄ and PGE₂ levels were expressed in pictograms per milligrams protein per 20 min.

Myeloperoxidase (MPO) activity

Supernatants generated for the eicosanoid assays were also used to determine peroxidase activity by measuring oxidation of 3,3',5,5'-tetramethylbenzidine as described previously (16). Briefly, supernatants were incubated with equal volumes of 3,3',5,5'-tetramethylbenzidine peroxidase substrate (Kirkegaard & Perry) for 45 min. The reaction was stopped by the

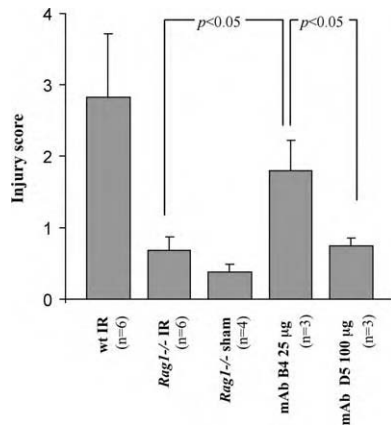


FIGURE 2. Restoration of IR injury in *Rag1*^{-/-} mice by mAb B4. Sixty minutes before the induction of ischemia by mesenteric artery occlusion, 25 µg of purified mAb B4, or 100 µg of control IgM mAb D5, were injected i.v. After completion of the IR protocol, mice were sacrificed, and Giemsa-stained intestinal sections from each treatment group were scored for mucosal injury (0–6) as described in *Materials and Methods*. mAb B4 injected into *Rag1*^{-/-} mice induced substantial injury in the mice undergoing IR (mAb B4 IR) in contrast to sham-operated mice (*Rag1*^{-/-} sham) or *Rag1*^{-/-} mice undergoing IR (*Rag1*^{-/-} IR). mAb D5-treated *Rag1*^{-/-} mice (mAb D5 IR) did not demonstrate substantial injury. As a positive control for the level of intestinal injury, wt C57BL/6 mice undergoing IR were included (wt IR). All measurements were obtained at $\times 200$. The figure is a representative of two independent experiments. Each bar is the average \pm SEM with three to six animals per group. Statistical analysis was performed by Student's *t* test.

addition of 0.18 M sulfuric acid, and the OD_{450 nm} was determined. The concentration of total peroxidase was determined using HRP (Sigma-Aldrich) as a standard and plotted as picograms of MPO activity per milligram of tissue.

Purification of IEC protein reactive with mAb B4

To purify protein reactive with mAb B4 for identification, a three-step purification procedure based on the method described by Vossenaar et al. (57) was performed. In the first step, IEC lysates were resolved using preparative 8% SDS-PAGE. Two lanes from the gel were cut. The first lane was transferred to a membrane and probed with mAb B4, and the second lane was stained with Coomassie brilliant blue to localize precisely the position of the proteins. The rest of the gel was stained with a nonfixing gel stain GeBA SeeBand stain (Gentaur), and protein-containing areas were excised and stored at 4°C. In the next step, the gel strips were washed in a freshly prepared, warm (37°C) washing solution (2 mM Tris-HCl (pH 8.0), 8 M urea, and 1% Nonidet P-40). The washed gel strips were then loaded on an isoelectric focusing (IEF) gel (6 M urea, 1% Nonidet P-40, 15% (of total volume) acrylamide mix (39:1), 2% ampholytes (3–10), 0.47 µg/ml ammonium persulfate, and 0.66 µl/ml tetramethylethylenediamine). IEF was performed on a gel (15 \times 15 cm) overnight at 200 V. The upper and lower buffers were 0.09 M NaOH and 0.85% phosphoric acid, respectively. Immediately after migration, the gel was fixed in the 20% trichloroacetic acid for 20 min and then stained with Coomassie brilliant blue. Regions containing proteins in the IEF were excised and separated by 8% SDS-PAGE. Protein was localized by staining with GeBA SeeBand stain, and areas of interest were excised and used for identification of proteins using mass spectrometry (MS) (University of Chicago). A parallel SDS-PAGE was performed, and after transfer to polyvinylidene difluoride membrane, Western blot analysis was performed to confirm the location of the Ag in the gel.

Protein identification by MS

After separation the protein was digested in-gel with trypsin according to a modified protocol (University of Chicago). The aqueous peptide extract (10 µl) was analyzed using electrospray liquid chromatography MS (LC/MS/MS). An HPLC instrument (Agilent) was connected with an XCT ion trap MS (Agilent). Sample was loaded automatically at 10 µl/min. Chromatography buffer solutions (buffer A, 2.5% methanol, and 0.1% formic acid; buffer B, 99.9% acetonitrile and 0.1% formic acid) were used to make

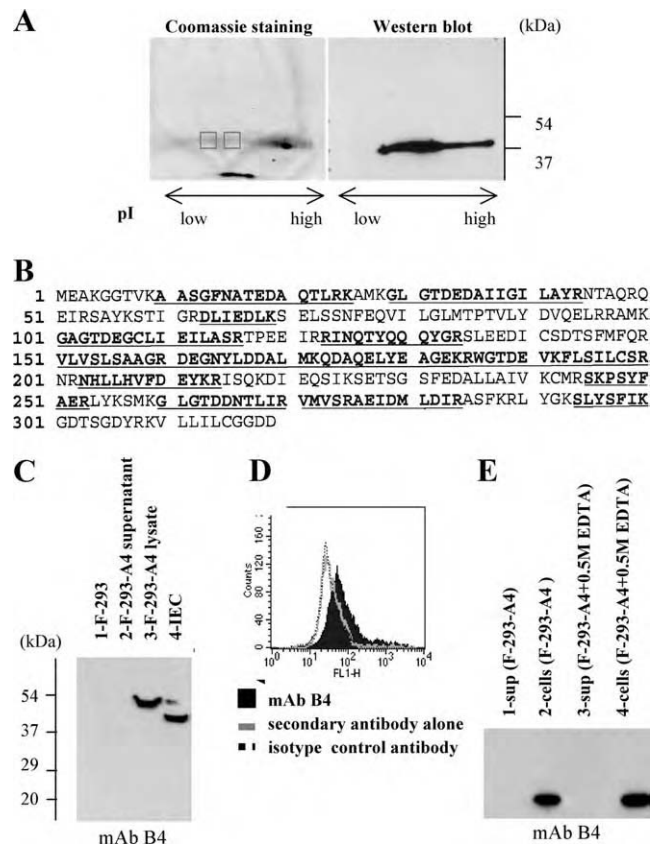


FIGURE 3. Identification of the Ag recognized by mAb B4. *A*, Lysates prepared from isolated IEC were separated using a sequential three gel separation protocol as described in *Materials and Methods*. The presence of the B4 Ag was confirmed by Western blot analysis (*right panel*). Two gel samples (□) were analyzed by MS. *B*, The MASCOT search results for the protein isolated from first sample were identified as mouse annexin IV based on the highest score number of 785; 78 matched peptides covering 53% of the annexin IV sequence were identified (underlined bold letters). *C*, Lysates of untransformed F-293 cells (*lane 1*) and F-293 cells transformed with the pSecTag2/Hygro B expression vector carrying annexin IV insert (F-293-A4) (*lane 2*) together with culture supernatants from transformed cells (*lane 3*) were probed by Western blot analysis with mAb B4. *D*, Flow cytometric analysis of F-293 cells expressing recombinant annexin IV. F-293-A4 cells were probed in flow cytometry with mAb B4. *E*, Supernatant (*lane 1*) and lysate (*lane 2*) from F-293-A4 cells expressing recombinant annexin IV that had been incubated in PBS alone, or supernatant (*lane 3*) and lysate (*lane 4*) from the same cells incubated with 0.5 M EDTA, were probed by Western blot analysis with mAb B4. Recombinant annexin IV was not released from F-293-A4 cells in the absence of free Ca²⁺.

a 90-min gradient (8 min to 10% buffer B, 32 min from 10 to 45%, hold 5 min, 5 min from 45 to 90%, hold for 20 min, then 5 min to 0% B, hold for 15 min). A flow rate of 0.25 µl/min was used. The MASCOT program was used to search the mouse protein sequence database. Probability-based mouse score ($-10 \log P$) was used for protein identification, where P is the probability that the observed match is a random event. Individual ion scores > 40 indicate identity or extensive homology ($p < 0.05$).

Annexin IV constructs

The original cDNA sequence of mouse annexin IV was taken from Invitrogen clone no. 4947415 placed into the pET-32 Xa/LIC bacterial expression vector (Novagen). To accomplish this task, cDNAs encoding for annexin IV were amplified by PCR. The forward primer used was 5'-GGT ATT GAG GGT CGC ATG GAA GCC AAA GGA GGA AC-3'. The reverse primer was 5'-AGA GGA GAG TTA GAG CCT TAA TCA TCT CCT CCA CAG AGA AT-3'. The ligation-independent cloning (LIC) was done in pETXa/LIC vector. The vector adds a Trx-Tag, His-Tag, and S-Tag to the N terminus of the protein. These tags are cleavable with Factor Xa

leaving a native version of the N terminus. To express protein in mammalian cells the forward and reverse primers were 5'-CTG GTA CCA GCA TGG AAG CCA AAG GAG-3' and 5'-TCT CGA GAA TCA TCT CCT CCA CAG AGA ATG-3', respectively. The primers add restriction sites *Acc65I* (or *KpnI*) to the start of annexin IV and *XhoI* restriction site to the end of annexin IV. The *KpnI/XhoI* fragment was amplified by PCR from genomic DNA using *Pfu* polymerase (Novagen). The *KpnI/XhoI* fragment was subsequently cloned into pSecTag2/Hygro B expression vector (Invitrogen), and expression of the protein was accomplished in the F-293 cell line (Invitrogen). The vector adds an Ig κ -chain leader sequence to the N terminus of the protein for secretion. After leader peptide is cleaved ~15 aa are left on the N terminus of the protein. The vector adds also a myc epitope and a 6 \times His tag to the C terminus of the protein.

Expression and purification of recombinant annexin IV

The expression construct pETXa/LIC-A4 was transformed into *E. coli* Rosetta 2 (DE3) cells. Bacterial expression cultures were incubated at 37°C in Luria-Bertani medium containing ampicillin (50 μ g/ml) until an $A_{600\text{ nm}}$ of 0.6 was reached. Recombinant protein expression was induced by an addition of isopropyl β -D-thiogalactoside (Sanland-Chem) to a final concentration of 0.3 mM. After 6 h of incubation at 32°C, bacteria were harvested by centrifugation at 10,000 \times g for 10 min at 4°C. After harvesting the cells, they were resuspended in PBS with Complete, EDTA-Free Protease Inhibitor Cocktail Tablets (Roche Molecular Biochemicals). Bacteria were lysed by four freeze-thaw cycles. The lysate was then incubated with DNase and RNase for 30 min. Cell lysate was then centrifuged (10,000 \times g for 40 min), and cell pellet was resuspended in 6 M urea for 30 min. Centrifugation by 10,000 \times g for 40 min was then used to remove undissolved debris. The precleared supernatant was diluted (2:1) by PBS, its pH adjusted to 7.6 with NaOH and then applied to a TALON resin column (BD Clontech) equilibrated with 4 M urea. Bound protein was refolded on the column using a discontinuous gradient from 4 to 0.25 M urea, starting with the equilibration buffer and finishing with a buffer containing 10 mM imidazole in PBS (pH 7.0). The refolded protein was eluted with a buffer containing a stepwise gradient of 19, 38, 75, and 150 mM imidazole. The presence of the protein and its purity was confirmed by SDS-PAGE and staining with Coomassie brilliant blue.

Annexin IV ELISA

Immulon 1B plates (Dynatech Laboratories) were coated with 5 μ g/ml annexin IV-purified protein in PBS. Wells were blocked with 1% BSA in PBS. Serial dilution of serum samples were made in blocking buffer, and samples were applied to wells. After incubation and washing, bound Abs were detected using AP-conjugated anti-mouse IgG (Fc γ specific) or anti-mouse IgM (μ -chain specific) Abs, followed by *p*-nitrophenyl phosphate (Sigma-Aldrich) at 1 mg/ml. Plates were read at 405 nm.

Results

Generation of mAbs

As a strategy to identify mAbs that would recognize neo-epitopes on ischemic tissues, we hypothesized that intact intestinal epithelial cells (IEC), when isolated as a single-cell suspension, might expose on the surface the same neo-epitopes that are targets on the ischemic cells for pathogenic IgM Abs *in vivo* during intestinal IR. Consistent with this, in pilot experiments, we found that whole serum from *Cr2^{+/+}* mice exhibited higher binding of Igs to IEC than *Cr2^{-/-}* mice (data not shown). On the basis of this hypothesis, we used freshly isolated IEC to screen hybridomas obtained by fusion with the Sp2/0-Ag14 myeloma cell line of B cells from wt unmanipulated C57BL/6 mice derived from peritoneum, lymph nodes, and spleen. Wells were chosen for further subcloning based on the positive surface staining of IEC by flow cytometry or reactivity by Western blot analysis on tissue lysates. Cells were then serially recloned to obtain monoclonal cell lines stably producing a single mAb.

One such product of this strategy, designated mAb B4, was obtained from a fusion with spleen cells and is an IgM κ isotype Ab. As shown using flow cytometric analysis, mAb B4 binds a surface epitope on IEC but not on freshly isolated splenocytes or thymocytes (Fig. 1A). By Western blot analysis, mAb B4 recognizes a protein with a m.w. of 37 kDa in IEC lysates but not lysates

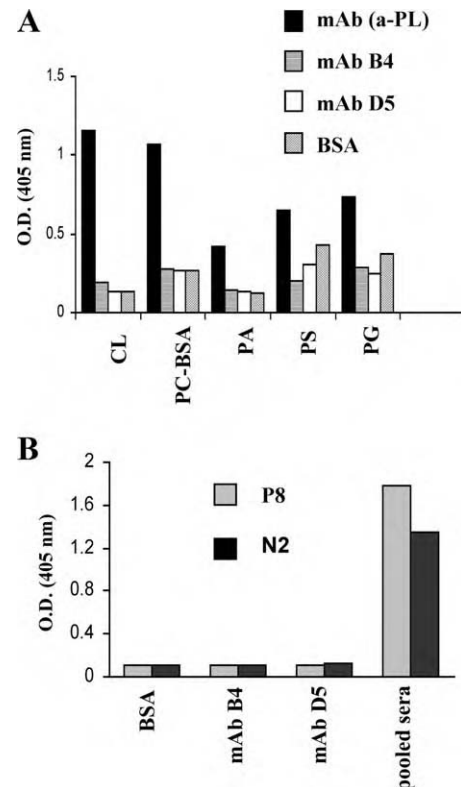


FIGURE 4. mAb B4 does not cross-react with previously published Ags recognized by pathogenic natural Abs in intestinal IR injury. *A*, mAb B4 was tested in an anti-phospholipid Ab ELISA for the binding to cardiolipin (CL), phosphorylcholine-BSA (PC-BSA), phosphatidic acid (PA), phosphatidylserine (PS), and phosphatidylglycerol (PG). A broadly reactive IgM anti-phospholipid mAb (our unpublished data) was used as a positive control. Bound Abs were detected by AP-conjugated goat anti-mouse IgM. Data are shown as OD_{405 nm}. *B*, Bar graph shows the lack of reactivity of mAb B4 in ELISA with synthetic peptides reported to be targets for the pathogenic CM22 IgM mAb. Synthetic peptides coated to an ELISA plate were incubated with either mAb B4 or control mAb D5. Bound Abs were detected by AP-conjugated goat anti-mouse IgM Ab. Pooled sera from C57BL/6 mice at a dilution of 1/50 were used as a positive control. Data are shown as OD_{405 nm} and are representative of two independent experiments.

from freshly isolated splenocytes or thymocytes (Fig. 1B). When other tissue lysates were probed by Western blot with mAb B4, the epitope was found to be widely distributed, with the highest relative expression in lung and isolated IEC (Fig. 1C). As an isotype control we used mAb D5 directed to an epitope on mouse cytokeratin 19 (our unpublished data). The results shown in Fig. 1C demonstrate that when the whole spleen was taken to make lysates, a weak band corresponding to the B4 Ag is seen, and a band of the same size was seen in lysates from whole thymus (data not shown). These data suggest that the mAb B4 epitope is expressed in nonlymphoid stromal cells, perhaps of epithelial origin, in these tissues.

To determine whether mAb B4 is typical of polyreactive natural Abs or has a more restricted reactivity, microarray analysis was performed using a series of Ags typically found to be targets of this class of Abs (29, 30). The accession number for the data is GSE14862; the data can be accessed on the website www.ncbi.nlm.nih.gov/geo/query/acc.cgi?acc=GSE14862. Positive controls for the assay were mAb NC17-D8 that recognizes phosphatidylcholine (58, 59) and polyclonal mouse IgM. As shown in Fig. 1D, mAb B4 demonstrates only minimal reactivity with a subset of

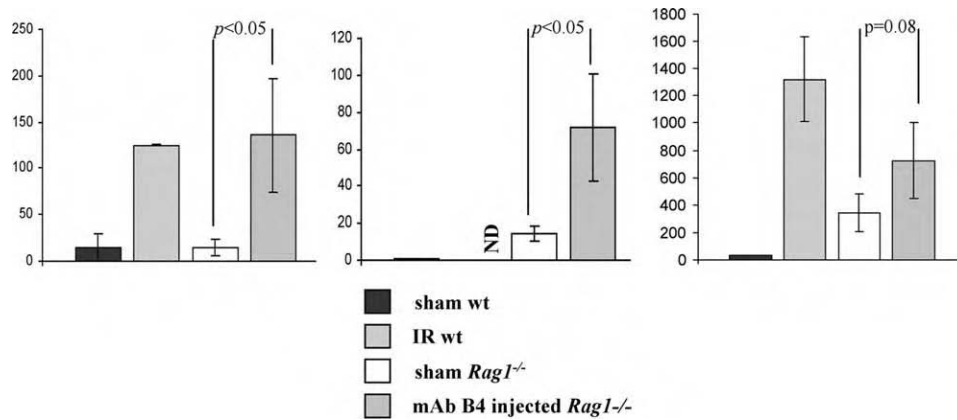


FIGURE 5. Association of neutrophil infiltration and eicosanoid generation with IR in *Rag1*^{-/-} mice treated with mAb B4. Intestinal tissue from sham-operated, wt C57BL/6 mice (■), wt mice undergoing IR (▨), or sham-operated *Rag1*^{-/-} mice (□), and *Rag1*^{-/-} mice preinjected with mAb B4 and undergoing IR (▩) were collected. The concentrations of MPO (left panel), LTB₄ (middle panel), and PGE₂ (right panel) were determined ex vivo using enzyme immunoassays. The data are presented as picograms per milligram of tissue for LTB₄ and PGE₂, and as MPO activity. Each bar is the average ± SEM with four to six animals per group. Statistical significance was determined using an unpaired two-tailed Student's *t* test. ND, data not obtained.

Ags that is far below that demonstrated by mAb NC17-D8 or polyclonal IgM. mAb B4 also does not recognize negatively charged phospholipids when using ELISA analysis (see Fig. 5 below). Thus, mAb B4 does not appear to be typical of the polyreactive subset of natural Abs.

Monoclonal Ab B4 restores IR injury in *Rag1*^{-/-} mice

To determine whether mAb B4 exhibited the desired characteristic of induction of intestinal IR injury, we used *Rag1*^{-/-} mice that are normally protected from IR injury (19). Purified mAb B4 or control IgM mAb D5 was injected i.v. 60 min before the reperfusion phase, and the intestines from mice undergoing IR were examined for injury.

Analysis of intestinal injury revealed that the sham treated *Rag1*^{-/-} mice as well as *Rag1*^{-/-} mice that underwent the IR protocol did not show significant damage as compared with wt C57BL/6 mice that demonstrated an injury score of 2.82 ± 0.9 (Fig. 2). In contrast, *Rag1*^{-/-} mice injected with 25 μ g of mAb B4 Ab demonstrated an injury score of 1.8 ± 0.42 . In contrast to the effects of mAb B4, the isotype control mAb D5, generated during the same screening protocol, did not cause IR injury in *Rag1*^{-/-} mice even at a dose of 100 μ g per mouse (score 0.75 ± 0.09). In other experiments, treatment of mice with doses of mAb B4 ranging from 9 to 81 μ g also led to significantly increased IR injury (data not shown), and thus, there is not a narrow dose-response interval for its biologic effect.

Monoclonal Ab B4 recognizes annexin IV

The finding that mAb B4 was able to mediate intestinal IR injury in *Rag1*^{-/-} mice led us to perform further studies and identify the protein specifically recognized by this mAb on IEC. We used a multistep process described in *Materials and Methods*, which culminated in a 2D gel separation of the proteins according to their m.w. and charge, following which the protein reactive with mAb B4 was characterized by proteolysis and MS analysis (Fig. 3). Of note, the IEF gel, wherein the separation of proteins occurs based on charge, revealed that the protein of interest formed a long smear, thus making it difficult to localize it in a single spot (Fig. 3A). To overcome the problem, we cut two separate areas from the gel and analyzed the proteins in each of these areas, considering that the same protein would be found in each section. MS analysis of fragmented protein in the two areas identified the same protein recognized by mAb B4 as mouse annexin IV (Fig. 3B). Consistent

with this result, using commercial polyclonal Abs to annexin IV, we were able to determine that anti-annexin IV Abs recognize the same extended band on the IEF gel to which mAb B4 binds (data not shown).

Monoclonal Ab B4 recognizes recombinant annexin IV expressed in mammalian cells

To confirm that murine annexin IV is the protein recognized by mAb B4, we expressed recombinant annexin IV in mammalian and bacterial cell systems. When recombinant annexin IV was expressed in the human F-293 cell line using the pSecTag2/Hygro B expression vector, Western blot analysis showed that the recombinant

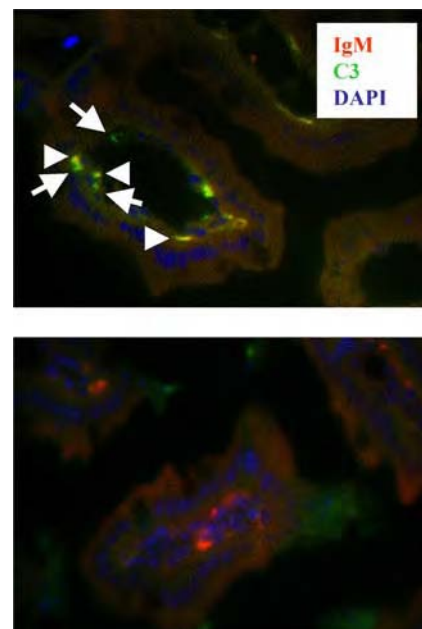


FIGURE 6. mAb B4, when injected into *Rag1*^{-/-} mice and inducing IR injury, clusters in the microvillus beneath the enterocyte layer. Three-color immunofluorescence staining for C3 (green), mouse Ig (red), and DAPI (blue) was performed. Clusters of C3 deposition colocalized with mouse Ig (arrow head) and C3 deposition alone (arrow) were seen in intestine from *Rag1*^{-/-} mice reconstituted by mAb B4 before IR (upper panel). Slides made from the same intestine were probed with anti-mouse Ig and isotype control Ab for C3 Ab (lower panel). Note absence of the yellow-color clusters therein.

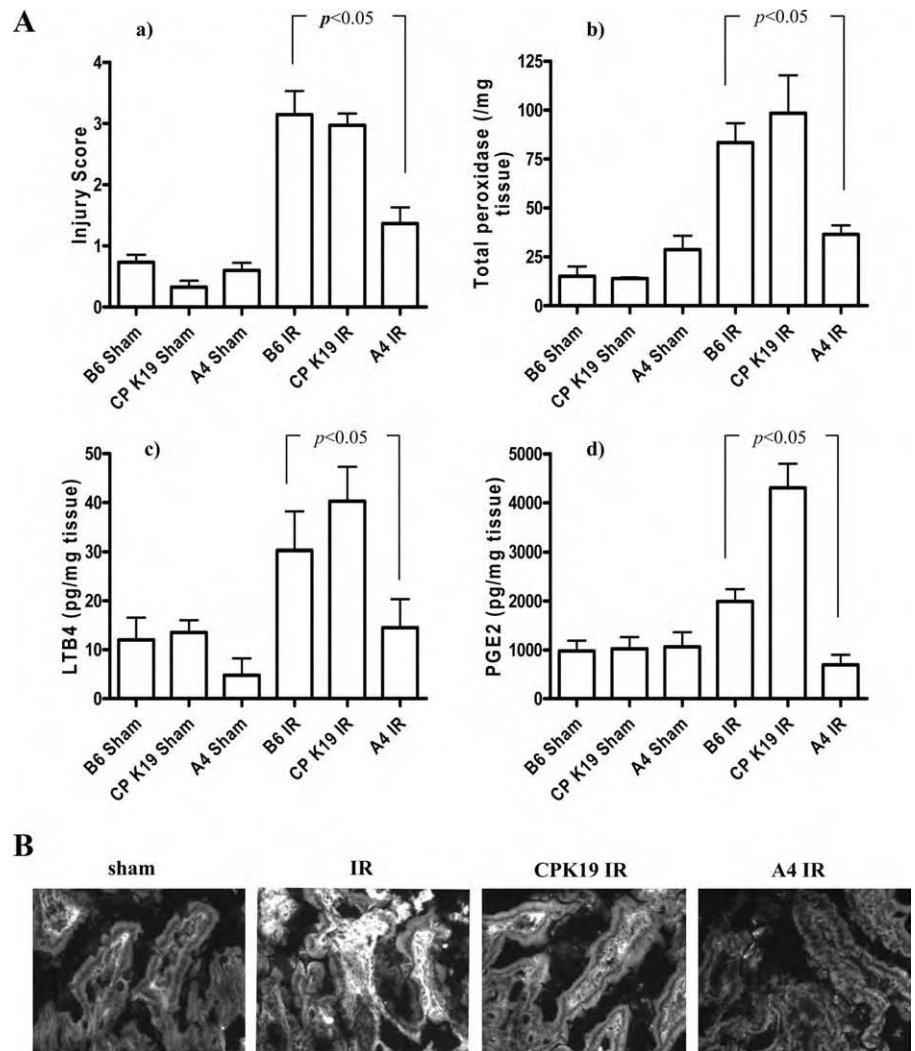


FIGURE 7. A, Intestinal IR injury is ameliorated in wt C57BL/6 mice receiving recombinant annexin IV before the ischemic phase. Reduction of the of IR-induced injury to the level of sham-operated animals (B6 sham) was observed in wt mice when they were injected with 50 $\mu\text{g}/\text{mouse}$ of annexin IV 5 min before the reperfusion phase (A4 IR). Injury in mice preinjected with control CPK19 protein (CP K19 IR) was comparable with the injury in C57BL/6 mice undergoing IR (B6 IR) (a). Small intestine tissue samples were processed as in Fig. 6 for MPO activity (b) and the eicosanoids LTB₄ (c) and PGE₂ (d). Each bar is the average \pm SEM with three to six animals per group. Statistical significance was determined using one-way ANOVA. B, Small intestine of annexin IV-preinjected mice (far right), similarly to sham-operated, wt mice (far left), does not show C3 deposition in IR induced injury, in contrast to wt mice (second from left) and mice preinjected with the CPK19 control protein undergoing IR (second from right).

annexin IV protein expressed was recognized by mAb B4 (Fig. 3C). The presence of annexin IV on the Western blot was confirmed by probing the membrane with polyclonal anti-annexin IV and anti-6 \times His Abs (data not shown). We also performed flow cytometric analysis of transfected F-293 cells to show that mAb B4 recognizes cells expressing recombinant murine annexin IV (Fig. 3D).

When transfected F-293-A4 cells were probed with mAb B4 using flow cytometric analysis, the protein was found to be localized on the surface of the cells (Fig. 3D). These results are consistent with the known localization of annexin IV whereby the protein is found to be closely associated with the plasma membrane. Previous results have suggested that annexin proteins may bind to the plasma membrane through a Ca²⁺-dependent mechanism (41, 60). However, when the recombinant annexin IV-expressing F-293-A4 cells were incubated in a buffer containing 0.5 M EDTA, immunoreactive protein was not released from the cell surface (Fig. 3E). These data correlate with the observation that IEC isolated in EDTA-containing buffer display the mAb B4 epitope on the surface of IEC as detected by flow cytometric analysis. In sum, several lines of evidence using mammalian recombinant protein expression methods confirm that mAb B4 specifically recognizes mouse annexin IV.

Monoclonal Ab B4 does not recognize Ags previously shown to be targets for pathogenic Abs in intestinal IR injury

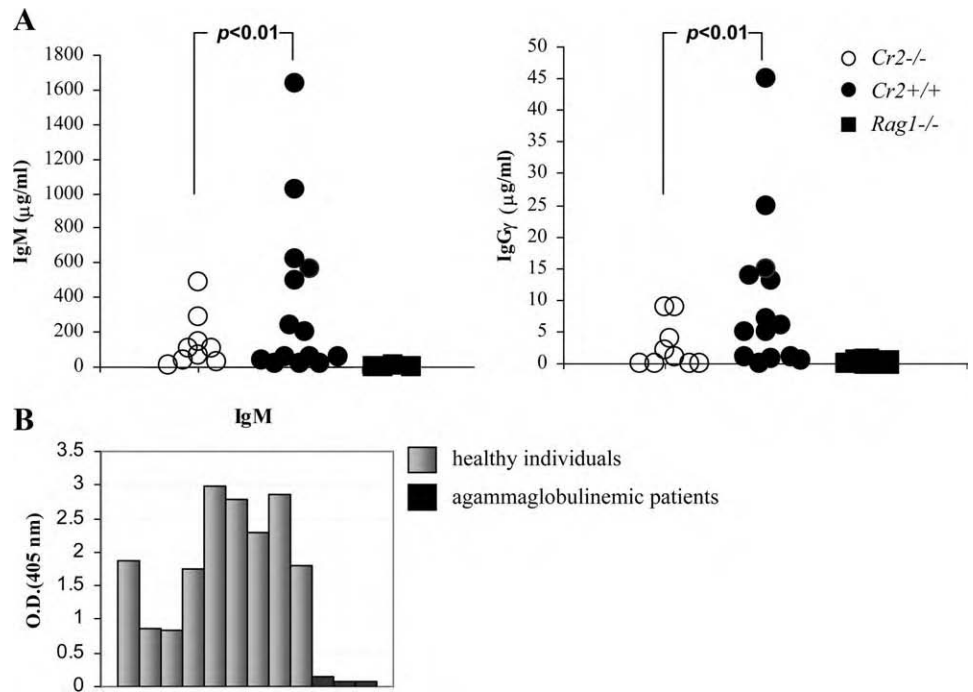
Two classes of Ags have previously been suggested as candidates for IR-related neo-epitopes and as targets for pathogenic

natural Abs. Although mAb B4 was found to recognize annexin IV, we wanted to specifically determine whether it would also cross-react with these other Ags. First, since it had been shown previously that *Cr2*^{-/-} and *Rag1*^{-/-} mice reconstituted with Abs recognizing negatively charged phospholipids demonstrated IR injury (21), we used an anti-phospholipid Ab ELISA to determine whether mAb B4 would recognize this class of Ags. We were unable to detect any binding of mAb B4 to the same phospholipids recognized in previous studies (Fig. 4A). Second, as reported by the Carroll group, the CM22 IgM mAb (37, 38) that is capable of inducing IR injury in *Rag1*^{-/-} mice recognizes a synthetic peptide (designated N2) derived from one of its Ags, nonmuscle myosin, or a mimicking peptide (designated P8) that was identified from a phage display library. When the same synthetic peptides were probed in ELISA for binding by mAb B4, no detectable signal was apparent, in contrast to pooled sera from wt C57BL/6 mice that demonstrated robust binding to both peptides (Fig. 4B). Thus, mAb B4 does not appear to cross-react with previously described Ags or epitopes important in this process.

IR injury restored by mAb B4 in *Rag1*^{-/-} mice is accompanied by neutrophil infiltration and the local generation of proinflammatory eicosanoids

To confirm that the intestinal IR injury in *Rag1*^{-/-} mice reconstituted with mAb B4 demonstrated similar characteristics to wt mice, we evaluated complement C3 deposition (see Fig. 6) as well

FIGURE 8. Presence of natural Abs to annexin IV. *A*, $Cr2^{+/+}$ in contrast to $Cr2^{+/-}$ mice demonstrate higher levels of IgM natural Ab to annexin IV. Serum samples from three cohorts of mice, $Cr2^{+/-}$ ($n = 9$), $Cr2^{+/+}$ mice ($n = 14$), and negative control $Rag1^{-/-}$ ($n = 5$) mice, were evaluated for the presence of natural IgM (left panel) and IgG (right panel) Abs to bacterial annexin IV. The figures are representative of two independent experiments. Statistical significance was determined using a Wilcoxon test. *B*, Nine serum samples from healthy humans and three from agammaglobulinemic patients were tested in the anti-annexin IV ELISA. Substantial levels of anti-annexin IV IgM Ab are present in the sera of normal humans.



as the infiltration of neutrophils and generation of eicosanoids (Fig. 5), all of which have been found in wt mice undergoing IR injury (16). To measure the level of neutrophil invasion into injured tissue, we performed biochemical analyses of MPO activity (Fig. 5). $Rag1^{-/-}$ mice reconstituted with mAb B4 demonstrated elevated MPO activity indistinguishable from wt mice undergoing IR injury. Previous studies have shown that the neutrophil chemoattractant LTB_4 is rapidly produced in response to intestinal IR injury (14, 16), and consistent with the increases in neutrophil invasion, the level of LTB_4 in $Rag1^{-/-}$ mice reconstituted with mAb B4 was greatly increased as compared with LTB_4 generation in sham-operated animals (Fig. 5). Finally, the proinflammatory eicosanoid PGE_2 also was elevated in samples from mice injected with mAb B4, but with marginal significance. In toto, mAb B4 appears to induce a proinflammatory response in $Rag1^{-/-}$ mice that is similar in nature to those in wt mice.

In situ analysis of mAb B4 localization and complement C3 deposition

It has been previously shown that complement C3 is deposited during intestinal IR injury (19, 23). The deposition of C3 in relation to mAb B4 in the intestines of mAb B4 treated $Rag1^{-/-}$ mice subjected to IR was determined by multicolor immunofluorescence microscopy (Fig. 6). As shown, when $Rag1^{-/-}$ mice were reconstituted with mAb B4 and IR injury was induced, mAb B4 was detected in the intestinal microvillus under the enterocyte layer, possibly being attached to the basal membrane of these cells, and colocalizing with C3.

Recombinant annexin IV blocks intestinal IR injury in wt mice

Although our data using mAb B4 in $Rag1^{-/-}$ mice revealed that this Ab was sufficient to mediate intestinal IR injury, it was uncertain as to whether this reactivity was necessary in context of the entire natural Ab repertoire in wt mice to develop injury. To address this question, we used recombinant annexin IV as an “inhibitor” of the annexin IV reactive natural Ab repertoire. We used annexin IV made in bacteria because of the low yields and inability to purify large amounts of recombinant protein from F-293 cell

membranes. Bacterial annexin IV was produced as described in *Materials and Methods* and was >95% pure by SDS-PAGE (data not shown). As a control for the experiments, we also produced and purified to a similar level a soluble fragment of cytokeratin 19, to which the control mAb D5 reacted (data not shown).

Following i.v. injection of wt mice 5 min before intestinal reperfusion phase with 50 µg/mouse of purified recombinant annexin IV or cytokeratin 19 as a relevant control, it was observed that the injection of annexin IV significantly reduced intestinal injury to the level of the sham-operated animals (Fig. 7Aa). Reduction of IR injury in the intestine of mice injected with annexin IV was confirmed using additional approaches. First, the tissue MPO content (Fig. 7Ab), which correlates with neutrophil activation and invasion, was also specifically reduced when compared with controls. Absence of inflammation in intestine of mice injected by annexin IV before reperfusion phase was also confirmed by the finding of specifically reduced levels of LTB_4 and PGE_2 (Fig. 7A, c and d). Finally, immunofluorescence analysis revealed a greatly diminished C3 deposition in annexin IV-treated mice as compared with controls (Fig. 7B). These data demonstrate that natural Ab reactivity with annexin IV is required for the full elaboration of intestinal IR injury.

Natural Abs to annexin IV are diminished in $Cr2^{-/-}$ mice

Because of the protection from the development of intestinal IR injury in $Cr2^{-/-}$ mice, we sought to determine whether differential reactivity to this particular Ag might underlie the difference in IR susceptibility. To address this question, we used an annexin IV ELISA to directly compare the level of anti-annexin IV Ab in serum samples from $Cr2^{+/+}$ and $Cr2^{-/-}$ mice. As a negative control, sera from $Rag1^{-/-}$ mice were used (Fig. 8A). Although we were not able to see complete abrogation of anti-annexin IV Ab in $Cr2^{-/-}$ mice, it is likely that the diminished natural Ab reactivity found is one reason that $Cr2^{-/-}$ mice are protected from IR injury.

Human annexin IV is a similar protein to mouse annexin IV and exhibits a 92% protein identity. We reasoned that it was relevant to determine whether similar natural Ab reactivity to annexin IV is present in humans. Indeed, when compared with sera from patients

with agammaglobulinemia, there is IgM reactivity to annexin IV demonstrable in human serum (Fig. 8B). These data suggest that a similar process of neo-epitope recognition could be present in humans with IR injury.

Discussion

At the initiation of these studies, we hypothesized that neo-epitopes necessary for the development of IR injury could be identified by creating mAbs reactive with IEC, a major cellular target of reperfusion injury. Using this approach, we successfully identified a pathogenic IgM mAb, designated B4, that could alone mediate the induction of IR injury in *Rag1*^{-/-} mice. In this experimental setting mAb B4 could lead to the fixation of complement C3 as well as the infiltration of neutrophils and elaboration of proinflammatory leukotrienes. Using several approaches, annexin IV was demonstrated to be the specific target Ag of mAb B4, and no evidence of cross-reactivity of mAb B4 with two previously suggested natural Ab targets, phospholipids and nonmuscle myosin, was found. Most importantly, the essential role for pathogenic natural Abs reactivity with annexin IV was confirmed by the specific inhibition of IR injury in wt mice using systemically administered recombinant annexin IV. Pretreatment of mice with annexin IV blocked tissue injury as measured by histologic criteria as well as greatly diminished the deposition of C3 and the elaboration of additional proinflammatory mediators in the intestine. Sera from *Cr2*^{-/-} mice, which are relatively protected from intestinal IR injury, showed diminished reactivity with annexin IV. Finally, sera from normal human subjects also demonstrated IgM Ab reactivity with annexin IV, suggesting that a similar recognition process may play a key role in IR injury in man. In sum, annexin IV and natural Ab reactivity to this membrane-associated protein play an essential role in this medically important pathologic process.

One major question is how access to annexin IV by natural Abs is regulated. It is likely, based on what is known regarding the normal distribution of annexin IV *in vivo*, that IEC have an intracellular or internal membrane bilayer-associated pool of protein that transfers to the extracellular membrane upon initial cellular injury. Whether endothelial cells also elaborate this protein during IR injury is not known but such a situation might also contribute to the initial recognition of annexin IV by natural Abs. There was no evidence of reactivity of mAb B4 with endothelial surfaces as shown in Fig. 6; however, recognition of endothelial cells may be below the level of detection of that immunofluorescence technique. Natural Abs then likely bind to several epitopes on annexin IV, activate complement and through this mechanism initiate the inflammatory cascade.

Annexin IV is a relatively widely distributed protein and a member of a family of largely membrane-associated proteins. Several annexin family members are expressed on the cell surface, for example, annexin II, which serves as an angiostatin receptor (61). Annexin VI and annexin II are found in the extracellular space and bind fetuin-A 43. The precise mechanisms by which annexins are transported to the surface of the cells are not certain. The N-terminal domain of annexins is responsible for binding to other proteins (62–64), and it is thus possible that the extracellular annexin IV we have detected is attached to the IEC membrane by being bound to another intrinsic membrane protein. Annexin IV has also been found in lipid rafts (65). The mechanism of raft inclusion is unknown; however, on the basis of this analogy to other lipid raft-associated proteins, this may be through attachment to a GPI anchor or through acylation with palmitate or myristate (66). A new ligand for annexin IV in the pancreas, GPI-anchored sialoprotein GP-2, was described recently (67). Our finding that annexin IV is detected on the IEC surface even if the purification

protocol for these cells contains EDTA, as well as the finding that recombinant annexin IV, despite of presence of a leader peptide, was not released from F-293 cells but rather remained attached to the surface in a Ca²⁺-independent manner, strongly suggests that it is not using the well-described Ca²⁺-dependent phospholipid binding mechanism (40). The possibility of such Ca²⁺-independent binding by annexins was recently shown by others while demonstrating that annexin IV could bind phosphatidylserine- and phosphatidic acid-containing liposomes at low pH in a Ca²⁺-independent manner (68) and that hypoxia sufficient to induce an intracellular pH change can promote certain annexins to translocate to the surface of the plasma membrane (69).

The histological analyses clearly showed that when mAb B4 was injected into *Rag1*^{-/-} mice, it was bound beneath the basal membrane of enterocytes in the villi. mAb B4 colocalizes with C3 deposition in intestine of mice undergoing IR injury, strongly suggesting that the binding of the mAb to the Ag results in complement activation. It is likely that annexin IV translocates to the cell surface when cells undergo hypoxia, early apoptosis, and perhaps necrosis. This translocation could also be facilitated by posttranslational modifications of annexin IV (53).

There is also a possibility that the chronic injury of epithelial cells may increase autoantibody production to annexin IV, as it has been demonstrated that patients with chronic alcoholism exhibit elevated levels of IgG autoantibodies to annexin IV (70, 71). This effect may increase the level of self-reactivity and promote the greater development of IR injury in the setting of similar levels of initial ischemia.

Natural Abs to IR related neo-epitopes are a component of the class of self-protein-directed Abs circulating in the body, the majority of which are products of B-1 B cells. The development of B-1 B cells secreting self-reactive Abs is believed to be Ag dependent (72). In this regard, it is notable that *Cr2*^{-/-} mice, despite exhibiting normal quantitative levels of IgG and IgM isotype Abs (24), clearly show differences in natural Ab reactivity to annexin IV. It is likely that the absence of mouse CR2 is the major cause of that difference (23, 25, 73). In addition, while it has been shown that there is a decrease in autoantibody production in experimental immunization-induced models of self-reactivity in the absence of CR2, for example, collagen-induced arthritis (74), this is the first report to our knowledge of a marked decrease in natural Ab reactivity to specific self-Ags in *Cr2*^{-/-} mice in the absence of directed immunization.

Of note, CD5⁺ B-1 cells do express mouse CR2; however, they do not amplify Ca²⁺ influx in response to BCR/C3dg coengagement (75) and also demonstrate a lower level of CR2 expression (76, 77). These data have been interpreted to indicate that, since these cells are already preactivated by Ag binding to the BCR, the cells are anergic due to chronic, low-grade, chronic stimulation *in vivo*. The lower levels of mouse CR2 may be due to receptor shedding or internalization after being engaged with its ligand (76, 77). If natural Ab reactivity to annexin IV is derived primarily from B-1 cells, and CR2 is required on B-1 cells for this process, this suggests that *in vivo* responses through CR2 are substantially different than those found *in vitro* using coligation as an analytic tool. Of course, since coligation of BCR with CR2 lowers the activation signal in B-2 cells several thousand-fold (78), it is also possible that B-2 cells play the major role in driving natural Ab self-reactivity to annexin IV. Finally, since the absence of mouse CR2 not only changes the B-2 cell activation threshold to immune complexes but also greatly alters follicular dendritic cell/immune complex networks (79) and diminishes Ab responses to T-independent Ags (73), additional mechanisms may play important roles

in the lack of development of natural Abs to annexin IV in the absence of this receptor.

Finally, it is worth considering how natural Ab reactivity to annexin IV relates to nonmuscle myosin and phospholipids, both of which have been previously suggested as targets for natural Abs in IR-induced injury and, at least with regard to nonmuscle myosin, as necessary for the development of tissue injury in vivo. There are several reasons that might explain these findings. One possibility is that serial recognition of several epitopes that are displayed in a stereotypic fashion during the development of cell apoptosis/necrosis is required to initiate complement-dependent injury. In that setting, interruption of reactivity of natural Abs to any one of the Ags could ameliorate the process. A second possibility is that epitopes are expressed at the same time but on unique cell populations, for example, nonmuscle myosin on endothelial cells and annexin IV on IECs, and recognition of each cell type is necessary for full injury development. A third possibility is that all of these proteins come together in protein/phospholipid complexes that are exposed during IR, and binding of natural Abs to several of the epitopes is necessary to activate complement and induce injury. What argues against these hypotheses is that individual IgM mAbs can transfer injury in *Rag1*^{-/-} mice. However, it is possible that a high dose of individual injected IgM mAbs can overcome restriction points that would be present in wt mice with lower levels of natural Abs. Certainly going forward, it will be necessary to better understand the physicochemical and quantitative relationships between the various neo-epitopes that are important in injury as well as the natural Abs that recognize them.

In summary, we propose that annexin IV is a major IR related neo-epitope that is recognized by pathogenic natural Abs. Further explorations of the mechanisms of natural Ab induced injury, a determination of how and where annexin IV epitopes are displayed, and the development of a better understanding of how this component of the natural Ab repertoire is positively selected by the presence of CR2 are particularly relevant areas for future investigation.

Disclosures

The authors have no financial conflict of interest.

References

- Ozmen, S., S. Ayhan, Y. Demir, M. Siemionow, and K. Atabay. 2007. Impact of gradual blood flow increase on ischaemia-reperfusion injury in the rat cremaster microcirculation model. *J. Plast. Reconstr. Aesthet. Surg.* 61: 939–948.
- Zimmerman, B. J., and D. N. Granger. 1994. Mechanisms of reperfusion injury. *Am. J. Med. Sci.* 307: 284–292.
- Mack, W. J., M. E. Sughrue, A. F. Ducruet, J. Mocco, S. A. Sosunov, B. G. Hassid, J. Z. Silverberg, V. S. Ten, D. J. Pinsky, and E. S. Connolly, Jr. 2006. Temporal pattern of C1q deposition after transient focal cerebral ischemia. *J. Neurosci. Res.* 83: 883–889.
- Mocco, J., D. A. Wilson, R. J. Komotar, M. E. Sughrue, K. Coates, R. L. Sacco, M. S. Elkind, and E. S. Connolly, Jr. 2006. Alterations in plasma complement levels after human ischemic stroke. *Neurosurgery* 59: 28–33.
- Vinten-Johansen, J., Z. Q. Zhao, R. Jiang, and A. J. Zatta. 2005. Myocardial protection in reperfusion with postconditioning. *Expert. Rev. Cardiovasc. Ther.* 3: 1035–1045.
- Zweier, J. L., and M. A. Talukder. 2006. The role of oxidants and free radicals in reperfusion injury. *Cardiovasc. Res.* 70: 181–190.
- Macfie, J., C. O'Boyle, C. J. Mitchell, P. M. Buckley, D. Johnstone, and P. Sudworth. 1999. Gut origin of sepsis: a prospective study investigating associations between bacterial translocation, gastric microflora, and septic morbidity. *Gut* 45: 223–228.
- Fukatsu, K., S. Sakamoto, E. Hara, C. Ueno, Y. Maeshima, I. Matsumoto, H. Mochizuki, and H. Hiraide. 2006. Gut ischemia-reperfusion affects gut mucosal immunity: a possible mechanism for infectious complications after severe surgical insults. *Crit. Care Med.* 34: 182–187.
- Deitch, E. A. 2001. Role of the gut lymphatic system in multiple organ failure. *Curr. Opin. Crit. Care* 7: 92–98.
- Burns, B. J., and L. J. Brandt. 2003. Intestinal ischemia. *Gastroenterol. Clin. North Am.* 32: 1127–1143.
- Simpson, R., R. Alon, L. Kobzik, C. R. Valeri, D. Shepro, and H. B. Hechtman. 1994. Neutrophil and nonneutrophil-mediated injury in intestinal ischemia-reperfusion. *Ann. Surg.* 218: 444–453.
- Hernandez, L. A., M. B. Grisham, B. Twhig, K. E. Arfors, J. M. Harlan, and D. N. Granger. 1987. Role of neutrophils in ischemia-reperfusion-induced microvascular injury. *Am. J. Physiol.* 253: H699–H703.
- Crawford, M. H., F. L. Grover, W. P. Kolb, C. A. McMahan, R. A. O'Rourke, L. M. McManus, and R. N. Pinckard. 1988. Complement and neutrophil activation in the pathogenesis of ischemic myocardial injury. *Circulation* 78: 1449–1458.
- Eror, A. T., A. Stojadinovic, B. W. Starnes, S. C. Makrides, G. C. Tsokos, and T. Shea-Donohue. 1999. Anti-inflammatory effects of soluble complement receptor type 1 promote rapid recovery of ischemia/reperfusion injury in rat small intestine. *Clin. Immunol.* 90: 266–275.
- Pemberton, M., G. Anderson, V. Vetvicka, D. E. Justus, and G. D. Ross. 1993. Microvascular effects of complement blockade with soluble recombinant CR1 on ischemia/reperfusion injury of skeletal muscle. *J. Immunol.* 150: 5104–5113.
- Rehrig, S., S. D. Fleming, J. Anderson, J. M. Guthridge, J. K. Rakstang, C. McQueen, V. M. Holers, G. C. Tsokos, and T. Shea-Donohue. 2001. Complement inhibitory Crry-Ig attenuates intestinal damage after the onset of mesenteric ischemia/reperfusion injury in mice. *J. Immunol.* 167: 5921–5927.
- Chan, R. K., S. I. Ibrahim, K. Takahashi, E. Kwon, M. McCormack, A. Ezekowitz, M. C. Carroll, F. D. Moore, Jr., and W. G. Austen, Jr. 2006. The differing roles of the classical and mannose-binding lectin complement pathways in the events following skeletal muscle ischemia-reperfusion. *J. Immunol.* 177:8080–8085.
- Jordan, J. E., M. C. Montalto, and G. L. Stahl. 2001. Inhibition of mannose-binding lectin reduces postischemic myocardial reperfusion injury. *Circulation* 104: 1413–1418.
- Williams, J. P., T. T. Pechet, M. R. Weiser, R. Reid, L. Kobzik, F. D. Moore, Jr., M. C. Carroll, and H. B. Hechtman. 1999. Intestinal reperfusion injury is mediated by IgM and complement. *J. Appl. Physiol.* 86: 938–942.
- Stahl, G. L., Y. Xu, L. Hao, M. Miller, J. A. Buras, M. Fung, and H. Zhao. 2003. Role for the alternative complement pathway in ischemia/reperfusion injury. *Am. J. Pathol.* 162: 449–455.
- Fleming, S. D., R. P. Egan, C. Chai, G. Girardi, V. M. Holers, J. Salmon, M. Monestier, and G. C. Tsokos. 2004. Anti-phospholipid antibodies restore mesenteric ischemia/reperfusion-induced injury in complement receptor 2/complement receptor 1-deficient mice. *J. Immunol.* 173: 7055–7061.
- Zhang, M., L. H. Michael, S. A. Grosjean, R. A. Kelly, M. C. Carroll, and M. L. Entman. 2006. The role of natural IgM in myocardial ischemia-reperfusion injury. *J. Mol. Cell. Cardiol.* 41: 62–67.
- Fleming, S. D., T. Shea-Donohue, J. M. Guthridge, L. Kulik, T. J. Waldschmidt, M. G. Gipson, G. C. Tsokos, and V. M. Holers. 2002. Mice deficient in complement receptors 1 and 2 lack a tissue injury-inducing subset of the natural antibody repertoire. *J. Immunol.* 169: 2126–2133.
- Zhang, M., W. G. Austen, Jr., I. Chiu, E. M. Alicot, R. Hung, M. Ma, N. Verna, M. Xu, H. B. Hechtman, F. D. Moore, Jr., and M. C. Carroll. 2004. Identification of a specific self-reactive IgM antibody that initiates intestinal ischemia/reperfusion injury. *Proc. Natl. Acad. Sci. USA* 101: 3886–3891.
- Reid, R. R., S. Woodstock, A. Shimabukuro-Vornhagen, W. G. Austen, Jr., L. Kobzik, M. Zhang, H. B. Hechtman, F. D. Moore, Jr., and M. C. Carroll. 2002. Functional activity of natural antibody is altered in Cr2-deficient mice. *J. Immunol.* 169: 5433–5440.
- Hardy, R. R. 2006. B-1 B cell development. *J. Immunol.* 177: 2749–2754.
- Hardy, R. R. 2006. B-1 B cells: development, selection, natural autoantibody and leukemia. *Curr. Opin. Immunol.* 18: 547–555.
- Kawahara, T., H. Ohdan, G. Zhao, Y. G. Yang, and M. Sykes. 2003. Peritoneal cavity B cells are precursors of splenic IgM natural antibody-producing cells. *J. Immunol.* 171: 5406–5414.
- Herzenberg, L. A. 2000. B1 cells: the lineage question revisited. *Immunol. Rev.* 175: 9–22.
- Martin, F., and J. F. Kearney. 2001. B1 cells: similarities and differences with other B cell subsets. *Curr. Opin. Immunol.* 13: 195–201.
- Baumgarth, N., O. C. Herman, G. C. Jager, L. E. Brown, L. Herzenberg, and J. Chen. 2000. B-1 and B-2 cell-derived immunoglobulin M antibodies are non-redundant components of the protective response to influenza virus. *J. Exp. Med.* 192: 271–280.
- Baumgarth, N., J. W. Tung, and L. A. Herzenberg. 2005. Inherent specificities in natural antibodies: a key to immune defense against pathogen invasion. *Springer Semin. Immunopathol.* 26: 347–362.
- Buza, J., M. Sileghem, P. Gwakisa, and J. Naessens. 1997. CD5⁺ B lymphocytes are the main source of antibodies reactive with non-parasite antigens in *Trypanosoma congolense*-infected cattle. *Immunology* 92: 226–233.
- Binder, C. J., and G. J. Silverman. 2005. Natural antibodies and the autoimmunity of atherosclerosis. *Springer Semin. Immunopathol.* 26: 385–404.
- Shaw, P. X., S. Horkko, M.-K. Chang, L. K. Curtiss, W. Palinski, G. J. Silverman, and J. L. Witztum. 2000. Natural antibodies with the T15 idiotype may act in atherosclerosis, apoptotic clearance, and protective immunity. *J. Clin. Invest.* 105: 1731–1740.
- Silverman, G. J., P. X. Shaw, L. Luo, D. Dwyer, M. Chang, S. Horkko, W. Palinski, A. Stall, and J. L. Witztum. 2000. Neo-self antigens and the expansion of B-1 cells: lessons from atherosclerosis-prone mice. *Curr. Top. Microbiol. Immunol.* 252: 189–200.
- Chan, R. K., N. Verna, J. Afnan, M. Zhang, S. Ibrahim, M. C. Carroll, and F. D. Moore, Jr. 2005. Attenuation of skeletal muscle reperfusion injury with intravenous 12 amino acid peptides that bind to pathogenic IgM. *Surgery* 139:236–243.

38. Zhang, M., E. M. Alicot, I. Chiu, J. Li, N. Verna, T. Vorup-Jensen, B. Kessler, M. Shimaoko, R. Chan, D. Friend, et al. 2006. Identification of the target self-antigens in reperfusion injury. *J. Exp. Med.* 203: 141–152.
39. Morgan, R. O., S. Martin-Almedina, J. M. Iglesias, M. I. Gonzalez-Florez, and M. P. Fernandez. 2004. Evolutionary perspective on annexin calcium-binding domains. *Biochim. Biophys. Acta* 1742: 133–140.
40. Rescher, U., and V. Gerke. 2004. Annexins—unique membrane binding proteins with diverse functions. *J. Cell Sci.* 117: 2631–2639.
41. Gerke, V., C. E. Creutz, and S. E. Moss. 2005. Annexins: linking Ca^{2+} signalling to membrane dynamics. *Nat. Rev. Mol. Cell Biol.* 6: 449–461.
42. Kim, J., and K. A. Hajjar. 2002. Annexin II: a plasminogen-plasminogen activator co-receptor. *Front. Biosci.* 7: d341–d348.
43. Kundranda, M. N., S. Ray, M. Saria, D. Friedman, L. M. Matrisian, P. Lukyanov, and J. Ochieng. 2004. Annexins expressed on the cell surface serve as receptors for adhesion to immobilized fetuin-A. *Biochim. Biophys. Acta* 1693: 111–123.
44. Perretti, M., and F. N. Gavins. 2003. Annexin I: an endogenous anti-inflammatory protein. *News Physiol. Sci.* 18: 60–64.
45. Massey-Harroche, D., N. Mayran, and S. Maroux. 1998. Polarized localizations of annexins I, II, VI and XIII in epithelial cells of intestinal, hepatic and pancreatic tissues. *J. Cell Sci.* 111(Pt. 20): 3007–3015.
46. Massey, D., V. Traverso, A. Rigal, and S. Maroux. 1991. Cellular and subcellular localization of annexin IV in rabbit intestinal epithelium, pancreas and liver. *Biol. Cell* 73: 151–156.
47. Mayran, N., V. Traverso, S. Maroux, and D. Massey-Harroche. 1996. Cellular and subcellular localizations of annexins I, IV, and VI in lung epithelia. *Am. J. Physiol.* 270: L863–L871.
48. Piljic, A., and C. Schultz. 2006. Annexin A4 self-association modulates general membrane protein mobility in living cells. *Mol. Biol. Cell* 17: 3318–3328.
49. Seville, R. A., S. Nijjar, M. W. Barnett, K. Masse, and E. A. Jones. 2002. Annexin IV (Xanx-4) has a functional role in the formation of pronephric tubules. *Development* 129: 1693–1704.
50. Hill, W. G., M. A. Kaetzel, B. K. Kishore, J. R. Dedman, and M. L. Zeidel. 2003. Annexin A4 reduces water and proton permeability of model membranes but does not alter aquaporin 2-mediated water transport in isolated endosomes. *J. Gen. Physiol.* 121: 413–425.
51. Shi, T., F. Dong, L. S. Liou, Z. H. Duan, A. C. Novick, and J. A. Didonato. 2004. Differential protein profiling in renal-cell carcinoma. *Mol. Carcinog.* 40: 47–61.
52. Zimmermann, U., S. Balabanov, J. Giebel, S. Teller, H. Junker, D. Schmoll, C. Protzel, C. Scharf, B. Kleist, and R. Walther. 2004. Increased expression and altered location of annexin IV in renal clear cell carcinoma: a possible role in tumour dissemination. *Cancer Lett.* 209: 111–118.
53. Herzog, A., S. Kuntz, H. Daniel, and U. Wenzel. 2004. Identification of biomarkers for the initiation of apoptosis in human preneoplastic colonocytes by proteome analysis. *Int. J. Cancer* 109: 220–229.
54. Sohma, H., H. Ohkawa, E. Hashimoto, R. Sakai, and T. Saito. 2002. Ethanol-induced augmentation of annexin IV expression in rat C6 glioma and human A549 adenocarcinoma cells. *Alcohol Clin. Exp. Res.* 26: 44S–48S.
55. Grossmann, J., J. M. Maxson, C. M. Whitacre, D. E. Orosz, N. A. Berger, C. Fiochi, and A. D. Levine. 1998. New isolation technique to study apoptosis in human intestinal epithelial cells. *Am. J. Pathol.* 153: 53–62.
56. Grossmann, J., K. Walther, M. Artinger, S. Kiessling, and J. Scholmerich. 2001. Apoptotic signaling during initiation of detachment-induced apoptosis (“anoikis”) of primary human intestinal epithelial cells. *Cell Growth Differ.* 12: 147–155.
57. Vossenaar, E. R., N. Despres, E. Lapointe, H. A. van der, M. Lora, T. Senshu, W. J. van Venrooij, and H. A. Menard. 2004. Rheumatoid arthritis specific anti-Sa antibodies target citrullinated vimentin. *Arthritis Res. Ther.* 6: R142–R150.
58. Mercolino, T. J., L. W. Arnold, L. A. Hawkins, and G. Haughton. 1988. Normal mouse peritoneum contains a large population of Ly-1⁺ (CD5) B cells that recognize phosphatidyl choline: relationship to cells that secrete hemolytic antibody specific for autologous erythrocytes. *J. Exp. Med.* 168: 687–698.
59. Mercolino, T. J., A. L. Locke, A. Afshari, D. Sasser, W. W. Travis, L. W. Arnold, and G. Haughton. 1989. Restricted immunoglobulin variable region gene usage by normal Ly-1 (CD5⁺) B cells that recognize phosphatidyl choline. *J. Exp. Med.* 169: 1869–1877.
60. Junker, M., and C. E. Creutz. 1994. Ca^{2+} -dependent binding of endonexin (annexin IV) to membranes: analysis of the effects of membrane lipid composition and development of a predictive model for the binding interaction. *Biochemistry* 33: 8930–8940.
61. Syed, S. P., A. M. Martin, H. M. Haupt, C. P. Renas-Elliot, and J. J. Brooks. 2007. Angiostatin receptor annexin II in vascular tumors including angiosarcoma. *Hum. Pathol.* 38: 508–513.
62. Cheng, C. W., A. Rifai, S. M. Ka, H. A. Shui, Y. F. Lin, W. H. Lee, and A. Chen. 2005. Calcium-binding proteins annexin A2 and S100A6 are sensors of tubular injury and recovery in acute renal failure. *Kidney Int.* 68: 2694–2703.
63. Hayes, M. J., U. Rescher, V. Gerke, and S. E. Moss. 2004. Annexin-actin interactions. *Traffic* 5: 571–576.
64. Willshaw, A., K. Grant, J. Yan, N. Rockliffe, S. Ambavarapu, G. Burdya, A. Varro, S. Fukuoka, and D. Gawler. 2004. Identification of a novel protein complex containing annexin A4, rabphilin and synaptotagmin. *FEBS Lett.* 559: 13–21.
65. Nguyen, H. T., A. B. Amine, D. Lafitte, A. A. Waheed, C. Nicoletti, C. Villard, M. Letisse, V. Deyris, M. Roziere, L. Tchiakpe, et al. 2006. Proteomic characterization of lipid rafts markers from the rat intestinal brush border. *Biochem. Biophys. Res. Commun.* 342: 236–244.
66. Brown, D. 2002. Structure and function of membrane rafts. *Int. J. Med. Microbiol.* 291: 433–437.
67. Tsujii-Hayashi, Y., M. Kitahara, T. Yamagaki, K. Kojima-Aikawa, and I. Matsumoto. 2002. A potential endogenous ligand of annexin IV in the exocrine pancreas. Carbohydrate structure of GP-2, a glycosylphosphatidylinositol-anchored glycoprotein of zymogen granule membranes. *J. Biol. Chem.* 277: 47493–47499.
68. Zschornig, O., F. Opitz, and M. Muller. 2007. Annexin A4 binding to anionic phospholipid vesicles modulated by pH and calcium. *Eur. Biophys. J.* 36: 415–424.
69. Monastyrskaya, K., F. Tschumi, E. B. Babychuk, D. Stroka, and A. Draeger. 2008. Annexins sense changes in intracellular pH during hypoxia. *Biochem. J.* 409: 65–75.
70. Sohma, H., H. Ohkawa, E. Hashimoto, S. Toki, H. Ozawa, Y. Kuroki, and T. Saito. 2001. Alteration of annexin IV expression in alcoholics. *Alcohol Clin. Exp. Res.* 25: 55S–58S.
71. Sohma, H., H. Ohkawa, R. Sakai, E. Hashimoto, W. Ukai, and T. Saito. 2003. Augmentation of ethanol-induced cell damage and activation of nuclear factor- κ B by annexin IV in cultured cells. *Alcohol Clin. Exp. Res.* 27: 64S–67S.
72. Hayakawa, K., M. Asano, S. A. Shinton, M. Gui, D. M. Allman, C. L. Steward, J. Silver, and R. R. Hardy. 1999. Positive selection of natural autoreactive B cells. *Science* 285: 113–116.
73. Holers, V. M., and L. Kulik. 2007. Complement receptor 2, natural antibodies and innate immunity: inter-relationships in B cell selection and activation. *Mol. Immunol.* 44: 64–72.
74. Kuhn, K. A., C. L. Cozine, B. Tomooka, W. H. Robinson, and V. M. Holers. 2008. Complement receptor CR2/CR1 deficiency protects mice from collagen-induced arthritis and associates with reduced autoantibodies to type II collagen and citrullinated antigens. *Mol. Immunol.* 45: 2808–2819.
75. Lyubchenko, T., J. dal Porto, J. C. Cambier, and V. M. Holers. 2005. Co-ligation of the B cell receptor with complement receptor type 2 (CR2/CD21) using its natural ligand C3dg: activation without engagement of an inhibitory signaling pathway. *J. Immunol.* 174: 3264–3272.
76. Tessier, J., A. Cuvillier, F. Glaudet, and A. A. Khamlichi. 2007. Internalization and molecular interactions of human CD21 receptor. *Mol. Immunol.* 44: 2415–2425.
77. Masilamani, M., D. Kassahn, S. Mikkat, M. O. Glocker, and H. Illges. 2003. B cell activation leads to shedding of complement receptor type II (CR2/CD21). *Eur. J. Immunol.* 33: 2391–2397.
78. Fearon, D. T., and R. H. Carter. 1995. The CD19/CR2/TAPA-1 complex of B lymphocytes: linking natural to acquired immunity. *Ann. Rev. Immunol.* 13: 127–149.
79. Fang, Y., C. Xu, V. M. Holers, and H. Molina. 1998. Expression of complement receptors 1 and 2 on follicular dendritic cells is necessary for the generation of a normal antigen-specific IgG response. *J. Immunol.* 160: 5273–5279.



This article appeared in a journal published by Elsevier. The attached copy is furnished to the author for internal non-commercial research and education use, including for instruction at the authors institution and sharing with colleagues.

Other uses, including reproduction and distribution, or selling or licensing copies, or posting to personal, institutional or third party websites are prohibited.

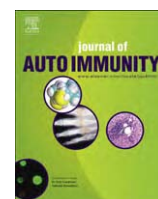
In most cases authors are permitted to post their version of the article (e.g. in Word or Tex form) to their personal website or institutional repository. Authors requiring further information regarding Elsevier's archiving and manuscript policies are encouraged to visit:

<http://www.elsevier.com/copyright>



Contents lists available at ScienceDirect

Journal of Autoimmunity

journal homepage: www.elsevier.com/locate/jautimm

B cells contribute to ischemia/reperfusion-mediated tissue injury

Jie Chen^a, José C. Crispín^a, Thomas F. Tedder^b, Jurandir Dalle Lucca^c, George C. Tsokos^{a,*}

^a Division of Rheumatology, Beth Israel Deaconess Medical Center, Harvard Medical School, 330 Brookline Avenue, CLS-937, Boston, MA 02115, USA

^b Department of Immunology, Duke University Medical Center, Durham, NC, USA

^c Department of Cellular Injury, Walter Reed Army Institute of Research, Silver Spring, MD, USA

ARTICLE INFO

Article history:

Received 3 January 2009

Accepted 11 February 2009

Keywords:

B cell

CXCL13

Inflammation

Ischemia/reperfusion

ABSTRACT

Multiple elements are known to participate in ischemia/reperfusion (I/R)-mediated tissue injury. Amongst them, B cells have been shown to contribute by the production of antibodies that bind to ischemic cells and fix complement. It is currently unknown whether B cells participate through antibody-independent mechanisms in the pathogenesis of I/R. In a mesenteric I/R model we found that B cells infiltrate the injured intestine of normal and autoimmune mice 2 h after reperfusion is established. B cell depletion protected mice from the development of I/R-mediated intestinal damage. The protection conferred by B cell depletion was significantly greater in MRL/lpr mice. Finally, we show that ischemic tissue expressed the B cell-attractant CXCL13 and infiltrating B cells expressed the corresponding receptor CXCR5. Our data grant B cells an antibody-independent role in the pathogenesis of intestinal I/R and suggest that B cells accumulate in the injured tissue in response to the chemokine CXCL13.

© 2009 Elsevier Ltd. All rights reserved.

1. Introduction

An intense inflammatory reaction is produced in tissues transiently deprived of blood flow during reperfusion. The mechanisms that trigger inflammation in this model known as ischemia/reperfusion (I/R) and the pathways involved in its development and amplification have been identified only partially [1]. The rapid kinetics with which inflammation and tissue damage occur in organs affected by I/R indicates that the involved elements are triggered directly by signals originated in the ischemic cells and implies that more complex mechanisms such as antigen uptake and presentation followed by expansion of clones of specific lymphocytes do not participate. Indeed, constituents of the innate immune system including reactive oxygen species, cytokines and chemokines, complement, natural antibodies, and neutrophils have been shown to be key players in I/R-induced tissue injury [1]. Interestingly, T cells have also been implicated in the pathogenesis of I/R [2]. They accumulate in damaged areas of the intestine of mice subjected to mesenteric artery occlusion as early as 1 h into the reperfusion phase [3]. The ability of infiltrating T cells to cause tissue damage in the setting of I/R has been demonstrated to depend on the production of the pro-inflammatory cytokine IL-17 [3]. This suggests that T cells amplify the inflammatory response by

producing factors that attract and activate effector cells such as neutrophils.

B cells have been shown to play central roles in the development of human and murine autoimmune inflammatory diseases [4]. Likewise, they have been implicated in the pathogenesis of I/R-mediated tissue injury [5]. Mainly regarded as cells that differentiate into antibody-producing cells, B lymphocytes perform several tasks aside from producing antibodies. They detect and process soluble antigens and present them to T cells; produce cytokines and express surface molecules that activate other cells. Moreover, they are equipped with receptors that allow them to become activated in the presence of inflammatory signals. B cells have been shown to be able to instigate the inflammatory response by mechanisms not limited to antibody production even in settings such as murine lupus in which antibodies are considered as a pathogenic element [6]. Antibodies and complement are known to be central in the pathogenesis of I/R [1]. In fact, antibody-containing serum has been shown to restore disease in B cell-deficient animals in models of renal [7] and intestinal I/R [8,9]. In this work we investigated whether B cells contribute to I/R injury in an antibody-independent manner in normal and autoimmune mice. We demonstrate that ischemia up-regulates the expression of the B cell-chemoattractant CXCL13 which induces B cell recruitment to damaged areas of the intestine and we show that B cell depletion in mice with intact levels of circulating antibodies ameliorates tissue injury in a model of mesenteric I/R.

* Corresponding author. Tel.: +1 617 735 4161; fax: +1 617 435 4170.
E-mail address: gtsokos@bidmc.harvard.edu (G.C. Tsokos).

2. Methods

2.1. Mice

Adult male B6.MRL*Tnfrsf6*^{lpr} (B6.MRL/*lpr*) and C57BL/6 mice were obtained from The Jackson Laboratory (Bar Harbor, ME), and housed in the animal facility of the Beth Israel Deaconess Medical Center.

2.2. Reagents

The following antibodies were used for immunofluorescence studies: FITC-labeled anti-mouse B220 (BD Pharmingen) was used in flow cytometry studies. Anti-mouse CXCL13 (R&D systems), rat anti-mouse B220 (BD Pharmingen), rat anti-mouse CXCR5 (BD Pharmingen) were used in immunohistochemistry studies. FITC-labeled anti-B220 and PE-labeled anti-CXCR5 (BD Pharmingen) were used for immunofluorescence and confocal microscope imaging.

2.3. Ischemia/reperfusion protocol

After an acclimation period of at least 7 days, mice were prepared for surgery. Anesthesia was induced with ketamine (10 mg/kg), xylazine (2 mg/kg), and acepromazine (0.3 mg/kg), administered by i.p. injection. Anesthesia was maintained during the entire experiment. All procedures were performed with the animals breathing spontaneously and body temperature maintained at 37 °C using a water-circulating heating pad. Research was conducted in compliance with the Animal Welfare Act and other Federal statutes and regulations relating to animals and experiments involving animals, and adheres to principles stated in the Guide for the Care and Use of Laboratory Animals, NRC Publication, 1996 edition. All procedures were reviewed and approved by the Institute's Animal Care and Use Committee, and performed in a facility accredited by the Association for Assessment and Accreditation of Laboratory Animal Care, International.

Animals were subjected to I/R as previously described [10]. Briefly, a midline laparotomy was performed before a 30-min equilibration period. The superior mesenteric artery was identified and isolated, and a small non-traumatic vascular clamp was applied for 30 min. After this ischemic phase, the clamp was removed and the intestine was allowed to reperfuse for 3 h. As sham procedure, animals were subjected to the same surgical intervention without artery occlusion. The laparotomy incisions were sutured and the animals were monitored during the reperfusion period. Additional ketamine and xylazine was administered by i.m. injection immediately before euthanasia. There was no significant difference in survival between treatment and control groups. After euthanasia, the small intestine (20 cm distal to the gastroduodenal junction) was removed for histological and immunofluorescence analysis as described below.

2.4. B cell depletion

In some experiments, B cells were depleted using a monoclonal anti-mouse CD20 antibody as previously described [11]. Briefly, anti-mouse CD20 or a control IgG2a monoclonal antibody was administered in a single i.p. injection 9 days prior to the I/R procedure. Control C57BL/6 mice received 20 µg (per mice) of antibody. In MRL/*lpr* mice the antibody dose had to be escalated to 250 µg (per mice) to achieve comparable B cell depletion.

2.5. Histology and immunofluorescence

To prepare specimens for histological analysis, 20-cm segments of small intestine specimens were fixed in 10% buffered Formalin phosphate immediately after euthanasia. Next, tissues were embedded in paraffin, sectioned transversely in 5 µm sections, and stained with Giemsa. In each section, 50–100 villi were graded on a six-tiered scale, as previously described [10]. Briefly, a score of 0 was assigned to a normal villus; villi with tip distortion were scored as 1; villi lacking goblet cells and containing Guggenheims' spaces were scored as 2; villi with patchy disruption of the epithelial cells were scored as 3; villi with exposed but intact lamina propria and epithelial cell sloughing were assigned a score of 4; villi in which the lamina propria was exuding were scored as 5; and finally, villi displaying hemorrhage or denudation were scored as 6. All histological analysis was performed in a blinded manner.

B cell infiltration into intestinal tissue was quantified using Nikon NIS-Elements software in four to six fields per animal. Pictures of the immunohistochemistry stained (anti-B220) and control sides of each slide were taken at 200× magnification. Objects above threshold level were counted as square pixels in areas of the same size. These numbers were entered into a Microsoft Excel spreadsheet for each animal and treatment group.

For immunofluorescence, small intestine sections were snap-frozen to –70 °C, and sections were cut with a cryostat and fixed in acetone. Samples were blocked in PBS + 10% FCS. Sections were incubated overnight with the primary antibodies (1:100). After thorough washing, secondary antibodies were incubated for 1 h. Sections were counterstained with DAPI (0.5 µg/mL) and mounted using anti-fade solution (Slowfade Gold, Invitrogen). Finally, slides were scanned in a Nikon Eclipse Ti confocal microscope. Images were analyzed with EZ-C1 v.3.6 software.

2.6. Reverse transcription PCR

Total RNA was isolated from intestine tissue using Trizol (Invitrogen). It was reverse transcribed into cDNA using Superscript preamplification kit and amplified with specific primers (CXCL13, sense 5'-TCTCTCCAGGCCACGGTATTCT-3', anti-sense 5'-ACCATTTG GCACGAGGATTAC-3'; CXCR5, sense 5'- GCTGTCGTCTGCTACTGG TC-3', anti-sense 5'-ACATCTTCTGTTTTATT-3').

2.7. Statistical analyses

Data are presented as mean ± SEM. All data were subjected to statistical analysis using Microsoft Excel software and GraphPad Prime 4 software. A $p < 0.05$ was considered significant.

3. Results

3.1. Increased numbers of B cells enter intestinal tissue subjected to I/R injury

To investigate the trafficking pattern of B cells during I/R intestinal injury, we subjected C57BL/6 mice to 30 min mesenteric artery occlusion followed by either 1 or 3 h reperfusion. Significant ($p < 0.001$) numbers of B220⁺ B cells were detected in the intestinal tissue 3 h after the initiation of the reperfusion phase. B cell accumulation was mostly observed in the basal portions of the intestinal villi and within Payer's patches (Fig. 2A). The numbers of intestinal B cells did not differ between animals subjected to sham procedure and animals allowed to reperfuse for only 1 h (Fig. 1).

In order to corroborate the histological data, we isolated Payer's patches from mice subjected to I/R and sham procedures and

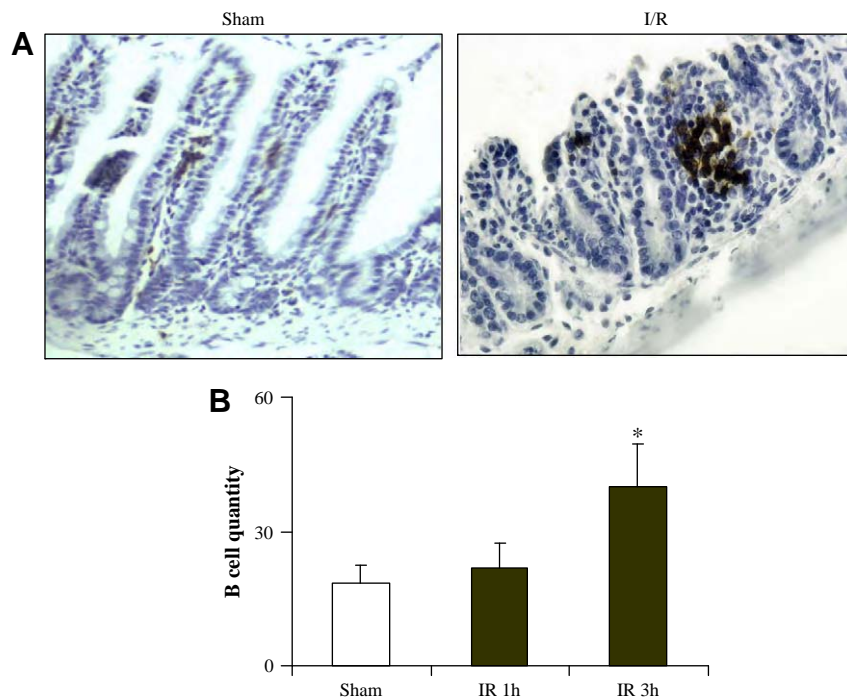


Fig. 1. B cells infiltrate ischemic intestine during reperfusion. (A) C57Bl/6 mice were subjected to sham procedure or I/R. Immunohistochemistry was performed with an anti-B220 antibody. Magnification 200 \times . (B) B cell infiltration was quantified with image analysis software. * $p < 0.001$ when compared to sham mice.

quantified the percentage of cells positive for the B cell marker B220 with flow cytometry. As shown in Fig. 2B and C, the B220⁺ Payer's patch cell fraction increased from 36.8 ± 5.5 in sham operated mice to 60.0 ± 7.0 in mice subjected to ischemia and 2 h reperfusion and to 66.7 ± 6.1 in mice after ischemia and 3 h reperfusion. These results confirm that I/R increases the number of intestinal B cells and indicate that B cells infiltrate ischemic intestine after 2 h of reperfusion.

3.2. I/R induces B cell infiltration into I/R injured intestinal tissue in MRL/lpr mice

I/R-mediated tissue injury has been shown to be amplified in autoimmune-prone MRL/lpr mice [3,8]. Circulating auto-antibodies [8], as well as increased infiltration of IL-17-producing T cells [3] have been reported to contribute to this phenomenon. In order to determine whether MRL/lpr mice exhibit increased B cell

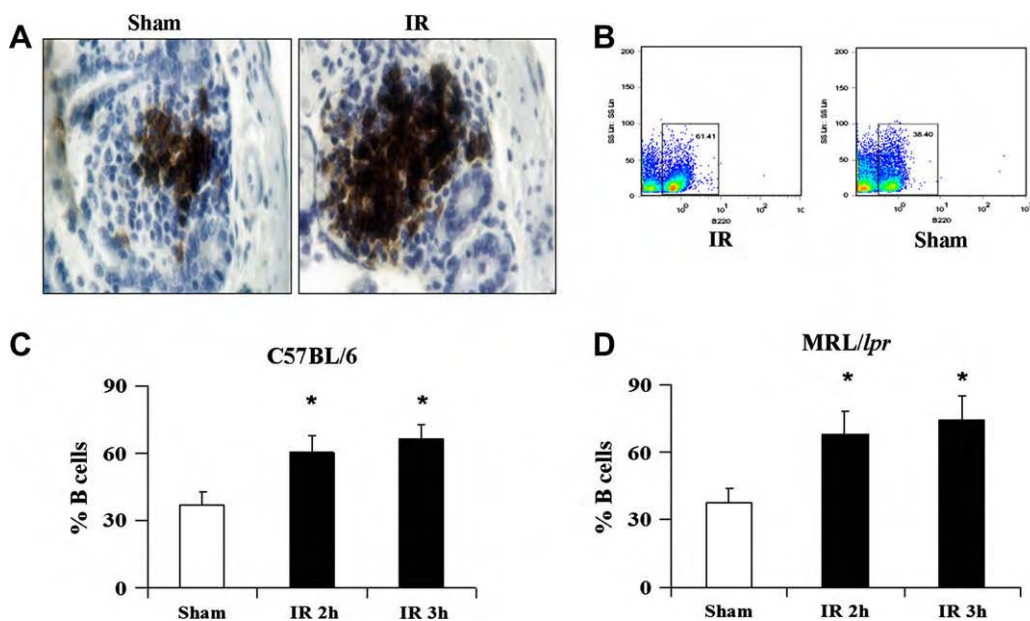


Fig. 2. I/R leads to an increase in the number of B cells within Payer's patches. (A) The number of B220⁺ cells in Payer's patches increases following I/R (magnification 200 \times). (B) Payer's patches were isolated and cells were stained with anti-B220 antibody. B cells were quantified in a flow cytometer. (C) Cumulative data of flow cytometry experiments ($n = 7$ per group). * $p < 0.001$ when compared to Sham.

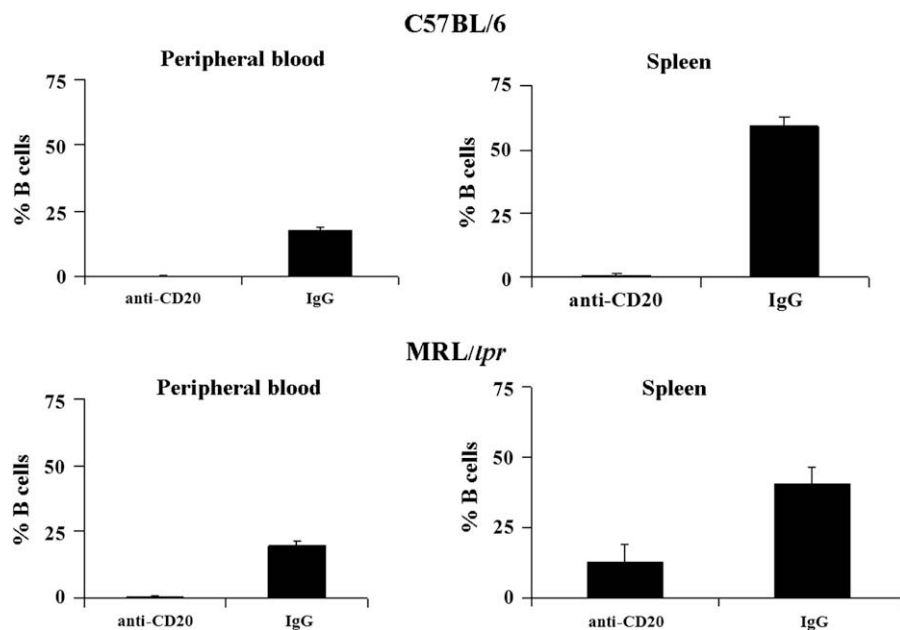


Fig. 3. MRL/lpr mice are resistant to complete B cell depletion. A depleting anti-mouse CD20 antibody was administered in a single dose to mice 9 days before I/R was induced. C57Bl/6 mice received 20 μ g per mouse; MRL/lpr received 250 μ g per mouse. Cellular suspensions from blood and spleen were stained with anti-B220 and analyzed by flow cytometry.

infiltration into tissue subjected to I/R, we subjected twenty month-old MRL/lpr mice to sham or I/R procedures. Kinetics and intensity of B cell tissue infiltration were similar to those observed in normal C57Bl/6 mice suggesting that B cell infiltration into ischemic tissue is guided by the same mechanism in both normal and autoimmunity-prone mice (Fig. 2D).

3.3. B cell depletion reduces I/R-mediated intestinal injury

To establish whether B cell infiltration has pathogenic significance in intestinal I/R, we depleted B cells from C57Bl/6 and MRL/lpr mice. B cells were depleted with a single injection of an anti-CD20 antibody, 9 days before I/R [11]. Complete B cell depletion was achieved in peripheral blood, Payer's patches, peritoneum, and spleen of C57Bl/6 mice using 20 μ g per mouse. In contrast, total B cell depletion was not observed in spleen and Payer's patches from MRL/lpr mice, even when a much higher antibody dose (250 μ g per mouse) was used (Fig. 3 and data not shown).

As shown in Fig. 4A, B cell depletion significantly reduced intestinal tissue damage. Injury score in B cell-sufficient C57Bl/6 mice was 5.1 ± 0.04 . After B cell depletion, tissue injury was reduced to 3.9 ± 0.11 ($p < 0.01$). Intestinal injury was also reduced in MRL/lpr mice from 5.75 ± 0.07 to 3.58 ± 0.23 after B cells were depleted ($p < 0.01$). Albeit complete B cell depletion could not be achieved in MRL/lpr mice, the reduction in tissue injury score was significantly greater in MRL/lpr mice than in control littermates ($p < 0.05$). Antibody titers are not immediately modified by anti-CD20 treatment [11]. Thus, these results indicate that B cells play an antibody-independent role in I/R-induced intestinal injury.

3.4. CXCL13 expression is locally induced by I/R injury

We hypothesized that the B cell-chemoattractant CXCL13 could be involved in the migration of B cells into areas of injured intestine. CXCL13 is known to guide the entry of B cells into follicles and inflamed tissues [12,13]. Thus, we sought the expression of this chemokine by immunohistochemistry in intestinal tissue from

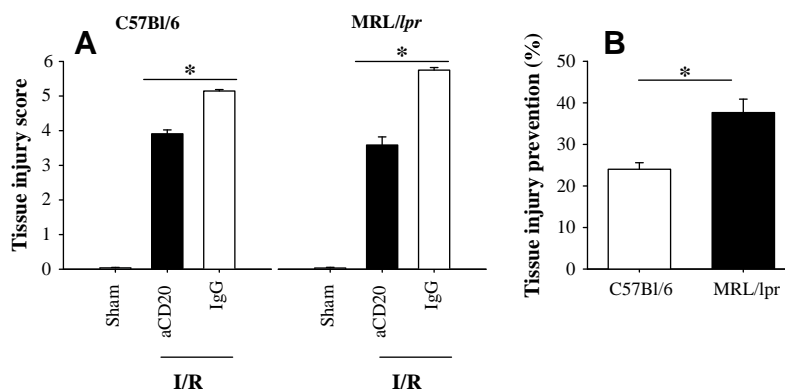


Fig. 4. B cell depletion reduces I/R-induced intestinal tissue injury. (A) Tissue injury score was significantly reduced in C57Bl/6 (left panel) and MRL/lpr (right panel) mice depleted of B cells (black bars) when compared to B cell-sufficient mice (white bars). * $p < 0.01$. (B) The reduction in tissue injury scores was significantly greater in MRL/lpr mice than in control mice. * $p < 0.05$.

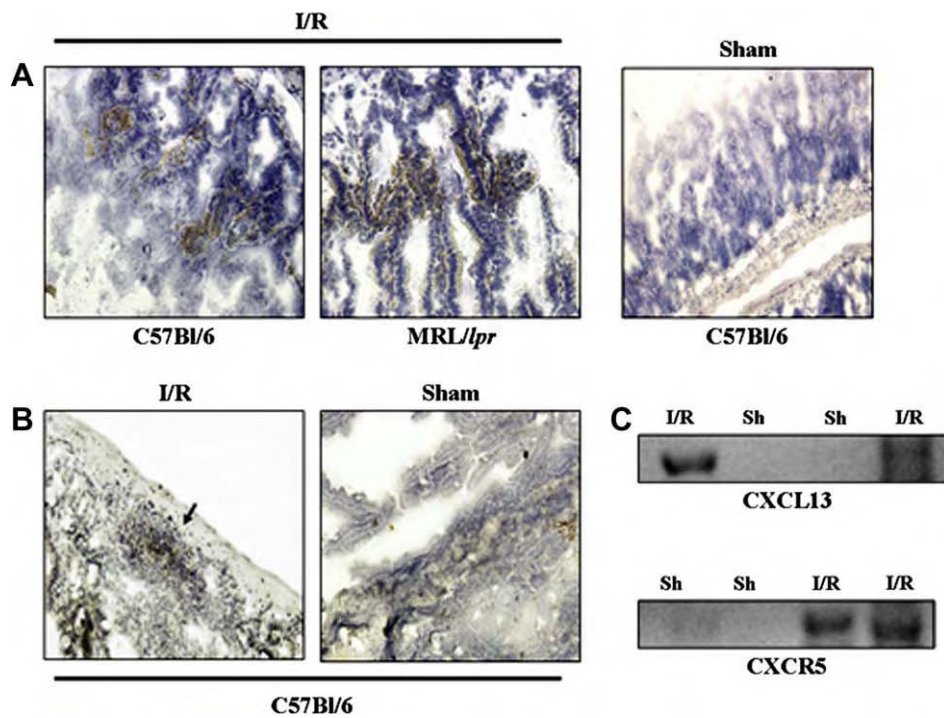


Fig. 5. CXCL13 expressed by injured tissue recruits CXCR5⁺ cells. Anti-CXCL13 (A) and anti-CXCR5 (B) antibodies were used to stain frozen sections from C57Bl/6 and MRL/lpr mice subjected to I/R (left panels) or sham (right panel) procedures ($n = 5$). Magnification 200 \times . (C) Total RNA was extracted from intestinal tissue of mice that had undergone I/R or sham (Sh) procedures. CXCL13 and CXCR5 transcripts were amplified by reverse transcriptase-PCR.

mice subjected to sham and I/R procedures. CXCL13 was not observed in intestine not subjected to ischemia (sham). In contrast, CXCL13 was abundantly expressed in injured areas of intestine damaged by I/R (Fig. 5A). To confirm this finding, we isolated total RNA from intestinal tissue. We were able to detect specific CXCL13

and CXCR5 transcripts only in lysates from mice subjected to I/R. Congruent with the histological findings, CXCL13 and CXCR5 mRNA were completely absent in control intestine (Fig. 5C).

To confirm the importance of this finding, we stained intestinal tissue with an antibody against the receptor of CXCL13 (CXCR5). As

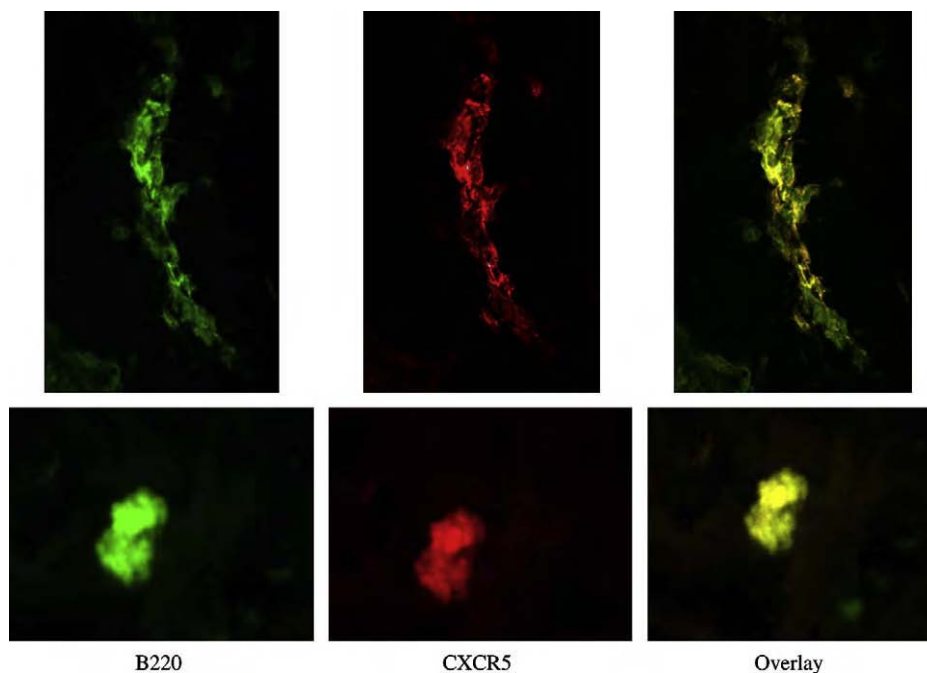


Fig. 6. CXCR5 expression is limited to B cells. Intestinal sections C57Bl/6 mice subjected to I/R were stained with FITC-labeled anti-B220 and PE-labeled anti-CXCR5 antibody and scanned in a confocal microscope.

expected, CXCR5 was exclusively present in intestinal sections from mice subjected to I/R (Fig. 5B). In order to exclude the expression of CXCR5 in cells different than B cells, we performed dual color immunofluorescence with FITC-labeled anti-B220 and PE-labeled anti-CXCR5. As shown in Fig. 6, confocal microscope scanning demonstrated colocalization of B220 and CXCR5 in intestine of animals subjected to I/R.

Taken together, our results indicate that intestine affected by I/R expresses the chemokine CXCL13 that attracts CXCR5⁺ B cells into damaged areas. B cell infiltration is involved to some extent in the tissue injury process, as demonstrated by B cell depletion experiments.

4. Discussion

Experiments reported in this communication grant B cells an antibody-independent role in I/R-mediated intestinal injury. Further, we describe the kinetics with which they infiltrate the ischemic tissue and identify a chemokine involved in their recruitment. Our data indicate that an analogous process occurs in MRL/lpr mice with similar kinetics and intensity.

B cells contribute to tissue pathology in immune-mediated disorders not only by producing antibody but also through other mechanisms which may involve antigen presentation and cytokine production [4,14]. The development of anti-B cell therapies that spare plasma cells and thus circulating antibodies has demonstrated that B cells are involved in autoimmune and inflammatory conditions in an antibody-independent fashion [6,15]. Although antibodies, particularly cationic auto-antibodies capable of binding negatively-charged phospholipids exposed after cell injury, have been considered the main mechanism by which B cells contribute to I/R-induced tissue injury [7–9,16–18], our data demonstrate that B cell depletion decreases tissue injury in mice which carry intact levels of circulating antibodies [19]. Interestingly, the protective effect of B cell depletion was significantly greater in the autoimmune mouse strain suggesting that B cells in the MRL/lpr mouse are capable of causing more damage than in the normal mouse (Fig. 4B).

Our results indicate that B cells appear in the ischemic tissue between 2 and 3 h after circulation is restored. This behavior contrasts with the earlier time in which T cells are observed to infiltrate intestine subjected to I/R [3]. Interestingly, we have previously shown that infiltrating T cells produce IL-17 [3]. This suggests that T cells might contribute to B cell infiltration by producing the B cell-chemoattractant CXCL13. This chemokine has been shown to be a product of IL-17-producing T cells [20]; this fact, added to the kinetics of infiltration of each cell type suggests that products secreted by early infiltrating T cells play a role in the amplification of the inflammatory response by recruiting effector cells. The whole process seems to be enhanced in autoimmune-prone mice. Should our results be reproduced in additional models of I/R injury and particularly in those closely resembling myocardial infarction and organ transplant, B cell depletion may prove of clinical value in multiple related clinical conditions.

Acknowledgments

This work was supported by Medical Research and Material Command grants W81XWH-07-1-0286, W81XWH-06-1-0486 and by NIH grants CA105001 and AI56363. We are grateful to Dr. Tong Shi for help with animal surgery and data analysis.

References

- [1] Fleming SD, Tsokos GC. Complement, natural antibodies, autoantibodies and tissue injury. *Autoimmun Rev* 2006;5:89–92.
- [2] Huang Y, Rabb H, Womer KL. Ischemia–reperfusion and immediate T cell responses. *Cell Immunol* 2007;248:4–11.
- [3] Edgerton C, Crispin JC, Moratz CM, Simovic M, Zacharia A, Egan R, et al. IL-17 producing CD4⁺ T cells mediate accelerated ischemia/reperfusion-induced injury in autoimmunity-prone mice. *Clin Immunol* 2009;130:313–321.
- [4] Tsokos GC. B cells, be gone – B-cell depletion in the treatment of rheumatoid arthritis. *N Engl J Med* 2004;350:2546–8.
- [5] Burne MJ, Daniels F, El Ghandour A, Mauyyedi S, Colvin RB, O'Donnell MP, et al. Identification of the CD4(+) T cell as a major pathogenic factor in ischemic acute renal failure. *J Clin Invest* 2001;108:1283–90.
- [6] Chan OT, Hannum LG, Haberman AM, Madaio MP, Shlomchik MJ. A novel mouse with B cells but lacking serum antibody reveals an antibody-independent role for B cells in murine lupus. *J Exp Med* 1999;189:1639–48.
- [7] Burne-Taney MJ, Ascon DB, Daniels F, Racusen L, Baldwin W, Rabb H. B cell deficiency confers protection from renal ischemia reperfusion injury. *J Immunol* 2003;171:3210–5.
- [8] Fleming SD, Monestier M, Tsokos GC. Accelerated ischemia/reperfusion-induced injury in autoimmunity-prone mice. *J Immunol* 2004;173:4230–5.
- [9] Fleming SD, Egan RP, Chai C, Girardi G, Holers VM, Salmon J, et al. Anti-phospholipid antibodies restore mesenteric ischemia/reperfusion-induced injury in complement receptor 2/complement receptor 1-deficient mice. *J Immunol* 2004;173:7055–61.
- [10] Rehrig S, Fleming SD, Anderson J, Guthridge JM, Rakstang J, McQueen CE, et al. Complement inhibitor, complement receptor 1-related gene/protein γ -Ig attenuates intestinal damage after the onset of mesenteric ischemia/reperfusion injury in mice. *J Immunol* 2001;167:5921–7.
- [11] Hamaguchi Y, Xiu Y, Komura K, Nimmerjahn F, Tedder TF. Antibody isotype-specific engagement of Fc γ receptors regulates B lymphocyte depletion during CD20 immunotherapy. *J Exp Med* 2006;203:743–53.
- [12] Roy MP, Kim CH, Butcher EC. Cytokine control of memory B cell homing machinery. *J Immunol* 2002;169:1676–82.
- [13] Kanemitsu N, Ebisuno Y, Tanaka T, Otani K, Hayasaka H, Kaisho T, et al. CXCL13 is an arrest chemokine for B cells in high endothelial venules. *Blood* 2005;106:2613–8.
- [14] Youinou P. B cell conducts the lymphocyte orchestra. *J Autoimmun* 2007;28:143–51.
- [15] Blank M, Shoenfeld Y. B cell targeted therapy in autoimmunity. *J Autoimmun* 2007;28:62–8.
- [16] Weiser MR, Williams JP, Moore FD Jr, Kobzik L, Ma M, Hechtman HB, et al. Reperfusion injury of ischemic skeletal muscle is mediated by natural antibody and complement. *J Exp Med* 1996;183:2343–8.
- [17] Williams JP, Pechet TT, Weiser MR, Reid R, Kobzik L, Moore FD Jr, et al. Intestinal reperfusion injury is mediated by IgM and complement. *J Appl Physiol* 1999;86:938–42.
- [18] Avrameas S, Ternynck T, Tsonis IA, Lymberi P. Naturally occurring B-cell autoreactivity: a critical overview. *J Autoimmun* 2007;29:213–8.
- [19] DiLillo DJ, Hamaguchi Y, Ueda Y, Yang K, Uchida J, Haas KM, et al. Long-lived plasma cells and serological memory do not require ongoing contributions from the memory B cell pool. *J Immunol* 2008;180:361–71.
- [20] Takagi R, Higashi T, Hashimoto K, Nakano K, Mizuno Y, Okazaki Y, et al. B cell chemoattractant CXCL13 is preferentially expressed by human Th17 cell clones. *J Immunol* 2008;181:186–9.



This article appeared in a journal published by Elsevier. The attached copy is furnished to the author for internal non-commercial research and education use, including for instruction at the authors institution and sharing with colleagues.

Other uses, including reproduction and distribution, or selling or licensing copies, or posting to personal, institutional or third party websites are prohibited.

In most cases authors are permitted to post their version of the article (e.g. in Word or Tex form) to their personal website or institutional repository. Authors requiring further information regarding Elsevier's archiving and manuscript policies are encouraged to visit:

<http://www.elsevier.com/copyright>

available at www.sciencedirect.comwww.elsevier.com/locate/yclim

IL-17 producing CD4⁺ T cells mediate accelerated ischemia/reperfusion-induced injury in autoimmunity-prone mice[☆]

Colin Edgerton^{a,1}, José C. Crispín^{b,1}, Chantal M. Moratz^{a,d}, Estelle Bettelli^c, Mohamed Oukka^c, Milomir Simovic^{a,d}, Athina Zacharia^a, Ryan Egan^d, Jie Chen^b, Jurandir J. Dalle Lucca^d, Yuang-Taung Juang^b, George C. Tsokos^{b,*}

^a Department of Medicine, Uniformed Services University for the Health Sciences, Bethesda, MD 20814, USA

^b Department of Medicine, Beth Israel Deaconess Medical Center, Harvard Medical School, 330 Brookline Avenue, CLS-937 Boston, MA 02115, USA

^c Center for Neurologic Diseases, Brigham and Women's Hospital, Harvard Medical School, Boston, MA 02115, USA

^d Department of Cellular Injury, Walter Reed Army Institute of Research, Silver Spring, MD 20910, USA

Received 14 August 2008; accepted with revision 23 September 2008

Available online 5 December 2008

KEYWORDS

Autoimmunity;
IL-17;
IL-23;
Inflammation;
Ischemia reperfusion;
MRL/lpr mice;
p19^{-/-} mice;
Systemic lupus erythematosus;
T cell

Abstract Elements of the innate and adaptive immune response have been implicated in the development of tissue damage after ischemic reperfusion (I/R). Here we demonstrate that T cells infiltrate the intestine of C57BL/6 mice subjected to intestinal I/R during the first hour of reperfusion. The intensity of the T cell infiltration was higher in B6.MRL/lpr mice subjected to intestinal I/R and reflected more severe tissue damage than that observed in control mice. Depletion of T cells limited I/R damage in B6.MRL/lpr mice, whereas repletion of B6.MRL/lpr lymph node-derived T cells into the I/R-resistant Rag-1^{-/-} mouse reconstituted tissue injury. The tissue-infiltrating T cells were found to produce IL-17. Finally, IL-23 deficient mice, which are known not to produce IL-17, displayed significantly less intestinal damage when subjected to I/R. Our data assign T cells a major role in intestinal I/R damage by virtue of producing the pro-inflammatory cytokine IL-17.

© 2008 Elsevier Inc. All rights reserved.

Introduction

Ischemia/reperfusion (I/R) represents a model of tissue injury in which circulation is reinstated in an organ transiently deprived of blood flow. The ischemic insult alters the affected tissue making it susceptible to inflammatory damage during reperfusion. Furthermore, mediators produced in the ischemic areas diffuse when circulation is restored and cause inflammation in remote organs not

[☆] The opinions expressed herein are those of the authors and do not represent those of the Department of Defense.

* Corresponding author. Fax: +1 617 435 4170.

E-mail address: gtsokos@bidmc.harvard.edu (G.C. Tsokos).

¹ C. E. and J. C. C. contributed equally to this work.

exposed to ischemia [1]. Several molecules and cells have been implicated in I/R. These include mainly elements of the innate immune response such as reactive oxygen species, cytokines and chemokines, complement, natural antibodies, and neutrophils [1]. The adaptive immune system has not yet been assigned a definitive role in the production of tissue injury in classical models of I/R. Nevertheless, recent evidence suggests that T cells participate actively in I/R injury as they have been found to enter the damaged tissue early after circulation is restored [2]. T cell depletion has been shown to diminish organ damage in intestinal [3], hepatic [4], and kidney models of I/R [5]. Although the mechanism by which T cells contribute to tissue injury is not completely understood, secretion of pro-inflammatory cytokines is probably involved. Hence, IFN- γ and TNF- α have been linked to tissue damage in the setting of I/R [5,6].

I/R-mediated organ damage has relevance to a number of clinical settings that include acute organ infarction, shock, and organ transplantation [1]. The model is also relevant in the study of systemic lupus erythematosus (SLE), a chronic inflammatory disease of autoimmune etiology strongly associated with vascular injury [7,8]. In patients with SLE, a number of pathogenic pathways converge to cause vascular damage. These include thrombotic diathesis [9], accelerated atherosclerosis [8], and vasculitis [10]. In this setting, the aforementioned factors are concomitant to an abnormal pro-inflammatory skewed immune response [11]. The coincidence of an inflammatory milieu with the proclivity to vascular damage makes patients with SLE prone to develop organ damage due to I/R phenomena. The importance of this fact is evidenced by the finding that mice with lupus-like disease are more susceptible to organ damage due to I/R than non-autoimmune mice [12]. Several facts could account for the increased susceptibility of lupus-prone mice to I/R. In a previous communication, we demonstrated that the presence of autoantibodies significantly increased the tissue injury score after I/R [12].

In this communication, we confirm that tissue injury after I/R is increased in lupus-prone mice (B6.MRL/lpr) when compared to normal non-autoimmune mice. Depletion of T cells suppresses the development of I/R injury, whereas transfer of MRL/lpr T cells to the I/R injury-resistant *Rag-1*^{-/-} mouse, reconstitutes tissue damage. We show that tissue-infiltrating T cells produce IL-17, and demonstrate the pathogenic importance of this cytokine using a mouse deficient in IL-23. Although T cell infiltration is not modified in IL-23 deficient mice, T cells fail to produce IL-17 and tissue injury is significantly reduced. Thus, we propose a model in which T cells infiltrate ischemic tissues early during reperfusion and secrete IL-17 that acts as a major pathogenic element in intestinal I/R tissue damage.

Materials and methods

Mice

Adult male B6.MRL*Tnfrsf6*^{lpr} (B6.MRL/lpr), B6.*Rag-1* (*Rag-1*^{-/-}), and control C57BL/6 mice were obtained from The Jackson Laboratory (Bar Harbor, ME), and housed in the animal facility of the Uniformed Services University for

the Health Sciences. IL-23p19^{-/-} (IL-23-deficient mice) and their WT controls were generated on a mixed B6 X 129 background.

Reagents

The following antibodies were used for immunofluorescence studies: FITC-labeled Armenian hamster anti-mouse CD3 ϵ (Clone 145-2C11); FITC-labeled rat anti-mouse CD4 (Clone RM4-5); FITC-labeled rat anti-mouse CD8 (Clone 53-6.7); FITC-labeled rat-anti mouse Ly-6G and Ly-6C (Gr-1; Clone RB6-8C5); FITC-labeled rat anti-mouse CD11b (Integrin α_M chain; Clone M1/70); rat anti-mouse IL-17A (Clone TC11-18H10); FITC-labeled rat IgG, all from BD Biosciences (San Jose, CA). As secondary antibody, affinity purified Texas Red-labeled goat-anti rat IgG was used (Jackson ImmunoResearch Laboratories, West Grove, PA).

Ischemia reperfusion protocol

After an acclimation period of at least 7 days, mice were prepared for surgery. Anesthesia was induced with ketamine (16 mg/kg) and xylazine (8 mg/kg) administered by i.p. injection. All procedures were performed with the animals breathing spontaneously and body temperature maintained at 37 °C using a water-circulating heating pad. Research was conducted in compliance with the Animal Welfare Act and other Federal statutes and regulations relating to animals and experiments involving animals, and adheres to principles stated in the Guide for the Care and Use of Laboratory Animals, NRC Publication, 1996 edition. All procedures were reviewed and approved by the Institute's Animal Care and Use Committee, and performed in a facility accredited by the Association for Assessment and Accreditation of Laboratory Animal Care, International.

Animals were subjected to I/R as previously described [13]. Briefly, a midline laparotomy was performed before a 30-min equilibration period. The superior mesenteric artery was identified and isolated, and a small non-traumatic vascular clamp (Roboz Surgical Instruments, Rockville, MD) was applied for 30 min. After this ischemic phase, the clamp was removed and the intestine was allowed to reperfuse for 1 or 3 h. In some experiments, 1 day prior to surgery, 250 μ g of rat anti-mouse CD4 IgG monoclonal Ab (BD Biosciences, Clone RM4-5) was administered by i.p. injection. As sham procedure, animals were subjected to the same surgical intervention without artery occlusion. The laparotomy incisions were sutured and the animals were monitored during the reperfusion period. Additional ketamine and xylazine was administered by i.m. injection immediately before euthanasia. There was no significant difference in survival between treatment and control groups. After euthanasia, the small intestine 10–20 cm distal to the gastroduodenal junction was removed for histological and immunofluorescence analysis as described below.

T. cell adoptive transfer

Mesenteric lymph nodes from B6.MRL/lpr mice were isolated, rinsed, and disrupted to form a cell suspension. The suspension was then filtered through a sterile nylon mesh

screen (0.45 μm , BD) to obtain a single cell suspension. T cells were isolated by negative selection using a combination of biotinylated antibodies (anti-B220, anti-CD11b, anti-Ter119, and anti-CD49b) and streptavidin coated magnetic beads (Dyna, M-280). T cells (5×10^6 per mouse) were transferred into *Rag-1*^{-/-} mice by tail vein injection. One week later, mice were subjected to I/R.

Histology and immunofluorescence

To prepare specimens for histological analysis, 2-cm segments of small intestine specimens were fixed in 10% buffered Formalin phosphate immediately after euthanasia. Next, tissues were embedded in paraffin, sectioned transversely in 5- to 7- μm sections, and stained with Giemsa. In each section, 50–100 villi were graded on a six-tiered scale, as previously described [13]. Briefly, a score of 0 was assigned to a normal villus; villi with tip distortion were scored as 1; villi lacking goblet cells and containing Guggenheims' spaces were scored as 2; villi with patchy disruption of the epithelial cells were scored as 3; villi with

exposed but intact lamina propria and epithelial cell sloughing were assigned a score of 4; villi in which the lamina propria was exuding were scored as 5; and finally, villi displaying hemorrhage or denudation were scored as 6. All histological analysis was performed in a blinded manner.

For immunofluorescence, small intestine sections were snap-frozen to -70°C , and sections were cut with a cryostat and fixed in acetone. Samples were blocked in PBS + 10% FCS. Sections were incubated overnight with the primary antibodies (1:100). After thorough washing, secondary antibodies were incubated for 1 h. Sections were counterstained with DAPI (0.5 $\mu\text{g}/\text{mL}$) and mounted using anti-fade solution (Slowfade Gold, Invitrogen). Finally, slides were scanned in a Nikon Eclipse Ti confocal microscope. Images were analyzed with EZ-C1 v.3.6 software. To quantify cellular infiltrates, digital photomicrographs of stained sections were processed with the ImageJ software (ImageJ 1.35, NIH) which quantifies the pixel density (pixel density per area unit) of stained cells present in each field. Five random fields (at a power of 200 \times) were examined per tissue per animal in a blinded fashion.

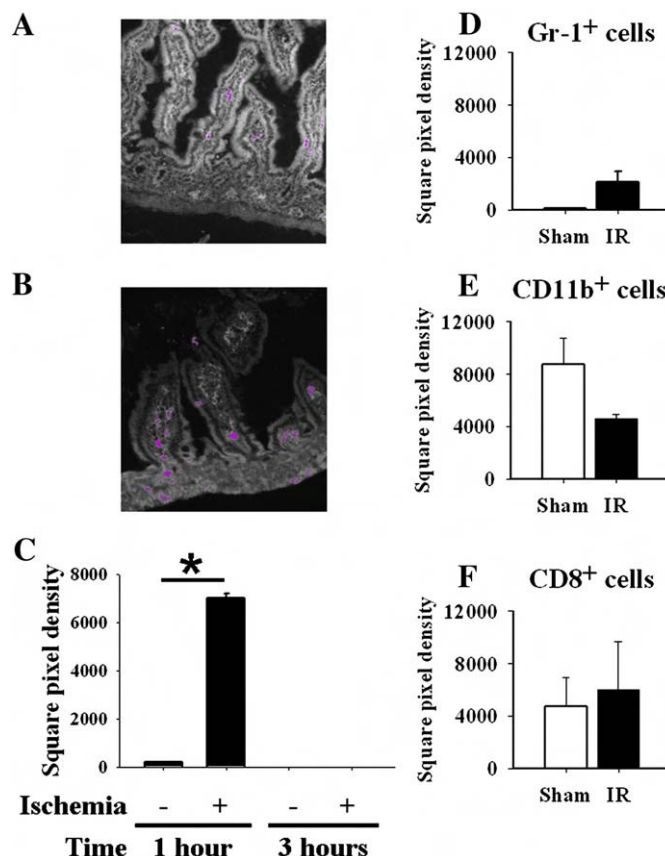


Figure 1 CD4⁺ T cells infiltrate ischemic intestine early during reperfusion. Representative processed photomicrographs of a B6 mouse subjected to sham (A) or I/R (B) procedure (CD4⁺ cells are highlighted in magenta). Increased numbers of CD4⁺ T cells were observed in intestines from mice subjected to I/R (B), as compared to non-ischemic intestines from control mice (A). (C) Cumulative data expressed as square pixel density from sham and I/R mice sacrificed at 1 and 3 h after reperfusion. (D) Infiltration of Gr-1⁺ cells in intestinal tissue of mice subjected to sham surgery (white bars) or superior mesenteric artery occlusion (black bars). Intestines were stained 1 h after reperfusion and cell infiltration was quantified as square pixel density. Although Gr-1⁺ cells showed a trend to increase in I/R mice (D), the difference did not reach statistical significance ($p=0.26$). Likewise, there was no significant difference in the number of CD11b⁺ ($p=0.12$) and CD8⁺ cells ($p=0.75$) in mice subjected to I/R injury when compared to mice that underwent the sham procedure (E and F, respectively). * $p<0.001$.

Statistical analysis

Data are presented as mean \pm SEM. Data were compared by one-way ANOVA with post hoc analysis using Newman-Keuls test (GraphPad/Instat Software). For nonparametric analysis of mucosal injury, data was compared using Kruskal-Wallis test with Dunn post analysis. A $p < 0.05$ was considered significant.

Results

CD4⁺ T cells infiltrate damaged intestine early during reperfusion

To determine which cell types are involved in I/R injury, C57BL/6 mice were subjected to intestinal ischemia by applying a clamp to the superior mesenteric artery for 30 min. After either 1 or 3 h of reperfusion, mice were sacrificed and the intestine was stained for immunofluorescence analysis. As shown in Figs. 1A and B, a significant increase in the number of CD4⁺ T cells present in the intestinal tissue was observed in mice that had been subjected to I/R, as compared to mice in which sham surgery had been performed ($p < 0.001$). Interestingly, the CD4⁺ T cell infiltration appeared rapidly, within the first hour of reperfusion, and was short lived. It could no longer be observed 3 h after reperfusion (Fig. 1C). CD4⁺ T cells were mainly observed in central areas of the villi, where they formed small aggregates adjacent to blood vessels and lamina propria (Figs. 1A and B). The early tissue infiltration response was highly specific for CD4⁺ T cells and analogous phenomena were not observed when other cell types were studied. The numbers of CD8⁺ T cells, granulocytes (Gr-1⁺ cells), and CD11b⁺ cells (monocytes and granulocytes), did not increase significantly when we compared intestines subjected to I/R injury with intestines in which sham procedures had been performed (Figs. 1D, E, F).

CD4⁺ T cell infiltration is amplified in MRL mice

Mice deficient in Fas molecule (MRL/*lpr*) develop a T cell driven autoimmune disease that resembles SLE [14]. T cells from MRL/*lpr* mice exhibit an activated phenotype and have been shown to induce auto-antibody production from auto-reactive B cells [15], secrete pro-inflammatory cytokines [16], and infiltrate organ tissues [17]. Likewise, in humans with SLE, peripheral blood T cells have been shown to share an activated phenotype with the T cells that infiltrate kidneys affected by lupus nephritis [18]. These facts suggest that T cells from MRL/*lpr* mice and from humans with SLE have a propensity to infiltrate tissues and cause inflammation. To test this hypothesis we subjected B6.MRL/*lpr* mice to intestinal ischemia and compared the CD4⁺ T cell infiltration after 1 h of reperfusion to that observed in congenic B6 mice. As shown in Fig. 2, intestinal infiltration by CD4⁺ T cells was significantly increased in B6.MRL/*lpr* mice when compared to non-autoimmune B6 mice ($p < 0.001$). B6.MRL/*lpr* mice showed an increased amount of CD4⁺ T cells even in the absence of ischemic insult. After I/R, the number of CD4⁺ T cells was dramatically amplified ($p < 0.001$). The distribution of the infiltrating CD4⁺ T cells was not different in MRL/*lpr* mice than in wild type mice. CD4⁺ T cells were mostly found close to the vasculature at the base of the villi and within the lamina propria.

Infiltrating CD4⁺ T cells play a role in I/R-mediated tissue damage

The amplified intestinal CD4⁺ T cell infiltration observed in B6.MRL/*lpr* mice could be a non-pathogenic phenomenon. However, tissue injury scores were significantly higher in B6.MRL/*lpr* mice than in non-autoimmune B6 mice indicating that the autoimmune proclivity of B6.MRL/*lpr* mice leads to enhanced susceptibility to ischemic injury. The degree of tissue damage (Fig. 3A) was mirror-imaged in the overall

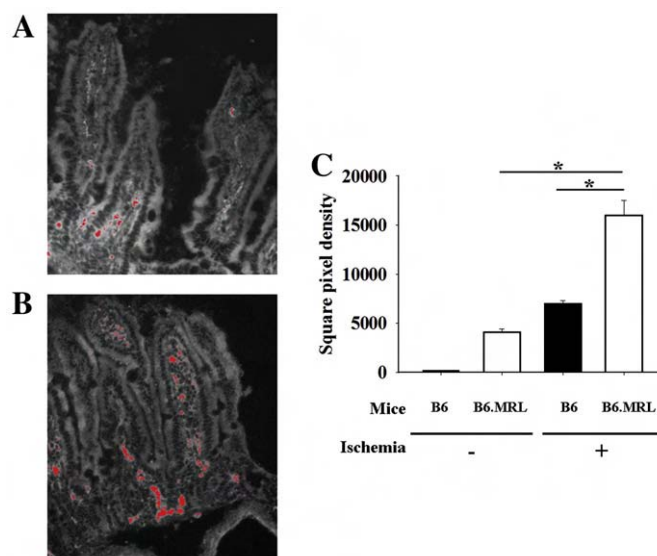


Figure 2 I/R-induced CD4⁺ T cell infiltration is increased in lupus-prone mice. B6 (black bars) and B6.MRL/*lpr* (white bars) mice were subjected to intestinal ischemia followed by 1 h reperfusion. The magnitude of the induced CD4⁺ T cell infiltration was significantly larger in B6.MRL/*lpr* mice (B) than in congenic control B6 mice (A). (C) Cumulative data expressed as square pixel density. * $p < 0.001$.

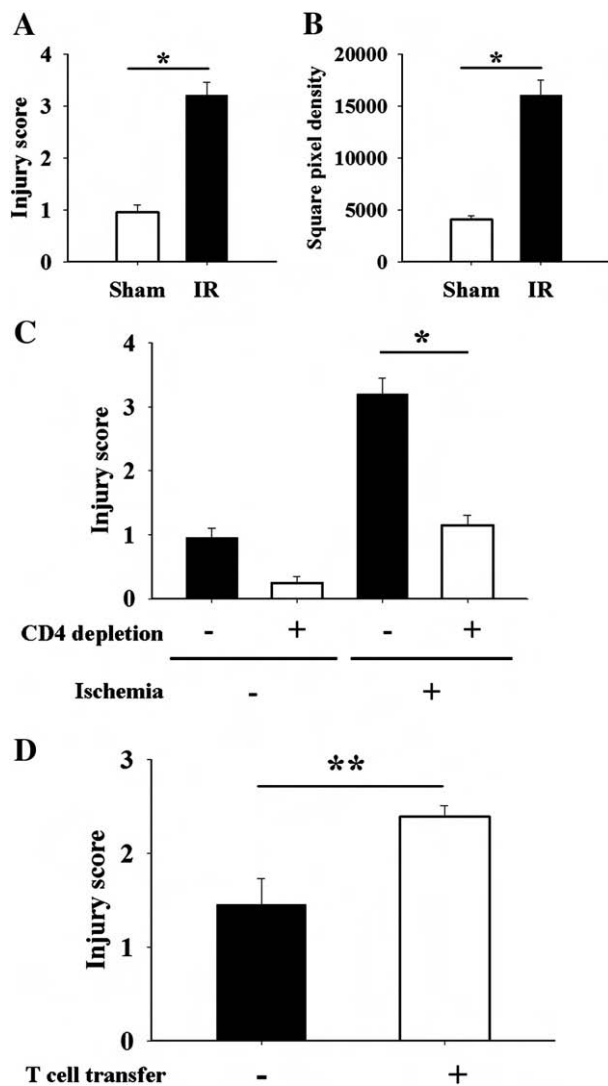


Figure 3 CD4⁺ T cells mediate I/R-induced injury in B6.MRL/*lpr* mice. Tissue injury (A) closely paralleled CD4⁺ T cell infiltration (B). (C) CD4⁺ cell depletion caused a decrease in tissue injury scores in B6.MRL/*lpr* mice and abrogated the effect of I/R diminishing the intestinal damage to levels similar to those of sham operated mice. (D) Transfer of T cells obtained from B6.MRL/*lpr* lymph nodes restored tissue damage in I/R-resistant *Rag-1*^{-/-} mice. **p*<0.001; ***p*<0.05.

intensity of the T cell infiltration (Fig. 3B), suggesting a role for CD4⁺ T cells in the enhanced tissue damage. To test this hypothesis, CD4⁺ T cells were depleted from B6.MRL/*lpr* mice 24 h prior to the induction of I/R. As expected, cell depletion with anti-CD4 Ab resulted in a decrease in the amount of infiltrating CD4⁺ T cells (data not shown). As shown in Fig. 3C, CD4⁺ T cell depletion decreased basal tissue injury levels, indicating that the low level intestinal damage observed in sham-operated B6.MRL/*lpr* mice is caused by the spontaneously infiltrating CD4⁺ T cells observed in lupus-prone mice. Importantly, CD4⁺ T cell depletion reduced intestinal injury scores in B6.MRL/*lpr* mice subjected to I/R to levels similar to those found in sham-operated mice (*p*<0.001), providing further evidence of the pathogenic role of CD4⁺ T cells in I/R-mediated intestinal injury.

To further establish the contribution of CD4⁺ T cells in the I/R-mediated bowel injury, we transferred lymph node T cells from B6.MRL/*lpr* mice into mice deficient in lymphocytes (*Rag-1*^{-/-}). *Rag-1*^{-/-} are known to be resistant to I/R damage [12]. Thus, this approach would allow the evaluation of the degree of damage caused by T cells in the absence of other possible pathogenic factors such as antibodies and B cells. As shown in Fig. 3D, T cell repletion increased significantly the degree of tissue damage induced by I/R in *Rag-1*^{-/-} mice (*p*=0.02) confirming the claim that the mere presence of B6.MRL/*lpr* T cells is capable of promoting tissue injury upon an I/R insult.

Infiltrating T cells produce IL-17

T cells can induce inflammation and tissue damage using different mechanisms. However, the kinetics with which they appeared and disappeared from ischemic tissue during reperfusion suggested that their mechanism of action was the production of cytokines that could induce tissue damage by acting on resident cells and attracting inflammatory cells to the injured site. IL-17 is a potent pro-inflammatory cytokine produced by the effector CD4⁺ T cell subset known as Th17 [19]. IL-17 has been linked to several inflammatory disease models such as experimental autoimmune encephalomyelitis [20] and collagen-induced arthritis [21]. The receptor(s) for IL-17 is expressed by a large variety of cells and thus it has a wide array of effects including the recruitment of macrophages and neutrophils to inflamed tissues [22]. Therefore, we stained intestinal sections from B6 and B6.MRL/*lpr* mice subjected to ischemia followed by 1 h reperfusion with FITC-labeled anti-CD3 and rat anti-mouse anti-IL-17 antibodies (followed by Texas Red-labeled goat anti-rat) and analyzed them using confocal microscopy. As shown in Fig. 4A, we found neither T cells nor IL-17 in the intestinal tissue of normal mice subjected to sham surgery. I/R led to an increase in the number of T cells infiltrating the tissues as well as to the deposition of IL-17. A majority of the T cells co-expressed IL-17 and CD3 (Fig. 4B, yellow color). We could also detect IL-17 in other cells that lacked CD3 expression. Congruent with our earlier findings, we could observe both T cells and IL-17 in intestinal villi from B6.MRL/*lpr* mice even in the absence of ischemic injury (Fig. 4). I/R was associated with a dramatic increase in the number of infiltrating IL-17⁺ CD3⁺ T cells in MRL mice, confirming that T cells produce IL-17 during reperfusion of intestinal tissue subjected to an ischemic assault.

Absence of IL-17 diminishes I/R intestinal injury

To test the hypothesis that IL-17 plays a pathogenic role in tissue damage induced by I/R, we used IL-23p19^{-/-} mice. These mice lack the 19 kD subunit that constitutes IL-23 when coupled to a 40 kD subunit shared with IL-12. In consequence, they exhibit a markedly reduced IL-17 response [19] and are resistant to IL-17-mediated diseases such as EAE [20]. We subjected p19 KO mice to I/R and analyzed the intensity of tissue damage, T cell infiltration, and IL-17 expression after 1 h reperfusion. As shown in Fig. 5A, the tissue injury score decreased significantly (*p*=0.002) in p19 KO mice when compared to congenic controls. The results were highly reproducible within groups and the

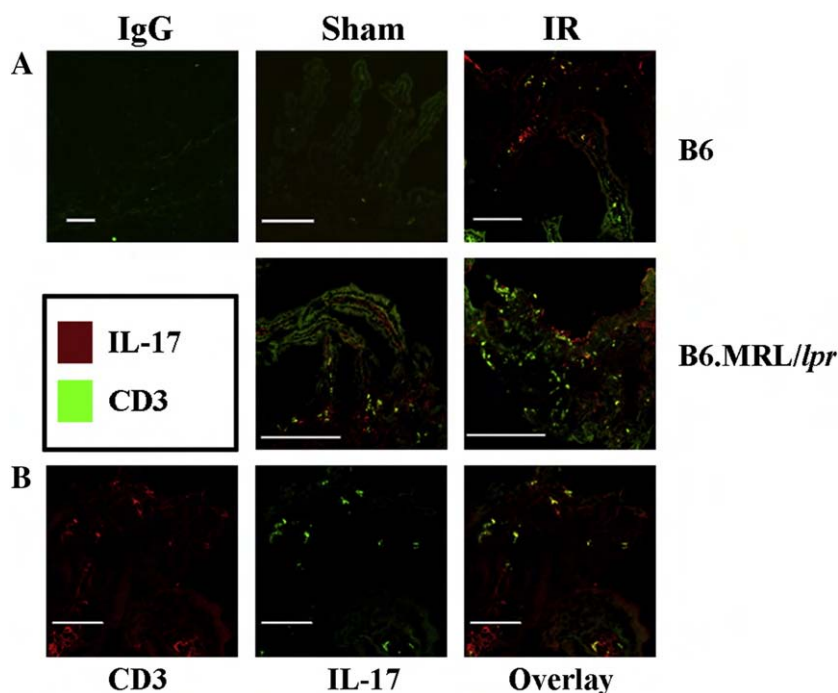


Figure 4 Intestine-infiltrating T cells produce IL-17. Tissues from B6.MRL/*lpr* and control mice subjected to sham-surgery and I/R were stained with FITC-labeled anti-CD3 Ab and rat anti-mouse IL-17 Ab (followed by Texas Red-labeled goat anti-rat Ab). Sections were scanned in a confocal microscope. (A) A scarce number of T cells can be observed in normal intestinal villi from a sham-operated B6 mouse. In contrast, I/R leads to the accumulation of T cells and IL-17 (upper panels). In intestinal sections from B6.MRL/*lpr* mice, T cells are present in sham-operated animals. Ischemic injury leads to a massive infiltration of IL-17⁺ T cells (lower panels). White bars represent 150 μ m. (B) Higher magnification demonstrates that a majority of infiltrating T cells produce IL-17. White bars represent 50 μ m.

experiment was only performed once ($n=3$ per group). As expected, IL-17 was virtually absent in intestinal tissue from p19 KO mice. However, T cell infiltration was not modified (Fig. 5B). These results indicate that IL-17 production, rather than the mere presence of infiltrating T cells, is necessary for the development of full-blown I/R-mediated intestinal tissue injury.

Discussion

In this communication, we confirm that T cells play a fundamental role in the early phase of the intestinal I/R-mediated tissue injury and demonstrate that they do so by means of producing the pro-inflammatory cytokine IL-17. Lupus prone mice which are known to suffer more intestinal I/R damage [12], display more intense T cell infiltration, as well as a more pronounced IL-17 tissue expression. The claim that T cells are important in I/R damage is supported by two experiments. First, depletion of CD4⁺ T cells in the B6.MRL/*lpr* mouse limits significantly T cell infiltration and tissue damage, and second, replenishment of the I/R-resistant Rag-1^{-/-} mouse with B6.MRL/*lpr* lymph node T cells reconstitutes the intestinal I/R damage. Finally, we provide first evidence that the infiltrating T cells produce IL-17, and demonstrate the pathogenic importance of this cytokine which apparently enables the subsequent steps of tissue damage.

The fast kinetics with which T cell infiltration occurs, indicates that the observed CD4⁺ cells are memory T cells since they migrate to inflamed tissues and produce inflam-

matory cytokines. This behavior is characteristic of the inflammatory response in the setting of I/R and it has been documented in previous work [4]. In agreement with our findings, T cell infiltration has shown to be negligible after 3 h of reperfusion [4]. A different communication, however reported peak T cell adhesion to intestinal endothelial cells 6 h after reperfusion [3]. We assume that methodological differences may account for the discrepant kinetics. We have found that the timing of the transfer is particularly relevant for the behavior of T cells, because their homing ability may be diminished during the first hour after reperfusion (Moratz CM, unpublished observation). Interestingly, the same report [3] demonstrated that early I/R-induced phenomena (i.e. albumin leakage and neutrophil accumulation) depended on the presence of T cells, since they were abolished in SCID mice and restored after T cell reconstitution [3]. Thus even though they detected late T cell-endothelial cell adhesion, their data supports an early role for T cells in the I/R injury process.

Tissue injury produced by I/R is increased in mice from autoimmune strains [11]. In this paper we confirm this fact and add T cells as central effector players in I/R injury. T cells from patients with SLE and mice with lupus-like diseases exhibit a number of biochemical abnormalities that alter their activation and effector functions. In patients with SLE, T cells have been found to infiltrate the kidney [23]. Because peripheral blood T cells and kidney infiltrating cells express the adhesion molecule CD44 and its signaling partner pERM, it has been claimed that CD44 guides the kidney infiltrating T cells [18]. T cells from lupus-prone mice express more CD44

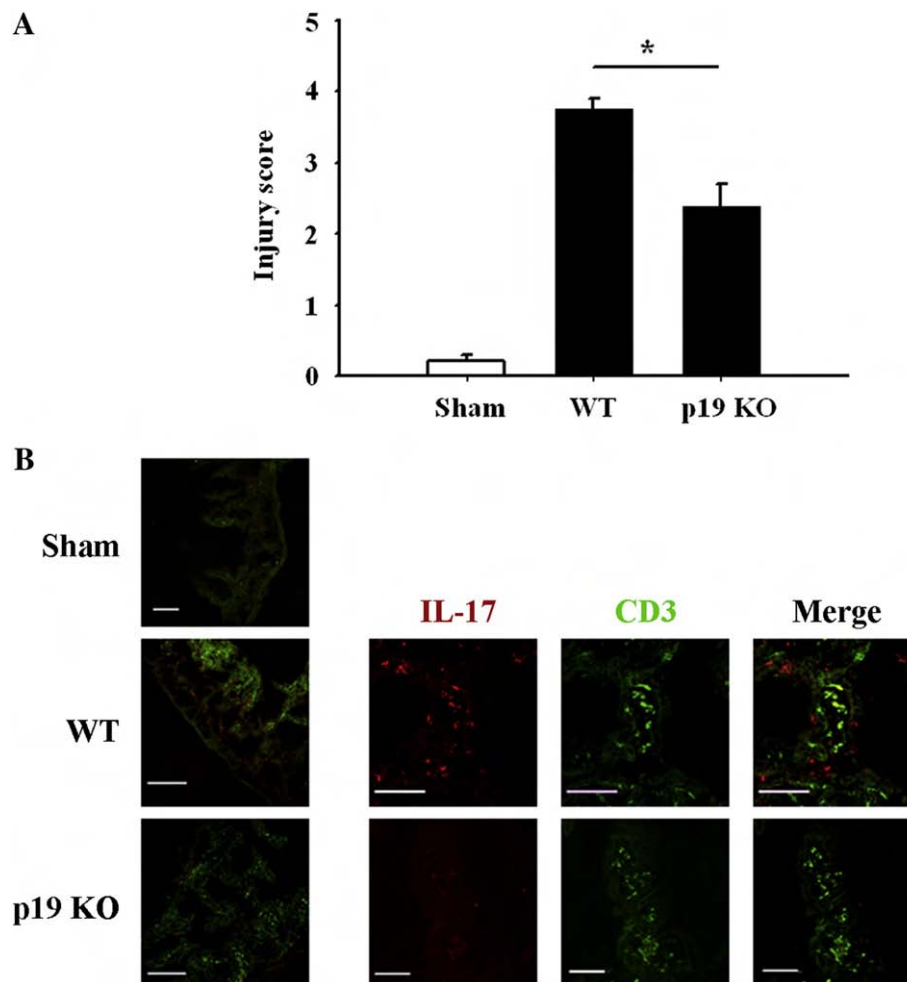


Figure 5 IL-23 deficient mice are protected from I/R-mediated intestinal injury. p19 deficient and congenic control mice ($n=3$ per group) were subjected to 30 min mesenteric occlusion followed by 1 h reperfusion. (A) Tissue injury was significantly inhibited in p19 KO mice when compared to control mice ($*p=0.002$). (B) Staining with Armenian hamster anti-mouse CD3-FITC and rat anti-mouse IL17A (followed by goat anti-rat Texas red) showed comparable T cell infiltration in p19 KO and control mice, but demonstrated absence of IL-17 expression in p19 KO mice. Representative images are shown. The three left side panels show panoramic views (100 \times ; white bars represent 150 μ m). The six panels on the right show representative villi. White bars represent 50 μ m.

(Ref. [24], and unpublished data from the Tsokos lab). This may account for the increased density of infiltrating T cells into the I/R-damaged intestine observed in this report (Fig. 2). It is possible that tissues affected by I/R express more hyaluronic acid –the ligand for CD44. Alternatively, chemokine receptor expression may be altered in SLE T cells [25,26] and the I/R intestine may produce more of the corresponding chemokines.

Th17 cells represent a CD4⁺ T cell subset which produces increased amounts of IL-17 [19]. IL-17 participates in the immune response against various infections, particularly extracellular bacteria and fungi, and has been linked to inflammatory and autoimmune diseases in humans and mice [27]. In particular, IL-17 has proved to play a key role in experimental autoimmune encephalomyelitis [28,29] and collagen-induced arthritis [21,30]. The action of IL-17 is particularly broad, since its receptor is expressed by a large array of immune and non-immune cells, especially epithelial tissues [27]. The production of IL-17 leads to the induction of multiple pro-inflammatory effects including the production

of cytokines and chemokines (IL-6, IL-8, GM-CSF, G-CSF, CXCL1, CXCL10) [19]. In addition, it plays a role in the local recruitment and activation of neutrophils [31]. These functional characteristics, along with the demonstration of its early presence in I/R-damaged tissues, suggested that IL-17 plays a pivotal role in I/R injury. Functionally, IL-17A and IL-17F are very similar, and the presence of one can compensate for the absence of the other. Thus, deletion of either gene does not lead to any phenotypic difference. Moreover, the distance that separates both genes has precluded the production of double KO mice. For this reason, IL-23 deficient (p19^{-/-}) mice that fail to produce IL-17 have been extensively used as a surrogate IL-17 deficient model [20,32–34]. IL-23 p19 KO mice have a decreased capacity to develop T cell-dependent humoral immune responses and their ability to mount delayed type hypersensitivity responses is impaired [35]. The presence of IL-23 is particularly relevant for the production of IL-17 in the intestine [19,36]. Thus, we believe that the p19 KO mouse is an ideal model for the study of the IL-23-IL17 axis in

intestinal I/R. Our results indicate that the powerful pro-inflammatory effect of IL-17 produced by T cells is responsible for a large proportion of the immune-mediated tissue damage triggered by ischemia. However, we cannot rule out the importance of other IL-23-associated factors.

IL-17 production in response to I/R is present in both normal and lupus-prone mice; however, it is exaggerated in the autoimmune mice. Although we do not have sufficient information to explain why this happens, it is possible that the intestinal local cytokine and chemokine milieu that results following I/R injury may account for the increased rate of Th17 cell infiltration. IL-2, which is able to restrain Th17 cell development [37], is produced in abnormally low levels in lupus-prone mice [38]. Conversely, the secretion of IL-6, which has Th17-inducing capacity [32,39], is increased [40].

In conclusion, we have presented evidence that IL-17 producing T cells infiltrate intestinal tissue after mesenteric I/R and that this response is amplified in lupus-prone mice. Our data suggest that control of IL-17 production may be of benefit to the I/R-instigated tissue damage which represents a component of various clinical conditions including organ transplant, coronary blood flow reinstatement following myocardial infarction and autoimmune diseases where the vascular bed is frequently affected.

Acknowledgments

This work was supported by the National Institutes of Health Grant R01 AI42269 and Medical Research Command grants W81XWH-07-1-0286 and W81XWH-06-1-0486.

References

- [1] S.D. Fleming, G.C. Tsokos, Complement, natural antibodies, autoantibodies and tissue injury, *Autoimmune Rev.* 5 (2006) 89–92.
- [2] Y. Huang, H. Rabb, K.L. Womer, Ischemia-reperfusion and immediate T cell responses, *Cell. Immunol.* 248 (2007) 4–11.
- [3] T. Shigematsu, R.E. Wolf, D.N. Granger, T-lymphocytes modulate the microvascular and inflammatory responses to intestinal ischemia-reperfusion, *Microcirculation* 9 (2002) 99–109.
- [4] R.M. Zwacka, Y. Zhang, J. Halldorson, H. Schlossberg, L. Dudus, J.F. Engelhardt, CD4⁽⁺⁾ T-Lymphocytes mediate ischemia/reperfusion-induced inflammatory responses in mouse liver, *J. Clin. Invest.* 100 (1997) 279–289.
- [5] M.J. Burne, F. Daniels, A. El Ghandour, et al., Identification of the CD4(+) T cell as a major pathogenic factor in ischemic acute renal failure, *J. Clin. Invest.* 108 (2001) 1283–1290.
- [6] M.O. Le, H. Louis, A. Demols, et al., Cold liver ischemia-reperfusion injury critically depends on liver T cells and is improved by donor pretreatment with interleukin 10 in mice, *Hepatology* 31 (2000) 1266–1274.
- [7] M.B. Urowitz, D. Gladman, D. Ibanez, et al., Clinical manifestations and coronary artery disease risk factors at diagnosis of systemic lupus erythematosus: data from an international inception cohort, *Lupus* 16 (2007) 731–735.
- [8] M.B. Urowitz, D. Gladman, D. Ibanez, et al., Accumulation of coronary artery disease risk factors over three years: data from an international inception cohort, *Arthritis Rheum.* 59 (2008) 176–180.
- [9] E. Somers, L.S. Magder, M. Petri, Antiphospholipid antibodies and incidence of venous thrombosis in a cohort of patients with systemic lupus erythematosus, *J. Rheumatol.* 29 (2002) 2531–2536.
- [10] M. Ramos-Casals, N. Nardi, M. Lagrutta, et al., Vasculitis in systemic lupus erythematosus: prevalence and clinical characteristics in 670 Patients, *Medicine (Baltimore)* 85 (2006) 95–104.
- [11] J.C. Crispin, V.C. Kyttaris, Y.T. Juang, G.C. Tsokos, How signaling and gene transcription aberrations dictate the systemic lupus erythematosus T cell phenotype, *Trends Immunol.* 29 (2008) 110–115.
- [12] S.D. Fleming, M. Monestier, G.C. Tsokos, Accelerated ischemia/reperfusion-induced injury in autoimmunity-prone mice, *J. Immunol.* 173 (2004) 4230–4235.
- [13] S. Rehrig, S.D. Fleming, J. Anderson, et al., Complement inhibitor, complement receptor 1-related gene/protein Y-Ig attenuates intestinal damage after the onset of mesenteric ischemia/reperfusion injury in mice, *J. Immunol.* 167 (2001) 5921–5927.
- [14] K. Liu, C. Mohan, What do mouse models teach us about human SLE? *Clin. Immunol.* 119 (2006) 123–130.
- [15] K. Deusch, R. Fernandez-Botran, M. Konstadoulakis, K. Bauer, R. S. Schwartz, M.P. Madaio, Autoreactive T cells from MRL-Lpr/Lpr mice secrete multiple lymphokines and induce the production of IgG anti-DNA antibodies, *J. Autoimmun.* 4 (1991) 563–576.
- [16] D. Balomenos, R. Rumold, A.N. Theofilopoulos, Interferon-gamma is required for lupus-like disease and lymphoaccumulation in MRL-Lpr mice, *J. Clin. Invest.* 101 (1998) 364–371.
- [17] H.K. Kang, M. Liu, S.K. Datta, Low-dose peptide tolerance therapy of lupus generates plasmacytoid dendritic cells that cause expansion of autoantigen-specific regulatory T cells and contraction of inflammatory Th17 cells, *J. Immunol.* 178 (2007) 7849–7858.
- [18] Y. Li, T. Harada, Y.T. Juang, et al., Phosphorylated ERM is responsible for increased T cell polarization, adhesion, and migration in patients with systemic lupus erythematosus, *J. Immunol.* 178 (2007) 1938–1947.
- [19] T. Korn, M. Oukka, V. Kuchroo, E. Bettelli, Th17 cells: effector T cells with inflammatory properties, *Semin. Immunol.* 19 (2007) 362–371.
- [20] C.L. Langrish, Y. Chen, W.M. Blumenschein, et al., IL-23 drives a pathogenic T cell population that induces autoimmune inflammation, *J. Exp. Med.* 201 (2005) 233–240.
- [21] S. Nakae, A. Nambu, K. Sudo, Y. Iwakura, Suppression of immune induction of collagen-induced arthritis in IL-17-deficient mice, *J. Immunol.* 171 (2003) 6173–6177.
- [22] C. Dong, TH17 cells in development: an updated view of their molecular identity and genetic programming, *Nat. Rev. Immunol.* 8 (2008) 337–348.
- [23] R.A. Cohen, G. Bayliss, G.F. Kane-Wanger, et al., T cells and *in situ* cryoglobulin deposition in the pathogenesis of lupus nephritis, *Clin. Immunol.* 128 (2008) 1–7.
- [24] F.R. Bahjat, P.R. Pine, A. Reitsma, et al., An orally bioavailable spleen tyrosine kinase inhibitor delays disease progression and prolongs survival in murine lupus, *Arthritis Rheum.* 58 (2008) 1433–1444.
- [25] L.G. Perez de, H. Maier, T.J. Franz, et al., Chemokine receptor Ccr2 deficiency reduces renal disease and prolongs survival in MRL/Lpr lupus-prone mice, *J. Am. Soc. Nephrol.* 16 (2005) 3592–3601.
- [26] H. Hasegawa, Chemokine blockade for lupus model mice, *Front. Biosci.* 13 (2008) 2900–2908.
- [27] W. Ouyang, J.K. Kolls, Y. Zheng, The biological functions of T helper 17 cell effector cytokines in inflammation, *Immunity* 28 (2008) 454–467.
- [28] Y. Komiyama, S. Nakae, T. Matsuki, et al., IL-17 plays an important role in the development of experimental autoimmune encephalomyelitis, *J. Immunol.* 177 (2006) 566–573.

- [29] H.H. Hofstetter, S.M. Ibrahim, D. Koczan, et al., Therapeutic efficacy of IL-17 neutralization in murine experimental autoimmune encephalomyelitis, *Cell. Immunol.* 237 (2005) 123–130.
- [30] K. Sato, A. Suematsu, K. Okamoto, et al., Th17 functions as an osteoclastogenic helper T cell subset that links T cell activation and bone destruction, *J. Exp. Med.* 203 (2006) 2673–2682.
- [31] J.K. Kolls, A. Linden, Interleukin-17 family members and inflammation, *Immunity* 21 (2004) 467–476.
- [32] M. Veldhoen, R.J. Hocking, C.J. Atkins, R.M. Locksley, B. Stockinger, TGFbeta in the context of an inflammatory cytokine milieu supports de novo differentiation of IL-17-producing T cells, *Immunity* 24 (2006) 179–189.
- [33] D.J. Cua, J. Sherlock, Y. Chen, et al., Interleukin-23 rather than interleukin-12 is the critical cytokine for autoimmune inflammation of the brain, *Nature* 421 (2003) 744–748.
- [34] S. Aggarwal, N. Ghilardi, M.H. Xie, F.J. de Sauvage, A.L. Gurney, Interleukin-23 promotes a distinct CD4 T cell activation state characterized by the production of interleukin-17, *J. Biol. Chem.* 278 (2003) 1910–1914.
- [35] N. Ghilardi, N. Kljavin, Q. Chen, S. Lucas, A.L. Gurney, F.J. de Sauvage, Compromised humoral and delayed-type hypersensitivity responses in IL-23-deficient mice, *J. Immunol.* 172 (2004) 2827–2833.
- [36] H.H. Uhlig, B.S. McKenzie, S. Hue, et al., Differential activity of IL-12 and IL-23 in mucosal and systemic innate immune pathology, *Immunity* 25 (2006) 309–318.
- [37] A. Laurence, C.M. Tato, T.S. Davidson, et al., Interleukin-2 signaling via STAT5 constrains T helper 17 cell generation, *Immunity* 26 (2007) 371–381.
- [38] A. Altman, A.N. Theofilopoulos, R. Weiner, D.H. Katz, F.J. Dixon, Analysis of T cell function in autoimmune murine strains. Defects in production and responsiveness to interleukin 2, *J. Exp. Med.* 154 (1981) 791–808.
- [39] E. Bettelli, Y. Carrier, W. Gao, et al., Reciprocal developmental pathways for the generation of pathogenic effector TH17 and regulatory T cells, *Nature* 441 (2006) 235–238.
- [40] P. Decker, I. Kotter, R. Klein, B. Berner, H.G. Rammensee, Monocyte-derived dendritic cells over-express CD86 in patients with systemic lupus erythematosus, *Rheumatology (Oxford)* 45 (2006) 1087–1095.